

GENOMIC INSTABILITY IN DEVELOPING B-CELLS AND B-CELL LEUKEMIA:

EXPLORING THE ROLE OF THE
RAG1/2 COMPLEX



Katarína Ochodnická

**Genomic instability in developing B-cells and B-cell leukemia:
exploring the role of the RAG1/2 complex**

Katarína Ochodnická

Genomic instability in developing B-cells and B-cell leukemia: exploring the role of the RAG1/2 complex

Academic thesis, University of Amsterdam, Amsterdam, the Netherlands

Author: Katarína Ochodnická
Printing: Ridderprint, ridderprint.nl
Cover design: Marcel Jansen, ziehoe.nl
Layout and design: Bart Roelofs, persoonlijkproefschrift.nl
ISBN: 978-94-6506-063-7

Printing of this thesis was financially supported by:

Department of Pathology, University Medical Centers, location AMC, Amsterdam, the Netherlands

Nordic Pharma BV

Copyright ©2024, **Katarína Ochodnická**, Amsterdam, the Netherlands

All rights reserved. No part of this thesis may be reproduced or transmitted in any form or by any means, without express written permission from the author.

**Genomic instability in developing B-cells and B-cell leukemia:
exploring the role of the RAG1/2 complex**

ACADEMISCH PROEFSCHRIFT

ter verkrijging van de graad van doctor
aan de Universiteit van Amsterdam
op gezag van de Rector Magnificus
prof. dr. ir. P.P.C.C. Verbeek
ten overstaan van een door het College voor Promoties ingestelde commissie,
in het openbaar te verdedigen in de Aula der Universiteit
op woensdag 23 oktober 2024, te 11.00 uur

door

Katarína Ochođnická

geboren te Bratislava

Promotiecommissie

Promotor: prof. dr. C.J.M. van Noesel AMC-UvA

Copromotor: dr. J.E.J. Guikema AMC-UvA

Overige leden: prof. dr. S.T. Pals AMC-UvA
prof. dr. E.F. Eldering AMC-UvA
prof. dr. M.C. van Zelm Erasmus Universiteit Rotterdam
dr. M. van der Burg Universiteit Leiden
dr. H.B. Jacobs NKI
prof. dr. C.E. van der Schoot AMC-UvA

Faculteit der Geneeskunde

to my daughters


Table of content

Chapter 1	General introduction and outline of this thesis	9
Chapter 2	Role of RAG1 and RAG2 in B-cell development, signaling and (off) target DNA damage	15
Chapter 3	RAG1/2 induces double-stranded DNA breaks at non- <i>Ig</i> loci in the proximity of single sequence repeats in developing B cells	53
Chapter 4	The DNA damage response regulates RAG1/2 expression in pre-B cells through ATM-FOXO1 signaling	81
Chapter 5	NF- κ B and AKT signaling prevent DNA damage in transformed pre-B cells by suppressing RAG1/2 expression and activity	115
Chapter 6	DNA damage-induced p53 downregulates expression of RAG1 through a negative feedback loop involving miR-34a and FOXP1	147
Chapter 7	General discussion	167
Appendix	English summary	194
	Nederlandse samenvatting	197
	Zhrnutie v slovenčine	201
	Authors' contributions & Research funding	204
	PhD portfolio & Publications	208
	About the author	211
	Acknowledgements	212



CHAPTER

General introduction and outline of the thesis



1

The **immune system** is a collection of molecules, cells, and tissues, which protect an individual from infectious microbes and eliminate foreign substances, and consists of two main branches: the innate immune system and the adaptive immune system.

The **innate immune system** provides immediate, nonspecific defense mechanisms, including physical barriers like the skin, as well as immune cells that engulf and destroy pathogens. The innate immune system responds always in the same way to repeated infections and it is not able to escalate the responses with each successive exposure to a particular microbe or antigen. The innate immune system is phylogenetically the oldest system of host defense.

The **adaptive immune system**, on the other hand, develops a more specific and targeted response over time, that can recognize and “remember” specific pathogens, providing a more tailored and long-lasting defense. The most characteristic feature of adaptive immunity is its unique specificity for distinct molecules. Lymphocytes and antigen-presenting cells (APC) are the main components of adaptive immunity. There are distinct subpopulations of lymphocytes that differ in their function and how they recognize antigens. **B lymphocytes (B cells)** recognize extracellular antigens, and are endowed with the unique property to produce antibodies. Antibodies are effectors of humoral immunity; they are serum proteins that initiate processes leading to the neutralization of antigens. **T lymphocytes (T cells)**, on the other hand, mediate cellular immunity. T cells are able to directly kill the infected cells and they also direct immune responses by helping B cells to eliminate the pathogens.

The communication between immune cells is crucial for an effective immune response, and various signaling molecules, such as cytokines, help coordinate these interactions. The immune system’s ability to distinguish self from non-self prevents it from attacking the body’s own cells, a condition known as autoimmunity.

B cells are specialized white blood cells that are responsible for producing antibodies, which are proteins that recognize and neutralize specific pathogens like bacteria and viruses. The total of antibodies with different specificities is called the B-cell repertoire, a vast and unique collection of distinct receptor molecules on the surface of B cells. The B-cell repertoire is generated through a process known as **V(D)J recombination**, occurring in the bone marrow during the early stages of B- and T-cell development. This genetic rearrangement process creates an enormous variety of potential antibody specificities, allowing the B and T cells to recognize a wide range of antigens. Upon maturation in the bone marrow, B cells migrate to the bloodstream and lymphoid tissues, where they can be activated, e.g. in response to foreign invaders. The diversity and adaptability of the B-cell repertoire contribute significantly to the immune system’s ability to defend the body against a myriad of pathogens. This intricate system ensures that the immune response is tailored to the specific challenges posed by different infectious agents, providing a key defense mechanism for maintaining overall health and well-being.

At the same time, this system poses a serious threat to genome stability if not tightly regulated. The V(D)J gene recombination process requires the activity of the **recombination-activating gene-1 (RAG1)** and **recombination-activating gene-2 (RAG2)** protein complex. RAG1 and RAG2 form a complex that cuts DNA at specific sites within the immunoglobulin (*Ig*) and T-cell receptor (*Tcr*) loci, thereby initiating gene recombination. DNA cleavage in genes outside of the *Ig* regions could give rise to potentially oncogenic genetic lesions such as chromosomal translocations or deletions. As a matter of fact, there is compelling evidence that some of the genomic lesions identified in subsets of **B-cell acute lymphoblastic leukemia (B-ALL)** result from aberrant RAG1/2 recombination activity. Though in the last couple of decades the physiological mechanisms of the regulation RAG1/2 regulations have extensively been studied, the mechanisms of pathological regulation of RAG1/2 are less well described.

This thesis aims to provide a deeper understanding of the mechanisms that regulate the expression and the activity of RAG1 and RAG2 in response to exogenous DNA damage, but also to DNA damage originating from RAG-dependent V(D)J recombination activity itself. Understanding the intricacies of RAG1/2 regulation is important for our understanding of how the integrity of the genome is maintained in developing B cells that have to deal with DNA damage during the *Ig* receptor formation. The misregulation of RAG1/2, or the illegitimate targeting of RAG1/2, might also pose a threat to genome integrity, as off-target DNA cleavage (outside the *Ig* loci), could potentially give rise to genomic lesions that may result in oncogenic mutations.

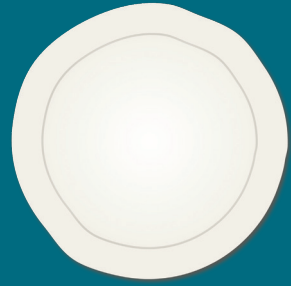
In **Chapter 2**, the current understanding of B-cell development and the regulation of RAG1 and RAG2 expression and activity is extensively summarized. The responses of pre-B cells to DNA damage, and specifically the regulatory role of the double-stranded DNA breaks (DSBs) are described in detail. This chapter reviews also the evidence for a possible role of RAG1/2 in the etiology of B-cell malignancies, and the targeting properties of RAG1/2 in this context.

Aberrant RAG1/2 targeting during B-cell development has been implicated in the development of lymphoid malignancies. In **Chapter 3** we developed a method that allows the identification of RAG1/2-induced DSBs on a genome-wide scale in developing pre-B cells. We found that many of the RAG1/2-induced DNA breaks can be detected outside of the *Ig* loci, providing *in vivo* evidence for the off-target activity of RAG1/2. Moreover, analysis of the common denominators with regard to the genomic locations and sequence motifs of the RAG1/2-induced DNA breaks revealed an enrichment of simple sequence repeats (SSR) and GC-rich regions in the proximity of the RAG1/2-induced DNA breaks. To gain a further understanding of the implications of programmed DNA damage in developing lymphocytes, it is essential to unravel the intricacies of the regulation of RAG1/2 activity during B-cell development, especially in the context of the DNA damage originating from V(D)J recombination itself. Inappropriate regulation of RAG1/2 expression may result in per-

sistent RAG1/2 activity, thereby potentially increasing the occurrence of genomic lesions resulting in oncogenic events. In chapters 4, 5, and 6 we describe the interplay between DNA breaks and RAG1/2 activity and regulation.

In **Chapter 4** we showed that extrinsic DNA damage leads to the downregulation of RAG1/2 expression in pre-B cells. We identified the ataxia telangiectasia mutated (ATM) kinase as a key player in the DNA damage-dependent regulation of RAG1/2 transcription, which primarily impinges on the transcription factor forkhead box O1 (FOXO1). In **Chapter 5** we showed that the nuclear factor kappa-B (NF- κ B) and phosphoinositol-3 kinase (PI3K)/AKT signaling pathways act in concert to suppress inappropriate RAG1/2 expression and activity in human and mouse pre-B cells and in B-cell acute lymphoblastic leukemia (B-ALL) patients. Finally, in **Chapter 6** we identified an additional regulatory mechanism that regulates RAG1/2 expression in response to DNA damage, involving the p53-dependent expression of microRNA-34a (miR-34a), which acts by inhibiting forkhead box protein P1 (FOXP1), a transcription factor that drives RAG1/2 expression.

In summary, the studies presented in this thesis show that RAG1/2 is capable of introducing DNA breaks outside of the *Ig* loci, located in the proximity of SSR sequences. In addition, our studies show that DNA breaks in developing pre-B cells also have an important regulatory function by instigating regulatory feedback loops that limit the expression and activity of RAG1/2, thereby contributing to safeguarding genome stability and integrity in developing B cells. These findings are further summarized and discussed in **Chapter 7**, outlining their potential implications and perspectives.



CHAPTER

Role of RAG1 and RAG2 in B-cell development, signaling and (off) target DNA damage

Katarina Ochodnicka-Mackovicova, Jeroen E.J. Guikema

A large, stylized number '2' in a light pink color, positioned on the right side of the page. It is partially enclosed by a vertical teal line that runs from the top of the chapter title down to the bottom of the page.

Abstract

This review explores the intricate regulatory mechanisms governing RAG1 and RAG2 expression and activity during the development of B cells, with a particular focus on their implications in the development of lymphoid malignancies such as B-cell acute lymphoblastic leukemia (B-ALL). We summarize current knowledge on B-cell development, the mechanism of V(D)J recombination, and the role of the RAG1 and RAG2 (RAG1/2) complex. We discuss the role of the DNA damage response (DDR) during V(D)J recombination, shedding light on its involvement in the regulation of the activity and expression of RAG1/2. Understanding the interplay between the various regulatory processes provides insights into the potential links between aberrant V(D)J recombination, dysregulation of RAG1/2, and the onset of lymphoid malignancies, contributing to our understanding of the molecular events underlying these diseases.

Adaptive immune system

The **adaptive immune** system evolved into a system that allows specific and targeted responses, capable of recognizing particular pathogens after repeated encounters, ensuring a long-lasting defense. The hallmark feature of the adaptive immune system is its unique specificity for distinct molecules, primarily facilitated by lymphocytes and antigen-presenting cells (APCs). Among lymphocytes, **B cells** specialize in recognizing extracellular antigens and producing antibodies, essential for humoral immunity. The antibodies initiate processes leading to antigen neutralization. On the other hand, T cells play a vital role in cellular immunity by recognizing antigens from intracellular microbes and eliminating infected cells. Unlike B cells, T cells do not produce antibodies.

Antibodies have a polypeptide structure consisting of four protein chains: two identical heavy (H) chains and two identical light (L) chains, connected by disulfide bonds and non-covalent interactions. These chains come together to form a Y-shaped structure known as the basic antibody monomer. Each chain consists of a constant region and a variable region. The variable regions of the heavy and light chains contain antigen-binding sites and it is responsible for pathogen recognition. To achieve an efficient adaptive immune response, the immune system is equipped with the capability to generate an enormously large array of antibodies of different specificities, recognizing the different pathogens. In a cell, single proteins are typically coded by single genes. The number of antibodies that are required to fight off hundreds of thousands of different pathogens is so high, that one's genome would have to accommodate hundreds of thousands of genes to make the various antigen receptors available for immune response. However, today it is clear that the genome of vertebrates contains just around 20,000 genes and thus not enough to give rise to the large repertoire of antibodies¹. In B and T cells, an intricate system has evolved allowing the flexible generation of a virtually unlimited number of different antibodies, also referred to as **immunoglobulins (Ig) or B-cell receptor (BCR)** in B cells, and **T-cell receptors (TCR)** in T cells, or collectively, antigen receptors. In this system, the recombination of gene segments is responsible for the generation of genetic variation. This is achieved by the ordered recombination of so-called variable (V), diversity (D), and joining (J) gene segments, which together code for the antigen-binding portion of the antigen receptor. These genes are non-functional in their germline configuration but become functional following the process of somatic gene recombination, also called **V(D)J recombination**, where one of the V-genes, one of the D-genes (only for the Ig heavy chain) and one of the J-genes are ligated together and the intervening parts are excised from the genome. V(D)J recombination is initiated by recombination-activating gene 1 (RAG1) and recombination-activating gene 2 (RAG2) proteins, which introduce a double-stranded DNA breaks into the V(D)J genes – first, the heavy chain is recombined, followed by the recombination of the light chain. This newly assembled sequence encodes

for the hypervariable (antigen-binding) part of the **B-cell antigen receptor or antibody**. The BCR diversity in developing B cells is further increased by terminal deoxynucleotidyl transferase (TdT), which catalyzes the addition of nucleotides to the 3' end of DNA during the formation of the V(D)J junction. V(D)J recombination is a site-specific recombination process that takes place only at BCR/T-cell receptor (TCR) gene segments and occurs only in developing lymphocytes in a lineage-specific manner². The process of gene recombination, coupled with the induction of junctional diversity, exhibits remarkable complexity, facilitating the creation of an extensive array of antigen receptors boasting millions of specificities, all while requiring modest gene coding capacity. However, the induction of DNA breaks necessary for recombination and the generation of billions of antigen receptors over an organism's lifespan poses a substantial **threat to genomic integrity** and requires stringent fidelity mechanisms.

T cells during their development also undergo RAG1/2-mediated gene recombination to express highly variable surface T-cell receptor (TCR) receptors alpha (α) and beta (β) chains, present in the majority of T cells, or gamma (γ) and delta (δ) chains present only in a minor population of T cells^{3,4}. Though the order of TCR loci recombination differs from the order of BCR recombination, the molecular basis of the gene recombination is the same in B and T cells. Considering the scope of this thesis, only B-cell-related gene recombination processes, and their regulation, will be discussed. T-cell development and TCR recombination have extensively been reviewed elsewhere⁵⁻⁷.

Aberrant V(D)J recombination has been demonstrated to be an underlying cause of several lymphoid malignancies, and therefore, the basic regulatory mechanisms safeguarding the genome integrity during V(D)J recombination are of great interest^{8,9}. To understand the pathogenesis of lymphoid malignancies, a deep knowledge of the inner workings of our immune system is needed. The following chapters summarize the current knowledge of the physiological B-cell development and gene recombination.

B-cell development, gene recombination, and B-cell activation

B-cell development

All lymphocytes develop from common lymphoid progenitors (CLPs) that are derived from hematopoietic stem cells (HSCs). The commitment of CLPs to either B- or T-lineage is coordinated by a set of transcription factors¹⁰. Commitment to the B-lineage is at first instance mediated by early B-cell factor (EBF) and E2A transcription factors, and subsequently by Paired Box 5 (Pax-5)¹¹. Commitment to the T-cell lineage is mainly orchestrated by Neurogenic locus notch homolog protein 1 (Notch-1) and GATA-3 transcription factors¹². Pro-B cells are the earliest committed B-cell precursors. The early stage of B-cell development is characterized by the sequential recombination of the *Ig* loci (**Figure 1**). At the end of this stage, **RAG1** and **RAG2** proteins are expressed for the first time and the first

recombination of *Ig* genes takes place at the **immunoglobulin heavy chain locus (*Igh*)**. Typically, the D_H to J_H recombinations take place first, followed by a recombination of the upstream V_H region to the already rearranged DJ segment. The successful recombination of *Igh* marks the transition to the pre-B cell stage¹⁰. The early pre-B cells express a **pre-B cell antigen receptor (pre-BCR)**, consisting of the μ -*Igh* chain and a surrogate light chain (SLC). The SLC is a heterodimer and consists of 2 proteins: $\lambda 5$ and VpreB. The pre-BCR can oligomerize and trigger downstream signaling in the absence of a specific antigen, so-called tonic pre-BCR signaling, which is crucial for the survival of the pre-B cells at this stage^{13,14}. Subsequently, pre-B cells may undergo 1 or 2 cell divisions and then proceed with the recombination of gene segments encoding for the **immunoglobulin light chain (*Igl*)**. At this stage the RAG1 and RAG2 are re-expressed and at first, **the immunoglobulin kappa chain (*Ig κ*)** is recombined. If the pre-B cells fail to productively recombine the first and the second allele of *Ig κ* , and when they have exhausted all the recombination possibilities, then they proceed with recombination of the **immunoglobulin lambda chain (*Ig λ*)**¹⁵. The human *Ig κ* is located on chromosome 2 (the mouse *Ig κ* is located on chromosome 6), and the human *Ig λ* on chromosome 22 (mouse *Ig λ* is located on chromosome 16). The light chain loci consist of V_L and J_L segments, and the constant region C_L but lack D gene segments, in contrast to the *Igh* locus. Following a successful recombination, an IgM BCR is expressed on the cell surface. Once the recombination has successfully been performed, the RAG1/2 expression is in general suppressed throughout the mature stage of the B cells, though there are instances when RAG1/2 can be re-expressed at immature B cells and mediate secondary rearrangements in *Ig* loci, so-called receptor editing¹⁶. In the process of receptor editing, the functionally unresponsive or the self-reactive BCR may acquire a new specificity, and thus escape the apoptosis. Secondary rearrangements in mature peripheral B cells may also take place, the so-called receptor revision, which further diversifies the repertoire¹⁷. Each B-cell expresses a BCR of only one particular specificity. This is achieved by allowing only one functional recombined allele to be expressed. This phenomenon called **allelic exclusion**, guarantees specificity of immune responses and prevents auto-immune reactions. More details on the mechanism of allelic exclusion are discussed elsewhere in this review.

After successful recombination, IgM-expressing immature B cells complete their maturation outside of the BM, they enter the circulation or migrate to the lymph nodes or spleen.

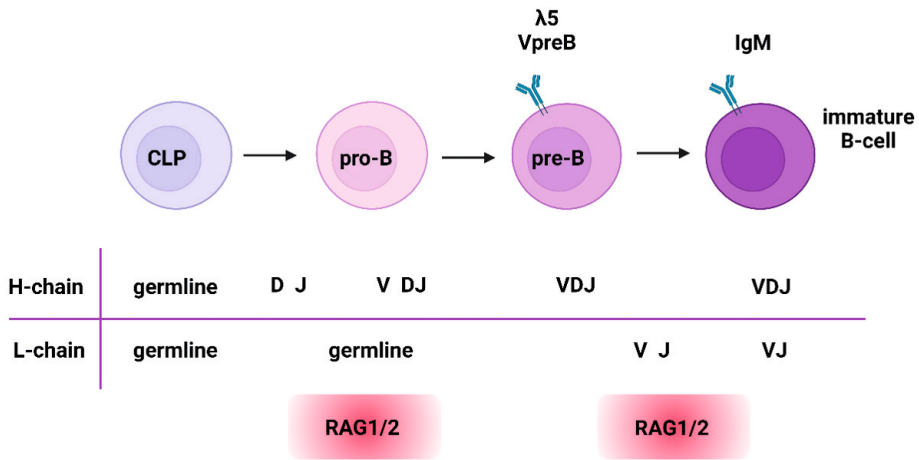


Figure 1.

Schematic depiction of B-cell development in the bone marrow. B cells develop from common lymphoid progenitor (CLP). At this stage, both the heavy and the light chains are present in their germline configurations. Subsequently, at the pro-B cell stage, RAG1/2 is expressed (here depicted in red) and gene recombination at the Ig heavy chain locus is initiated. First, a D to J segment recombination takes place, followed by V to DJ recombination. Successful recombination at the early pre-B cell stage leads to the expression of pre-BCR, composed of the recombined heavy chain – μ -Igh, and the surrogate light chain, composed of λ 5 and VpreB. At the late pre-B cell stage, the RAG1/2 recombinase is expressed for the second time and the recombination of Ig light chain genes is initiated. Following the successful Ig light chain recombination, the B-cell receptor (BCR/IgM) is expressed at the immature B-cell stage. Created with BioRender.com

RAG1 and RAG2 proteins are essential for V(D)J recombination and normal B-cell development, this has been clearly illustrated in mice where the biallelic disruption of *Rag1* and *Rag2* genes resulted in a complete developmental block of B and T cells at their progenitor stage due to the inability to initiate V(D)J recombination^{18,19}. Biallelic *RAG1* or *RAG2* null mutations in human result in severe combined immunodeficiency (SCID) presented with absent B- and T-cell lymphocytes²⁰. Recent advances in genetic engineering allowed successful replacement of the *RAG1* or *RAG2* null mutations using CRISPR-Cas9 editing of the hematopoietic stem cells in mice and patients, which led to successful production of mature B and T cells with diverse antigen receptor repertoires^{21,22}. Omenn syndrome (OS) presents as an additional clinical phenotype linked to hypomorphic mutations in *RAG1* and *RAG2*, where only residual enzymatic RAG activity is observed. This condition is characterized by the presence of oligoclonal lymphocytes and infiltrating activated T cells, which cause damage to target tissues. Atypical SCID (AS) and delayed onset combined immunodeficiency with granulomas or autoimmunity (CID-G/AI) are some of the other clinical phenotypes associated with RAG1/2 mutations²³.

Receptor editing and allelic exclusion

Considering the vast diversity of antibody specificities, B cells must continuously ensure the specificities against pathogens, while averting autoreactivity. Consequently, B cells undergo multiple screening checkpoints during their development to assess their autoreactivity levels. The initial screening occurs following the differentiation of pro-B cells into pre-B cells. The antigen-independent tonic pre-BCR promotes the progression of pre-B cells with non-autoreactive pre-BCR to the next developmental stage. Lack of tonic pre-BCR signaling leads to apoptosis. However, several studies addressing the mechanism of central tolerance have uncovered that autoreactive B cells may undergo another round of *Ig* chain gene recombination as an attempt to “edit” the autoreactive pre-BCR or BCR and thus escape apoptosis. This ongoing gene recombination, known as receptor editing, may change receptor specificity and this contributes to repertoire diversification^{24,25}. At the same time, receptor editing, and the ongoing exposure of the pre-B cells to RAG1/2-recombinase, may be a potential source of genomic instability.

The concept of B-cell monospecificity has long been pivotal in explaining the targeted production of antibodies against specific pathogens. Referred to as the ‘one B-cell - one antibody’ rule, this paradigm finds substantial support in numerous experimental studies. At the genetic level, the monospecificity of B cells arises from the so-called allelic exclusion, mechanism ensuring that each B cell produces antibodies with a single specificity. B cells with multiple different specificities could lead to autoimmune reactions or ineffective immune responses^{26,27}. It has been demonstrated that successful recombination on one allele initiated signaling suppressing bi-allelic recombination by terminating RAG1 and RAG2 expression as well as the accessibility of the *Ig* locus. Several mechanisms have been proposed to explain how simultaneous rearrangement of both alleles is prevented. The *asynchronous recombination models* rely on mechanisms regulating the accessibility. These models propose two main mechanisms: the probabilistic model and the instructive model. In the probabilistic model, the chromatin (in)accessibility leads to asynchronous recombination, as the inaccessible *Ig* chromatin/allele leads to slow and inefficient recombinations, limiting the frequency of recombination events to one allele per cell. The instructive model is based on the asynchronous replication timing of the two alleles. The early-replicating allele is recombined first, while the late-replicating allele is recombined only if the recombination attempt on the first allele failed^{27,28}. The *stochastic model* suggests that while *Ig* recombination is highly efficient, it typically yields only one functional *Ig* allele per cell. This concept implies that *Ig* allelic exclusion occurs due to the low probability of rearranging an allele in the correct reading frame, resulting in a functional *Ig* chain, compared to the higher likelihood of generating a non-functional allele. Consequently, no coordination between the two *Ig* alleles is deemed necessary, rendering asynchrony of allelic recombination inconsequential in this model²⁹. On the other hand, *feedback inhibition models* propose that the recombination process of *Ig* genes is inhibited by their

products or intermediates. In the classical feedback inhibition model, successful *Ig* gene rearrangements activate signals through pre-BCRs or B-cell receptors (BCRs), leading to the suppression of further allelic recombination^{30,31}. This model explains the observed ratios of peripheral B cells with *Igh* and *Igl* loci in different configurations³². A more recent study proposes a mechanistic explanation based on the fact that only the mRNA transcripts from productively rearranged *Igh* allele are stable, whereas the non-productive *Igh* mRNA transcripts carry multiple stop-codons and are degraded by nonsense-mediated mRNA decay. Therefore, it was hypothesized that it is the stable mRNA transcript of productively rearranged *Igh* is responsible for the allelic exclusion³³. However, a more detailed investigation of this mechanism provided compelling evidence showing that the *Igh* mRNA actually does not play a role in allelic exclusion, and that it is the *Igh* protein complex that enforces the allelic exclusion and drives B cell development³⁴.

In addition, the RAG2 C-terminus and ataxia-telangiectasia mutated (ATM) were shown to prevent the bi-allelic gene recombination³⁵. In fact, the double-stranded DNA breaks (DSBs) arising from the RAG1/2 activity, which activate the DNA damage sensor ATM, have been proposed to trigger a negative feedback loop limiting the RAG expression. Inhibition or deletion of ATM resulted in bi-allelic recombinations and an increase in genomic instability in developing B cells³⁶.

From mature B-cell to plasma cell

Immature B cells exit the bone marrow and travel to the spleen, where they complete their early development by differentiating into naïve, follicular, or marginal zone (MZ) B cells. In secondary lymphoid organs, mature B cells encounter antigens presented by antigen-presenting cells (APCs), such as dendritic cells. Upon recognition of specific antigens by their BCRs, B cells become activated and undergo clonal expansion. Activated B cells that receive appropriate signals from helper T cells differentiate into plasma cells. Plasma cells are specialized for antibody production and secrete large quantities of antibodies. A subset of activated B cells differentiates into memory B cells, which persist long-term and provide a rapid and robust secondary immune response upon re-exposure to the same antigen³⁷.

The first antibodies produced in a humoral immune response are always of the IgM isotype. However, mature B cells may undergo so-called class-switch recombination (CSR) changing the antibody isotype. There are 5 antibody isotypes: IgG (subclasses IgG1, IgG2, IgG3, and IgG4), IgA (subclasses IgA1 and IgA2), IgM, IgD, and IgE. Exons that encode for these antibody classes are named γ (γ 1, γ 2, γ 3, and γ 4), α (α 1 and α 2), μ , δ , and ϵ . Different isotypes have adapted to function in different body compartments, for instance, IgA is predominantly present in secretions such as saliva, digestive tract, or nasal secretions, while IgG is primarily present in the blood serum³⁸. In addition to CSR, the affinity and other biological properties of the immunoglobulins can be further modified without changing their specificity in a process termed somatic hypermutation (SHM). Both CSR and SHM are

initiated by activation-induced cytidine deaminase (AID), an enzyme that is required for the execution of both mechanisms^{39–41}. The exact molecular backgrounds of the CSR and SHM mechanisms are provided elsewhere^{42–44}. AID has been shown to bind non-*Ig* loci and introduce collateral DNA damage throughout the genome of mature B cells^{44–46}. Thus, throughout their lifespan, B cells encounter numerous challenges to maintain genome integrity, highlighting the critical need for meticulous processes to safeguard genomic fidelity.

RAG1, RAG2 and the molecular mechanisms of V(D)J recombination

The evolution of RAG

The human *RAG1* and *RAG2* genes are situated in close proximity on chromosome 11p (the mouse *Rag1* and *Rag2* are located on chromosome 2p), each containing one large exon, separated by only 8kb⁴⁷. Such locus configuration is rather unusual and the lack of introns within the coding region is reminiscent of transposable elements. Indeed, the evolution studies of RAG1 and RAG2 structure and biochemical function indicate that RAGs originate from RAG-like (RAGL) transposable elements and evolved through so-called “molecular domestication” to their current form⁴⁸. Transposons are considered fragments of “selfish DNA,” acting as molecular parasites capable of replicating within the host’s genome without offering any discernible benefit. These mobile genetic elements spread within genomes by excising or copying themselves from one location and inserting into another^{49,50}. The first transposition event that led to the formation of the split antigen receptor gene occurred probably in early jawed vertebrate ancestors by invading the *Ig*-domain gene receptor exon by the *RAGL_A* family transposon. After this event, the *RAGL_A* transposon became a functional host protein, and its DNA-cleaving activity became essential for the expression of the split gene. A selective pressure caused an evolutionary adaptation of the *RAGL_A* in the way that it maintained its excision activity to allow the gene assembly, but at the same time suppressed the integrase activity of *RAGL_A* to limit its liability to genome integrity^{48,51,52}. Such an evolutionary change, termed the “molecular transposon domestication”, might have occurred when the early jawed vertebrates acquired the arginine 848 mutation in RAG1L (R848). In most invertebrates, methionine would be found in this position (M848). Interestingly, the methionine to arginine mutation does not seem to increase the efficiency of DNA cleavage, but it strongly suppresses the transposition activity and improves the odds of maintaining the genome integrity during the gene recombination^{53,54}.

RAG1 and RAG2 proteins

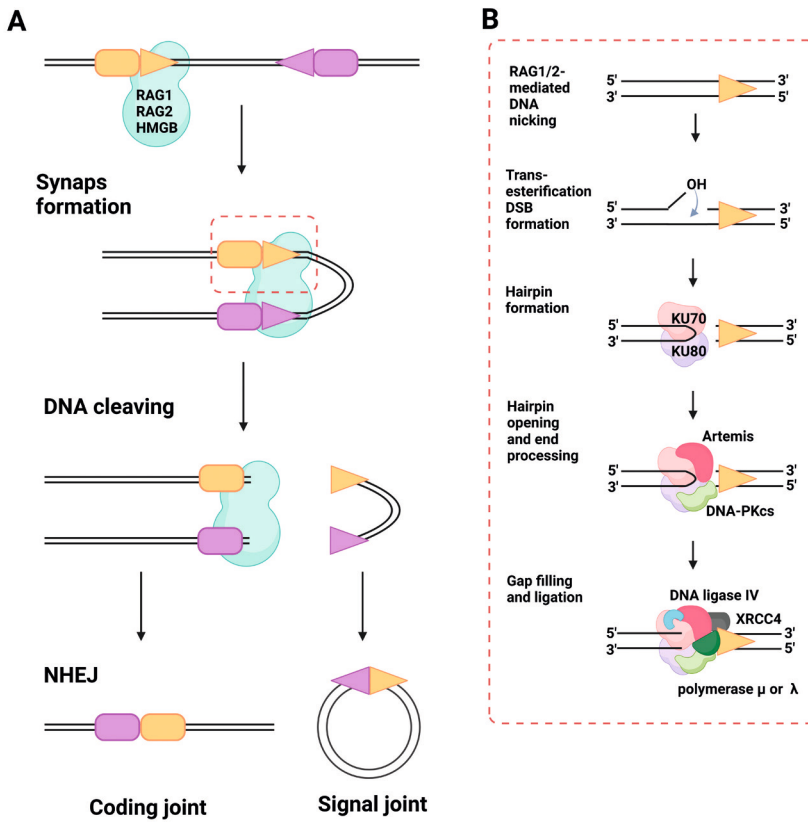
The human RAG1 contains 1043 amino acids (murine RAG1 contains 1040 amino acids) and is composed of 7 distinct structural domains. It contains a catalytic site that is responsible

for DNA cleavage⁵⁵. The human and murine RAG2 is composed of only 527 residues and has no direct contribution to DNA cutting, but enhances the RAG1 DNA cleavage activity by hundreds of folds. The RAG2 is folded into a six-bladed β -propeller or Kelch-repeat structure⁵⁶. The diverse domains in both RAGs can be categorized as either catalytically essential “core” domains or “non-core” domains, which are dispensable for the enzymatic activity but have a regulatory function⁵⁷. For instance, non-core RAG2, consisting of approximately one-third of the full-length protein, mediates its nuclear localization, association with specific histone-modified chromatin, and facilitates the long-range recombination reactions^{58–60}. The non-core RAG2 also contains a zinc-binding domain called plant homology domain (PHD), which coordinates with two zinc ions, and it specifically binds the histone H3 trimethylated on Lysine 4 (H3K4me3). Mutations in this region lead to severe defects in V(D)J recombination activity and failure of RAG2-PHD to bind H3K4me3 and has been linked to Omenn syndrome⁶¹. Non-core RAG1 increases the efficiency and fidelity of V(D)J recombination^{62,63}. An important feature in the N-terminal of non-core RAG1 is the zinc-binding dimerization domain (ZDD). ZDD contains two sub-domains, the C2H2 zinc finger and the Really Interesting New Gene (RING) finger, which act as an E3 ubiquitin ligase mediating (auto)ubiquitination of Histone H3. Point mutations in this domain result in decreased V(D)J recombination activity^{64,65}.

Structural studies in mice and zebrafish revealed that RAG1 and RAG2 interact and form together a Y-shaped heterodimer of 230kDa size, the RAG complex is composed of two core subunits, forming a heterotetramer that holds the two paired DNA strands, where RAG1 catalyzes the DNA nicking step. RAG2 is in particular responsible for stabilizing the protein-protein interaction between the two halves of the RAG tetramer, and for conferring the specificity to the interaction of RAG1 with the DNA substrate^{66,67}.

Molecular mechanism of V(D)J recombination

V(D)J recombination is initiated by the RAG1/2 endonuclease heterotetramer,⁵⁶ introducing a single-stranded DNA nick in the RSSs flanking the two participating coding sequences (**Figure 2A and 2B**) The RSSs contain conserved palindromic heptamer (CACAGTG) and an AT-rich nonamer (ACAAAACC), separated by 12 or 23 nucleotides of a less-conserved spacer sequence. The nucleotide sequence of the RSS may vary, however, the gene recombination can (normally) occur only between genes flanked by the RSS segments, and it is only efficient when it takes place between RSSs with different space lengths, this is also known as the “12/23 rule”. In the recombination of T-cell receptor beta and delta loci, additional spatial restrictions apply, so-called “beyond 12/23 restriction”^{68,69}. The RSSs are limiting sequence structures required for V(D)J recombination; recombination on artificial substrates can be successfully achieved *in vitro* and *in vivo* when the substrates are flanked by canonical RSSs^{70,71}. The orientation of RSS also determines if the joining of the coding segments proceeds by inversion or by deletion of the intervening sequence⁷².

**Figure 2.**

(A) Schematic representation of DNA cleavage process during V(D)J recombination. RAG1 and RAG2, assisted by high-mobility group proteins (HMGB), binds the V(D)J segments (here represented by the yellow/purple box) at recombination signal sequences (RSS) (represented by the yellow/purple triangles). Next, a synapse is formed and nicked by the RAG1/2 at the RSS. The cleaved DNA is then repaired in the process of non-homologous end joining (NHEJ), leading to the formation of a coding joint (the recombines loci) and a formation of a signal joint, also called the excised signal circle “ESC” (the intervening loci) (B) A more detailed schematic representation of the molecular mechanism of V(D)J recombination. RAG1/2 recombinase introduces a nick on one DNA strand. Subsequently, the free -OH group, created by the nick, attacks the other DNA strand by transesterification, leading to the formation of a break at the other DNA strand, which ultimately creates a double-stranded DNA break (DSB). A hairpin is formed at the broken end, and the Ku70 and Ku80 bind and stabilize the loose DNA end, they also attract other proteins involved in the DNA repair process. To resolve the DSB, first, the hairpin is opened by Artemis, which in the presence of DNA-dependent protein kinase catalytic subunit (DNA-PKcs) acts as an endonuclease. Upon hairpin opening, the shorter DNA strand is extended by the addition of palindromic nucleotides (P-nucleotides) at the coding end, and the terminal deoxynucleotidyl transferase (TdT) further diversifies the junction by catalyzing the addition of non-templated nucleotides (N-nucleotides). The ends are filled by the Polymerase X family of polymerases (Pol μ and Pol λ) and finally, the broken DNA is sealed by Ligase IV/XRCC4. Created with BioRender.com

More detailed studies of the initiation of V(D)J recombination revealed that DNA melting of the conserved RSS heptamer proceeds the nicking and suggested that the conservation of the heptamer is determined by its ability to unwind at CAC/GTG sequences⁷³. Subsequently, trans-esterification takes place during which the nicked 3'OH of the coding strand invades the opposite DNA strand, creating a DSB, which contains a closed hairpin at the coding end and a blunt 5'RSS end (signal end). RAG1 and RAG2 are supported by high-mobility group proteins belonging to the HMG-box family (HMGB1 and HMGB2), which facilitate the association of two signal ends. The HMG proteins interact with the nonamer-binding domain of RAG1 even in the absence of DNA, amplifying its natural DNA-binding activity⁷⁴. Following the DNA cutting, Ku70 (also known as X-ray repair cross-complementing group 5 or XRCC5) and Ku80 (also known as X-ray repair cross-complementing group 6 or XRCC6) heterodimerize and bind the broken DNA ends and attract DNA-dependent protein kinase catalytic subunit (DNA-PKcs), which controls the interaction of the broken DNA ends. The Ku70/Ku80 heterodimer also attracts other factors containing Ku-binding motifs^{75,76}. Even though they form a heterodimer, striking differences in their mutant phenotypes have been observed, while the *ku80*^{-/-} mice were reported to show early aging signs without the increased incidence of cancer, the *ku70*^{-/-} mice exhibited defective B-cell maturation and high incidence of thymic lymphomas⁷⁷. Silencing of Ku70 in the Jurkat T-cell leukemia cell line resulted in accumulation of DSBs, cell cycle arrest, and increased apoptosis as a consequence of the impairment of the DNA repair pathways by the Ku70 deficiency⁷⁸.

Next, from the four broken DNA ends two are covalently sealed forming a hairpin (termed "coding end"), and the other two are blunt DNA ends (termed "signal ends"). For this reaction no external energy is required, the necessary energy is derived from the DNA breakage. The binding of RAG1/2 complex to the DNA does not form a covalent complex and while the nicking occurs within minutes, the hairpinning might take several hours⁷⁹. Subsequently, the hairpins must first be opened in order to proceed with the joining and repair of the broken DNA. A characteristic feature of V(D)J recombination is the asymmetric processing of the signal and coding end. The blunt-ended signal ends can directly be ligated with almost no processing, while the coding ends must first undergo further processing, such as small deletions or small insertions^{80,81}. In the process of V(D)J recombination, Artemis is a nuclease with an indispensable role in resolving and repairing the DSBs. Artemis exhibits an inherent 5'-3'exonuclease activity while upon an association with DNA-PKcs, Artemis acts as a 5'-3'endonuclease. The hairpin is opened asymmetrically on the coding end, creating a shorter and a longer strand. The shorter strand is extended by the addition of nucleotides complementary to the longer strand, giving rise to the insertion of palindromic nucleotides (P-nucleotides) at the coding end. These are never observed at the signal end. In addition, the single-strand extensions increase the chances of loss of nucleotides from the coding end, thereby further increasing the diversity of the

antigen-binding sites⁸². In addition, the terminal deoxynucleotidyl transferase (TdT) further augments the diversity of the junctional sequences by catalyzing the addition of the non-templated nucleotides (N-nucleotides) to the coding ends. This process of junctional diversification can potentially expand the diversity from around 10^6 up to 10^{11} possible combinations⁸³. Typically, the ends are filled in by the Pol X family of polymerases, namely Pol μ and Pol λ . Defects in these polymerases in mice resulted in shorter *Igh* and *Igl D* to J and V to DJ junctions. Next, the Ligase IV/XRCC4 complex ligates the processed ends. This DNA repair pathway is known as classical non-homologous end joining (c-NHEJ) where Ku70, Ku80, Artemis, XRCC4, and DNA Ligase IV are considered to be indispensable for this process, conserved throughout the evolution in different cell types⁸⁴. Finally, the DNA between the two recombining segments is removed and covalently sealed at the signal ends, forming a so-called excised signal circle (ESC). It has been estimated that the production of every functional antigen receptor gene can generate up to 10 ESCs, depending on the level of non-productive recombinations. ESCs are non-replicative elements that are likely to be lost or diluted in the subsequent cell divisions^{85,86}.

Aberrant V(D)J recombination and aberrant RAG mistargeting

Aberrant V(D)J recombination

Next to the typical outcome of the V(D)J recombination – the formation of the coding and the signal ends, alternative outcomes have been reported. For instance, formation of so-called “hybrid joints” (HJ) when the coding end of one exon is joined to the signal end of another cleaved exon. Such events can occur in a small percentage of murine and human B cells. HJs do not contribute to the repertoire diversity and their role in oncogenic transformation remains inconclusive⁸⁷. Increased formation of hybrid joints was observed in mice harboring inactivating mutation in Nijmegen breakage syndrome 1 protein (NBS1). NBS1 is part of the MRE11-RAD50-NBS1 complex (MRN), which plays a crucial role in DNA repair. The NBS1 mutation was shown to promote DNA repair through the alternative NHEJ pathway, known for its error-prone nature, often leading to small insertions or deletions⁸⁸. In mice overexpressing coreRAG1 (cRAG1) and coreRAG2 (cRAG2) proteins, extremely high frequencies of HJ formation were observed as compared to cells derived from mice overexpressing full-length RAG1 and RAG2, suggesting that the non-core RAG regions suppress HJ formation under physiological conditions. In addition, leukemia that the mice expressing cRAG1 and cRAG2 developed was more aggressive and showed more genomic instability, as judged by the percentage of γ H2AX-positive cells, which is a marker for DSBs⁸⁹. However, the formation of HJ in endogenous wildtype/unmanipulated context seems to be rather rare.

In other cases, the original pairs of coding and signal, cleaved by RAGs, are rejoined leading to a formation of “open-shut joints”. These are rather difficult to detect if there are

no further modifications of the joint⁹⁰. An *in vitro* cell-free RAG activity assay showed that the truncated but catalytically active forms of RAG easily catalyzed the formation of hybrid joints and open-shut joints suggesting that the full-length forms repress their formation. The *in vitro* transposition activity of full-length RAG2 was dramatically reduced as opposed to the full-length RAG1 transposition activity⁹¹.

Several studies have shown that the ESCs do not seem to be as inert as initially thought, and in fact, in various *in vitro* assays they display the capacity to re-integrate elsewhere in the genome. However, it is supposed that the *in vivo* threat to the integrity of the genome caused by RAG-mediated transposition is rather limited. Only a few *in vivo* RAG-mediated transposition events have been described to date, and the evidence linking leukemia or lymphoma cases to RAG-mediated transposition events remains inconclusive^{86,92-95}. The RAG/ESC complex could, so far only theoretically, catalyse the formation of DSBs as it still contains two RSSs (**Figure 2A**). It has been observed that upon cleavage of the ESC is opened at the RSS but the RAG1/2, which is still bound to the ESC, is able to introduce DSBs at the next RSS, a process termed as “cut-and-run”. Recently, a next-generation genome-wide sequencing of the leukemic B cells revealed similarities between the “cut-and-run” breakpoints and the breakpoints observed in B-cell leukemia that harbor the *ETV6/RUNX1* chromosomal translocation^{96,97}. These studies argue that the lack of evidence is caused by the limitations of the previously used techniques and suggest that the advances in the next-generation sequencing techniques of the whole genome could provide a much better resolution of the genomic events, and thus in the future deliver the missing evidence of RAG-mediated ESCs re-integration in lymphoid malignancies^{98,99}.

RAG mistargeting

Sequences that resemble RSS, termed cryptic RSS (cRSS), were shown to be very abundant in the vertebrate genome, with a remarkable estimate of one cRSS per each 600bp¹⁰⁰. A study employing genome-wide chromatin immunoprecipitation (ChIP) of RAG1 and RAG2 in mouse pre-B cells, followed by next-generation sequencing (ChIP-seq), clearly demonstrated that RAG1 and RAG2 binding in the genome is not solely limited to the *Ig* loci, as around 3400 RAG1 and around 18300 RAG2 binding sites were identified throughout the genome of mouse pre-B cells. However, the presence of RSS alone seems to be a poor indicator of RAG1-binding sites; the heptamer and cRSS sequences were even found to be depleted from the RAG1-binding sites. Also, in this study no translocations were detected of the selected examples of genes with high content of cRSS in their proximity, concluding that RAG1/2 binding outside of the *Ig/Tcr* loci only rarely results in translocation events⁷¹. On the other hand, the RAG2 binding throughout the lymphocyte genome coincided significantly with regions containing high levels of histone H3 trimethylated at lysine 4 (H3K4me3)^{101,102}, which was not entirely surprising considering that the PHD finger of RAG2 was shown to specifically recognize and bind H3K4me3 in mammalian cells. Mutations

that abrogate RAG2's ability to bind H3K4me3 severely impaired V(D)J recombination *in vivo*⁶¹. Furthermore, the junction analysis of mice bearing RAG2 with truncated C-terminus showed the formation of genomic lesions in the proximity of cRSSs, including several oncogenes¹⁰³, and similar lesions have also been observed in human pre-B cells derived from B-ALL patients¹⁰⁴. Next to the lesions observed in the proximity of the individual cRSS, the genomic events can also take place between pairs of cRSS. This may result in a chromosome translocation as seen in several cases of human pre-T cells derived from patients suffering from T-cell acute lymphoblastic leukemia (T-ALL), bearing recombination between TCR gene segments and the Ikaros locus (*Ikzf1*)¹⁰⁵, neurogenic locus notch homolog protein 1 (*Notch1*)¹⁰⁶, phosphatase and tensin homolog (*PTEN*)¹⁰⁷ or stem cell leukemia (SCL)/ SCL interrupting locus (*SIL*)^{108,109}.

Besides being a sequence-specific recombinase, RAG1/2 has also been shown to recognize specific DNA structures and cleave DNA even without the presence of RSS motifs, thus acting as a structure-specific nuclease, cleaving, for instance, heterologous loops of G-quadruplexes^{110,111}. For example, RAG1/2 shows 3'-flap endonuclease activity that is able to remove single-strand (ss) extensions from branched DNA¹¹². In follicular lymphoma, non-B DNA structures were also identified around the *BCL2* major breakpoint region (Mbr) of the t(14;18) translocation, where the *BCL2* gene is juxtaposed to the *Igh* locus. RAG complex was shown to bind and nick at non-B DNA structures in the proximity of *BCL2* Mbr, resulting in double-strand breaks *in vitro*, thus demonstrating the transposase activity of RAG1/2¹¹³. Simple repeat sequences have also been shown to assume non-B DNA structures and become a RAG1/2 target. For instance, CA-repeats were shown to function as a type of cryptic RSS (cRSS) as RAG1/2 was able to cleave such structures¹¹⁴. In addition, the GC-rich regions are also able to adopt structures such as hairpins, cruciform or triple-stranded DNA, and the GC-rich motif 5'-GCCGCCGGCG-3' was identified as RAG1/2 transposition hotspot¹¹⁵. In our study (manuscript under consideration) we identified RAG1/2-dependent DSBs on genome-wide scale by using NBS1 ChIP-seq. Though the RAG1/2 DSBs were clearly enriched at Ig light chain regions, where they associated with RSS motifs as expected, the majority of the RAG-dependent DNA breaks were found outside of the *Ig* loci and showed no appreciable association with cRSSs. Interestingly, simple repeat sequences such as GA and CA repeats, but also GC-rich motifs were found to be enriched in the 500-1000bp proximity of the RAG1/2-dependent DSBs, further underscoring the propensity of the repeat regions to become RAG1/2 target. Next to aberrant RAG1/2 targeting in developing lymphocytes, the aberrant or persistent expression of RAG1/2 also represents a significant threat to genome integrity, various aspects of which are outlined in the next chapters.

RAGulation: the intricate regulation of RAG expression and activity

RAG1 and RAG2 proteins are regulated on multiple levels. In the next paragraphs, various levels of RAG regulation are outlined.

Cell cycle and post-translational regulation

The cell cycle is an important regulator of RAG2 expression, ensuring that RAG2 is only expressed in the G0/G1 phase, whereas it is almost undetectable in the S and the G2/M phases of the cell cycle. The RAG2 availability is modified by cyclin-dependent kinases (CDK), which initiate the rapid proteasomal degradation when entering the S phase. RAG2 is phosphorylated at Thr-490, which is a consensus substrate sequence for CDK2, CDK2, and CDK4, providing the conserved degradation signal¹¹⁶. Consequently, V(D)J recombination occurs exclusively in the G1 phase. In contrast to the cell cycle-dependent oscillation of RAG2, the levels of RAG1 remain rather consistent throughout the cell cycle¹¹⁷.

Though not cell-cycle-dependent, post-translational modifications of RAG1 have also been described. The N-terminus of RAG1 contains a functional E3 ubiquitin ligase RING domain¹¹⁸. This domain has been shown to be involved in the ubiquitination of histone H3 as well as RAG1 itself. Recently, it was found that mouse mutants carrying the P326G mutation in the RAG1 RING domain accumulate RAG1 protein, likely due to the impaired ability to degrade RAG1 through autoubiquitylation^{119,120}. Interestingly, we observed that DNA damage negatively impacts the protein stability of RAG1. Specifically, in human pre-B cell line harboring BCR-ABL1 translocation, co-treatment with the DNA damaging agent neocarzinostatin (NCS) and the protein synthesis inhibitor cycloheximide (CHX) resulted in a shorter RAG1 half-life compared to treatment with CHX alone, possibly due altered post-translational modification of RAG1¹²¹.

Spatial and temporal regulation

The subcellular spatial regulation of RAG proteins has been shown to be an important regulator of V(D)J recombination. In T cells, the different regions of T-cell receptor b (*Tcrb*) were shown to interact with the nuclear lamina and at the same time, the RAG2 abundance in the nuclear periphery was found to be decreased. The spatial distributions of RAG2 and the *Tcrb* locus may thus be involved in the regulation of V(D)J recombination by limiting accessibility, and may even be one of the mechanisms enforcing allelic exclusion¹²². Not only RAG2 but also RAG1 has been shown to be spatially regulated; in mouse pre-B cells RAG1 localized with nucleolar markers and disruption of nucleoli lead to increased V(D)J recombination activity. The nucleolar sequestration of RAG1, controlled by N-terminal regions of RAG1, contributes to the regulation of the V(D)J recombination activity¹²³. In addition, PAX5, known mostly for being an important B-cell commitment factor controlling transcription, also regulates the spatial positioning of chromatin towards the central nucleus regions

ensuring active is in an extended state and promotes *Ig* locus contraction¹²⁴. CCCTC-binding factor (CTCF) is a zinc-finger protein with various functions in transcriptional regulation, was also shown to influence chromosomal contacts genome-wide and on the *Ig* locus through CTCF-binding elements (CBEs), a 14bp conserved regions within the *Ig* loci. Deletion of CTCF hampers the B-cell maturation and arrests the cell at pre-B cell stage^{125,126}.

Protein aggregation

Protein aggregation and condensation were proposed to be an additional layer of regulation of RAG expression and activity. In the absence of RAG2, the human RAG1 has been shown to form aggregates scattered throughout the nucleus. RAG2 by itself does not aggregate but interacts with RAG1 aggregates. The disruption of the RAG1 oligomers leads to initiation of V(D)J recombination, as only the dimeric RAG1 form has the ability to interact with RAG2 and RSS and thus exhibits the catalytic activity¹²⁷. In addition, temperature plays also a role in the self-association properties of RAG1¹²⁸.

Transcriptional regulation

Multiple cis-regulatory elements have been identified in the RAG locus, which restrict the *Rag* expression during the development of B and T cells. Interestingly, these regulatory elements differ in B and the T cells. While the murine and human *Rag1* promoters were found to be active in lymphoid and non-lymphoid cell lines,¹²⁹ the Alt group showed that the 2-kb and 2-7kb 5' regions upstream of the *Rag2* promoter can independently drive the development of murine B cells but not T cells.¹³⁰ Multiple transcription factors binding both promoters were identified, including PAX5, specificity protein1 (SP1), lymphoid enhancer-binding factor-1 (LEF1), myoblastosis viral oncogene homolog (c-MYB), nuclear transcription factor Y (NF-Y), the longest isoform of B-cell lymphoma/leukemia 11A (BCL11A-XL) and Myc-associated zinc finger protein (MAZ)¹³¹⁻¹³⁵. Similar to the previous finding, the Muraguchi group identified, using a gene reporter assay, two enhancer elements in the 5'-upstream region of *Rag2*, one of which (D3) was not active in CD4⁺CD8⁺ or CD4⁺CD8⁻ thymocytes, but only in CD4⁻CD8⁻ lymphocytes, specifically in B220⁺IgM⁻, but not in B220⁺IgM⁺, cells in the bone marrow. This suggests a strict lineage and developmental stage-specific regulation of *Rag2* by the cis-regulatory enhancer elements¹³⁶.

Erag was discovered to be a *bona fide* B cell-specific *Rag* enhancer, identified ~22kb upstream from the *Rag2* promoter. Deletion of *Erag* results in a dramatic decrease of *Rag* expression and a partial block in the development of B cells, but not T cells¹³⁷. Multiple transcription factors were shown to bind the *Erag* enhancer and positively regulate its activity such as forkhead box O1 (FOXO1), forkhead box P1 (FOXP1), and E2A¹³⁸. Loss of FOXP1 transcription resulted in severe impairment of B-cell development and function¹³⁹. Decreased FOXO1 protein levels diminished the transcription of the *Rag* locus, impaired development and receptor editing of primary bone-marrow B-cells¹⁴⁰. The *Erag* is nega-

tively regulated by Gfi1b, Ebf1, and c-Myb^{141,142}. The chromosomal architecture of the *Rag* locus is further summarized in great detail elsewhere¹⁴³.

Signaling pathways controlling RAG expression

The many signaling pathways and their interplay at the different stages of B-cell development are still the subject of active investigations. In this section, important signaling pathways that affect Rag expression are summarized, amongst which are IL7 receptor (IL7R) signaling, pre-B cell receptor (pre-BCR) signaling, and B-cell receptor (BCR) signaling.

IL7R signaling

Developing B cells in the bone marrow receive proliferative signals from stromal cells. Prior to the gene recombination, the processes in early pro-B cells are controlled mainly by the IL7 receptor (IL7R) and two tyrosine kinase receptors: c-kit and Flt3, activating downstream signaling pathways that are interconnected. The binding of stem cell factor present on BM stromal cells causes dimerization and transphosphorylation of the c-kit receptor, which leads to an activation of various downstream pathways, including phosphatidylinositol-3 kinase (PI3K) and mitogen-activated protein kinase (MAPK), which are signaling pathways that promote survival and proliferation¹⁴⁴. Similar to c-kit, Flt3 also dimerizes upon binding of the Flt3-ligand (Flt3L) and activates Ras and PI3K pathways, further stimulating the proliferation of developing B cells¹⁴⁵. Upon binding of IL7 to the IL7 α chain, the IL7 α and IL7 γ subunits heterodimerize, which results in an activation and transmission of the signals through pathways including the Janus kinase/signal transducer and activator of transcription (JAK/STAT) and the PI3K/AKT pathway. In developing B cells, the PI3K/AKT activation inhibits forkhead box O1 (FOXO1) and forkhead box O3 (FOXO3) transcription factors through AKT-mediated phosphorylation,^{146,147} which causes their nuclear export, sequestration, or degradation.¹⁴⁸ B-cell specific deletion of *Foxo1* using the conditional CD19-Cre mouse model showed only a partial block in B-cell development, suggesting a certain degree of redundancy with other transcription factors. However, the peripheral lymphoid organs from these mice clearly showed an aberrant representation of B-cell subsets, and even B220⁺ B cells without surface Ig were detected^{147,149}. Similarly, FOXO3a deficient mouse shows a lower number of pre-B cells but not a complete block¹⁴⁶.

IL7R activation triggers association of JAK1 with JAK3. The activated tyrosine kinases phosphorylate in return the α -subunit of IL7R, which creates binding sites for STAT protein. Amongst the 7 different STAT proteins, the STAT5a and STAT5b isoforms mediate the IL7R specifically in developing lymphocytes¹⁵⁰. STAT5 conveys the survival signals in developing B cells by activating pro-survival factors such as B-cell lymphoma 2 (Bcl2), B-cell lymphoma extra-large (Bcl-xl), and myeloid cell leukemia sequence 1 (Mcl1)¹⁵¹. In addition, STAT5 increases the expression of *Ccnd3*, encoding for Cyclin D3, which drives prolifera-

tion. The proliferative signals resulting from IL7R/STAT5 activation, mediated through the MAPK pathway, result in FOXO1 inhibition, which also keeps the expression of *Rag1* and *Rag2* low¹⁵². In addition, the extracellular signal-regulated kinase (ERK)/ mitogen-activated protein kinase (MAPK) pathway also regulates E2A (also known as TCF3), which is a RAG transcription factor and a regulator of *Ig* light chain accessibility^{153,154}.

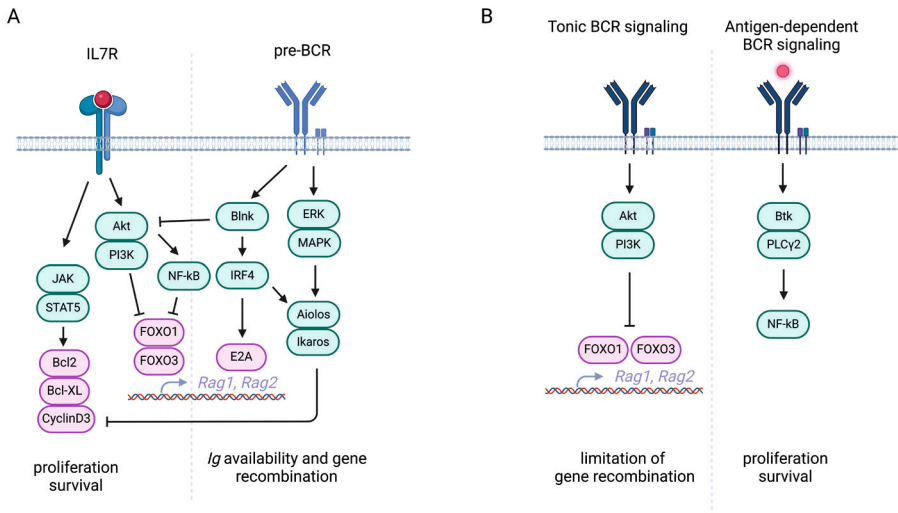


Figure 3.

(A) Schematic representation of the interplay between IL7R signaling and pre-BCR signaling. The signals from IL7R activate PI3K/AKT, which on the one hand negatively regulates Rag1/2 transcription factor FOXO1, and on the other hand activates NF-κB, which in turn further suppresses RAG expression. Moreover, the IL7 signals activate the JAK/STAT5 pathway, which in turn leads to the upregulation of anti-apoptotic proteins, such as Bcl2 or Bcl-XL, but also to the upregulation of CyclinD3 which drives cell proliferation. The pre-BCR counteracts many of the IL7R-driven signals. For instance, AKT signaling is inhibited through pre-BCR-driven B-cell linker (BLNK) upregulation. BLNK also drives the expression of interferon regulatory factor 4 (IRF4), which helps to counteract the IL7R-mediated proliferative signals through Aiolos and Ikaros. IRF4 also increases Ig light chain availability and promotes the binding of RAG1/2 transcription factor E2A to the RAG promoter. The pre-BCR driven extracellular signal-regulated kinase (ERK) and mitogen-activated protein kinase (MAPK) signals further aid to counteract the IL7R proliferative and pro-survival signals. **(B)** Schematic representation of BCR-mediated signals regulating RAG expression. Tonic BCR signaling activates the PI3K/AKT pathway, leading to the downregulation of the RAG1/2 transcription factors FOXO1 and FOXO3. Antigen-dependent BCR signaling activates NF-κB, which conveys the pro-survival and proliferation signals. Created with BioRender.com

pre-BCR signaling

Following the successful V- to (D)J- recombination at the heavy chain (HC), resulting in the expression of μ HC, giving rise to the pre-B cell receptor (pre-BCR), composed of μ HC

homodimer, two surrogate light chains (SLC) and the Ig α and Ig β units which possess the signaling capacity¹⁵⁵. At this stage, the rapid clonal expansion comes to a halt, mainly because of the cell-cycle arrest, which is required for the *Rag1/2* expression and *Ig* gene recombination. The pre-BCR signal promotes the expansion of large pre-B cells, which remain dependent on IL7 signaling. The IL7R-induced STAT5 signaling also inhibits the Ig κ recombination, presumably through direct binding to Ig κ intron enhancer^{156,157}. Therefore, in order to initiate Ig κ or Ig λ recombination, IL7 signaling must attenuate so that the large pre-B cells can escape their proliferative state. The crosstalk between the IL7R signaling and the pre-BCR signaling ensures successful progression of B-cell development and the maintenance of genome integrity by ensuring that proliferation and gene recombination are mutually exclusive.

Importantly, pre-BCR signaling has the ability to counteract the IL7-dependent proliferation of pre-B cells through B-cell linker (BLNK)-mediated inhibition of the PI3K-AKT pathway¹⁵⁸⁻¹⁶⁰. The rapid clonal expansion is limited by the pre-BCR-driven RAS-ERK signaling pathway that operates to diminish proliferation. This occurs through the activation of the developmentally restricted transcription factor Aiolos (an Ikaros family member encoded by *Ikzf3*¹⁶¹). Aiolos then suppresses the transcription of *Myc* and *Cyclin D3*. In addition, in response to pre-BCR signaling, BLNK also mediates upregulation of interferon regulatory factor 4 (IRF4), which on the one hand further enhances the expression of Ikaros and Aiolos, aiding to limit the cell proliferation, and on the other hand, promotes light chain rearrangement by attenuating the IL7 signaling and promoting the binding of E2A to *Rag* promoter^{160,162}.

BCR signaling

BCR serves as a regulator controlling the initial stages of development within the bone marrow. Even in the absence of an antigen, in resting B lymphocytes, there is an observable low-level phosphorylation of signaling intermediates, so-called "tonic signaling", driven by the surface expression of BCR. The tonic BCR signaling is crucial for cell survival and its deletion results in loss of mature B cells¹⁶³. These survival signals are mediated primarily through PI3K: while constitutive activity of nuclear factor kappa B (NF- κ B) or MAPK or overexpression of BCL2 failed to prevent the loss of mature B cells in B cells with conditionally deleted BCR (BCR^{neg} cells), the conditional PI3K signaling was sufficient to sustain the survival of mature B cells in BCR^{neg} cells¹⁶⁴. Following the discovery of AKT being the effector of PI3K¹⁶⁵, it has been demonstrated that Akt (also known as protein kinase B or PKB) is recruited to the membrane and activated downstream of BCR¹⁶⁶. In immature B cells with competent BCR the tonic BCR-signaling is low, which was shown to turn off RAG expression through the downstream effectors of PI3K: AKT, but also phospholipase C (PLC) γ 2 (PLC γ) and Bruton's tyrosine kinase (BTK)^{140,167,168} and in this way thought to protect the stability of the genome in developing B cells against excessive RAG1/2 ac-

tivity. Interestingly, it has also been shown that in Btk/Slp65-deficient mouse pre-B cells, malignancies can also arise independently from V(D)J recombination¹⁶⁹.

Additionally, BCR signaling plays a crucial role in initiating processes such as clonal deletion and receptor editing, which are essential for removing autoreactive B cells. As opposed to the cells with competent BCRs, the immature B cells with a self-reactive BCR lacking CD19, which functions as a BCR co-receptor, show attenuated PI3K activation. Also, the self-reactive immature B cells show increased tonic BCR signaling leading to re-expression of RAGs in the effort of the self-reactive B cell to attempt to “edit” the autoreactive BCR and escape apoptosis²⁴. B cells undergoing receptor editing internalize the BCR, which leads to a decrease in PI3K/AKT signaling¹⁷⁰. Already in the 1980s, the notion was put forward that NF- κ B is a critical trans-acting factor that mediates the B-cell-specific expression of *Ig κ* genes¹⁷¹. The NF- κ B transcription factor family consists of five proteins: RelA (also known as p65), RelB, c-Rel, p100, and p150. The p100 and p150 are precursors, which after proteolysis produce p50 and p52 subunits¹⁷². The p50 subunit was shown to suppress *Rag1* and *Rag2* expression in mice. Members of NF- κ B were shown to associate with the RAG locus and this transcriptional regulation was demonstrated to be limiting for *IgI* gene recombination¹⁷³. Another study showed that crosslinking of the BCR by self-antigen signals through NF- κ B drove the IRF4 expression and thereby increased the accessibility of *IgI* to RAG1/2 endonuclease and enabling receptor editing¹⁶².

Besides the role in receptor editing and allelic exclusion, the NF- κ B signaling pathway was shown to have an important role in RAG1/2 regulation and B-cell development. Single-gene knock-in/knock-out experiments, involving the manipulation of a single gene within the NF- κ B pathway occasionally yielded conflicting outcomes likely attributed to redundancies existing between the classical and alternative pathways. However, even more sophisticated mouse models targeting both pathways or simultaneously deleting several NF- κ B components, did not always provide consistent results, all of which make studying NF- κ B a challenging task, as illustrated by the following examples: mice expressing a dominant negative form of I κ B α showed reduced numbers of pre-B cells, probably due to the altered expression of PAX5 and IRF4¹⁷⁴. The deletion of p100 led to the activation of the alternative NF- κ B pathway through a process involving the liberation of NF- κ B dimers. Normally, p100 functions as an inhibitor of the alternative pathway by sequestering NF- κ B dimers, particularly RelB/p52 complexes, in an inactive form within the cytoplasm. However, upon deletion of p100, this inhibition is alleviated. Such constitutive activation of the alternative NF- κ B through p100 deletion showed arrested B-cell development at pro-B cell stage¹⁷⁵. However, in other studies, the constitutive activation of the alternative NF- κ B pathway¹⁷⁶ or the classical NF- κ B pathway¹⁷⁷ showed no impact on B-cell development in bone marrow. TNF receptor-associated factors 2 and 3 (TRAF2 and TRAF3) participate in the NF- κ B pathway, namely, they inhibit the alternative NF- κ B pathway by targeting NF- κ B-inducing kinase (NIK) for ubiquitin-mediated degradation and thereby preventing the p100

precursor from forming p52¹⁷⁸. A B-cell specific TRAF2 and TRAF3 double deficiency in mice caused B cells to be more resistant to DNA damage-induced apoptosis, probably due to cellular inhibitor of apoptosis 2 (cIAP2) and X-linked inhibitor of apoptosis (XIAP), which in turn attenuates caspase-3 activation. However, in this model, apart from oligoclonal B-cell repertoire, no evidence was found that TRAF2/3 double deficiency would induce genomic instability in primary B cells¹⁷⁹. Another more recent study generated mice that have either or both NF- κ B pathways constitutively active as of the early pro-B cell stage, by crossing the TRAF3 conditional knock-out mice (Traf3^{flx/flx}) and the I κ B-kinase 2 (IKK2) transgenic mice (IKK2^{ca}) mice, which lead to a systemic loss of B cells¹⁸⁰. In one of our studies, we demonstrated that in murine cycling pre-B cells, NF- κ B signaling represses RAG expression through the inhibition of CDK4 and FOXO1 and thereby protects pre-B cells from RAG-induced genomic instability. Interestingly, we showed that AKT signaling at this stage feeds into the NF- κ B/FOXO1 axis and potentiates its inhibitory effect on RAG expression. Furthermore, NF- κ B and AKT also inhibit RAG expression in primary human pre-B acute lymphoblastic leukemia cells from patients. Therefore, targeting parts of this regulatory pathway with new therapies could accidentally increase the risk of malignant pre-B cell transformation by allowing uncontrolled RAG expression¹⁸¹.

The regulatory function of RAG-induced DSBs

Throughout their development, B cells have to repeatedly deal damage to their genetic material. Next to homeostatic sources of DNA damage, B cells sustain DNA damage as a result of V(D)J recombination during development and as a result of CSR and SHM upon activation and antigen encounter. Though DNA breaks can have devastating effects on genome integrity, they can also be exploited for precise regulation of various biological processes or decision-making activities.

The DSBs trigger a conserved DNA damage response (DDR) in order to repair the genetic lesions, such a response is shared by most cell types. Sometimes, the activation of DDR kinases results in cell-type specific processes that do not have a known function in DNA damage repair, but instead seem to regulate other processes¹⁸². There are 2 central kinases in DDR: ATM kinase and ATM- and Rad3-related kinase (ATR). ATM is recruited to the sites containing DSBs upon MRN activation¹⁸³. ATR primarily responds to a broad spectrum of DNA damage lesions, including single-stranded DNA. Both ATM and ATR are essential for checkpoint responses to the DSBs. Upon binding to the MRN complex, ATM activation takes place through autophosphorylation, which subsequently activates the heterodimer of KU70 (XRCC6) and KU80 (XRCC5) and other kinases involved in DNA repair^{184,185}.

The DSBs-induced phosphorylation of ATM at Ser¹⁹⁸¹ subsequently initiates phosphorylation of checkpoint kinase 2 (Chk2) at Thr68. Once activated, Chk2 phosphorylates more than 20 different proteins, mainly involved in cell cycle progression and apoptosis, such as p53,

MDM4, and E2F1^{186–188}. The Chk2-mediated stabilization of p53 drives the transcription of p21^{CIP} and halts the progression of the cell cycle through inhibition of CDKs¹⁸⁹. In developing B cells, the RAG1/2-generated DSBs were shown to activate apoptotic factors that promote cell survival to enable additional V(D)J recombination events, for instance, Igk-derived DSBs were shown to promote p53-mediated activation of the pro-apoptotic BAX protein as well as the ATM-mediated up-regulation of the pro-survival protein Pim2¹⁹⁰. The balance between the pro-apoptotic and the pro-survival signals determines the outcome.

Our lab demonstrated that in response to external or RAG-derived DSBs, several related negative feedback mechanisms are triggered that limit the availability of RAG1 and RAG2, thereby dampening the V(D)J recombination activity, and thus preventing further genomic instability. The activation of ATM, as a response to external, but also to the RAG-created DNA breaks, resulted in the rapid downregulation of RAG1 and RAG2 expression. This downregulation was shown to be mediated on one hand through the ATM-dependent release of FOXO1 from binding to *Erag*, and on the other hand by ATM-dependent reduction of FOXO1 levels. Strikingly, PI3K/AKT did not show any involvement in the DNA damage-mediated downregulation of RAG1/2, suggesting under the genotoxic stress conditions, this pathway does not regulate RAG expression, unlike observed under the normal, non-stressed conditions¹²¹. In addition, our work also indicates that the ATM-mediated activation of p53 constitutes an additional regulatory circuit, resulting in decrease of FOXP1 levels, possibly through the p53-dependent activation of microRNA-34a (miR-34a), which targets and downregulates FOXP1 expression, and thereby limits the expression of RAGs in response to external and RAG-mediated DSBs (Ochodnicka-Mackovicova et al, manuscript under consideration). In this negative feedback regulation, the RAG-dependent DSBs limit themselves and protect the genomic stability of B cells from excessive RAG activity (**Figure 4**).

The RAG-induced DSBs introduced on one *Igk* allele suppress, through ATM signaling, RAG expression and thereby suppresses RAG-mediated cleavage on the other allele, contributing to Igk allelic exclusion. It was demonstrated that immature B cells from ATM-deficient mice demonstrated increased frequencies of bi-allelic cleavage at *Igh* and *Igl*. It was proposed that the activation of ATM results in the down-regulation of growth arrest and DNA damage-inducible alpha (GADD45 α), which subsequently represses its targets *Rag1* and *Rag2*^{236,191}. It has been proposed that in this way, the RAG activity creates a negative feedback loop limiting its own expression and protecting the genomic stability, though in our previous study, the genotoxic stress in mouse *v-Abl*-transformed pre-B cells did not confirm the ATM-dependent effect on the levels of GADD45 α ¹²¹.

In eukaryotic cells the DSB-prompted ATM activation initiates phosphorylation of the histone variant H2AX at Ser¹³⁹, giving rise to so-called γ H2AX. γ H2AX accumulates in the proximity of the DSBs and serves as a landing pad for other components of the DDR cascade¹⁹². In murine cells, γ H2AX promotes the hairpin processing by Artemis. In the absence

of γ H2AX, carboxy-terminal binding protein (CtBP)-interacting protein (CtIP) endonuclease takes over the hairpin opening and processing activities. Though CtIP can open the hairpin, in G1-phase lymphocytes the CtIP-generated joints are not efficiently processed by NHEJ. CtIP uses microhomologies to process the joints, which results in frequent chromosomal deletions. Thus, the DSBs-recruited γ H2AX ensures the maintenance of genomic integrity in the G1 phase¹⁹².

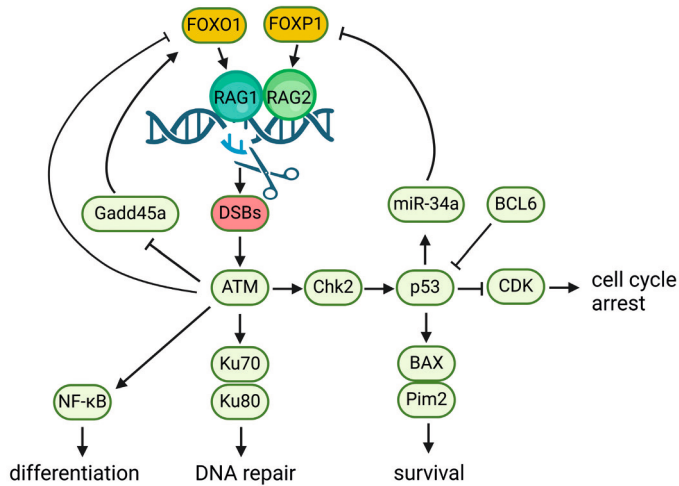


Figure 4.

Schematic depiction of B-cell-specific regulatory processes impinging on RAG expression triggered by the formation of DSBs. The formation of DSBs leads to autophosphorylation of the DNA damage sensor Ataxia-telangiectasia mutated (ATM). The activation of ATM triggers several negative feedback mechanisms that limit the expression of RAG1 and RAG2, such as the inhibition of FOXO1 and FOXP1 transcription factors either directly or through downstream intermediates. The ATM-driven stabilization of p53 drives the expression of miR-34a, which is a negative regulator of FOXP1. Next to the effect of DSBs on RAG expression, the activated ATM also triggers the DNA damage response, activates cell-cycle arrest, and, depending on the extent of the DNA damage, the pro-apoptotic or the pro-survival and differentiation signals. Created with BioRender.com

RAG: driver of lymphoid malignancies

Acute lymphoblastic leukemia (ALL) is the most common pediatric cancer in developed countries, accounting for 81% of childhood leukemias and one-third of all cancers diagnosed in children of age 0-14 years¹⁹³. ALL is characterized by the rapid proliferation of lymphoid progenitor cells. B-cell acute lymphoblastic leukemia (B-ALL) originates from abnormal progenitor B cells, while T-ALL originates from abnormal progenitor T cells. These malignant progenitor cells, immature lymphoblasts, do not mature properly and

instead, they accumulate in bone marrow, crowding out the normal cells. The presence of mutations, translocations, or other genomic abnormalities is a hallmark of ALL. There are several hypotheses regarding the underlying cause and mechanisms that give rise to B-ALL, including the so-called “2 hit theory” postulating that for the development of cancer, at least 2 different mutations are needed: suggests that two separate genetic mutations are necessary for the development of cancer. The first hit, often a dominantly inherited predisposition to cancer may entail a germline mutation. The second hit occurs when the other copy of the gene also becomes mutated, either through environmental factors (like exposure to carcinogens) or random errors in DNA replication. This second mutation is usually acquired later in life. This model helps explain why certain individuals with a hereditary predisposition to cancer may be more susceptible to developing the disease and why cancer development often involves multiple genetic alterations¹⁹⁴. The most prevalent chromosomal lesion in ALL is the t(12;21)(p13;q22) translocation, creating the *ETV6/RUNX1* fusion gene (also known as *TEL/AML1*)¹⁹⁵. This translocation is present in 25% of the childhood ALL cases¹⁹⁶. The detection of *ETV6/RUNX1* fusion gene presence in the neonatal blood suggests that the first event takes place *in utero*. Moreover, the *ETV6/RUNX1* fusion gene is present in 1-5% of newborns, but the actual incidence of *ETV6/RUNX1*⁺ B-ALL is much lower (0.0001%), suggesting that a secondary hit is needed for the malignant transformation and the development of clinically relevant B-ALL¹⁹⁷. The *ETV6/RUNX1* gene product was associated with increased levels of reactive oxygen species (ROS)¹⁹⁸. It has been proposed that the ROS-mediated formation of DSBs may be one of the sources of genomic instability, delivering the secondary hits¹⁹⁹. Because RAG1/2 is a source of DBSs in progenitor B cells, its dysregulation was also suspected to be a significant source of secondary mutations. Exome and whole-genome DNA sequencing of ALL cells carrying *ETV6/RUNX1* translocation revealed the presence of RSS motifs near the translocation breakpoints, as well as the presence of N-nucleotides at the junctions, a typical signature of RAG activity⁹⁷. Inactivating deletions in *PTEN* are detected in 8% of childhood T-ALL cases. The breakpoints in *PTEN* inactivation deletions were found to be flanked by cRSS and the presence of N-nucleotides inserted in between the breakpoints, implicating aberrant RAG1/2 activity^{107,200}. Besides the *ETV6/RUNX1*⁺ cytogenetic subgroup, hyperdiploid B-ALL cases revealed recurrent RAG-mediated copy number alterations (CNAs) in genes including *PAX5*, *IKZF1*, and *ETV6*. In addition, hyperdiploid B-ALL shows frequent mutations in receptor tyrosine kinase (RTK)-RAS pathways and mutations affecting histone modifiers²⁰¹. The BCR-ABL1 translocation, or the so-called Philadelphia chromosome-positive ALL (Ph⁺ALL), constitutes approximately 5% of childhood ALL cases and 20% of adult ALL cases²⁰². In adult cases of B-ALL carrying the BCR-ABL1 t(9;22) translocation, the presence of cRSS and N-nucleotides was reported in the breakpoint regions, as well as abundant RAG binding in the breakpoint proximity²⁰³.

The notion that there might be a causal relation between infectious diseases and the development of ALL is now more than 100 years old²⁰⁴. It has been observed that infants in highly sanitized environments in developed societies experienced delayed exposure to infections. As a result, when they did encounter these infections, their immune responses were prolonged and exaggerated, leading to significant collateral damage. On the other hand, early exposure to common infections reduced this risk. Systemic introduction of vaccination programs in early childhood significantly decreased the risk of childhood ALL, presumably by reducing the chronic infections and the responses they instigate^{205,206}. Indeed, repeated exposure to inflammatory stimuli has been shown to drive RAG1/2 and AID, which did not only enhanced the genetic diversity within B cells but also facilitated the acquisition of genetic abnormalities, thus promoting the clonal evolution toward leukemia²⁰². For instance, the detailed analysis of the breakpoints provides evidence that the chromosomal recombination in human B-cell malignancies may originate from the collaboration between RAG1/2 and AID^{207,208}, though the expression of these 2 enzymes was thought to be strictly segregated and confined to specific developmental stages of the B-cell development¹⁰. Taken together, all these findings underscore the potential threat that V(D)J recombination, SHM, and CSR pose to B cells throughout their development and maturation and the need for tight regulation of these processes.

Concluding remarks and future perspectives

Next to the conceptual breakthroughs in the topic of gene recombination from several decades ago, also in recent years, important discoveries have been made, especially adding to our understanding of RAG1/2 binding, targeting, and regulation. It became clear that the gene recombination system evolved in a way that allows for the generation of a staggering diversity in antigen receptors, at the expense of the risk imposed by the generation and repair of DNA breaks. In lymphocytes these risks are mitigated by various regulatory mechanisms, protecting the stability of their genome.

The DNA breaks generated by V(D)J recombination have important regulatory functions, activating DDR responses, which in return control the availability of their substrates. On the signaling level, ATM, p53, and NF- κ B pathways, activated by the DSBs, seem to on one end converge towards the same effect – control of RAG1/2 endonuclease availability and the V(D)J recombination efficiency^{121,171,185,191}, and at the same time branch out to influence many other cellular processes as well. The qualitative and temporal crosstalk between these pathways is not fully understood yet.

The occurrence of genomic lesions resulting from the off-target V(D)J recombination and the RAG1/2 activity seems to be rare, despite the genome-wide binding of RAG1 and RAG2 in mouse lymphocytes⁷¹. In cell systems that are unable to repair the DSBs, the location of the off-target RAG-dependent DSBs can be studied in more detail and the

results can provide valuable insights into the off-target preferences of RAG1/2 recombinase (Ochodnicka-Mackovicova K *et al*, manuscript under consideration). In addition, understanding how cells maintain genome stability may provide insights into mutagenic processes in other cell types as well.

The exploration of links between the B-cell-specific regulatory pathways and lymphoid malignancies may provide insights into novel targeted therapies. For instance, tyrosine kinase inhibitors, and specifically, ABL kinase inhibitors have already revolutionized the treatment of Philadelphia chromosome-positive B-ALL. The PI3K/AKT or mTOR pathway inhibitors (e.g., idelalisib or everolimus) showed promising results in inhibiting leukemia cell proliferation and enhancing the cytotoxic effects of chemotherapy^{209–211}. Targeting the anti-apoptotic BCL2 (e.g. venetoclax) has demonstrated efficacy in inducing apoptosis and enhancing the sensitivity of leukemia cells to chemotherapy²¹². Inhibitors targeting JAK/STAT proteins (e.g., ruxolitinib) may disrupt aberrant signaling and inhibit leukemia cell growth^{213,214}. Immunotherapies targeting pre-B cell surface marker CD19, such as chimeric antigen receptor (CAR) T-cell therapy and bispecific T-cell engagers (BiTEs), redirect the patient's immune system to selectively eliminate leukemia cells expressing CD19^{215,216}.

Additionally, investigating the role RAG-induced genomic instability in cancer development could lead to new diagnostic and prognostic advances. For instance, expression patterns of specific microRNAs hold promise for non-invasive early detection. In chronic lymphocytic leukemia (CLL), low expression of miR-34a was associated with shorter overall survival and worse responses to fludarabine, cyclophosphamide, rituximab (FCR) therapy. MiR-34a is induced in response to DDR activation and p53 stabilisation and was shown to limit the BCR signaling in CLL during DDR by down-modulating FOXP1²¹⁷. Overexpression of miR-196b has been associated with poor prognosis and chemotherapy resistance in B cell ALL. It regulates the expression of HOXA9, a transcription factor involved in hematopoietic development, and contributes to leukemogenesis by promoting cell proliferation and inhibiting apoptosis²¹⁸.

References

1. Bonilla, F. A. & Oettgen, H. C. Adaptive immunity. *J. Allergy Clin. Immunol.* **125**, S33-40 (2010).
2. Chaplin, D. D. Overview of the immune response. *J. Allergy Clin. Immunol.* **125**, S3-23 (2010).
3. Weiss, A. Structure and function of the T cell antigen receptor. *J. Clin. Invest.* **86**, 1015–22 (1990).
4. Wilson, I. A. & Garcia, K. C. T-cell receptor structure and TCR complexes. *Curr. Opin. Struct. Biol.* **7**, 839–48 (1997).
5. Livák, F. & Petrie, H. T. Access roads for RAG-ged terrains: control of T cell receptor gene rearrangement at multiple levels. *Semin. Immunol.* **14**, 297–309 (2002).
6. Smith-Garvin, J. E., Koretzky, G. A. & Jordan, M. S. T cell activation. *Annu. Rev. Immunol.* **27**, 591–619 (2009).
7. Zhu, J. & Paul, W. E. CD4 T cells: fates, functions, and faults. *Blood* **112**, 1557–69 (2008).
8. Marculescu, R., Le, T., Simon, P., Jaeger, U. & Nadel, B. V(D)J-mediated translocations in lymphoid neoplasms: a functional assessment of genomic instability by cryptic sites. *J. Exp. Med.* **195**, 85–98 (2002).
9. Krem, M. M., Press, O. W., Horwitz, M. S. & Tidwell, T. Mechanisms and clinical applications of chromosomal instability in lymphoid malignancy. *Br. J. Haematol.* **171**, 13–28 (2015).
10. Pieper, K., Grimbacher, B. & Eibel, H. B-cell biology and development. *J. Allergy Clin. Immunol.* **131**, 959–971 (2013).
11. Kwon, K. *et al.* Instructive role of the transcription factor E2A in early B lymphopoiesis and germinal center B cell development. *Immunity* **28**, 751–762 (2008).
12. Van de Walle, I. *et al.* GATA3 induces human T-cell commitment by restraining Notch activity and repressing NK-cell fate. *Nat. Commun.* **7**, 11171 (2016).
13. Rickert, R. C. New insights into pre-BCR and BCR signalling with relevance to B cell malignancies. *Nat. Rev. Immunol.* **13**, 578–591 (2013).
14. Mårtensson, I.-L., Keenan, R. A. & Licence, S. The pre-B-cell receptor. *Curr. Opin. Immunol.* **19**, 137–142 (2007).
15. Collins, A. M. & Watson, C. T. Immunoglobulin Light Chain Gene Rearrangements, Receptor Editing and the Development of a Self-Tolerant Antibody Repertoire. *Front. Immunol.* **9**, 2249 (2018).
16. Wilson, A., Held, W. & MacDonald, H. R. Two waves of recombinase gene expression in developing thymocytes. *J. Exp. Med.* **179**, 1355–1360 (1994).
17. Zouali, M. Receptor editing and receptor revision in rheumatic autoimmune diseases. *Trends Immunol.* **29**, 103–109 (2008).
18. Mombaerts, P. *et al.* RAG-1-deficient mice have no mature B and T lymphocytes. *Cell* **68**, 869–877 (1992).
19. Shinkai, Y. *et al.* RAG-2-deficient mice lack mature lymphocytes owing to inability to initiate V(D)J rearrangement. *Cell* **68**, 855–867 (1992).
20. Schwarz, K. *et al.* RAG mutations in human B cell-negative SCID. *Science* **274**, 97–99 (1996).
21. Allen, D. *et al.* CRISPR-Cas9 engineering of the RAG2 locus via complete coding sequence replacement for therapeutic applications. *Nat. Commun.* **14**, 6771 (2023).
22. Garcia-Perez, L. *et al.* Successful Preclinical Development of Gene Therapy for Recombinase-Activating Gene-1-Deficient SCID. *Mol. Ther. Methods Clin. Dev.* **17**, 666–682 (2020).
23. Delmonte, O. M., Schuetz, C. & Notarangelo, L. D. RAG Deficiency: Two Genes, Many Diseases. *J. Clin. Immunol.* **38**, 646–655 (2018).
24. Nemazee, D. Mechanisms of central tolerance for B cells. *Nat. Rev. Immunol.* **17**, 281–294 (2017).
25. Luning Prak, E. T., Monestier, M. & Eisenberg, R. A. B cell receptor editing in tolerance and autoimmunity. *Ann. N. Y. Acad. Sci.* **1217**, 96–121 (2011).

26. Brady, B. L., Steinel, N. C. & Bassing, C. H. Antigen receptor allelic exclusion: an update and reappraisal. *J. Immunol.* **185**, 3801–3808 (2010).
27. Vettermann, C. & Schlissel, M. S. Allelic exclusion of immunoglobulin genes: models and mechanisms. *Immunol. Rev.* **237**, 22–42 (2010).
28. Liang, H.-E., Hsu, L.-Y., Cado, D. & Schlissel, M. S. Variegated transcriptional activation of the immunoglobulin kappa locus in pre-b cells contributes to the allelic exclusion of light-chain expression. *Cell* **118**, 19–29 (2004).
29. Coleclough, C., Perry, R. P., Karjalainen, K. & Weigert, M. Aberrant rearrangements contribute significantly to the allelic exclusion of immunoglobulin gene expression. *Nature* **290**, 372–378 (1981).
30. Alt, F. W., Enea, V., Bothwell, A. L. & Baltimore, D. Activity of multiple light chain genes in murine myeloma cells producing a single, functional light chain. *Cell* **21**, 1–12 (1980).
31. Mostoslavsky, R., Alt, F. W. & Rajewsky, K. The lingering enigma of the allelic exclusion mechanism. *Cell* **118**, 539–544 (2004).
32. Yancopoulos, G. D. & Alt, F. W. Regulation of the assembly and expression of variable-region genes. *Annu. Rev. Immunol.* **4**, 339–368 (1986).
33. Lutz, J. *et al.* Pro-B cells sense productive immunoglobulin heavy chain rearrangement irrespective of polypeptide production. *Proc. Natl. Acad. Sci. U. S. A.* **108**, 10644–10649 (2011).
34. Aslam, M. A. *et al.* The Ig heavy chain protein but not its message controls early B cell development. *Proc. Natl. Acad. Sci. U. S. A.* **117**, 31343–31352 (2020).
35. Chaumeil, J. *et al.* The RAG2 C-terminus and ATM protect genome integrity by controlling antigen receptor gene cleavage. *Nat. Commun.* **4**, 2231 (2013).
36. Hewitt, S. L. *et al.* RAG-1 and ATM coordinate monoallelic recombination and nuclear positioning of immunoglobulin loci. *Nat. Immunol.* **10**, 655–664 (2009).
37. Netea, M. G., Schlitzer, A., Placek, K., Joosten, L. A. B. & Schultze, J. L. Innate and Adaptive Immune Memory: an Evolutionary Continuum in the Host's Response to Pathogens. *Cell Host Microbe* **25**, 13–26 (2019).
38. Charles A Janeway, J., Travers, P., Walport, M. & Shlomchik, M. J. The structure of a typical antibody molecule. (2001).
39. Stavnezer, J., Guikema, J. E. J. & Schrader, C. E. Mechanism and regulation of class switch recombination. *Annu. Rev. Immunol.* **26**, 261–92 (2008).
40. Charles A Janeway, J., Travers, P., Walport, M. & Shlomchik, M. J. Structural variation in immunoglobulin constant regions. (2001).
41. Matthews, A. J., Zheng, S., DiMenna, L. J. & Chaudhuri, J. Regulation of immunoglobulin class-switch recombination: choreography of noncoding transcription, targeted DNA deamination, and long-range DNA repair. *Adv. Immunol.* **122**, 1–57 (2014).
42. Chi, X., Li, Y. & Qiu, X. V(D)J recombination, somatic hypermutation and class switch recombination of immunoglobulins: mechanism and regulation. *Immunology* **160**, 233–247 (2020).
43. Stavnezer, J., Guikema, J. E. J. & Schrader, C. E. Mechanism and regulation of class switch recombination. *Annu. Rev. Immunol.* **26**, 261–292 (2008).
44. Staszewski, O. *et al.* Activation-induced cytidine deaminase induces reproducible DNA breaks at many non-Ig Loci in activated B cells. *Mol. Cell* **41**, 232–242 (2011).
45. Hasham, M. G. *et al.* Activation-induced cytidine deaminase-initiated off-target DNA breaks are detected and resolved during S phase. *J. Immunol.* **189**, 2374–2382 (2012).
46. Khair, L., Baker, R. E., Linehan, E. K., Schrader, C. E. & Stavnezer, J. Nbs1 ChIP-Seq Identifies Off-Target DNA Double-Strand Breaks Induced by AID in Activated Splenic B Cells. *PLoS Genet.* **11**, e1005438 (2015).
47. Oettinger, M. A. *et al.* The recombination activating genes, RAG 1 and RAG 2, are on chromosome 11p in humans and chromosome 2p in mice. *Immunogenetics* **35**, 97–101 (1992).

48. Liu, C., Zhang, Y., Liu, C. C. & Schatz, D. G. Structural insights into the evolution of the RAG recombinase. *Nat. Rev. Immunol.* **22**, 353–370 (2022).
49. Doolittle, W. F. & Sapienza, C. Selfish genes, the phenotype paradigm and genome evolution. *Nature* **284**, 601–603 (1980).
50. Orgel, L. E., Crick, F. H. & Sapienza, C. Selfish DNA. *Nature* vol. 288 645–646 (1980).
51. Lescale, C. & Deriano, L. The RAG recombinase: Beyond breaking. *Mech. Ageing Dev.* **165**, 3–9 (2017).
52. Helmink, B. A. & Sleckman, B. P. The response to and repair of RAG-mediated DNA double-strand breaks. *Annu. Rev. Immunol.* **30**, 175–202 (2012).
53. Zhang, Y. *et al.* Transposon molecular domestication and the evolution of the RAG recombinase. *Nature* **569**, 79–84 (2019).
54. Martin, E. C. *et al.* Identification of RAG-like transposons in protostomes suggests their ancient bilaterian origin. *Mob. DNA* **11**, 17 (2020).
55. Schatz, D. G., Oettinger, M. A. & Baltimore, D. The V(D)J recombination activating gene, RAG-1. *Cell* **59**, 1035–48 (1989).
56. Oettinger, M. A., Schatz, D. G., Gorka, C. & Baltimore, D. RAG-1 and RAG-2, adjacent genes that synergistically activate V(D)J recombination. *Science* **248**, 1517–1523 (1990).
57. Kim, M.-S., Lapkouski, M., Yang, W. & Gellert, M. Crystal structure of the V(D)J recombinase RAG1-RAG2. *Nature* **518**, 507–511 (2015).
58. Liang, H.-E. *et al.* The ‘dispensable’ portion of RAG2 is necessary for efficient V-to-DJ rearrangement during B and T cell development. *Immunity* **17**, 639–651 (2002).
59. Corneo, B., Benmerah, A. & Villartay, J.-P. de. A short peptide at the C terminus is responsible for the nuclear localization of RAG2. *Eur. J. Immunol.* **32**, 2068–2073 (2002).
60. Mizuta, R., Mizuta, M., Araki, S. & Kitamura, D. RAG2 is down-regulated by cytoplasmic sequestration and ubiquitin-dependent degradation. *J. Biol. Chem.* **277**, 41423–41427 (2002).
61. Matthews, A. G. W. *et al.* RAG2 PHD finger couples histone H3 lysine 4 trimethylation with V(D)J recombination. *Nature* **450**, 1106–1110 (2007).
62. Chao, J., Rothschild, G. & Basu, U. Ubiquitination events that regulate recombination of immunoglobulin Loci gene segments. *Front. Immunol.* **5**, 100 (2014).
63. Jones, J. M. & Simkus, C. The roles of the RAG1 and RAG2 ‘non-core’ regions in V(D)J recombination and lymphocyte development. *Arch. Immunol. Ther. Exp. (Warsz.)* **57**, 105–116 (2009).
64. Jones, J. M. *et al.* The RAG1 V(D)J recombinase/ubiquitin ligase promotes ubiquitylation of acetylated, phosphorylated histone 3.3. *Immunol. Lett.* **136**, 156–162 (2011).
65. Singh, S. K. & Gellert, M. Role of RAG1 autoubiquitination in V(D)J recombination. *Proc. Natl. Acad. Sci. U. S. A.* **112**, 8579–8583 (2015).
66. Ru, H., Zhang, P. & Wu, H. Structural gymnastics of RAG-mediated DNA cleavage in V(D)J recombination. *Curr. Opin. Struct. Biol.* **53**, 178–186 (2018).
67. Swanson, P. C. The DDE motif in RAG-1 is contributed in trans to a single active site that catalyzes the nicking and transesterification steps of V(D)J recombination. *Mol. Cell. Biol.* **21**, 449–458 (2001).
68. Banerjee, J. K. & Schatz, D. G. Synapsis alters RAG-mediated nicking at Tcrb recombination signal sequences: implications for the “beyond 12/23” rule. *Mol. Cell. Biol.* **34**, 2566–2580 (2014).
69. Bassing, C. H. *et al.* Recombination signal sequences restrict chromosomal V(D)J recombination beyond the 12/23 rule. *Nature* **405**, 583–586 (2000).
70. Hesse, J. E., Lieber, M. R., Gellert, M. & Mizuuchi, K. Extrachromosomal DNA substrates in pre-B cells undergo inversion or deletion at immunoglobulin V-(D)-J joining signals. *Cell* **49**, 775–783 (1987).
71. Teng, G. *et al.* RAG Represents a Widespread Threat to the Lymphocyte Genome. *Cell* **162**, 751–765 (2015).
72. Tonegawa, S. Somatic generation of antibody diversity. *Nature* **302**, 575–81 (1983).

73. Ru, H. *et al.* DNA melting initiates the RAG catalytic pathway. *Nat. Struct. Mol. Biol.* **25**, 732–742 (2018).
74. Aidinis, V. *et al.* The RAG1 homeodomain recruits HMG1 and HMG2 to facilitate recombination signal sequence binding and to enhance the intrinsic DNA-bending activity of RAG1-RAG2. *Mol. Cell. Biol.* **19**, 6532–6542 (1999).
75. Grundy, G. J., Moulding, H. A., Caldecott, K. W. & Rulten, S. L. One ring to bring them all—the role of Ku in mammalian non-homologous end joining. *DNA Repair (Amst)*. **17**, 30–38 (2014).
76. Frit, P., Ropars, V., Modesti, M., Charbonnier, J. B. & Calsou, P. Plugged into the Ku-DNA hub: The NHEJ network. *Prog. Biophys. Mol. Biol.* **147**, 62–76 (2019).
77. Li, G. C. *et al.* Ku70: a candidate tumor suppressor gene for murine T cell lymphoma. *Mol. Cell* **2**, 1–8 (1998).
78. Yu, W. *et al.* KU70 Inhibition Impairs Both Non-Homologous End Joining and Homologous Recombination DNA Damage Repair Through SHP-1 Induced Dephosphorylation of SIRT1 in T-Cell Acute Lymphoblastic Leukemia (T-ALL) [corrected]. *Cell. Physiol. Biochem. Int. J. Exp. Cell. Physiol. Biochem. Pharmacol.* **49**, 2111–2123 (2018).
79. Little, A. J., Matthews, A., Oettinger, M., Roth, D. B., and Schatz, D. G. Chapter 2—The Mechanism of V(D)J Recombination,” in *Molecular Biology of B Cells (Second Edition)*. London Acad. Press (2015).
80. Lewis, S., Gifford, A. & Baltimore, D. DNA elements are asymmetrically joined during the site-specific recombination of kappa immunoglobulin genes. *Science* **228**, 677–685 (1985).
81. Schlissel, M., Constantinescu, A., Morrow, T., Baxter, M. & Peng, A. Double-strand signal sequence breaks in V(D)J recombination are blunt, 5'-phosphorylated, RAG-dependent, and cell cycle regulated. *Genes Dev.* **7**, 2520–2532 (1993).
82. Lafaille, J. J., DeCloux, A., Bonneville, M., Takagaki, Y. & Tonegawa, S. Junctional sequences of T cell receptor gamma delta genes: implications for gamma delta T cell lineages and for a novel intermediate of V-(D)-J joining. *Cell* **59**, 859–870 (1989).
83. Desiderio, S. V. *et al.* Insertion of N regions into heavy-chain genes is correlated with expression of terminal deoxytransferase in B cells. *Nature* **311**, 752–755 (1984).
84. Ramsden, D. A. & Gellert, M. Formation and resolution of double-strand break intermediates in V(D)J rearrangement. *Genes Dev.* **9**, 2409–2420 (1995).
85. Mensen, A. *et al.* Utilization of TREC and KREC quantification for the monitoring of early T- and B-cell neogenesis in adult patients after allogeneic hematopoietic stem cell transplantation. *J. Transl. Med.* **11**, 188 (2013).
86. Sodora, D. L. *et al.* Quantification of thymic function by measuring T cell receptor excision circles within peripheral blood and lymphoid tissues in monkeys. *Eur. J. Immunol.* **30**, 1145–1153 (2000).
87. Raghavan, S. C., Tong, J. & Lieber, M. R. Hybrid joint formation in human V(D)J recombination requires nonhomologous DNA end joining. *DNA Repair (Amst)*. **5**, 278–285 (2006).
88. Deriano, L., Stracker, T. H., Baker, A., Petrini, J. H. J. & Roth, D. B. Roles for NBS1 in alternative nonhomologous end-joining of V(D)J recombination intermediates. *Mol. Cell* **34**, 13–25 (2009).
89. Yu, X. *et al.* RAG1 and RAG2 non-core regions are implicated in the leukemogenesis and off-target V(D)J recombination in BCR-ABL1-driven B cell lineage lymphoblastic leukemia. (2023) doi:10.1101/2023.09.29.560132.
90. Gellert, M. Molecular analysis of V(D)J recombination. *Annu. Rev. Genet.* **26**, 425–446 (1992).

91. Swanson, P. C., Volkmer, D. & Wang, L. Full-length RAG-2, and not full-length RAG-1, specifically suppresses RAG-mediated transposition but not hybrid joint formation or disintegration. *J. Biol. Chem.* **279**, 4034–4044 (2004).
92. Chatterji, M., Tsai, C.-L. & Schatz, D. G. Mobilization of RAG-generated signal ends by transposition and insertion in vivo. *Mol. Cell. Biol.* **26**, 1558–1568 (2006).
93. Reddy, Y. V. R., Perkins, E. J. & Ramsden, D. A. Genomic instability due to V(D)J recombination-associated transposition. *Genes Dev.* **20**, 1575–1582 (2006).
94. Messier, T. L., O'Neill, J. P., Hou, S.-M., Nicklas, J. A. & Finette, B. A. In vivo transposition mediated by V(D)J recombinase in human T lymphocytes. *EMBO J.* **22**, 1381–1388 (2003).
95. Curry, J. D. *et al.* Chromosomal reinsertion of broken RSS ends during T cell development. *J. Exp. Med.* **204**, 2293–2303 (2007).
96. Kirkham, C. M. *et al.* Cut-and-Run: A Distinct Mechanism by which V(D)J Recombination Causes Genome Instability. *Mol. Cell* **74**, 584-597.e9 (2019).
97. Papaemmanuil, E. *et al.* RAG-mediated recombination is the predominant driver of oncogenic rearrangement in ETV6-RUNX1 acute lymphoblastic leukemia. *Nat. Genet.* **46**, 116–25 (2014).
98. Smith, A. L., Scott, J. N. F. & Boyes, J. The ESC: The Dangerous By-Product of V(D)J Recombination. *Front. Immunol.* **10**, 1572 (2019).
99. Rommel, P. C., Oliveira, T. Y., Nussenzweig, M. C. & Robbiani, D. F. RAG1/2 induces genomic insertions by mobilizing DNA into RAG1/2-independent breaks. *J. Exp. Med.* **214**, 815–831 (2017).
100. Lewis, S. M., Agard, E., Suh, S. & Czyzyk, L. Cryptic signals and the fidelity of V(D)J joining. *Mol. Cell. Biol.* **17**, 3125–3136 (1997).
101. Rodgers, W., Byrum, J. N., Simpson, D. A., Hoolehan, W. & Rodgers, K. K. RAG2 localization and dynamics in the pre-B cell nucleus. *PLoS One* **14**, e0216137 (2019).
102. Teng, G. & Schatz, D. G. Regulation and Evolution of the RAG Recombinase. *Adv. Immunol.* **128**, 1–39 (2015).
103. Gigi, V. *et al.* RAG2 mutants alter DSB repair pathway choice in vivo and illuminate the nature of 'alternative NHEJ'. *Nucleic Acids Res.* **42**, 6352–6364 (2014).
104. Papaemmanuil, E. *et al.* RAG-mediated recombination is the predominant driver of oncogenic rearrangement in ETV6-RUNX1 acute lymphoblastic leukemia. *Nat. Genet.* **46**, 116–125 (2014).
105. Mullighan, C. G. *et al.* BCR-ABL1 lymphoblastic leukaemia is characterized by the deletion of Ikaros. *Nature* **453**, 110–114 (2008).
106. Haydu, J. E. *et al.* An activating intragenic deletion in NOTCH1 in human T-ALL. *Blood* **119**, 5211–5214 (2012).
107. Mendes, R. D. *et al.* PTEN microdeletions in T-cell acute lymphoblastic leukemia are caused by illegitimate RAG-mediated recombination events. *Blood* **124**, 567–578 (2014).
108. Aplan, P. D. *et al.* Disruption of the human SCL locus by 'illegitimate' V-(D)-J recombinase activity. *Science* **250**, 1426–1429 (1990).
109. Onozawa, M. & Aplan, P. D. Illegitimate V(D)J recombination involving nonantigen receptor loci in lymphoid malignancy. *Genes Chromosomes Cancer* **51**, 525–535 (2012).
110. Raghavan, S. C., Gu, J., Swanson, P. C. & Lieber, M. R. The structure-specific nicking of small heteroduplexes by the RAG complex: implications for lymphoid chromosomal translocations. *DNA Repair (Amst)*. **6**, 751–759 (2007).
111. Nambiar, M. *et al.* Formation of a G-quadruplex at the BCL2 major breakpoint region of the t(14;18) translocation in follicular lymphoma. *Nucleic Acids Res.* **39**, 936–948 (2011).
112. Santagata, S. *et al.* The RAG1/RAG2 complex constitutes a 3' flap endonuclease: implications for junctional diversity in V(D)J and transpositional recombination. *Mol. Cell* **4**, 935–947 (1999).
113. Raghavan, S. C., Swanson, P. C., Wu, X., Hsieh, C.-L. & Lieber, M. R. A non-B-DNA structure at the Bcl-2 major breakpoint region is cleaved by the RAG complex. *Nature* **428**, 88–93 (2004).

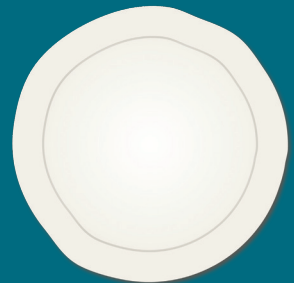
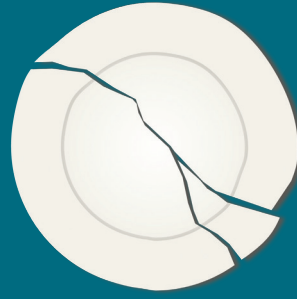
114. Agard, E. A. & Lewis, S. M. Postcleavage sequence specificity in V(D)J recombination. *Mol. Cell. Biol.* **20**, 5032–5040 (2000).
115. Tsai, C.-L., Chatterji, M. & Schatz, D. G. DNA mismatches and GC-rich motifs target transposition by the RAG1/RAG2 transposase. *Nucleic Acids Res.* **31**, 6180–6190 (2003).
116. Li, Z., Dordai, D. I., Lee, J. & Desiderio, S. A conserved degradation signal regulates RAG-2 accumulation during cell division and links V(D)J recombination to the cell cycle. *Immunity* **5**, 575–89 (1996).
117. Lee, J. & Desiderio, S. Cyclin A/CDK2 regulates V(D)J recombination by coordinating RAG-2 accumulation and DNA repair. *Immunity* **11**, 771–81 (1999).
118. Yurchenko, V., Xue, Z. & Sadofsky, M. The RAG1 N-terminal domain is an E3 ubiquitin ligase. *Genes Dev.* **17**, 581–585 (2003).
119. Grazini, U. *et al.* The RING domain of RAG1 ubiquitylates histone H3: a novel activity in chromatin-mediated regulation of V(D)J joining. *Mol. Cell* **37**, 282–293 (2010).
120. Beilinson, H. A. *et al.* The RAG1 N-terminal region regulates the efficiency and pathways of synapsis for V(D)J recombination. *J. Exp. Med.* **218**, (2021).
121. Ochodnicka-Mackovicova, K. *et al.* The DNA Damage Response Regulates RAG1/2 Expression in Pre-B Cells through ATM-FOXO1 Signaling. *J. Immunol.* **197**, 2918–2929 (2016).
122. Chan, E. A. W. *et al.* Peripheral subnuclear positioning suppresses Tcrb recombination and segregates Tcrb alleles from RAG2. *Proc. Natl. Acad. Sci. U. S. A.* **110**, E4628–37 (2013).
123. Brecht, R. M. *et al.* Nucleolar localization of RAG1 modulates V(D)J recombination activity. *Proc. Natl. Acad. Sci. U. S. A.* **117**, 4300–4309 (2020).
124. Fuxa, M. *et al.* Pax5 induces V-to-DJ rearrangements and locus contraction of the immunoglobulin heavy-chain gene. *Genes Dev.* **18**, 411–422 (2004).
125. Hu, J. *et al.* Chromosomal Loop Domains Direct the Recombination of Antigen Receptor Genes. *Cell* **163**, 947–959 (2015).
126. Degner, S. C. *et al.* CCCTC-binding factor (CTCF) and cohesin influence the genomic architecture of the Igh locus and antisense transcription in pro-B cells. *Proc. Natl. Acad. Sci. U. S. A.* **108**, 9566–9571 (2011).
127. Gan, T., Wang, Y., Liu, Y., Schatz, D. G. & Hu, J. RAG2 abolishes RAG1 aggregation to facilitate V(D)J recombination. *Cell Rep.* **37**, 109824 (2021).
128. De, P. *et al.* Thermal dependency of RAG1 self-association properties. *BMC Biochem.* **9**, 5 (2008).
129. Yu, W. *et al.* Coordinate regulation of RAG1 and RAG2 by cell type-specific DNA elements 5' of RAG2. *Science* **285**, 1080–1084 (1999).
130. Monroe, R. J., Chen, F., Ferrini, R., Davidson, L. & Alt, F. W. RAG2 is regulated differentially in B and T cells by elements 5' of the promoter. *Proc. Natl. Acad. Sci. U. S. A.* **96**, 12713–12718 (1999).
131. Lee, B.-S. *et al.* Corrected and Republished from: BCL11A Is a Critical Component of a Transcriptional Network That Activates RAG Expression and V(D)J Recombination. *Mol. Cell. Biol.* **38**, (2018).
132. Kishi, H. *et al.* Lineage-specific regulation of the murine RAG-2 promoter: GATA-3 in T cells and Pax-5 in B cells. *Blood* **95**, 3845–3852 (2000).
133. Brown, S. T. *et al.* Regulation of the RAG-1 promoter by the NF-Y transcription factor. *J. Immunol.* **158**, 5071–5074 (1997).
134. Jin, Z.-X. *et al.* Lymphoid enhancer-binding factor-1 binds and activates the recombination-activating gene-2 promoter together with c-Myb and Pax-5 in immature B cells. *J. Immunol.* **169**, 3783–3792 (2002).
135. Wu, C.-X. *et al.* Activation of mouse RAG-2 promoter by Myc-associated zinc finger protein. *Biochem. Biophys. Res. Commun.* **317**, 1096–1102 (2004).
136. Wei, X.-C. *et al.* Characterization of chromatin structure and enhancer elements for murine recombination activating gene-2. *J. Immunol.* **169**, 873–881 (2002).

137. Hsu, L.-Y. *et al.* A conserved transcriptional enhancer regulates RAG gene expression in developing B cells. *Immunity* **19**, 105–17 (2003).
138. Chen, Z. *et al.* Transcription factors E2A, FOXO1 and FOXP1 regulate recombination activating gene expression in cancer cells. *PLoS One* **6**, e20475 (2011).
139. Dekker, J. D. *et al.* Loss of the FOXP1 Transcription Factor Leads to Deregulation of B Lymphocyte Development and Function at Multiple Stages. *ImmunoHorizons* **3**, 447–462 (2019).
140. Amin, R. H. & Schlissel, M. S. Foxo1 directly regulates the transcription of recombination-activating genes during B cell development. *Nat. Immunol.* **9**, 613–22 (2008).
141. Schulz, D. *et al.* Gfi1b negatively regulates Rag expression directly and via the repression of FoxO1. *J. Exp. Med.* **209**, 187–199 (2012).
142. Timblin, G. A. & Schlissel, M. S. Ebf1 and c-Myb repress rag transcription downstream of Stat5 during early B cell development. *J. Immunol.* **191**, 4676–4687 (2013).
143. Miyazaki, K. & Miyazaki, M. The Interplay Between Chromatin Architecture and Lineage-Specific Transcription Factors and the Regulation of Rag Gene Expression. *Front. Immunol.* **12**, 659761 (2021).
144. Lennartsson, J. & Rönstrand, L. Stem cell factor receptor/c-Kit: from basic science to clinical implications. *Physiol. Rev.* **92**, 1619–1649 (2012).
145. Dolence, J. J., Gwin, K. A., Shapiro, M. B. & Medina, K. L. Flt3 signaling regulates the proliferation, survival, and maintenance of multipotent hematopoietic progenitors that generate B cell precursors. *Exp. Hematol.* **42**, 380–393.e3 (2014).
146. Hinman, R. M. *et al.* Foxo3^{-/-} mice demonstrate reduced numbers of pre-B and recirculating B cells but normal splenic B cell sub-population distribution. *Int. Immunol.* **21**, 831–842 (2009).
147. Dengler, H. S. *et al.* Distinct functions for the transcription factor Foxo1 at various stages of B cell differentiation. *Nat. Immunol.* **9**, 1388–98 (2008).
148. Burgering, B. M. T. A brief introduction to FOXOlogy. *Oncogene* **27**, 2258–2262 (2008).
149. Chen, J., Limon, J. J., Blanc, C., Peng, S. L. & Fruman, D. A. Foxo1 regulates marginal zone B-cell development. *Eur. J. Immunol.* **40**, 1890–1896 (2010).
150. Hu, X., Li, J., Fu, M., Zhao, X. & Wang, W. The JAK/STAT signaling pathway: from bench to clinic. *Signal Transduct. Target. Ther.* **6**, 402 (2021).
151. Malin, S., McManus, S. & Buslinger, M. STAT5 in B cell development and leukemia. *Curr. Opin. Immunol.* **22**, 168–176 (2010).
152. Zhang, L., Reynolds, T. L., Shan, X. & Desiderio, S. Coupling of V(D)J recombination to the cell cycle suppresses genomic instability and lymphoid tumorigenesis. *Immunity* **34**, 163–74 (2011).
153. Quong, M. W. *et al.* Receptor editing and marginal zone B cell development are regulated by the helix-loop-helix protein, E2A. *J. Exp. Med.* **199**, 1101–1112 (2004).
154. Novak, R., Jacob, E., Haimovich, J., Avni, O. & Melamed, D. The MAPK/ERK and PI3K pathways additively coordinate the transcription of recombination-activating genes in B lineage cells. *J. Immunol.* **185**, 3239–3247 (2010).
155. Reth, M. *et al.* The B-cell antigen receptor complex. *Immunol. Today* **12**, 196–201 (1991).
156. Heltemes-Harris, L. M. *et al.* Ebf1 or Pax5 haploinsufficiency synergizes with STAT5 activation to initiate acute lymphoblastic leukemia. *J. Exp. Med.* **208**, 1135–1149 (2011).
157. Malin, S. *et al.* Role of STAT5 in controlling cell survival and immunoglobulin gene recombination during pro-B cell development. *Nat. Immunol.* **11**, 171–179 (2010).
158. Herzog, S., Reth, M. & Jumaa, H. Regulation of B-cell proliferation and differentiation by pre-B-cell receptor signalling. *Nat. Rev. Immunol.* **9**, 195–205 (2009).
159. Zhang, L., Reynolds, T. L., Shan, X. & Desiderio, S. Coupling of V(D)J recombination to the cell cycle suppresses genomic instability and lymphoid tumorigenesis. *Immunity* **34**, 163–174 (2011).

160. Clark, M. R., Mandal, M., Ochiai, K. & Singh, H. Orchestrating B cell lymphopoiesis through interplay of IL-7 receptor and pre-B cell receptor signalling. *Nat. Rev. Immunol.* **14**, 69–80 (2014).
161. Lazorchak, A. S., Schlissel, M. S. & Zhuang, Y. E2A and IRF-4/Pip promote chromatin modification and transcription of the immunoglobulin kappa locus in pre-B cells. *Mol. Cell. Biol.* **26**, 810–821 (2006).
162. Johnson, K. *et al.* Regulation of immunoglobulin light-chain recombination by the transcription factor IRF-4 and the attenuation of interleukin-7 signaling. *Immunity* **28**, 335–345 (2008).
163. Myers, D. R., Zikherman, J. & Roose, J. P. Tonic Signals: Why Do Lymphocytes Bother? *Trends Immunol.* **38**, 844–857 (2017).
164. Srinivasan, L. *et al.* PI3 kinase signals BCR-dependent mature B cell survival. *Cell* **139**, 573–586 (2009).
165. Franke, T. F. *et al.* The protein kinase encoded by the Akt proto-oncogene is a target of the PDGF-activated phosphatidylinositol 3-kinase. *Cell* **81**, 727–736 (1995).
166. Aman, M. J., Lamkin, T. D., Okada, H., Kurosaki, T. & Ravichandran, K. S. The inositol phosphatase SHIP inhibits Akt/PKB activation in B cells. *J. Biol. Chem.* **273**, 33922–33928 (1998).
167. Llorian, M., Stamatakis, Z., Hill, S., Turner, M. & Mårtensson, I.-L. The PI3K p110delta is required for down-regulation of RAG expression in immature B cells. *J. Immunol.* **178**, 1981–1985 (2007).
168. Verkoczy, L. *et al.* Basal B cell receptor-directed phosphatidylinositol 3-kinase signaling turns off RAGs and promotes B cell-positive selection. *J. Immunol.* **178**, 6332–6341 (2007).
169. Ta, V. B. T., de Haan, A. B., de Bruijn, M. J. W., Dingjan, G. M. & Hendriks, R. W. Pre-B-cell leukemias in Btk/Slp65-deficient mice arise independently of ongoing V(D)J recombination activity. *Leukemia* **25**, 48–56 (2011).
170. Schram, B. R. *et al.* B cell receptor basal signaling regulates antigen-induced Ig light chain rearrangements. *J. Immunol.* **180**, 4728–4741 (2008).
171. Sen, R. & Baltimore, D. Inducibility of kappa immunoglobulin enhancer-binding protein Nf-kappa B by a posttranslational mechanism. *Cell* **47**, 921–928 (1986).
172. Zinatizadeh, M. R. *et al.* The Nuclear Factor Kappa B (NF- κ B) signaling in cancer development and immune diseases. *Genes Dis.* **8**, 287–297 (2021).
173. Verkoczy, L. *et al.* A role for nuclear factor kappa B/rel transcription factors in the regulation of the recombinase activator genes. *Immunity* **22**, 519–531 (2005).
174. Balkhi, M. Y. *et al.* IKK α -mediated signaling circuitry regulates early B lymphopoiesis during hematopoiesis. *Blood* **119**, 5467–5477 (2012).
175. Guo, F., Tänzler, S., Busslinger, M. & Weih, F. Lack of nuclear factor-kappa B2/p100 causes a RelB-dependent block in early B lymphopoiesis. *Blood* **112**, 551–559 (2008).
176. Xie, P., Stunz, L. L., Larison, K. D., Yang, B. & Bishop, G. A. Tumor necrosis factor receptor-associated factor 3 is a critical regulator of B cell homeostasis in secondary lymphoid organs. *Immunity* **27**, 253–267 (2007).
177. Sasaki, Y. *et al.* Canonical NF-kappaB activity, dispensable for B cell development, replaces BAFF-receptor signals and promotes B cell proliferation upon activation. *Immunity* **24**, 729–739 (2006).
178. Vallabhapurapu, S. *et al.* Nonredundant and complementary functions of TRAF2 and TRAF3 in a ubiquitination cascade that activates NIK-dependent alternative NF-kappaB signaling. *Nat. Immunol.* **9**, 1364–1370 (2008).
179. Vashisht, M. *et al.* TRAF2/3 deficient B cells resist DNA damage-induced apoptosis via NF- κ B2/XIAP/cIAP2 axis and IAP antagonist sensitizes mutant lymphomas to chemotherapeutic drugs. *Cell Death Dis.* **14**, 599 (2023).
180. Paun, A., Claudio, E. & Siebenlist, U. K. Constitutive activation of NF- κ B during early bone marrow development results in loss of B cells at the pro-B-cell stage. *Blood Adv.* **5**, 745–755 (2021).

181. Ochodnicka-Mackovicova, K. *et al.* NF- κ B and AKT signaling prevent DNA damage in transformed pre-B cells by suppressing RAG1/2 expression and activity. *Blood* **126**, 1324–1335 (2015).
182. Matsuoka, S. *et al.* ATM and ATR substrate analysis reveals extensive protein networks responsive to DNA damage. *Science* **316**, 1160–1166 (2007).
183. Lee, J.-H. & Paull, T. T. ATM activation by DNA double-strand breaks through the Mre11-Rad50-Nbs1 complex. *Science* **308**, 551–554 (2005).
184. Stracker, T. H. & Petrini, J. H. J. The MRE11 complex: starting from the ends. *Nat. Rev. Mol. Cell Biol.* **12**, 90–103 (2011).
185. Blackford, A. N. & Jackson, S. P. ATM, ATR, and DNA-PK: The Trinity at the Heart of the DNA Damage Response. *Mol. Cell* **66**, 801–817 (2017).
186. Shieh, S. Y., Ahn, J., Tamai, K., Taya, Y. & Prives, C. The human homologs of checkpoint kinases Chk1 and Cds1 (Chk2) phosphorylate p53 at multiple DNA damage-inducible sites. *Genes Dev.* **14**, 289–300 (2000).
187. Zannini, L., Delia, D. & Buscemi, G. CHK2 kinase in the DNA damage response and beyond. *J. Mol. Cell Biol.* **6**, 442–457 (2014).
188. Stevens, C., Smith, L. & La Thangue, N. B. Chk2 activates E2F-1 in response to DNA damage. *Nat. Cell Biol.* **5**, 401–409 (2003).
189. Harper, J. W., Adami, G. R., Wei, N., Keyomarsi, K. & Elledge, S. J. The p21 Cdk-interacting protein Cip1 is a potent inhibitor of G1 cyclin-dependent kinases. *Cell* **75**, 805–816 (1993).
190. Bredemeyer, A. L. *et al.* DNA double-strand breaks activate a multi-functional genetic program in developing lymphocytes. *Nature* **456**, 819–823 (2008).
191. Steinel, N. C. *et al.* The ataxia telangiectasia mutated kinase controls Igk allelic exclusion by inhibiting secondary V κ -to-J κ rearrangements. *J. Exp. Med.* **210**, 233–239 (2013).
192. Kinner, A., Wu, W., Staudt, C. & Iliakis, G. Gamma-H2AX in recognition and signaling of DNA double-strand breaks in the context of chromatin. *Nucleic Acids Res.* **36**, 5678–5694 (2008).
193. Woo, J. S., Alberti, M. O. & Tirado, C. A. Childhood B-acute lymphoblastic leukemia: a genetic update. *Exp. Hematol. Oncol.* **3**, 16 (2014).
194. Chernoff, J. The two-hit theory hits 50. *Mol. Biol. Cell* **32**, rt1 (2021).
195. Shurtleff, S. A. *et al.* TEL/AML1 fusion resulting from a cryptic t(12;21) is the most common genetic lesion in pediatric ALL and defines a subgroup of patients with an excellent prognosis. *Leukemia* **9**, 1985–1989 (1995).
196. Angione, S. D. A. *et al.* Fusion Oncoproteins in Childhood Cancers: Potential Role in Targeted Therapy. *J. Pediatr. Pharmacol. Ther. JPPT Off. J. PPAG* **26**, 541–555 (2021).
197. Schäfer, D. *et al.* Five percent of healthy newborns have an ETV6-RUNX1 fusion as revealed by DNA-based GIPFEL screening. *Blood* vol. 131 821–826 (2018).
198. Kantner, H.-P. *et al.* ETV6/RUNX1 induces reactive oxygen species and drives the accumulation of DNA damage in B cells. *Neoplasia* **15**, 1292–1300 (2013).
199. Ziech, D., Franco, R., Pappa, A. & Panayiotidis, M. I. Reactive oxygen species (ROS)-induced genetic and epigenetic alterations in human carcinogenesis. *Mutat. Res.* **711**, 167–173 (2011).
200. Kuiper, R. P. & Waanders, E. A RAG driver on the road to pediatric ALL. *Nat. Genet.* **46**, 96–98 (2014).
201. Paulsson, K. *et al.* The genomic landscape of high hyperdiploid childhood acute lymphoblastic leukemia. *Nat. Genet.* **47**, 672–676 (2015).
202. Aricò, M. *et al.* Outcome of treatment in children with Philadelphia chromosome-positive acute lymphoblastic leukemia. *N. Engl. J. Med.* **342**, 998–1006 (2000).

203. Mathijs A. Sanders, Anikó Szabó, Carla Exalto, Remco Hoogenboezem, Annelieke Zeilemaker, Jasper E. Koenders, Peter van Geel, Anita Schelen, H. Berna Beverloo, Jan J. Cornelissen, Anita W. Rijnveld, P. J. M. V. Extensive RAG-Mediated Rearrangements and Mutations in BCR-ABL1 and BCR-ABL1-like Adult Acute Lymphoblastic Leukemia. *Blood* **128**, 4067 (2016).
204. G, W. The infective theory of acute leukaemia. *Br J Child Dis* 10–20 (1917).
205. Ma, X. *et al.* Vaccination history and risk of childhood leukaemia. *Int. J. Epidemiol.* **34**, 1100–1109 (2005).
206. Auvinen, A., Hakulinen, T. & Groves, F. Haemophilus influenzae type B vaccination and risk of childhood leukaemia in a vaccine trial in Finland. *Br. J. Cancer* **83**, 956–958 (2000).
207. Mahowald, G. K., Baron, J. M. & Sleckman, B. P. Collateral damage from antigen receptor gene diversification. *Cell* **135**, 1009–1012 (2008).
208. Tsai, A. G. *et al.* Human chromosomal translocations at CpG sites and a theoretical basis for their lineage and stage specificity. *Cell* **135**, 1130–1142 (2008).
209. Place, A. E. *et al.* Phase I trial of the mTOR inhibitor everolimus in combination with multi-agent chemotherapy in relapsed childhood acute lymphoblastic leukemia. *Pediatr. Blood Cancer* **65**, e27062 (2018).
210. Ratti, S. *et al.* B-ALL Complexity: Is Targeted Therapy Still A Valuable Approach for Pediatric Patients? *Cancers (Basel)*. **12**, (2020).
211. Adam, E. *et al.* The PI3K δ Inhibitor Idelalisib Inhibits Homing in an in Vitro and in Vivo Model of B ALL. *Cancers (Basel)*. **9**, (2017).
212. Ferrari, A. *et al.* Venetoclax durable response in adult relapsed/refractory Philadelphia-negative acute lymphoblastic leukemia with JAK/STAT pathway alterations. *Front. cell Dev. Biol.* **11**, 1165308 (2023).
213. Kołodrubiec, J. *et al.* Efficacy of ruxolitinib in acute lymphoblastic leukemia: A systematic review. *Leuk. Res.* **121**, 106925 (2022).
214. Lee, S. *et al.* Ruxolitinib significantly enhances in vitro apoptosis in Hodgkin lymphoma and primary mediastinal B-cell lymphoma and survival in a lymphoma xenograft murine model. *Oncotarget* **9**, 9776–9788 (2018).
215. Deak, D. *et al.* Let's Talk About BiTEs and Other Drugs in the Real-Life Setting for B-Cell Acute Lymphoblastic Leukemia. *Front. Immunol.* **10**, 2856 (2019).
216. Ren, A. *et al.* CAR T-Cell Immunotherapy Treating T-ALL: Challenges and Opportunities. *Vaccines* **11**, (2023).
217. Rao, D. S. *et al.* MicroRNA-34a perturbs B lymphocyte development by repressing the forkhead box transcription factor Foxp1. *Immunity* **33**, 48–59 (2010).
218. de Oliveira, J. C. *et al.* Differential miRNA expression in childhood acute lymphoblastic leukemia and association with clinical and biological features. *Leuk. Res.* **36**, 293–298 (2012).



CHAPTER

RAG1/2 induces double-stranded DNA breaks at non-*Ig* loci in the proximity of single sequence repeats in developing B cells

Katarina Ochodnicka-Mackovicova, Michal Mokry,
Martin Haagmans, Ted E. Bradley, Carel J.M. van Noesel
and Jeroen E.J. Guikema

3



Abstract

In developing B cells, V(D)J gene recombination is initiated by the RAG1/2 endonuclease complex, introducing double-stranded DNA breaks (DSBs) in V, D, and J genes and resulting in the formation of the hypervariable parts of immunoglobulins (Ig). Persistent or aberrant RAG1/2 targeting is a potential threat to genome integrity. While RAG1 and RAG2 have been shown to bind various regions genome-wide, the *in vivo* off-target DNA damage instigated by RAG1/2 endonuclease remains less well understood. In the current study, we identified regions containing RAG1/2-induced DNA breaks in mouse pre-B cells on a genome-wide scale using a global DNA DSB detection strategy. 1489 putative RAG1/2-dependent DSBs were identified, most of which were located outside the *Ig* loci. DNA sequence motif analysis showed a specific enrichment of RAG1/2-induced DNA DSBs at GA- and CA-repeats and at GC-rich motifs. These findings provide further insights into RAG1/2 off-target activity. The ability of RAG1/2 to introduce DSBs on the non-Ig loci during the endogenous V(D)J recombination emphasizes its genotoxic potential in developing lymphocytes.

Introduction

During lymphocyte development in bone marrow, each lineage-committed B-cell undergoes V(D)J recombination to assemble functional gene segments that encode the heavy and the light chain variable regions of its antibody. These regions are critical for antigen recognition and antigen binding. V(D)J recombination is initiated by RAG1/2 endonuclease by binding the recombination signal sequences (RSS) flanking each variable (V), diversity (D), and joining (J) gene segment and consisting of conserved heptamer and nonamer sequences, separated by a less conserved spacer region. The cleavage of DNA by RAG1/2 endonuclease occurs in a coordinated manner, RAG1/2 first introduces a single-stranded nick between the heptamer and the gene segment. This creates a 3' hydroxyl group which then attacks the other strand and generates a double-stranded DNA break (DSB). This step is also referred to as hairpin formation because it generates a covalently sealed hairpin at the end of the gene segment¹. Hairpin formation only occurs in the paired complex and is thought to take place simultaneously at the two RSSs. The two blunt RSS ends are fused by classical non-homologous end-joining (c-NHEJ) pathway in which Artemis plays a pivotal role in successful gene recombination by opening the end-associated hairpins^{2,3}. The created DSBs are detected by the MRN complex, consisting of meiotic recombination 11 (MRE11), RAD50, and Nijmegen breakage syndrome 1 (NBS1; also known as Nibrin), which binds the DNA in the proximity of the DSBs⁴.

B-cell acute lymphoblastic leukemia (B-ALL) is one of the most common cancers affecting all age groups. In individuals under 20 years of age, it is the leading cause of cancer-related death. It is characterized by a high degree of genomic instability. A number of genomic aberrations have also been associated with B-ALL, including fusions such as *ETV6-RUNX1*, *BCR-ABL1*, mutations in *IKZF1*, *ZEB2*, *MEF2D* rearrangement or *PAX5* tandem duplication⁵⁻⁷. In the last decades, thanks to new innovative treatment options, the survival of young B-ALL patients improved dramatically^{8,9}. Nevertheless, the true root cause of the molecular formation of these genomic alterations remains not entirely understood.

Mistargeted activity of RAG1/2 recombinase can lead to an inappropriate DNA cleavage, resulting in to DNA breaks at unintended sites. Such genomic instability events may create a favorable condition for the acquisition of an oncogenic event. Several translocations or fusions have been described in B-ALL patients that bear signs of RAG1/2 activity¹⁰, including *ETV6/RUNX1* gene fusion¹¹ or *PAR1* deletion, where a conserved RSS was found near the breakpoint or *E2A-PBX1* translocation that harbors non-template nucleotides reminiscent of V(D)J joint¹².

Previous studies showed that RAG1 and RAG2 binding to DNA in B and T cells is not exclusively limited to *Ig* and *Tcr* genes. In fact, thousands of RAG1 and RAG2 binding sites were identified throughout the genome in mouse lymphocytes. Though outside of the *Ig* loci the presence of RSS was shown to be a poor predictor of RAG1 binding, a robust

accumulation of RAG1 and RAG2 was demonstrated near the cryptic RSS (cRSS), which are sequences that structurally resemble the canonical RSS. Interestingly, no endogenous recombination events were detected in the tested gene pairs of thymocyte genomes, concluding that despite the promiscuous RAG1 and RAG2 binding, recombination events must be rather rare^{13,14}. In extrachromosomal V(D)J recombination assays, or cell systems with artificially introduced cRSS-containing constructs, RAG1/2 was demonstrated to bind and cleave the non-*Ig* loci^{13,15,16}. However, the off-target activity of RAG1/2 in endogenous chromosomal V(D)J recombination context in pre-B cells is less well described.

In this study, we aimed to identify off-target RAG1/2-dependent DSBs on a genome-wide scale in *in vivo* endogenous chromosomal V(D)J recombination context, using pre-B cells that can be induced to undergo immunoglobulin kappa light chain (*Igκ*) recombination, expressing endogenous levels of RAG1/2, but that are unable to repair the DSBs. We made use of Artemis-deficient mouse v-Abl/E μ -Bcl2 pre-B cells where Artemis deficiency prevents the hairpins of the coding ends from being opened, thus leading to accumulation of the RAG-dependent DNA breaks that would otherwise be quickly resolved by c-NHEJ. We used the DNA-bound repair protein NBS1 as a proxy of coding ends. NBS1, being a member of the MRN DNA repair complex, binds the DNA in close proximity to DSBs. Performing an NBS1 chromatin immunoprecipitation followed by massive parallel sequencing (ChIP-Seq) in the pre-B cells undergoing *Igκ* recombination allows genome-wide determination of the position of DSBs, as has previously been demonstrated in a study investigating the off-target AID-derived DNA breaks in splenic B cells¹⁷. Comparing the NBS1 ChIP-Seq profiles of RAG-proficient pre-B cells to the RAG2-deficient cells allowed us to select and analyze the RAG-dependent DSBs. Using this approach, we identified 1489 RAG1/2-dependent DSBs throughout the genome. One of the common features of the off-targets is the presence of simple sequence repeats in the proximity of the putative RAG off-targets, further underscoring the vulnerability of such regions to DNA damage.

Material and methods

Cell culture and small molecule compounds

Mouse v-Abl transformed B-cell lines were used as a model to study the off-target activity of endogenous RAG1 and RAG2. The v-Abl-transformed cells are characterized by the surface expression of B220⁺CD43⁺CD25⁻IgM⁻, which is typical for B cells in the pro- or early pre-B cells stage. At this stage, the B cells proliferate rapidly and express very little or no RAG1 and RAG2. Also, their *Igκ* at this stage had not been yet rearranged. Treatment with Abelson kinase inhibitor (STI571/Imatinib), leads to G1 arrest, upregulation of RAG1 and RAG2, and initiation of *Igκ* recombination¹⁸. The treatment with STI571 also triggers an apoptosis within several hours. As such cell system would be sub-optimal to study the (off)-targeting activity of RAG1/2, the cell lines also carry an E μ -Bcl2 transgene, allowing

them to circumvent the STI571-induced cell-death¹⁹. The following v-Abl/Bcl2 cell lines were used: A70 wildtype (WT), *Rag2*^{-/-} (R2K3), *Artemis*^{-/-} (AH2), and *Rag2*^{-/-}/*Artemis*^{-/-} (R2K. Art) as a model for developing lymphocytes, cultured under the conditions as previously described²⁰. The cell lines were kindly provided by Dr. Craig Bassing (University of Pennsylvania School of Medicine, Philadelphia, PA). The cells were cultured in RPMI1640 (Life Technologies, Bleiswijk, the Netherlands) supplemented with 2 mM of L-glutamine, 100 U/ml penicillin, 100 µg/ml streptomycin, and 10% FCS. To introduce RAG1/2 expression, and the subsequent RAG1/2 endonuclease activity leading to *Igκ* recombination, the cells were treated with 5µM STI571 (imatinib methanesulfonate; LC Laboratories, Woburn, MA). The formation of V_κ6-23 to J_κ1 coding joins was determined by semiquantitative polymerase chain reaction (PCR) by using previously published primers¹⁹.

Chromatin immunoprecipitation (ChIP) and Real-time quantitative PCR

Cells were seeded at 2x10⁶ cell/mL density and cultured for 72h following an addition of 5µM STI571 to allow sufficient V(D)J recombination and accumulation of DSBs. At this timepoint the cell death is still minimal¹⁹. After 72h, the viable cells were isolated using 3mL Lympholyte M spun at 1200rcf/20min. The cells were washed in RPMI1640 containing a cocktail of protease and phosphatase inhibitors: 100 µM PMSF, 1 mM sodium ortho-vanadate, 2mM sodium fluoride, and 1.25mM β-glycero-phosphate. Crosslinking of the chromatin was achieved by adding 37% formaldehyde (1% final formaldehyde concentration) to the resuspended cells in RPMI1640 at 2x10⁶ cell/mL density, and incubating in a 37°C water bath for 5min. The crosslinking reaction was terminated by adding glycine to a final concentration of 125mM using 2.5M stock solution. The cells were washed in PBS and stored at -80°C for at least overnight. The cells were re-suspended at a concentration of 40x10⁶ cell/mL in sonication buffer (2% SDS, 10 mM EDTA, 50mM Tris-Cl at pH=8, and containing the cocktail of protease and phosphatase inhibitors as mentioned above) and subjected to ultrasound sonication to obtain DNA fragments of average length of 250bp. Following the sonication, the cells were diluted in a dilution buffer (0.01% SDS, 1.1% Triton X-100, 1.2 mM EDTA, 16.7 mM Tris-Cl pH=8, 167 mM NaCl) and incubated with 5µg of an antibody (rabbit anti-NBS1 antibody, Abcam; rabbit anti-histone H4 antibody, Millipore) per sample for 2.5h at 4°C, after with Protein A on beads was added to each sample and the incubation continued for another 2.5h at 4°C. The beads were washed with series of buffers, the low salt buffer (0.1% SDS, 1%, 2 mM EDTA, 20 mM Tris-Cl, pH=8, 150 mM NaCl), high-salt buffer (0.1% SDS, 1%, 2 mM EDTA, 20 mM Tris-Cl, pH=8, 500 mM NaCl), LiCl buffer (250 mM LiCl, 1% deoxycholate, 1% NP-40, 1mM EDTA, 10 mM Tris-Cl pH=8), TE buffer (10 mM Tris-Cl pH=8, 1mM EDTA) and finally the elution buffer (0.5% SDS, 5 mM EDTA, 10 mM Tris-Cl, pH=8, 300 mM NaCl) to elute the protein-chromatin complexes off the beads. The samples were heated overnight at 65°C to reverse the crosslinking, followed by the addition of Protease K and RNase A and subsequent overnight incubation at 55°C to destroy the remaining protein and RNA.

After reversal of the crosslinking the DNA was purified using phenol-chloroform-isomylalcohol DNA extraction, the DNA was quantified using the CFX384 (Bio-Rad, Hercules, CA) real-time PCR platform. The PCR master mix contained 5 μ l of Sso Fast EvaGreen supermix (Bio-Rad, Hercules, CA) and 0.5 μ l of 10 μ M reverse and forward primers (Biolegio, Nijmegen, the Netherlands). The final volume was adjusted to 9 μ l using PCR-grade water, to which 1 μ l of diluted cDNA was added. The following PCR conditions were used: initial denaturation at 95°C for 5 min, followed by 40 cycles of denaturation at 95°C for 15 s, annealing at 65°C for 5 s, and extension at 72°C for 10 s. The fluorescent product was measured by a single acquisition mode at 72°C after each cycle. For distinguishing specific from nonspecific products and primer dimers, a melting curve was obtained after amplification by holding the temperature at 65°C for 15 s followed by a gradual increase in temperature to 95°C at a rate of 2.5°C s⁻¹, with the signal acquisition mode set to continuous.

The following primers were used J_k1 forward (5'-TCTGTCAGAGAAGCCCAAGC-3'), J_k1 reverse (GGCTGTACAAAAACCTCCTC-3'), J_k2 forward (5'-CTGGAGAATGAATGCCAGTG-3'), J_k2 reverse (5'-CCCCATACAAAACTGAGC-3'), J_k5 forward (5'-GCTGAGCGAAAACCTCGTCTTAAGG-3') and J_k5 reverse (5'-AAAACCTGCCTGTGAAGCCAGTCC-3').

The binding of NBS1 to the *Plac8* region was considered as negative control. Primers that amplify the intronic region of *Plac8* on chromosome 5 were used as previously described²¹. *Plac8* was found to be highly active during placental development and embryogenesis^{22,23}. Though random RAG1/2 off-target breaks around this gene cannot be excluded, it is not expected to be a RAG1/2 hotspot as there are no antigen receptor loci located on chromosome 5. To calculate the NBS1 density, we normalized the NBS1 qPCR signal to the H4 qPCR signal at each location assayed and compared it to the NBS1/H4 ratio at *Plac8* control.

Library preparation and SOLiD Sequencing

The massive parallel sequencing was performed on the ABI SOLiD 5500 platform. First, the sonicated CHIP DNA samples were quantified by Quant-iT™ dsDNA High-Sensitivity Assay Kit (Thermo Fisher) according to the manufacturer's protocol. Next the libraries for high throughput sequencing were prepared using the Fragment Library Preparation kit for 5500 Series SOLiD Systems (Applied Biosystems) according to the manufacturer's protocol, briefly, the DNA fragments were first blunt-ended and phosphorylated at the 5' end. Next, the DNA fragment size selection was performed on Agencourt AMPure® XP beads and separated on 2% agarose gel. The fragments of 250bp bp size were selected by gel excision. Then, the dA-tail was ligated onto the size-selected DNA using the A-tailing enzyme, and using T4 DNA ligase the P1-T and Barcode-T adaptors and barcodes were ligated onto the DNA fragments. These adaptors/barcodes are designed to be compatible with the reverse-read sequencing on 5500 Series SOLiD™ sequencers. Prior to ligation-mediated PCR, the sample was incubated at 72°C for 20 minutes in PCR mix to let the DNA diffuse

out of the gel and to perform nick translation on non-ligated 3'-ends of DNA fragments. Finally, the libraries were amplified using Platinum® PCR amplification kit and the final size distribution was checked using Agilent Technologies 2100 Bioanalyzer™.

To sequence the libraries an amplification on P1 beads was performed in an emulsion PCR (ePCR), followed by enrichment of the templated beads. Templated bead preparation was performed using the SOLiD® EZ Bead™ System (Applied Biosystems) according to the manufacturers' protocol. The emulsion was dispensed into a 96-well plate and cycled for 60 cycles. After the amplification, emulsion was broken with butanol, beads were enriched for template positive beads, 3'-end extended and covalently attached to sequencing slides. Physically separated samples were deposited on one sequencing slide and sequenced using standard settings on the 5500 Series SOLiD™ sequencer.

Analysis of ChIP-Seq data

Color signal/SOLiD signal was base-called into reads with the manufacturer's software (Lifescape). Sequencing reads were quality trimmed by clipping at 3 consecutive nucleotides with a quality score of less than 10. Reads shorter than 18 nucleotides were discarded and the remaining reads were cleaned of PCR duplicates and mapped onto the mouse genome (MM9 assembly) using the Bowtie²⁴ tool available on the Galaxy platform. NBS1 peak calling was performed by MACS²⁵ in each cell line. Next, to identify the RAG-dependent NBS1 peaks, the peaks called in *Artemis*^{-/-}/*Rag2*^{-/-} (R2K.Art) were subtracted from breaks called in the RAG proficient *Artemis*^{-/-} cell (AH2). Finally, the peaks called in the Input sample were subtracted from the RAG-dependent NBS1 peaks to eliminate any background binding bias. Annotation of the resulting RAG-dependent NBS1 peaks cleaned of input background was performed using PAVIS algorithm²⁶ for which the RAG-dependent NBS1 peaks were first lifted over to MM10 assembly.

The unsupervised motif analysis was performed by STREME (Sensitive, Thorough, Rapid, Enrichment Motif Elicitation)²⁷. The program uses Fisher's Exact Test or the Binomial test to determine the significance of each motif found in the positive set as compared with its representation in the control set. Shuffled primary sequences were used as a control set. The identified motifs were then compared to known motifs using the Tomtom motif comparison tool²⁸. This tool compares the identified motifs against the database of known motifs, produces alignment for each identified motif, and assigns a rank. The supervised analysis of the simple repeat motif enrichment was performed by SEA (Simple Enrichment Analysis)²⁹, which compares the used-provided motifs in the primary dataset and compares them against the enrichment in the shuffled primary sequences used as a control data set. The cut-off for q-value, the minimal false discovery rate at which the observed similarity would be deemed significant, was set to 0.05 in all motif-finding analyses.

Results

Experimental model and accumulation of RAG-dependent NBS1 peaks at *Igk* locus

The mouse v-Abl/Bcl2-transformed *Artemis*^{-/-} (AH2) and *Artemis*^{-/-}*Rag2*^{-/-} (R2K.Art) pre-B cells were used as a model to study the (off-)targeting capacity of RAG1/2 endonuclease. Transformation of B cells with Abelson murine leukemia virus arrests B-cell development in the early pre-B cell-like stage at which the expression of *Rag1* and *Rag2* is low and the light chain recombination minimal. Treatment with Abelson kinase inhibitor STI571 alleviates the developmental block, resulting in an increase in *Rag1* and *Rag2* mRNA expression. The subsequent increase in RAG1/2 endonuclease activity leads to *Igk* recombination. In this experimental model, V_κ6-23/J_κ1 recombination was monitored by PCR (**Figure 1A**). In time, the V_κ6-23/J_κ1 PCR signal increases (**Figure 1B**), suggesting more cells have undergone successful recombination *Igk* recombination. RAG cleavage creates pairs of coding and signal DNA ends, which are processed and joined by the canonical non-homologous end-joining (c-NHEJ) pathway of DNA DSB repair³⁰. The DSB formation results in recruitment of the MRN complex (composed of MRE11, RAD50, and NBS1)³¹. The *Artemis* deficiency in v-Abl pre-B cells treated with STI571 enabled detection of unrepaired DSB as *Artemis* functions as an endonuclease providing a hairpin opening activity³². Using this model, we took advantage of DSB accumulation, and thus accumulation of MRN members including NBS1 near the DSBs. Importantly, based on the experiments including wildtype v-Abl-transformed mouse pre-B cells, *Artemis* deficiency proved to be instrumental in the robust detection of RAG1/2-dependent DSBs (data not shown).

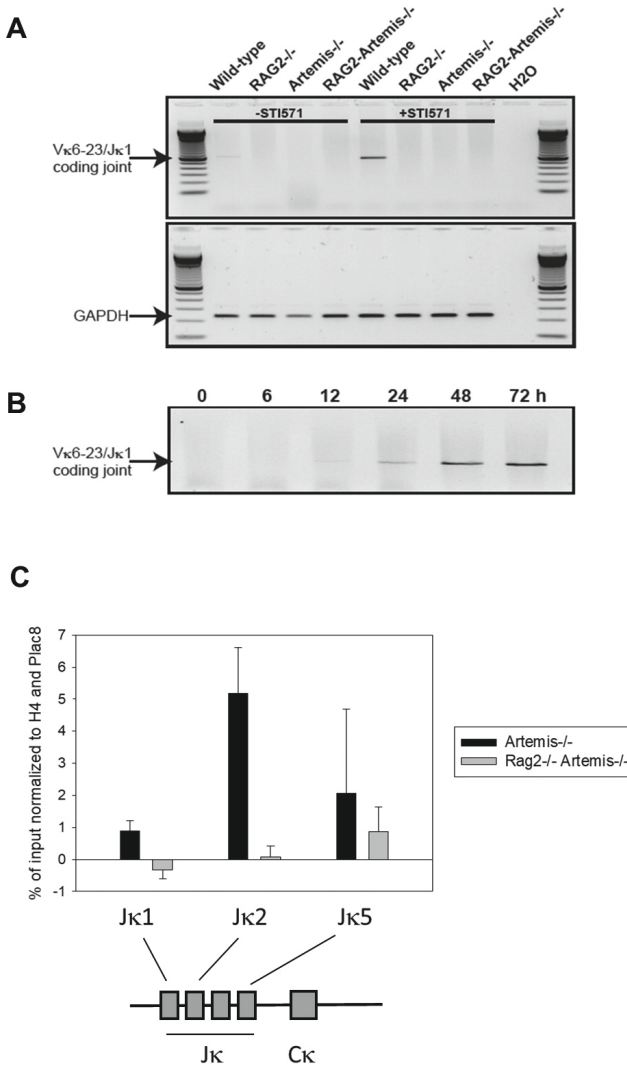
The suitability of the model to interrogate RAG targeting was tested by assessing the binding of NBS1 protein to *Jk* regions by chromatin immunoprecipitation (ChIP) of NBS1 at J_κ1, J_κ2 and J_κ5, and normalized to binding to *Plac8* intronic region, used as a control region,

► Figure 1.

(A) Wildtype (WT), *Rag2*^{-/-} (R2K3), *Artemis*^{-/-} (AH2) and *Artemis*^{-/-}*Rag2*^{-/-} (R2K.Art) v-Abl cells were treated with 5μM STI571 for 72h. Following the treatment, the recombination products of RAG1/2 activity were confirmed by assessing the presence of V_κ6-23/J_κ1 recombination with the means of PCR. The PCR products were analyzed on agarose gel stained with ethidium bromide. GAPDH was used as a housekeeping gene. **(B)** Wildtype v-Abl cells were treated with 5μM STI571 for 6h, 12h, 24h, 48h, and 72h. The presence of V_κ6-23/J_κ1 recombination can be detected as early as 24h following the STI571 treatment with the means of PCR. The PCR products were analyzed on agarose gel stained with ethidium bromide. GAPDH was used as a housekeeping gene. **(C)** Binding of NBS1 protein to DNA was assessed by chromatin-immunoprecipitation (ChIP). Even though no productive recombination takes place in *Artemis*^{-/-} cells (AH2), RAG1/2 endonuclease still creates DSBs at the *Igk* locus, thus prompting the NBS1 binding to the vicinity of the DSBs. PCR was performed on the precipitated material using J_κ1, J_κ2, and J_κ5 primer sets. The signal from NBS1 ChIP was normalized to the signal from Histone 4 (H4) ChIP, where H4 was used as a control antibody, its relative presence in both cell lines should be similar. PCR at *Plac8* was used as a negative control, this is not active in developing B cells and no accumulation of DNA breaks is expected here.

which is not expected to be a RAG1/2 recombinase hotspot. Substantially more binding to $J_{\kappa}1$ and $J_{\kappa}2$ regions was observed in *Artemis*^{-/-} cells (AH2) as compared to *Artemis*^{-/-}*Rag2*^{-/-} cells (R2K.Art). The binding of NBS1 to the *Plac8* control region was low and there was no notable difference between *Artemis*^{-/-} (AH2) and *Artemis*^{-/-}*Rag2*^{-/-} (R2K.Art) (**Figure 1C**).

To identify RAG off-targets on a genome-wide scale, we performed NBS1 ChIP followed by subsequent massive parallel sequencing of all immunoprecipitated material. The NBS1 ChIP-Seq reads were robustly accumulated at the *Ig* κ region on chromosome 6 (**Figure 2A**) in RAG1/2 proficient cells (AH2), whereas no accumulation of NBS1 reads is observed in RAG2-deficient cell line (R2K.Art). Input samples show only a background level of NBS1 reads at this region.



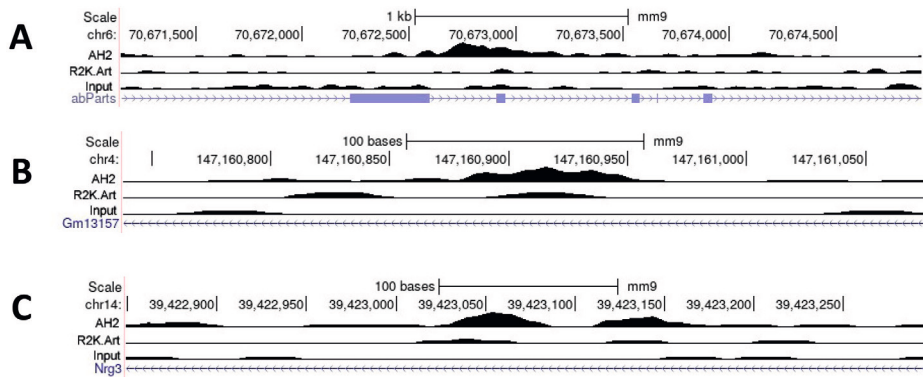


Figure 2.

(A) NBS1 ChIP-Seq in *Artemis*^{-/-} cells (AH2) and *Artemis*^{-/-}*Rag2*^{-/-} (R2K.Artm) cells showing *Igk* locus at chromosome 6. Distinct accumulation of reads in the AH2 cell line, and their absence in R2K.Artm cell line in this region, suggests that NBS1 binding, and thus the presence of DSBs at this locus is only found in the Rag-proficient cell line. Input ChIP-Seq sample shows the background level of the mapped reads. (B) and (C) examples of 2 NBS1 peaks outside of the *Ig* loci: chromosome 4 (147160850-147160999) and chromosome 14 (39423000-39423149), where AH2 shows the NBS1 reads in RAG-proficient cell line, R2K.Art shows the NBS1 reads in the RAG-deficient cell line and an untreated input sample shows the background levels of NBS1 in these regions.

In STI571-treated v-Abl cells, the *Igk* locus undergoes gene rearrangement, which was reflected in the frequency of RAG-dependent NBS1 peaks in this region, which was 8.8-fold higher (4.85 breaks per million bp) than the frequency of the RAG-dependent NBS1 peaks throughout the whole mouse genome (0.55 breaks per million bp; $p < 0.001$). Interestingly, we also found a hotspot at the *Igh* locus on chromosome 12, showing 33.1 fold higher frequency of RAG-dependent NBS1 peaks (18.2 peaks per million bp; $p < 0.001$), as compared to 0.5 peaks per million bp in the rest of the genome (SUPPL Table 1A), which is a 33-fold difference ($p < 0.001$), suggesting simultaneous RAG1/2 activity at *Igh* and the immunoglobulin light chain (*Ig*). This is rather unexpected as the v-Abl transformed pro-B cells have previously been shown to contain rearranged *Igh*, which should prevent any subsequent recombination on this locus¹⁸.

RAG1/2 induces DNA breaks outside of *Igk* locus

Using our approach, 1489 RAG-dependent NBS1 peaks were identified throughout the genome, 95,3% of which were located outside of the *Ig* loci (Figure 2B and Figure 2C are examples of RAG-specific NBS1 peaks identified outside of the *Igk* locus, SUPPL Table 2 for a complete overview of the RAG-specific NBS1 peaks). Interestingly, some of the RAG-specific NBS1 ChIP-Seq peaks, next to the 2 hotspots (*Igk* and *Igh*), were localized in or near

genes previously associated with B-cell malignancies in mouse and human, such as *Ikzf4*, *Abl2*, *Klf4*, *Tcf4*, *Tcf7*, *Rassf8*, *Mef2c*³³⁻³⁹ or involved in DNA repair, *Rad51ap1*⁴⁰ (**SUPPL Table 2**).

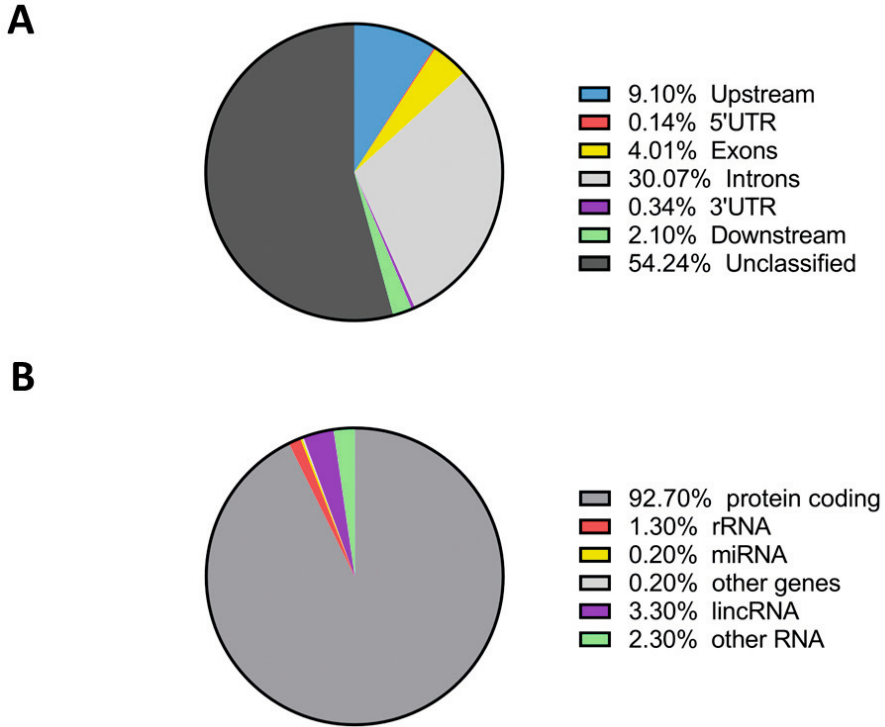


Figure 3.

(A) Pie chart showing the distribution of RAG1/2-dependent NBS1 peaks according to position within genes. (B) Pie chart showing the distribution of RAG1/2-dependent NBS1 peaks according to gene categories.

Of the 1489 RAG-dependent NBS1 peaks, 1473 peaks were annotated, of which 45,9% (674 of 1473) were associated with known genes. Of all the peaks, 4% (59 of 1473) were located in the gene exons and 30% (443 of 1473) were located in the gene introns (**Figure 3A**). 92.7% of genes that contained NBS1 peaks were protein-coding genes, the rest of the genes (7.3%) containing NBS1 peaks were regions coding for miRNA, rRNA, lincRNA, or other types of RNA (**Figure 3B**). Finally, 799 of 1473 RAG-dependent NBS1 peaks were not associated with any known genes.

Enrichment of cRSS motif at NBS1 binding sites at *Igκ*, but not in the rest of the genome

Simple Enrichment Analysis (SEA) of the canonical RSS in sequences directly at the RAG-specific NBS1 peaks, showed no significant enrichment for the nonamer 5'-ACAAAAACC-3', nor for the heptamer 5'-CACAGTG-3' (false discovery rate expressed as q-values > 0.05). Similar results were obtained when analyzing the sequences directly under the NBS1 peaks in the subset of *Igκ* peaks (**Figure 4A**), suggesting that NBS1 binding sites do not strictly co-localize with RSSs. We then extended the region around each NBS1 peak on each end by an additional 500bps or 1000bps, respectively. In the subset of 500bp-extended NBS1 peaks at the *Igκ* locus, a significant enrichment for both canonical RSS motifs was observed (3.75-fold enrichment of 5'-CACAGTG-3', $q=0.0006$ and 3.5-fold enrichment of 5'-ACAAAAACC-3' $q=0.0023$) (**Figure 4B**). The enrichment of the nonamer motif 5'-ACAAAAACC-3' further increased in the 1000bp-extended subset of NBS1 peaks at *Igκ* locus (4.67-fold enrichment, $q=0.0005$), whereas the enrichment of the heptamer motif CACAGTG in the 1000bp-extended dataset was lower compared to the 500bp-extended sequences (3.75-fold vs. 1.78-fold; q -values < 0.05) (**Figure 4C**). The nonamer, but not the heptamer, was also found to be moderately enriched in the 1000bp-extended sequences outside of the *Igκ* loci (enrichment ratio 1.69 q -value < 0.01) (**SUPPL Table 1B**).

Zinc-finger binding sites are the most dominant motifs associated with RAG-mediated DNA breaks

Next, we employed MEME motif analysis to identify motifs associated with the RAG-dependent NBS1 peak sequences directly under the peaks and in the 500bp- and 1000bp-extended sequences. Two unique motifs were identified in the sequences directly under the NBS1 peaks; 15 motifs in the 500bp-extended NBS1 peak sequences, and 41 motifs in the 1000bp-extended dataset (**SUPPL Table 1C**), p - and q - values cut-offs were both set to 0.05. Not all the identified motifs are known motifs already associated with specific protein binding sites. In the sequences directly under the NBS1 peaks (0bp off-set), 1 known motif was identified (CTGAGTTCVAGGCCA) (**Figure 5A**), in the sequences with 500bp off-set 3 known motifs were identified (CTGCCTCTGCCTCCC, CCCACCCACYCC, CCCTCCCCC) (**Figure 5B**) and 4 different motifs were identified in the sequences with 1000bp off-set (GAGTTC SAGGMCAGC, CCCACCCMC, CCCTCCCTCCCC, TATATATATATA) (**Figure 5C**). Though other associated motifs are not known protein binding sites, amongst these other motifs we observed several simple repeat motifs, such as CTCTCTCTCTCTCTC, ACACACACACACACA (**SUPPL Table 1C**). Except for the TATA-box binding motif (TATATATATATA) the rest of the known motifs are zinc-finger type motifs, and which are shared by multiple transcription factors or DNA binding proteins, amongst which proteins that play a role in

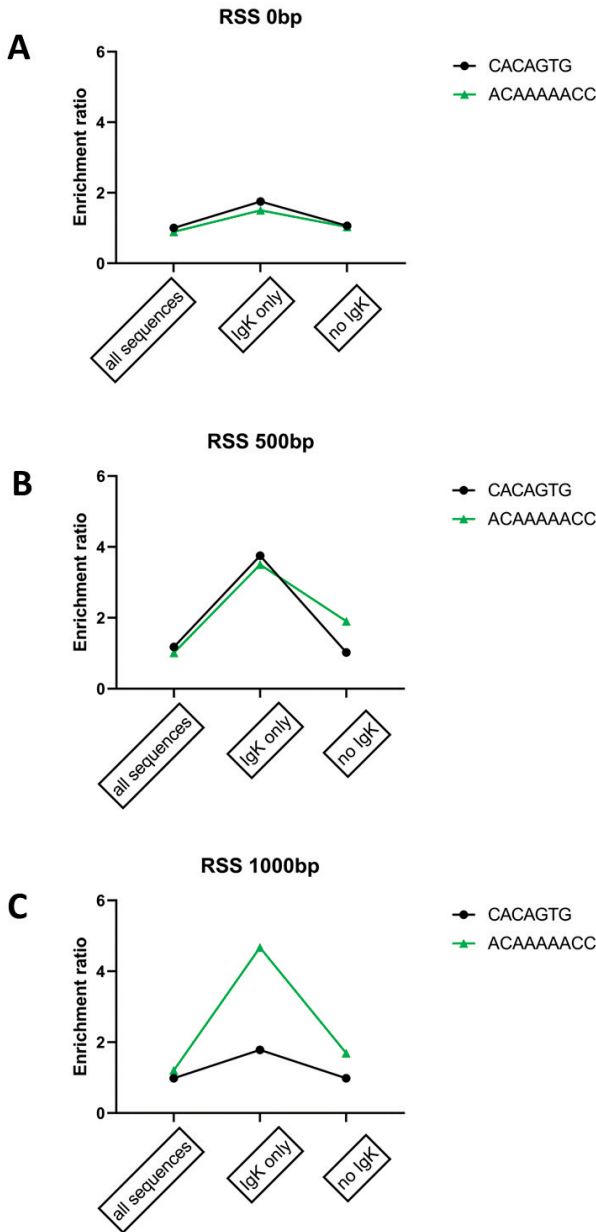


Figure 4.

Graphs showing the enrichment ratios of canonical RSS sequences (CACAGTG and ACAAAAACC) within RAG1/2-dependent NBS1 peaks, divided into 3 subsets: ‘all sequences’, ‘*IgK* only’ and in a subset where the *IgK* locus peaks were excluded (“no *IgK*”). The enrichment of canonical RSS sequences in these subsets was analyzed in sequences directly under NBS1 peaks (**A**), sequences extended by 500bp at each end (**B**), and sequences extended by 1000bp at each end (**C**).

DNA damage repair such as PRDM9, EGR1, MAZ or RREB1^{41–44}, in p53 signaling or apoptosis such as PATZ1 or SP1^{45,46}, or in B-cell development and proliferation such as KLF4⁴⁷.

RAG-dependent DNA breaks localized close to SSR such as CA- and GC-rich sequences

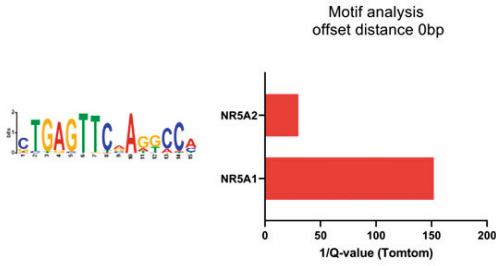
Several of the motifs identified by the unsupervised Simple, Thorough, Rapid, Enriched Motif Elicitation (STREME) analysis indicated an association with simple sequence repeats (SSR). SSRs have previously been associated with the formation of non-canonical (non-B) DNA structures, such as quadruplexes, hairpins, cruciform or triple-stranded DNA^{48,49}, and were suggested to be a possible target of RAG1/2 recombinase⁵⁰. Therefore, we investigated the presence of GA and CA repeats around the RAG-dependent NBS1 binding sites. Using unsupervised SEA analysis, each dataset was interrogated for the presence of [CACA]₁₋₂₀ and [GAGA]₁₋₂₀ repeats, where increases from 1 up to 20, the maximum repeat length corresponding to half of the average NBS1 peak length without any extension. While no notable enrichment for CA or GA repeats was observed in sequences directly under the peaks (**Figure 6A**), both 500bp and 1000bp-extended NBS1 peaks showed strong enrichment of both CA and GA repeats (**Figure 6B and 6C**).

Next to the SSR, GC-rich regions are also known to assume structures such as hairpins, cruciform or triple-stranded DNA, and the GC-rich motif 5'-GCCGCCGGGCG-3' was identified as RAG1/2 transposition hotspot^{51,52}. We next investigated the presence of this transposition hotspot motif, and 1 to 5 repeats thereof [5'-GCCGCCGGGCG-3']_{1-5'} around the putative RAG-off target DSBs. While no enrichment (all q-values > 0.05) has been identified in sequences directly under the RAG-dependent NBS1 peaks (**Figure 7A**), a moderate enrichment of 1.3-11 fold (q-value < 0.05) was found in the peaks with 500bp offset and 1.5-15 fold in the peaks with 1000bp offset (**Figure 7B and 7C**), further underscoring the strong association of RAG1/2 (off-) targets with the repeat regions.

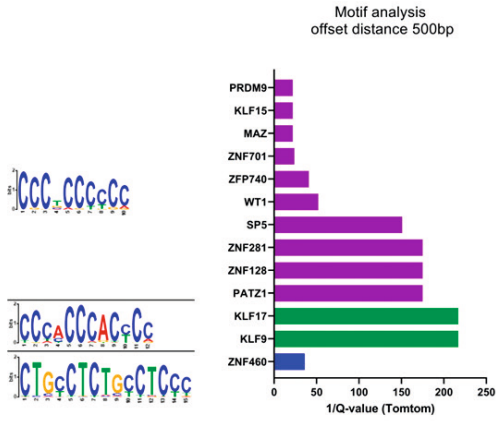
► Figure 5.

Motif analysis of RAG1/2-dependent NBS1 peaks motif logos are shown on the left side. For each motif, additional Tomtom analysis was performed to compare the obtained motif to known motifs (graphs on the right-hand side) in not extended NBS1 peak sequences (**A**), in sequences extended by 500bp on each end (**B**), and in sequences extended by 1000bp on each end (**C**).

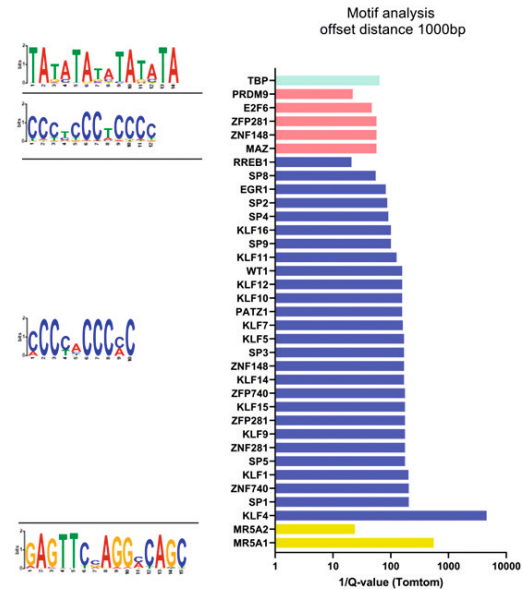
A

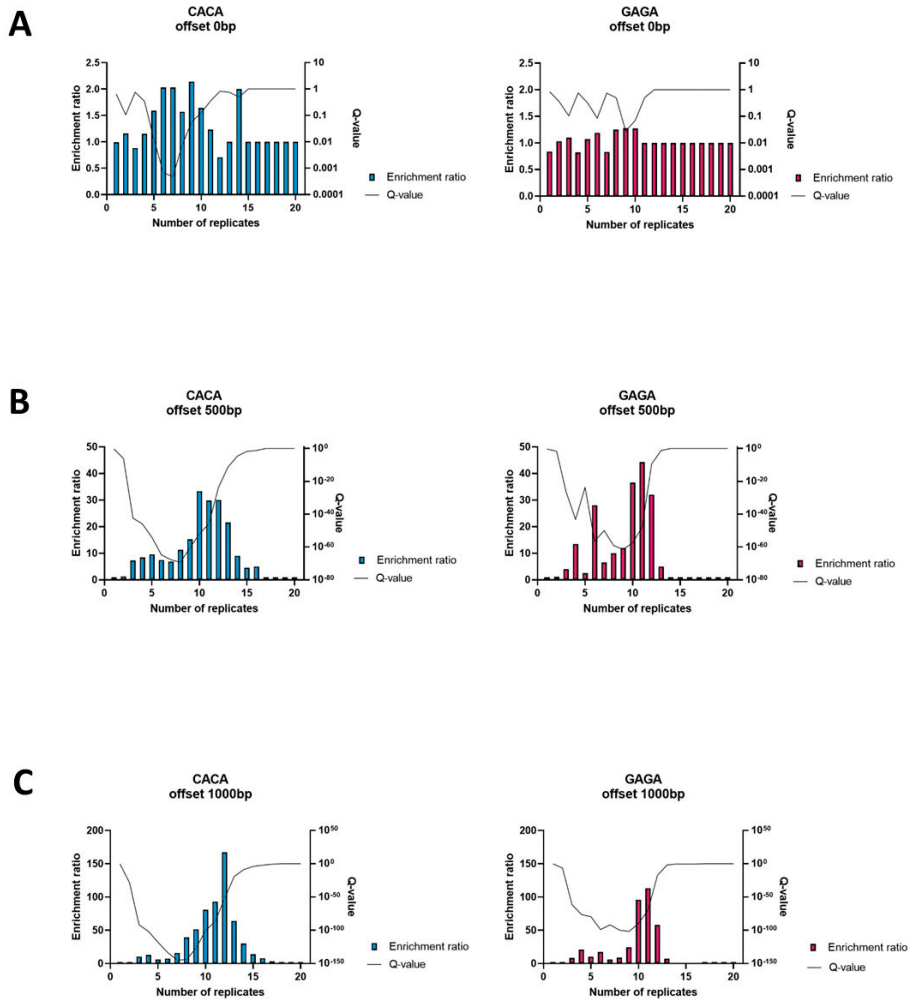


B

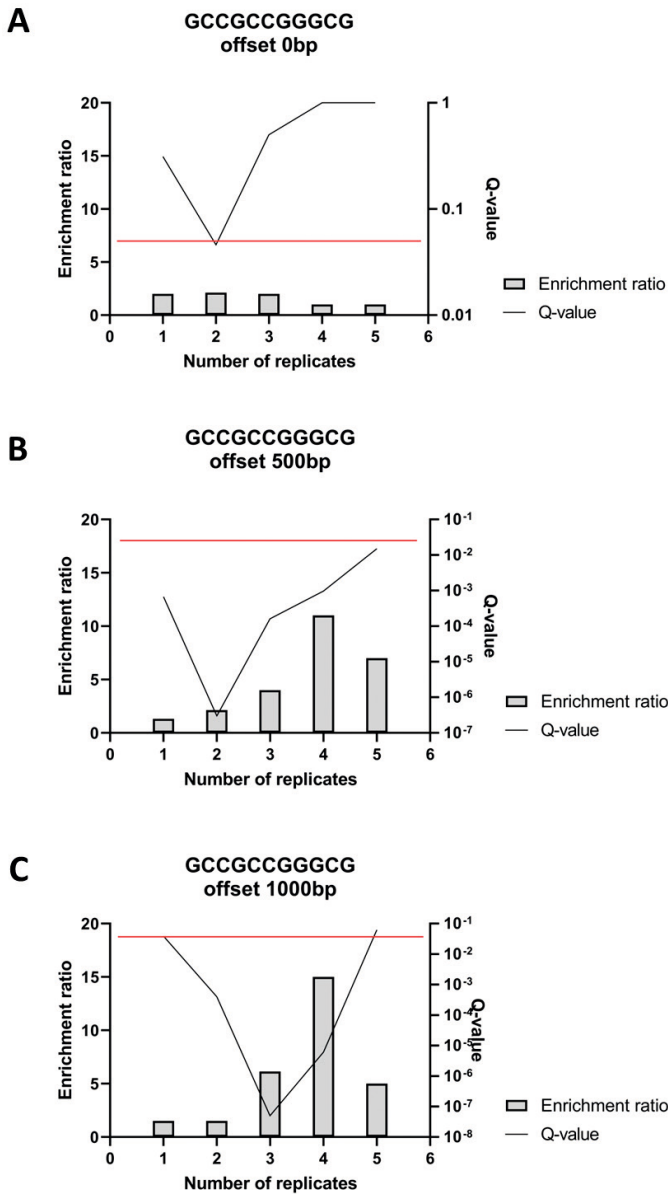


C



**Figure 6.**

Graphs depicting enrichment ratios of sequence motif $(CACA)_n$ and $(GAGA)_n$ repeats versus the number of repeats (repeat replicates: x-axis) in non-extended RAG1/2-dependent NBS1 peaks **(A)**, NBS1 peak sequences extended by 500bp **(B)** and by 1000bp **(C)** on each end. In all graphs, the left y-axis shows the enrichment ratios and the right y-axis shows the q-values, $q < 0.05$ was considered as the cut-off for minimal false discovery rate (FDR).

**Figure 7.**

Graphs depicting the enrichment ratios (y-axis) of known GC-rich RAG1 transposition hotspot (5'-GCCGCCGGGCG-3')_n versus the number of repeats (repeat replicates: x-axis) in non-extended RAG1/2-dependent NBS1 peaks (A), NBS1 peak sequences extended by 500bp (B) and by 1000bp (C) on each end. In all graphs, the left y-axis shows the enrichment ratios and the right y-axis shows the q-values, $q < 0.05$ was considered as the cut-off for minimal false discovery rate (FDR). The red line depicts the $q = 0.05$ cut-off value.

Discussion

In the past, the prevailing thought was that RAG1/2 binding and activity were restricted to regions containing RSSs, such as the immunoglobulin loci, and that this restriction limits the potential genotoxic threat of RAGs. However, in the last decade, it has been shown that RAG1 and RAG2 can bind DNA throughout the genome and that their DNA cleaving activity might not only be limited to the canonical RSS sequences. Using NBS1 as a surrogate marker for DSBs, we identified RAG1/2-specific DSBs in a mouse v-Abl cell line at the genome-wide scale. The off-target activity was examined through differential binding of NBS1 to DNA in RAG-proficient and RAG2-deficient cell lines, which lack the capacity to resolve the DSBs due to the absence of Artemis. This model allowed us to interrogate the DSBs in the chromosomal context of living pre-B cells undergoing *Ig* recombination. In the previous studies, RAG1 was shown to bind to ~3400 sites in mouse pre-B cells⁵³ and RAG2 to ~18300 sites throughout the mouse genome⁵³. In our study we identified only 1489 putative RAG1/2 DSBs, suggesting that binding or co-localization of RAG1 and RAG2 does not necessarily result in the creation of DSBs.

Next to *Igκ*, an accumulation of RAG-specific NBS1 peaks was observed at the *Igh* locus on chromosome 12. The v-Abl cell line has previously been shown to be arrested in a stage where the *Igh* recombination has already taken place¹⁸. B-cells ensure the preservation of successfully recombined *Igh* by allelic exclusion, not allowing any subsequent heavy chain recombination on the other allele⁵⁴. The abundant presence of NBS1 at the *Igh* region in this experimental set-up suggests that RAG1/2 endonuclease continues to introduce DSBs in this region following the treatment of the v-Abl cells with STI571 and their subsequent transition from pro to pre-B cell stage. Some of the earlier work suggests that v-Abl transformants are able to initiate but not terminate recombination⁵⁵. It has been suggested that v-Abl antagonizes the pre-B cell signaling pathway and the pre-B cells containing one functional *Igh* allele continue to transcribe and rearrange the allelic, unrecombined *Igh* locus, thus not adhering to the allelic exclusion rule⁵⁶. In addition, subsequent work showed that B cells with functional B-cell receptors may continue the recombination and “edit” their specificity, allowing the cells with auto-reactive receptors to escape their elimination⁵⁷.

The off-target activity of RAG1/2 has been associated with a number of genomic lesions often seen in B-ALL cases. Though our data showed RAG-dependent NBS1 peaks in the proximity of genes associated with B-cell malignancies, the genes that are most frequently translocated in B-ALL (ETV6/RUNX1 or BCR/ABL1) or deleted (E2A, EBF1, LEF1, IKZF1 or IKZF3)^{5-7,11} were not identified in our model. This could be attributed to several factors, for instance, differences in murine and human chromatin configuration, or to the fact that the v-Abl B cell line has already acquired the transforming genomic event, which may have changed the accessibility of some of the genes that are frequently translocated in human patients. Furthermore, only 2.7% of the RAG1/2-dependent NBS1 peaks (**SUPPL**

Table 3A and 3B) overlapped with the publicly available RAG1 ChIP-seq peaks published by another group¹³. The cells used for the previously reported RAG1 ChIP-seq were primary mouse pre-cells, whose DNA damage-response pathways are unimpaired, as opposed to the *Artemis*^{-/-} cell line used in our study, where the absence of Artemis would cause accumulation of the DNA breaks. In primary WT pre-B cells, the DSBs (including those caused by RAG1/2) would be efficiently repaired, which would perhaps result in a RAG1 binding pattern than in *Artemis*^{-/-} cells. Also, the binding of RAG1 to a certain place in the genome of WT bone marrow pre-B cells might be transient and represent a “snap-shot” at a particular time point, which could explain the low overlap degree. It should also be noted that our analyses represent a collective portrayal of the cell population and it remains uncertain to what degree the individual lymphocytes mirror the population averages as shown by the ChIP-seq.

The association of genomic lesions in B-ALL to RAG1/2 activity is based either on the proximity of conserved RSS near the breakpoint, the presence of N-nucleotides which are reminiscent of V(D)J joints at the breakpoints, or the proximity of the breakpoints to cRSS^{10,12}. Though sequences directly under the RAG-dependent NBS1 peaks did not show enrichment for RSSs, we found a clear enrichment especially for nonamers, and in a lesser extent also for heptamers 500bp and 1000bp around the NBS1 peaks on *Igκ* locus. In the rest of the genome a moderate enrichment for the nonamer, but not the heptamer, was observed. This seems to be in line with the observation that nonamers, but not heptamers, are enriched in the proximity of RAG1 binding regions in mouse v-Abl cell lines and mouse thymocytes¹³. Interestingly, the nonamer was found mostly enriched in the sequences with 1000bp offset, while the heptamer was mostly enriched in the sequences with 500bp offset. Though MRN complex, including NBS1, binds the DNA at the broken ends⁵⁸, it is possible that the association of NBS1 with the DNA around the DSBs takes place a few hundred bps away from the actual break, as also suggested by the NBS1-chromatin binding studies⁵⁹.

The motifs identified around RAG-dependent NBS1 peaks were associated with various zinc-finger binding domains, the most common structural motif in eukaryotic cells. Most of the known motifs were shared by several transcription factors or DNA-binding proteins. Interestingly, several of the identified motifs were known binding sites of DNA repair proteins, such as PRDM9, EGR1, MAZ, or RREB1⁴¹⁻⁴⁴, or transcription factors involved in p53 signaling and apoptosis such as PATZ1 or SP1^{45,46}, on one hand suggesting the susceptibility of these regions to RAG-mediated damage, on the other hand underscoring the potential threat that RAG1/2 off-target activity can inflict. Another identified motif was associated with MYC-associated zinc finger protein (MAZ), a transcription factor regulating the MYC oncogene expression and affecting large-scale genome organization through interaction with cohesin⁶⁰. Part of the MAZ binding motif is partially shared by other transcription

factors such as SP1⁶¹, which is also reflected in our findings (**Figure 5C**), this motif is also CG-rich, which further emphasizes the preference of RAG for GC-rich motifs.

Next to RSS enrichment, we found a strong enrichment for CA and GA simple repeats around the RAG-dependent NBS1 peaks. Repeat DNA has been associated with alternative, non-B DNA structures, which often assume an open chromatin configuration and are also prone to the acquisition of mutations⁶². Such DNA structures are thought to contribute to genomic instability, for instance, H-DNA forming regions have been identified near the breakpoints of the translocated *c-myc* in Burkitt's lymphoma and *t(12;15)* BALB/c plasmacytomas⁶³. Non-B DNA structures were also identified around the *Bcl-2* major breakpoint region (Mbr), where the RAG complex was shown to bind and nick at duplex–single-strand transitions of non-B DNA structures, resulting in double-strand breaks *in vitro*, thus demonstrating the transposase activity of RAGs¹². RAG1/2 has been shown to cleave non-B cell structure without the presence of RSS, thus also functioning as a structure-specific endonuclease⁵⁰. In fact, CA repeats have previously been shown to be a type of cRSS (mimicking the nonamer and the heptamer) and target of RAG1/2 activity, thus inadvertently introducing DNA breaks at CA-rich sites^{14,66}. A more recent study has even demonstrated that the Znc2 domain of RAG1 is required for binding to non-B DNA structures; mutations introduced in this domain hindered the nicking capacity of the endonuclease on DNA quadruplexes and single-stranded regions.⁶⁷ Therefore, the presence of the CA repeat regions and the GC-rich regions around the RAG-dependent NBS1 peaks may reflect the off-target activity of RAGs at the non-B DNA structures.

Taken together, RAG1/2 is able to introduce DNA breaks on non-*Ig* and repeat regions are one of the common denominators of the off-target lesions. Non-B DNA structures, previously also implicated in the off-target activity of AID in mature B cells⁶⁵, are more prone to DNA damage, putting lymphocytes under additional DNA damage stress during their development and maturation.

Acknowledgements

We thank Linda Koster, Core Facility Genomics, Amsterdam UMC, for helping with sample handling and library preparations. We also thank Ing. Ivan Mackovic EUR ING for providing a server space for the sequencing data, and to Ing. Jakub Mackovic for developing and testing a Python script to analyze the overlap between different ChIP-Seq peak data sets.

References

- Schatz DG, Swanson PC. V(D)J recombination: mechanisms of initiation. *Annu Rev Genet.* 2011;45:167-202. doi:10.1146/annurev-genet-110410-132552
- Zhao B, Rothenberg E, Ramsden DA, Lieber MR. The molecular basis and disease relevance of non-homologous DNA end joining. *Nat Rev Mol Cell Biol.* 2020;21(12):765-781. doi:10.1038/s41580-020-00297-8
- Lieber MR. The mechanism of double-strand DNA break repair by the nonhomologous DNA end-joining pathway. *Annu Rev Biochem.* 2010;79:181-211. doi:10.1146/annurev.biochem.052308.093131
- Bian L, Meng Y, Zhang M, Li D. MRE11-RAD50-NBS1 complex alterations and DNA damage response: implications for cancer treatment. *Mol Cancer.* 2019;18(1):169. doi:10.1186/s12943-019-1100-5
- Kaczmarek A, Derebas J, Pinkosz M, Niedźwiecki M, Lejman M. The Landscape of Secondary Genetic Rearrangements in Pediatric Patients with B-Cell Acute Lymphoblastic Leukemia with t(12;21). *Cells.* 2023;12(3). doi:10.3390/cells12030357
- Yeung DTO, Osborn MP, White DL. B-cell acute lymphoblastic leukaemia: recent discoveries in molecular pathology, their prognostic significance, and a review of the current classification. *Br J Haematol.* 2022;197(1):13-27. doi:10.1111/bjh.17879
- Ryan SL, Peden JF, Kingsbury Z, et al. Whole genome sequencing provides comprehensive genetic testing in childhood B-cell acute lymphoblastic leukaemia. *Leukemia.* 2023;37(3):518-528. doi:10.1038/s41375-022-01806-8
- Hunger SP, Mullighan CG. Acute Lymphoblastic Leukemia in Children. *N Engl J Med.* 2015;373(16):1541-1552. doi:10.1056/NEJMra1400972
- Malczewska M, Kośmider K, Bednarz K, Ostapińska K, Lejman M, Zawitkowska J. Recent Advances in Treatment Options for Childhood Acute Lymphoblastic Leukemia. *Cancers (Basel).* 2022;14(8). doi:10.3390/cancers14082021
- Wiemels J. Chromosomal translocations in childhood leukemia: natural history, mechanisms, and epidemiology. *J Natl Cancer Inst Monogr.* 2008;(39):87-90. doi:10.1093/jncimonographs/lgn006
- Papaemmanuil E, Rapado I, Li Y, et al. RAG-mediated recombination is the predominant driver of oncogenic rearrangement in ETV6-RUNX1 acute lymphoblastic leukemia. *Nat Genet.* 2014;46(2):116-125. doi:10.1038/ng.2874
- Wiemels JL, Leonard BC, Wang Y, et al. Site-specific translocation and evidence of postnatal origin of the t(1;19) E2A-PBX1 fusion in childhood acute lymphoblastic leukemia. *Proc Natl Acad Sci U S A.* 2002;99(23):15101-15106. doi:10.1073/pnas.222481199
- Teng G, Maman Y, Resch W, et al. RAG Represents a Widespread Threat to the Lymphocyte Genome. *Cell.* 2015;162(4):751-765. doi:10.1016/j.cell.2015.07.009
- Maman Y, Teng G, Seth R, Kleinstein SH, Schatz DG. RAG1 targeting in the genome is dominated by chromatin interactions mediated by the non-core regions of RAG1 and RAG2. *Nucleic Acids Res.* 2016;44(20):9624-9637. doi:10.1093/nar/gkw633
- Rahman NS, Godderz LJ, Stray SJ, Capra JD, Rodgers KK. DNA cleavage of a cryptic recombination signal sequence by RAG1 and RAG2. Implications for partial V(H) gene replacement. *J Biol Chem.* 2006;281(18):12370-12380. doi:10.1074/jbc.M507906200
- Zhang M, Swanson PC. V(D)J recombinase binding and cleavage of cryptic recombination signal sequences identified from lymphoid malignancies. *J Biol Chem.* 2008;283(11):6717-6727. doi:10.1074/jbc.M710301200

17. Khair L, Baker RE, Linehan EK, Schrader CE, Stavnezer J. Nbs1 ChIP-Seq Identifies Off-Target DNA Double-Strand Breaks Induced by AID in Activated Splenic B Cells. *PLoS Genet.* 2015;11(8):e1005438. doi:10.1371/journal.pgen.1005438
18. Muljo SA, Schlissel MS. A small molecule Abl kinase inhibitor induces differentiation of Abelson virus-transformed pre-B cell lines. *Nat Immunol.* 2003;4(1):31-37. doi:10.1038/ni870
19. Bredemeyer AL, Sharma GG, Huang CY, et al. ATM stabilizes DNA double-strand-break complexes during V(D)J recombination. *Nature.* 2006;442(7101):466-470. doi:10.1038/nature04866
20. Ochodnicka-Mackovicova K, Bahjat M, Maas C, et al. The DNA Damage Response Regulates RAG1/2 Expression in Pre-B Cells through ATM-FOXO1 Signaling. *J Immunol.* 2016;197(7):2918-2929. doi:10.4049/jimmunol.1501989
21. Savic V, Yin B, Maas NL, et al. Formation of dynamic gamma-H2AX domains along broken DNA strands is distinctly regulated by ATM and MDC1 and dependent upon H2AX densities in chromatin. *Mol Cell.* 2009;34(3):298-310. doi:10.1016/j.molcel.2009.04.012
22. El-Sheikh Ali H, Scoggin K, Linhares Boakari Y, et al. Kinetics of placenta-specific 8 (PLAC8) in equine placenta during pregnancy and placentitis. *Theriogenology.* 2021;160:81-89. doi:10.1016/j.theriogenology.2020.10.041
23. Tanaka TS, Jaradat SA, Lim MK, et al. Genome-wide expression profiling of mid-gestation placenta and embryo using a 15,000 mouse developmental cDNA microarray. *Proc Natl Acad Sci U S A.* 2000;97(16):9127-9132. doi:10.1073/pnas.97.16.9127
24. Langmead B, Trapnell C, Pop M, Salzberg SL. Ultrafast and memory-efficient alignment of short DNA sequences to the human genome. *Genome Biol.* 2009;10(3):R25. doi:10.1186/gb-2009-10-3-r25
25. Zhang Y, Liu T, Meyer CA, et al. Model-based analysis of ChIP-Seq (MACS). *Genome Biol.* 2008;9(9):R137. doi:10.1186/gb-2008-9-9-r137
26. Huang W, Loganantharaj R, Schroeder B, Fargo D, Li L. PAVIS: a tool for Peak Annotation and Visualization. *Bioinformatics.* 2013;29(23):3097-3099. doi:10.1093/bioinformatics/btt520
27. Bailey TL. STREME: accurate and versatile sequence motif discovery. *Bioinformatics.* 2021;37(18):2834-2840. doi:10.1093/bioinformatics/btab203
28. Gupta S, Stamatoyannopoulos JA, Bailey TL, Noble WS. Quantifying similarity between motifs. *Genome Biol.* 2007;8(2):R24. doi:10.1186/gb-2007-8-2-r24
29. Timothy L. Bailey and Charles E. Grant. SEA: Simple Enrichment Analysis of motifs. *BioRxiv.* Published online 2021.
30. Rooney S, Chaudhuri J, Alt FW. The role of the non-homologous end-joining pathway in lymphocyte development. *Immunol Rev.* 2004;200:115-131. doi:10.1111/j.0105-2896.2004.00165.x
31. Stracker TH, Theunissen JWF, Morales M, Petrini JHJ. The Mre11 complex and the metabolism of chromosome breaks: the importance of communicating and holding things together. *DNA Repair (Amst).* 2004;3(8-9):845-854. doi:10.1016/j.dnarep.2004.03.014
32. Wang J, Pluth JM, Cooper PK, Cowan MJ, Chen DJ, Yannone SM. Artemis deficiency confers a DNA double-strand break repair defect and Artemis phosphorylation status is altered by DNA damage and cell cycle progression. *DNA Repair (Amst).* 2005;4(5):556-570. doi:10.1016/j.dnarep.2005.02.001
33. Xia R, Cheng Y, Han X, Wei Y, Wei X. Ikaros Proteins in Tumor: Current Perspectives and New Developments. *Front Mol Biosci.* 2021;8:788440. doi:10.3389/fmolb.2021.788440
34. Canté-Barrett K, Meijer MT, Cordo' V, et al. MEF2C opposes Notch in lymphoid lineage decision and drives leukemia in the thymus. *JCI insight.* 2022;7(13). doi:10.1172/jci.insight.150363

35. Roberts KG. Genetics and prognosis of ALL in children vs adults. *Hematol Am Soc Hematol Educ Progr.* 2018;2018(1):137-145. doi:10.1182/asheducation-2018.1.137
36. Jain N, Roberts KG, Jabbour E, et al. Ph-like acute lymphoblastic leukemia: a high-risk subtype in adults. *Blood.* 2017;129(5):572-581. doi:10.1182/blood-2016-07-726588
37. Kharas MG, Yusuf I, Scarfone VM, et al. KLF4 suppresses transformation of pre-B cells by ABL oncogenes. *Blood.* 2007;109(2):747-755. doi:10.1182/blood-2006-03-011106
38. Rohil Y, Shetty D, Narula G, Banavali SD. A Novel Case of ABL2 Chromosomal Rearrangement in High-Risk B-Cell Acute Lymphoblastic Leukemia. *J Assoc Genet Technol.* 2019;45(2):73-76.
39. Volodko N, Gordon M, Salla M, Ghazaleh HA, Baksh S. RASSF tumor suppressor gene family: biological functions and regulation. *FEBS Lett.* 2014;588(16):2671-2684. doi:10.1016/j.febslet.2014.02.041
40. Bridges AE, Ramachandran S, Pathania R, et al. RAD51AP1 Deficiency Reduces Tumor Growth by Targeting Stem Cell Self-Renewal. *Cancer Res.* 2020;80(18):3855-3866. doi:10.1158/0008-5472.CAN-19-3713
41. Wang B, Guo H, Yu H, Chen Y, Xu H, Zhao G. The Role of the Transcription Factor EGR1 in Cancer. *Front Oncol.* 2021;11:642547. doi:10.3389/fonc.2021.642547
42. Paigen K, Petkov PM. PRDM9 and Its Role in Genetic Recombination. *Trends Genet.* 2018;34(4):291-300. doi:10.1016/j.tig.2017.12.017
43. Deng YN, Xia Z, Zhang P, Ejaz S, Liang S. Transcription Factor RREB1: from Target Genes towards Biological Functions. *Int J Biol Sci.* 2020;16(8):1463-1473. doi:10.7150/ijbs.40834
44. Wang T, Zhu X, Wang K, et al. Transcriptional factor MAZ promotes cisplatin-induced DNA damage repair in lung adenocarcinoma by regulating NEIL3. *Pulm Pharmacol Ther.* 2023;80:102217. doi:10.1016/j.pupt.2023.102217
45. Keskin N, Deniz E, Eryilmaz J, et al. PATZ1 Is a DNA Damage-Responsive Transcription Factor That Inhibits p53 Function. *Mol Cell Biol.* 2015;35(10):1741-1753. doi:10.1128/MCB.01475-14
46. Chuang JY, Wu CH, Lai MD, Chang WC, Hung JJ. Overexpression of Sp1 leads to p53-dependent apoptosis in cancer cells. *Int J cancer.* 2009;125(9):2066-2076. doi:10.1002/ijc.24563
47. Yusuf I, Kharas MG, Chen J, et al. KLF4 is a FOXO target gene that suppresses B cell proliferation. *Int Immunol.* 2008;20(5):671-681. doi:10.1093/intimm/dxn024
48. Zhao J, Bacolla A, Wang G, Vasquez KM. Non-B DNA structure-induced genetic instability and evolution. *Cell Mol Life Sci.* 2010;67(1):43-62. doi:10.1007/s00018-009-0131-2
49. Xu Q, Kowalski J. NBBC: a non-B DNA burden explorer in cancer. *Nucleic Acids Res.* 2023;51(W1):W357-W364. doi:10.1093/nar/gkad379
50. Naik AK, Lieber MR, Raghavan SC. Cytosines, but not purines, determine recombination activating gene (RAG)-induced breaks on heteroduplex DNA structures: implications for genomic instability. *J Biol Chem.* 2010;285(10):7587-7597. doi:10.1074/jbc.M109.089631
51. Posey JE, Pytlos MJ, Sinden RR, Roth DB. Target DNA structure plays a critical role in RAG transposition. *PLoS Biol.* 2006;4(11):e350. doi:10.1371/journal.pbio.0040350
52. Tsai CL, Chatterji M, Schatz DG. DNA mismatches and GC-rich motifs target transposition by the RAG1/RAG2 transposase. *Nucleic Acids Res.* 2003;31(21):6180-6190. doi:10.1093/nar/gkg819
53. Ji Y, Resch W, Corbett E, Yamane A, Casellas R, Schatz DG. The in vivo pattern of binding of RAG1 and RAG2 to antigen receptor loci. *Cell.* 2010;141(3):419-431. doi:10.1016/j.cell.2010.03.010
54. Vettermann C, Schlissel MS. Allelic exclusion of immunoglobulin genes: models and mechanisms. *Immunol Rev.* 2010;237(1):22-42. doi:10.1111/j.1600-065X.2010.00935.x

55. Schlissel MS, Corcoran LM, Baltimore D. Virus-transformed pre-B cells show ordered activation but not inactivation of immunoglobulin gene rearrangement and transcription. *J Exp Med*. 1991;173(3):711-720. doi:10.1084/jem.173.3.711
56. Muljo SA, Schlissel MS. Pre-B and pre-T-cell receptors: conservation of strategies in regulating early lymphocyte development. *Immunol Rev*. 2000;175:80-93.
57. Luning Prak ET, Monestier M, Eisenberg RA. B cell receptor editing in tolerance and autoimmunity. *Ann NY Acad Sci*. 2011;1217:96-121. doi:10.1111/j.1749-6632.2010.05877.x
58. Syed A, Tainer JA. The MRE11-RAD50-NBS1 Complex Conducts the Orchestration of Damage Signaling and Outcomes to Stress in DNA Replication and Repair. *Annu Rev Biochem*. 2018;87:263-294. doi:10.1146/annurev-biochem-062917-012415
59. Berkovich E, Monnat RJJ, Kastan MB. Roles of ATM and NBS1 in chromatin structure modulation and DNA double-strand break repair. *Nat Cell Biol*. 2007;9(6):683-690. doi:10.1038/ncb1599
60. Xiao T, Li X, Felsenfeld G. The Myc-associated zinc finger protein (MAZ) works together with CTCF to control cohesin positioning and genome organization. *Proc Natl Acad Sci U S A*. 2021;118(7). doi:10.1073/pnas.2023127118
61. O'Connor L, Gilmour J, Bonifer C. The Role of the Ubiquitously Expressed Transcription Factor Sp1 in Tissue-specific Transcriptional Regulation and in Disease. *Yale J Biol Med*. 2016;89(4):513-525.
62. Guiblet WM, Cremona MA, Harris RS, et al. Non-B DNA: a major contributor to small- and large-scale variation in nucleotide substitution frequencies across the genome. *Nucleic Acids Res*. 2021;49(3):1497-1516. doi:10.1093/nar/gkaa1269
63. Wang G, Vasquez KM. Naturally occurring H-DNA-forming sequences are mutagenic in mammalian cells. *Proc Natl Acad Sci U S A*. 2004;101(37):13448-13453. doi:10.1073/pnas.0405116101
64. Fortini P, Dogliotti E. Base damage and single-strand break repair: mechanisms and functional significance of short- and long-patch repair subpathways. *DNA Repair (Amst)*. 2007;6(4):398-409. doi:10.1016/j.dnarep.2006.10.008
65. Staszewski O, Baker RE, Ucher AJ, Martier R, Stavnezer J, Guikema JEJ. Activation-induced cytidine deaminase induces reproducible DNA breaks at many non-Ig loci in activated B cells. *Mol Cell*. 2011;41(2):232-242. doi:10.1016/j.molcel.2011.01.007
66. Agard EA, Lewis SM. Postcleavage sequence specificity in V(D)J recombination. *Mol Cell Biol*. 2000;20(14):5032-5040. doi:10.1128/MCB.20.14.5032-5040.2000
67. Nilavar NM, Nishana M, Paranjape AM, et al. Znc2 module of RAG1 contributes towards structure-specific nuclease activity of RAGs. *Biochem J*. 2020;477(18):3567-3582. doi:10.1042/BCJ20200361

Supplement

Supplemental Tables 1

Table showing peak enrichment on Igc and Igh locus (A), results of SEA motif analysis of the canonical RSS motifs in the dataset (B), and the results of the STREME and Tomtom motif-finding analyses of the RAG1/2-dependent NBS1 peaks (C).

Due to the table size, please use the link hereunder to view the tables, or contact the author.

<https://www.dropbox.com/scl/fi/964g6oncz7bipjvjy49k4/Chapter-3-Suppl-table-1ABC.xlsx?rlkey=wqltnna2r2phm4b1ssrpmu4is&st=a7ucxsug&dl=0>



Supplemental Table 2

List of RAG1/2-dependent NBS1 peaks. The sequencing reads were initially mapped onto the MM9 mouse genome (A). For annotation purposes, RAG1/2-dependent NBS1 peaks were lifted over to MM10 (using the UCSC Genome Browser). (B) The list of annotated peaks (those associated with known genes) in MM10. The annotation was performed using the Pavis annotation tool.

Due to the table size, please use the link hereunder to view the tables, or contact the author.

<https://www.dropbox.com/scl/fi/xtq1e4gzp1y0texb4k67w/Chapter-3-Suppl-table-2.xlsx?rlkey=cvfb0zp21tsidgavr7599v3uf&st=gx7o1j92&dl=0>



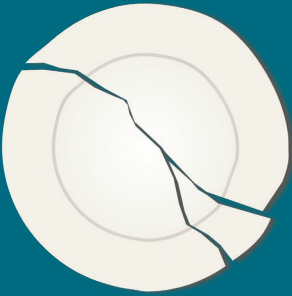
Supplemental Table 3

Using the in-house developed and tested Python algorithm, overlapping peaks were identified between the RAG1/2-dependent NBS1 peak dataset (using 1000bp, 2000bp, and 5000bp offset) (A) and the RAG1 CHIP-seq peaks in pre-B cells, available in Supplementary Table S1 (Supplement 8) of Teng G, Maman Y, Resch W, et al. RAG Represents a Widespread Threat to the Lymphocyte Genome. *Cell*. 2015;162(4):751-765. doi:10.1016/j.cell.2015.07.009. This supplement shows the list of overlapping sequences in the RAG1/2-dependent NBS1 peak dataset with 5000bp off-set (B).

Due to the table size, please use the link hereunder to view the tables, or contact the author.

<https://www.dropbox.com/scl/fi/q41tjitr2x03gwm6q729n/Chapter-3-Suppl-table-3.xlsx?rlkey=fia1wn6q5452lu5tanx1mxxog&st=tw91oxzw&dl=0>





CHAPTER

The DNA damage response regulates RAG1/2 expression in pre-B cells through ATM-FOXO1 signaling

Katarina Ochodnicka-Mackovicova, Mahnoush Bahjat,
Chiel Maas, Amélie van der Veen, Timon A. Bloedjes,
Alexander M. de Bruin, Harmen van Andel,
Carol E. Schrader, Rudi W. Hendriks, Els Verhoeyen,
Richard J. Bende, Carel J.M. van Noesel and
Jeroen E.J. Guikema

4



Abstract

The recombination activating gene (RAG) 1 and RAG2 protein complex introduces DNA breaks at *Tcr* and *Ig* gene segments that are required for V(D)J recombination in developing lymphocytes. Proper regulation of RAG1/2 expression safeguards the ordered assembly of antigen (Ag) receptors and the development of lymphocytes, while minimizing the risk of collateral damage. The ataxia telangiectasia mutated (ATM) kinase is involved in the repair of RAG1/2-mediated DNA breaks and prevents their propagation. The simultaneous occurrence of RAG1/2-dependent and -independent DNA breaks in developing lymphocytes exposed to genotoxic stress increases the risk of aberrant recombinations. Here we assessed the effect of genotoxic stress on RAG1/2 expression in pre-B cells and show that activation of the DNA damage response resulted in the rapid ATM-dependent down-regulation of RAG1/2 mRNA and protein expression. We show that DNA damage led to the loss of FOXO1-binding to the enhancer region of the RAG1/2 locus (*Erag*) and provoked FOXO1 cleavage. We also show that DNA damage caused by RAG1/2 activity in pre-B cells was able to down-modulate RAG1/2 expression and activity, confirming the existence of a negative feedback regulatory mechanism. Our data suggest that pre-B cells are endowed with a protective mechanism that reduces the risk of aberrant recombinations and chromosomal translocations when exposed to DNA damage, involving the ATM-dependent regulation of FOXO1-binding to the *Erag* enhancer region.

Introduction

In developing lymphocytes, Ag receptors are assembled by recombination of immunoglobulin heavy chain (*Igh*) and light chain (*Igl*) variable (V), diversity (D), and joining (J) gene segments. This recombination process is initiated by the recombination activating gene (RAG) proteins RAG1 and RAG2, which form a heterodimeric complex possessing endonuclease capacity, creating double-stranded DNA breaks (DSBs) at recombination signal sequences (RSS) adjacent to the immunoglobulin (*Ig*) and T-cell receptor (*Tcr*) gene segments^{1,2}. Subsequent to DNA cleavage, the RAG1/2 complex remains associated with the DNA ends to facilitate their repair by the non-homologous end-joining repair mechanism³. V(D)J recombination is initiated in a monoallelic fashion, and following a successful in-frame *Igh* V to DJ rearrangement in pro-B cells, RAG expression is rapidly down-regulated, thereby preventing biallelic recombinations and enforcing allelic exclusion. After productive *Igh* rearrangement the pre-B cell receptor (pre-BCR) is formed, expressed on the cell membrane, and as a result of pre-BCR expression, pre-B cells enter the cell cycle.

At the pre-B cell stage, an interplay between IL-7 receptor (IL-7R) signaling and pre-BCR signaling coordinates subsequent B-cell development and RAG expression⁴. IL-7R activates phosphoinositide 3-kinase (PI3K), which via AKT, represses forkhead box protein O1 (FOXO1), a major non-redundant RAG1 and RAG2 transcription factor. Moreover, IL-7R activates STAT5 that, on one hand, drives cyclin D3 expression and promotes cell proliferation, and on the other hand limits accessibility of the *Igk* light chain locus⁵. The pre-BCR regulates pre-B cell proliferation by activating spleen tyrosine kinase (SYK) and RAS-extracellular signal-regulated kinase (ERK) signaling, which represses cyclin D3 and drives early region 2A (E2A), an important regulator of *Igk* locus transcription^{6,7}. In addition, pre-BCR signals to pre-B cell linker (BLNK, also known as SLP-65), inhibiting the PI3K-AKT pathway and enhancing *Igk* accessibility by a redistribution of long-range chromatin interactions^{8,9}. Attenuation of IL7 signaling in mouse pre-B cells drives B-cell differentiation and is associated with up-regulation of FOXO1, re-expression of RAG1 and RAG2, and *Igk* rearrangement⁴.

RAG1 and RAG2 are convergently transcribed from the same locus. Cooperation of distant sequences in *cis*, the proximal enhancer, the distal enhancer, and the RAG enhancer (*Erag*), with RAG promoters is required for regulating RAG expression in lymphocytes¹⁰⁻¹². *Erag* is the strongest enhancer and a complex network of transcription factors, including Foxo1, forkhead box protein P1 (FoxP1), paired box protein 5 (Pax5), nuclear factor kappa-light-chain-enhancer of activated B cells (NF- κ B), and Ikaros, was shown to activate RAG transcription by binding to this element¹².

Unlike RAG1, termination of RAG2 expression is linked to cell-cycle progression. In dividing cells, RAG2 expression and activity are detected in the G1-phase whereas it is absent in the S- and G2/M-phases of the cell cycle¹³. It was shown that phosphorylation

of Thr490 of RAG2 by the CyclinA/CDK2 complex, which is active at the G1/S transition, signals the periodic destruction of RAG2. A threonine-to-alanine mutation at this residue (T490A) rendered RAG2 insensitive to this regulation and allowed its persistence in S- and G2/M-phases¹⁴. Such unrestricted expression of RAG2 throughout the cell cycle resulted in formation of aberrant recombinations¹⁵. In addition, on a p53-deficient background, the T490A RAG2 mutation led to the development of lymphoid malignancies harboring chromosomal translocations involving the antigen receptor loci¹⁶. Proper termination and restriction of RAG expression and activity are necessary to prevent formation of potentially dangerous recombinations and genomic instability.

A recent study suggested that aberrant RAG activity is a dominant driver of secondary genetic hits in ETV6-RUNX1-positive childhood acute lymphoblastic leukemia (ALL) cases, where many breakpoints map near RSS motifs¹⁷. Moreover, a large portion of B-ALL cases display constitutive RAG expression, which has been associated with ongoing *Igh* rearrangements even after the malignant clone transformation¹⁸, thereby contributing to secondary genetic hits that may be at the basis of therapy resistance¹⁹.

RAG-dependent chromosomal translocations occur as a result of the aberrant joining of RAG-induced DSBs with DSBs in other chromosomes. Therefore, B cells that are actively engaged in V(D)J recombination (pro-B cells and small pre-B cells) are especially at risk to procure such aberrant joining events when exposed to genotoxic stress. It is not very likely that cell cycle-dependent RAG2 degradation is the only protective mechanism that limits RAG-associated DNA damage. Rather, it is conceivable that mechanisms exist that down-regulate RAG activity when DNA damage is detected, irrespective of cell-cycle stage. However, it is not known whether B-lineage cells undergoing V(D)J recombination possess protective mechanisms that limit the formation of aberrant chromosomal rearrangements under such conditions. Given its oncogenic potential, mechanisms controlling RAG expression and activity in cells that have initiated V(D)J recombination need to be better understood. In this study we show that the DNA damage response limits the expression of RAG1/2 in pre-B cells, involving the Ataxia Telangiectasia mutated kinase (ATM) and FOXO1, thus preventing further formation of potentially dangerous lesions.

Materials and methods

Cell culture and small molecule compounds

The *v-Abl* transformed mouse pre-B cell lines were generated from wild type (WT) (A70) and *Rag2*^{-/-} (R2K3) mice that harbor the E μ -Bcl2 transgene and were kindly provided by Dr. Craig Bassing (University of Pennsylvania School of Medicine, Philadelphia, PA). The human BCR-ABL⁺ B-ALL cell lines BV173 and SUP-B15 were obtained from DSMZ (Braunschweig, Germany) and cultured in RPMI 1640 (Gibco Life Technologies, Bleiswijk The Netherlands) supplemented with 2mM L-glutamine, 100 U/mL penicillin, 100 μ g/mL streptomycin, 20%

fetal calf serum and 50 μ M β -mercaptoethanol. HEK293 cells were obtained from the ATCC and maintained in DMEM (Gibco Life Technologies) supplemented with 2 mM L-glutamine, 100 U/mL penicillin, 100 μ g/mL streptomycin, and 10% fetal calf serum. The following small molecule inhibitors/activators were used: STI571 (Imatinib methanesulfonate, LC Laboratories, Woburn, MA), GSK690693 (Selleckchem, Houston, TX), CAL101 (Idelalisib, Selleckchem), KU55933 (ATM-kinase inhibitor, Selleckchem), NCS (Neocarzinostatin, Sigma-Aldrich, Zwijndrecht, The Netherlands), Q-VD-OPH (Sigma-Aldrich), AKTi VIII (AKT inhibitor VIII, EMD Millipore, Billerica, MA). To induce RAG1/2 expression and *IgI* recombination, BV173, SUP-B15, and A70 were treated overnight with 5 μ M STI571, as previously established^{20,21}.

Primary mouse bone marrow cultures

ATM-deficient mice²², Jackson Laboratory stock 002753, were provided by Dr. Stephen Jones (University of Massachusetts Medical School, Worcester, MA). C57Bl/6 WT mice were housed in the animal research facility of the Academic Medical Center under specific pathogen-free conditions. Animal experiments were approved by the Animal Ethics Committee and performed in agreement with national and institutional guidelines. Bone marrow (BM) cells were harvested from 8- to 20-wk-old mice by flushing femurs and tibia. Total BM cells were cultured in six-wells plates in RPMI1640 with 2 mM L-glutamine, 100 U/mL penicillin, 100 μ g/mL streptomycin, 10% fetal calf serum, 50 μ M β -mercaptoethanol, 10 ng/mL recombinant mouse IL7, and 10 ng/mL Flt3L (both from ProSpec Inc., Ness-Ziona, Israel). Culture medium and cytokines were replaced every three days. Cells were harvested after 7-10 days and analyzed by flow cytometry, typically yielding >95% B220⁺, IgM⁺, CD43⁺ progenitor B cells (data not shown). To induce large to small pre-B cell transition, RAG1/2 expression, and *IgI* recombination, cells were washed 3 times in culture medium without cytokines and placed back in six-well plates at 2×10^6 cells/mL in medium without cytokines (IL7 withdrawal).

Induction of DNA damage

DNA damage in cultured cells (2×10^6 cells/ml) was induced by adding 50 ng/ml NCS to the culture medium. After 2 hours the cells were harvested for respective experiments. Additionally, where so mentioned, DNA damage was induced by irradiating the cells ($[^{137}\text{Cs}]$, 5 Gy, 0.50 Gy/min) at a dose of 5 Gy. Following irradiation, the cells were allowed to recover for 2 hours at 37°C in an atmosphere of 5% CO₂ and subsequently harvested.

Western blotting and immunoprecipitation

Cells ($2-5 \times 10^6$) were washed with ice-cold PBS and lysed in ice-cold lysis buffer (10 mM Tris-HCl pH 8, 150 mM NaCl, 1% NP-40, 20% glycerol, 5 mM EDTA supplemented with protease and phosphatase inhibitors (EDTA-free protease cocktail inhibitor (Roche Diagnostics, Almere, The Netherlands), 1 mM sodium-ortho-vanadate, 2 mM sodium phosphate, 1.25

mM β -glycerophosphate, and 100 μ M phenylmethanesulfonylfluoride (PMSF). The protein pellets were homogenized passing through a 27G needle and protein concentrations were measured using the bicinchoninic acid (BCA) assay (Sigma-Aldrich). For each sample, 15 μ g of protein lysate was used for protein separation in Precise™ 4-20% gradient Tris-SDS gels (Thermo Fisher Scientific, Landsmeer, The Netherlands). Subsequently, separated protein lysates were transferred onto polyvinylidene difluoride (PVDF) membranes (Immobilon-P, EMD Millipore), membranes were blocked in 5% BSA (BSA Fraction V, Roche Life Sciences, Almere, the Netherlands) in TBS-T or 5% milk in TBS-T for 2 hours. Primary antibodies were incubated overnight at 4°C. Following a series of thorough washes with TBS-T, membranes were incubated with secondary antibodies (goat-anti-rabbit-HRP or rabbit-anti-mouse HRP, DAKO, Agilent Technologies, Heverlee, Belgium) for 2 hours at room temperature. Antibody binding (protein expression) was visualized using Amersham ECL Prime Western Blotting detection reagent (GE Healthcare Bio-Sciences AB, Uppsala, Sweden). The following antibodies were used in this study: Rabbit-anti-RAG1 (D36B3), rabbit-anti-FOXO1 (C29H4), rabbit-anti-phospho-FOXO1 (Ser²⁵⁶) (9461), rabbit-anti-AKT (4691), rabbit-anti-phospho-AKT (Ser⁴⁷³) (D9E), rabbit-anti-phospho-p53 (Ser¹⁵) (9284), rabbit-anti-mTOR (2972), rabbit-anti-phospho-mTOR (Ser²⁴⁴⁸) (D9C2), rabbit-anti-cleaved caspase-3 (Asp¹⁷⁵) (9661), rabbit-anti-GADD45 α (D17E8) (all from Cell Signaling Technology, Danvers, MA), mouse-anti-phospho-ATM (Ser¹⁹⁸¹) (10H11.E12), and mouse-anti- β -actin (C4) (both from EMD Millipore).

For immunoprecipitation, nuclear extracts from 60x10⁶ cells were prepared according to the nuclear complex co-IP kit (active Motif, Carlsbad, CA). Cleared lysates were incubated overnight at 4°C with rabbit anti-phospho-(Ser/Thr) ATM/ATR substrate antibody (2851, Cell Signaling Technology), or polyclonal rabbit IgG (Santa Cruz Biotechnology, Dallas, TX) with 1% detergent in 150 mM NaCl. Antibody-bound proteins were captured by protein-A sepharose beads (CL-4B, GE Healthcare Bio-Sciences AB), thoroughly washed, resolved in Novex Bolt™ 10% Bis-Tris Plus gels (Thermo Fisher Scientific), and subjected to Western blotting. The following antibodies were used: rabbit-anti-FOXO1 (C29H4, Cell Signaling Technology), and rabbit-anti-NBS1 (Y112, Abcam, Bristol, UK).

Real-time quantitative RT-PCR

Levels of mRNA expression were determined using the CFX384 (Bio-Rad, Hercules, CA) real-time PCR platform. Briefly, RNA from cells was isolated by TRI reagent (Sigma-Aldrich) according to the manufacturer's protocol. For each sample cDNA was synthesized from 500 ng RNA, using random primers (Promega Benelux, Leiden, the Netherlands) and M-MLV reverse transcriptase (Invitrogen-Life Technologies, Bleiswijk, the Netherlands). For each sample, cDNA was diluted 1:5 with PCR-grade water. The PCR mastermix contained 5 μ l of Sso Fast EvaGreen supermix (Bio-Rad, Hercules, CA), and 0.5 μ l of 10 μ M reverse and forward primers (Biogio, Nijmegen, the Netherlands). The final volume was adjusted to

9 μ l using PCR-grade water, to which 1 μ l of diluted cDNA was added. The following PCR conditions were used: initial denaturation at 95°C for 5 minutes, followed by 40 cycles of denaturation at 95°C for 15 seconds, annealing at 65°C for 5 seconds, and extension at 72°C for 10 seconds. The fluorescent product was measured by a single acquisition mode at 72°C after each cycle. For distinguishing specific from non-specific products and primer dimers, a melting curve was obtained after amplification by holding the temperature at 65°C for 15 seconds followed by a gradual increase in temperature to 95°C at a rate of 2.5°C s⁻¹, with the signal acquisition mode set to continuous. For each cDNA preparation PCR reactions were performed at least in duplicate, and for each condition at least three independent experiments were performed. Expression of target gene mRNAs were normalized to the housekeeping genes large ribosomal protein PO (*RPLPO*) for human samples and 18S ribosomal RNA (*18S rRNA*) for mouse samples. Statistical significance was determined using the one-sample *t*-test in which the DMSO-treated control samples were set to a value of 1.

PCR primers used in this study: human RAG1-forward (5'-GGCAAGGAGAGAGCAGAG-GA-3'), human RAG1-reverse (5'-CTCACCCGGAACAGCTTAAA-3'), human CDKN1A/P21-forward (5'-GACTCTCAGGGTCGAAAACG-3'), human CDKN1A/P21-reverse (5'-GGATTAGG-GCTTCTCTTGG-3'), human FOXO1-forward (5'-AAGAGCGTGCCCTACTTCAA-3'), human FOXO1-reverse (5'-TTCCTTCATTCTGCACACGA-3'), human GADD45a-forward (5'-GAGCTCT-GCTCTTGGAGAC-3'), human GADD45a-reverse (5'-GCAGGATCCTTCCATTGAGA-3'), human RPLPO-forward (5'-GCTTCTGGAGGGGTGTCCGC-3'), human RPLPO-reverse (5'-TCCGTCTC-CACAGACAAGGCCA-3'), mouse Rag1-forward (5'-AGCTATCACTGGGAGGCAGA-3'), mouse Rag1-reverse (5'-GAGGAGGCAAGTCCAGACAG-3'), mouse Rag2-forward (5'-CTTCCCCAAGT-GCTGACAAT-3'), mouse Rag2-reverse (5'-AGTGAGAAGCCTGGCTGAAT-3'), mouse Cdkn1a/p21-forward (5'-TCCACAGCGATATCCAGACA-3'), mouse Cdkn1a/p21-reverse (5'-AGACAAC-GGCACACTTTGCT-3'), mouse Foxo1-forward (5'-AAGAGCGTGCCCTACTTCAA-3'), mouse Foxo1-reverse (5'-TGCTGTGAAGGGACAGATTG-3'), mouse Gadd45a-forward (5'-CCGAAAG-GATGGACACGGTG-3'), mouse Gadd45a-reverse (5'-TATCGGGGTCTACGTTGAGC-3'), mouse 18S rRNA-forward (5'-TGGTGGAGGGATTGTCTGG-3'), mouse 18S rRNA-reverse (5'-TCAATCTCGGGTGGCTGAAC-3').

Lentiviral and retroviral transductions

Lentiviral constructs for overexpression of WT and mutant kinase-dead AKT (K179M/T308A/S473A) were generated by cloning the BamHI/EcoRI fragments from Addgene plasmids 9011 and 9013²³ into the leGO-iG2 backbone. The leGO-iG2 was a gift from Boris Fehse (Addgene plasmid #27341)²⁴. Lentiviral particles incorporating measles virus glycoproteins H and F were generated by cotransfection of HEK293T cells with the D8.91 (gag/pol) and Hdel24 and Fdel30 plasmids²⁵ using GENIUS DNA transfection reagent (Westburg, Leusden, the Netherlands). In brief, virus supernatants were harvested 48h after transfection, and concentrated by overnight centrifugation at 3000xg at 4°C. BV173 cells

were exposed overnight to the concentrated virus in the presence of 7 $\mu\text{g}/\text{mL}$ polybrene (Sigma-Aldrich). Transduced cells were FACS-sorted based on green fluorescent protein (GFP) expression 5 days after transduction. To assess RAG recombination activity, A70 WT mouse *v-Abl* pre-B cells were transduced with a retroviral RAG-reporter construct²⁶, as described previously²⁷.

Chromatin immunoprecipitation

Protein-DNA binding was studied using the MAGnify™ Chromatin Immunoprecipitation system (Life Technologies) in accordance with the manufacturer's protocol. Briefly, 20×10^6 cells were used for each IP, which were performed in triplicate for each condition. The cells were fixed in 1% formaldehyde for 5 minutes at 37°C and quenched for 10 minutes with 125 mM glycine. Subsequently, cells were washed twice in ice-cold PBS and lysed using the enclosed lysis buffer and sonicated by Covaris S2 (intensity: 3, duty cycle: 5 %, and cycles per burst: 200) to obtain DNA fragments of an average length of 500bp. Protein concentration was measured after sonication by the BCA assay and equal amounts of fragmented chromatin-protein complexes were incubated for 2 hours with enclosed Dynabeads® that were first coupled to a cocktail of FOXO1-specific antibodies (rabbit-anti-FOXO1, C29H4 [Cell Signaling Technology], rabbit-anti-FOXO1, H-128, [Santa Cruz Biotechnology], rabbit-anti-acetyl-FOXO1, D-19, [Santa Cruz Biotechnology], rabbit-anti-FOXO1, ab70382, [Abcam], rabbit-anti-phospho-FOXO1 (Ser²⁵⁶), 9461, [Cell Signaling Technology]) (10 μg in total per ChIP), phospho-ATM (Ser¹⁹⁸¹) (10H11.E12, EMD MilliPore), or to polyclonal rabbit or mouse IgG (control ChIP) (Santa Cruz Biotechnology). Following a series of washes, chromatin was decross-linked for 15 minutes at 65°C and purified using the ChIP DNA Clean & Concentrator kit (Zymo Research, Freiburg, Germany). FOXO1 binding to *Erag* was assessed by quantifying ChIP-enriched DNA using CFX384 real-time PCR (Bio-Rad). *Erag* primers used: *Erag*-ChIP-forward (5'-TGCTGTGTAGCCTTTTGAG-3'), *Erag*-ChIP-reverse (5'-TGGAAGCATAAAGCTGGTCA-3').

Luciferase assay

Luciferase activity was measured using the Dual-Glo® Luciferase Assay System (Promega) according to the manufacturer's protocol. Mouse WT (A70) and *Rag2*^{-/-} (R2K3) cells were transfected (Fugene® 6 transfection reagent, Promega) with the *Erag-Rag1*-luciferase reporter (kindly provided by prof. M. Schlissel, University of Michigan, Ann Arbor, MI) and TK *Renilla* luciferase reporter vector (Promega) in the ratio 1:8 using in total 1.25 μg DNA per 100,000 cells. Following transfection cells were treated either with 5 μM KU55933 or vehicle (DMSO, Sigma) for 24h. Cells were harvested into 100 μl of passive lysis buffer. Firefly luciferase and *Renilla* luciferase activity were measured on a GloMax 96 microplate luminometer (Promega) according to the manufacturer's instructions. *Renilla* activity served as a control for transfection efficiency. Activity of RAG reporter for each sample was calculated as firefly/*Renilla* ratio, expressed as relative light units (RLU).

Proximity ligation assay

Protein colocalizations/interactions in cells were determined by the Duolink® proximity ligation assay as per manufacturer's directions (Sigma-Aldrich). BV173 cells exposed to different treatments were cytocentrifuged onto glass slides, fixed for 30 minutes in 4% paraformaldehyde, permeabilized in 0.25% Triton-X, washed and blocked in Duolink® blocking solution prior to overnight incubation with primary antibody combinations. The following combinations were applied: mouse-anti-phospho-ATM (Ser¹⁹⁸¹) (10H11.E12, EMD MilliPore) + rabbit-anti-FOXO1 (C29H4, Cell Signaling Technology), goat-anti-ATM (A300-136A, PLA-grade, Bethyl Laboratories Inc. Montgomery, TX) + rabbit-anti-FOXO1, goat-anti-ATM + rabbit-anti phospho-p53 (Ser¹⁵) (9284, Cell Signaling Technology). After washing, the slides were incubated with combinations of plus- and minus-PLA-probes (anti-mouse + anti-rabbit or anti-goat + anti-rabbit), followed by ligation and rolling circle amplification using the Duolink® in situ Red kit (Sigma-Aldrich). Nuclei were counterstained with 4,6-diamidino-2-phenylindole, dihydrochloride (DAPI) and slides were mounted with VECTASHIELD antifading mounting medium (Vectorlabs, Burlingame, CA). Protein interactions were quantified by assessing the number of PLA-foci in at least 20 cells for each experimental condition. Imaging was performed using a Leica DM5000B fluorescence microscope equipped with a Leica FDC500 camera and a 20x objective (Leica Microsystems BV, Son, the Netherlands).

Statistics

The GraphPad Prism software package (GraphPad Software, La Jolla, CA) was used for statistical testing.

Results

DNA breaks regulate RAG1 expression in pre-B cells

To assess the role of DNA damage in the regulation of RAG1 expression, BCR-ABL-positive human pre-B cells and *v-Abl*-transformed mouse pre-B cells were treated overnight with the specific Abl kinase-inhibitor STI571 (imatinib methanesulfonate) to induce RAG expression and *IgI* recombination and were subsequently exposed to the radiomimetic drug neocarzinostatin (NCS) for 2 hours to induce DNA damage. NCS rapidly induces chromosome breaks in quiescent cells, not requiring S-phase for its DNA-damaging effect²⁸. Such short exposure of pre-B cells to this DNA damaging agent did not result in detectable cell death at the time of sample collection, judging by the percent of apoptotic (propidium-iodide positive) cells as detected by flow cytometry (**SUPPL Figure 1A**), but generated substantial DNA damage as the levels of phospho-p53 (Ser¹⁵) and phospho-ATM (Ser¹⁹⁸¹) were strongly induced (**Figure 1A**). In addition, *p21* mRNA expression was increased by 13.5

fold in NCS-treated cells compared to DMSO-treated control cells (**Figure 1B**). Induction of DNA damage by NCS resulted in the rapid down-regulation of RAG1 protein in BV173 cells (**Figure 1A**). Similar results were obtained using a different human pre-B cell line, SUP-B15 (**SUPPL Figure 1B-C**). To determine the effect of DNA damage on RAG1 protein stability and turnover we blocked protein synthesis using cycloheximide (CHX) in STI571-treated BV173 cells. In accordance with previous reports^{29,30} we demonstrate that the RAG1 protein has a short half-life of about 30'-60' (**Figure 1C**, compare DMSO-treated to CHX-treated samples), which is decreased by NCS treatment (**Figure 1C**, compare CHX-treated to CHX+NCS-treated samples). These results indicate that DNA damage negatively affected RAG1 protein stability.

Interestingly, we found *RAG1* mRNA transcripts also being significantly down-regulated following the NCS treatment in BV173 cells: 59% of DMSO-treated controls ($p=0.01$), and in A70 (WT mouse *v-Abl*) pre-B cells: 10% of DMSO-treated controls ($p<0.001$), (**Figures 1D and 1E**). Furthermore, DNA damage induction by NCS treatment caused a comparable down-regulation (16% of untreated controls, $p=0.01$ as compared to untreated controls) of *Rag1* mRNA in primary mouse WT pre-B cells (**Figure 1F**), and of *Rag2* mRNA in A70 cells (**Figure 1G**).

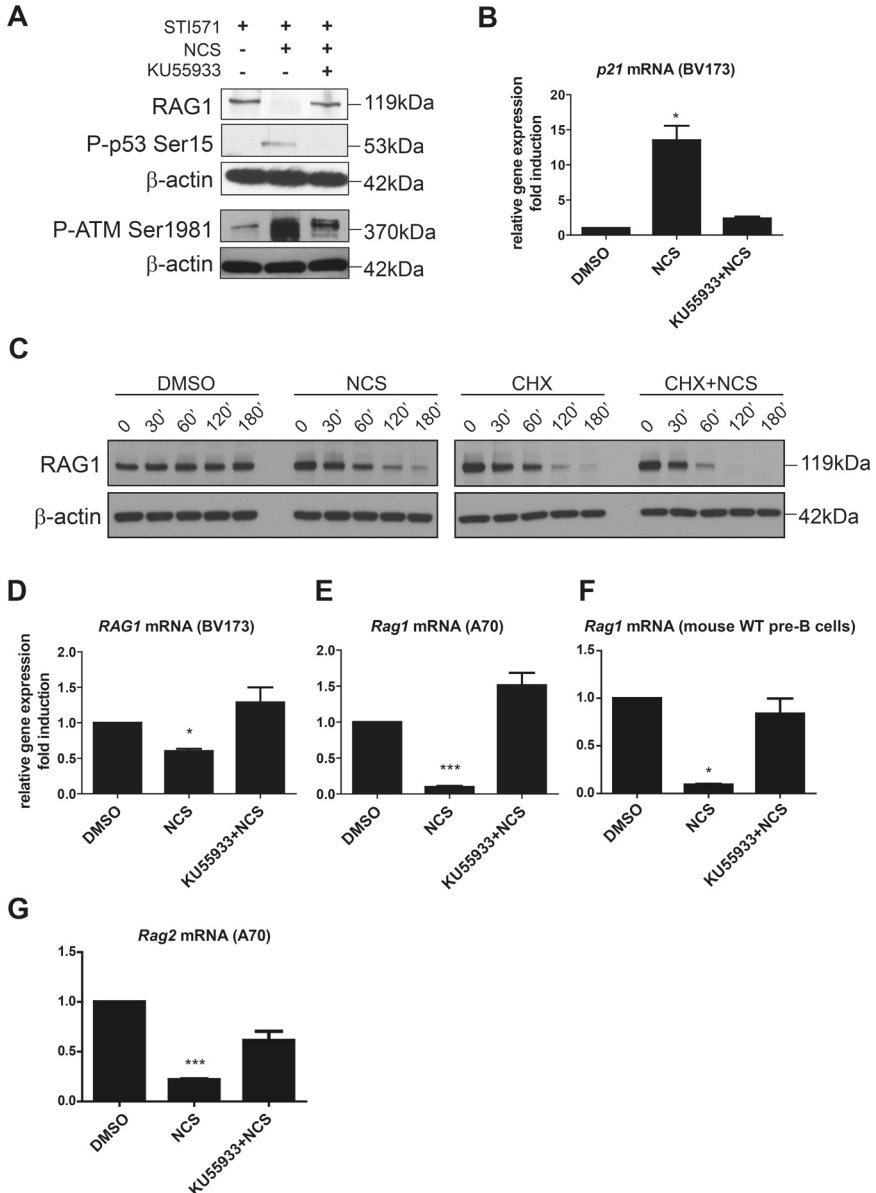
ATM kinase is involved in DNA damage-mediated regulation of RAG1/2

Inhibition of ATM kinase activity using the selective inhibitor KU55933 prevented NCS-induced down-regulation of RAG1 protein. It also effectively reduced ATM Ser¹⁹⁸¹ autophosphorylation in BV173 cells (**Figure 1A**). Moreover, KU55933 treatment prevented the DNA

► **Figure 1. DNA damage down-regulates RAG1 protein and mRNA expression.**

(A) Western blotting analysis of RAG1 expression in STI571-treated BV173 BCR-ABL-positive B-ALL cells. DNA damage induction by 2h treatment with 50 ng/mL NCS resulted in a rapid down-regulation of RAG1 protein expression, which was prevented by 2h pretreatment with 5 μ M KU55933. Phospho-p53 (Ser¹⁵) and phospho-ATM (Ser¹⁹⁸¹) blots were used to show the induction of the ATM-dependent DNA damage response. The β -actin blot was used to control for loading. **(B)** Realtime quantitative RT-PCR analysis of *CDKN1A* (*p21*) mRNA expression in BV173 cells treated as indicated in (A). Means \pm SEM are shown ($n=4$, * $p<0.05$, one-sample *t* test). **(C)** Western blot analysis of RAG1 protein stability after cycloheximide (CHX) treatment in BV173 cells treated overnight with 5 μ M STI571. Cells were treated for the indicated timepoints with DMSO (vehicle control), 50 ng/mL NCS, 20 μ g/mL CHX, or the combination of both. The β -actin blot was used to control for loading. **(D)** Realtime quantitative RT-PCR analysis of *RAG1* mRNA expression in BV173 cells treated as indicated in (A), means \pm SEM are shown ($n=4$, * $p=0.01$, one-sample *t* test). **(E)** Realtime quantitative RT-PCR analysis of *Rag1* mRNA expression in A70 WT mouse *v-Abl* cells treated as indicated in (A), means \pm SEM are shown ($n=4$, *** $p<0.001$, one-sample *t* test). **(F)** Realtime quantitative RT-PCR analysis of *Rag1* mRNA expression in WT mouse IL-7 dependent pre-B cell cultures, cells were treated as indicated in (B) 48h after IL7 withdrawal. Cultures from 3 mice were analyzed independently, means \pm SEM are shown ($n=3$, * $p=0.01$, one-sample *t* test). **(G)** Realtime quantitative RT-PCR analysis of *Rag2* mRNA expression in A70 cells

damage-induced down-regulation of *RAG1/2* mRNA transcripts in the BV173 and A70 cell lines and in primary mouse WT pre-B cells (**Figures 1D-1G**). In addition, expression of *Rag1* mRNA in primary pre-B cells derived from *Atm*^{-/-} mouse bone marrow remained unaffected by DNA damage (data not shown), supporting a central role for ATM kinase in the regulation of RAG1 expression following DNA damage.



Transcriptional regulation of RAG expression by DNA damage

Exposure of cells to DNA-damaging agents may result in the activation of a caspase cascade and subsequent proteolysis³¹. Accordingly, we observed that the 2-hour NCS treatment activated caspase-3 (**Figure 2A**). To provide evidence that NCS-induced RAG1 protein down-regulation is not merely a result of proteolysis by activated caspases, BV173 cells were pre-treated with the pan-caspase inhibitors Q-VD-OPH or Z-VAD (data not shown) one hour prior to NCS treatment. Subsequent treatment with NCS resulted in RAG1 down-modulation even in the presence of Q-VD-OPH, whereas cleavage of pro-caspase-3 was efficiently inhibited (**Figure 2A**), showing that caspase-mediated proteolysis did not account for the loss of RAG1 protein following DNA damage.

DNA damage significantly affected *RAG1* mRNA and protein expression levels in pre-B cells, indicating that regulation takes place at the transcriptional level as well as the post-translational level. To further dissect the relative contribution of these regulatory mechanisms, we ectopically expressed RAG1 protein from a heterologous promoter (i.e., plasmid-driven) in HEK293 cells. Surprisingly, while treatments with increasing doses of ionizing radiation or increasing concentrations of NCS clearly elicited a DNA damage response, as shown by increased phospho-p53 (Ser¹⁵) levels, DNA damage did not affect RAG1 protein levels under these conditions, suggesting that DNA damage-mediated regulation of RAG1 protein requires its endogenous transcriptional regulation and that the post-translational regulation of RAG1 protein expression is not conserved between different cell-types (**Figure 2B**).

► **Figure 2. RAG1 down-regulation upon DNA damage is caspase-3-independent, requires its endogenous transcriptional context, and coincides with loss of FOXO1-Erag binding.** (A) Western blotting analysis of RAG1 and cleaved caspase-3 expression in STI571-treated BV173 BCR-ABL-positive B-ALL cells. Cells were pre-treated with 10 μ M Q-VD-OPH 1h prior to 2h treatment with 50 ng/mL NCS treatment. The β -actin blot was used to control for loading. (B) Western blotting analysis of HEK293 cells transfected with pEBB-RAG1 encoding full-length mouse RAG1 (kind gift from Dr. M. van der Burg). Cells were treated as indicated and harvested 2h after induction of DNA damage. The phospho-p53 (Ser¹⁵) blot was used to show the induction of the DNA damage response. The β -actin blot was used to control for loading. (C) Schematic depiction of the human *RAG1/2* locus, numbers indicate chromosomal coordinates and arrows indicate transcriptional direction. *Erag* enhancer and ChIP-PCR target region are shown. (D) Binding of FOXO1 and control rabbit IgG, and (E) phospho-ATM (Ser¹⁹⁸¹) and control mouse IgG to the *Erag* enhancer in STI571-treated BV173 cells and SUP-B15 BCR-ABL-positive B-ALL cells as determined by ChIP and expressed as percent of input DNA. Cells were treated as indicated. ChIP experiments were performed in triplicate. Statistical significances were determined by one-way analysis of variance (ANOVA) using a Bonferroni's post-test, means \pm SEM are shown (** $p < 0.01$; *** $p < 0.001$).

ERRATUM II

Chapter 4, page 93, Figure 2 should be displayed as follows:

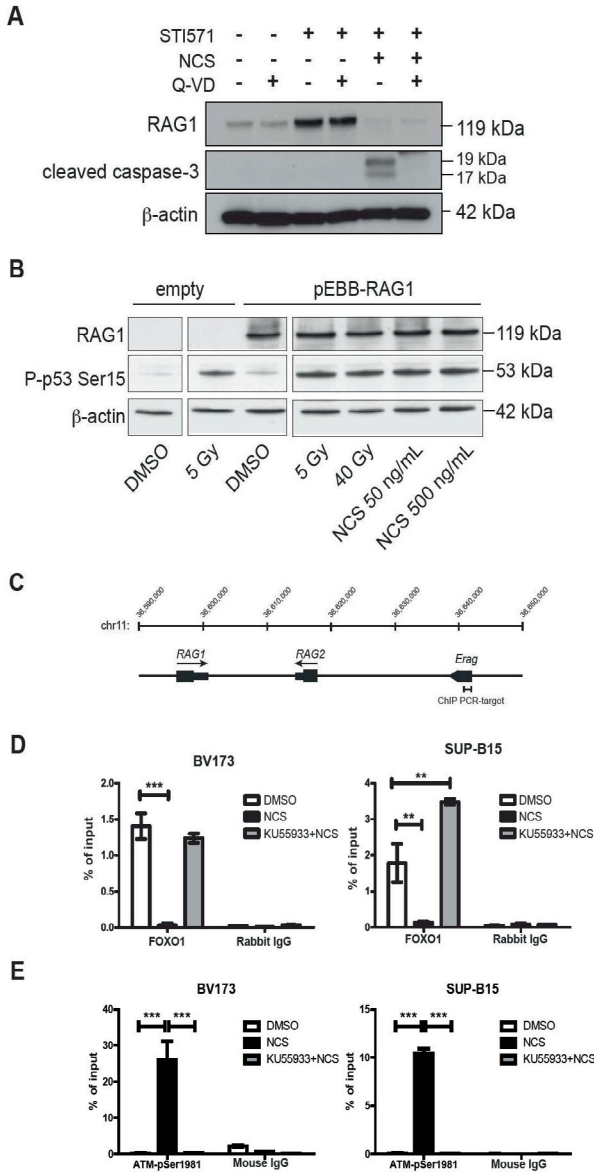


Figure 2. RAG1 down-regulation upon DNA damage is caspase-3-independent, requires its endogenous transcriptional context, and coincides with loss of FOXO1-Erag binding. (A) Western blotting analysis of RAG1 and cleaved caspase-3 expression in STI571-treated BV173 BCR-ABL-positive B-ALL cells. Cells were pre-treated with 10 μ M Q-VD-OPH 1h prior to 2h treatment with 50 ng/mL NCS treatment. The β -actin blot was used to control for loading. (B) Western blotting analysis of HEK293 cells transfected with pEBB-RAG1 encoding full-length mouse RAG1 (kind gift from Dr. M. van der Burg). Cells were treated as indicated and harvested 2h after induction of DNA damage. The phospho-p53 (Ser¹⁵) blot was used to show the induction of the DNA damage response. The β -actin blot was used to control for loading. (C) Schematic depiction of the human RAG1/2 locus, numbers indicate chromosomal coordinates and arrows indicate transcriptional direction. Erag enhancer and ChIP-PCR target region are shown. (D) Binding of FOXO1 and control rabbit IgG, and (E) phospho-ATM (Ser¹⁹⁸¹) and control mouse IgG to the Erag enhancer in STI571-treated BV173 cells and SUP-B15 BCR-ABL-positive B-ALL cells as determined by ChIP and expressed as percent of input DNA. Cells were treated as indicated. ChIP experiments were performed in triplicate. Statistical significances were determined by one-way analysis of variance (ANOVA) using a Bonferroni's post-test, means \pm SEM are shown (** p<0.01; *** p<0.001).

FOXO1 is involved in the DNA damage-induced regulation of RAG1

Based on these results we decided to study the effects of DNA damage on the transcriptional regulation of RAG expression in pre-B cells in further detail. FOXO1 is a crucial non-redundant transcription factor in developing B cells, and a key regulator of RAG1/2 expression at the pre-B cell stage^{32,33}. Transcription of the RAG locus in B cells is controlled by the evolutionary conserved enhancer element *Erag*¹¹. FOXO1 was shown to bind *Erag* in RAG-expressing small pre-B cells and is involved in driving RAG expression from this *cis*-acting sequence^{33,34}. To further establish the involvement of FOXO1 in the DNA damage-induced regulation of RAG1 expression we assessed the binding of FOXO1 to the *Erag* enhancer following DNA damage, using chromatin immunoprecipitation (ChIP) (**Figure 2C**). We found that the binding of FOXO1 to the *Erag* enhancer was abolished by NCS treatment in BV173 and SUP-B15 cells (**Figure 2D**). Pre-treatment with the ATM kinase inhibitor fully prevented the loss of FOXO1-*Erag* binding upon induction of DNA damage. In addition, we found that phosphorylated ATM (Ser¹⁹⁸¹) was present at the *Erag* enhancer region in NCS-treated cells (**Figure 2E**), indicating that regulation of FOXO1-binding by ATM possibly could take place in the context of chromatin.

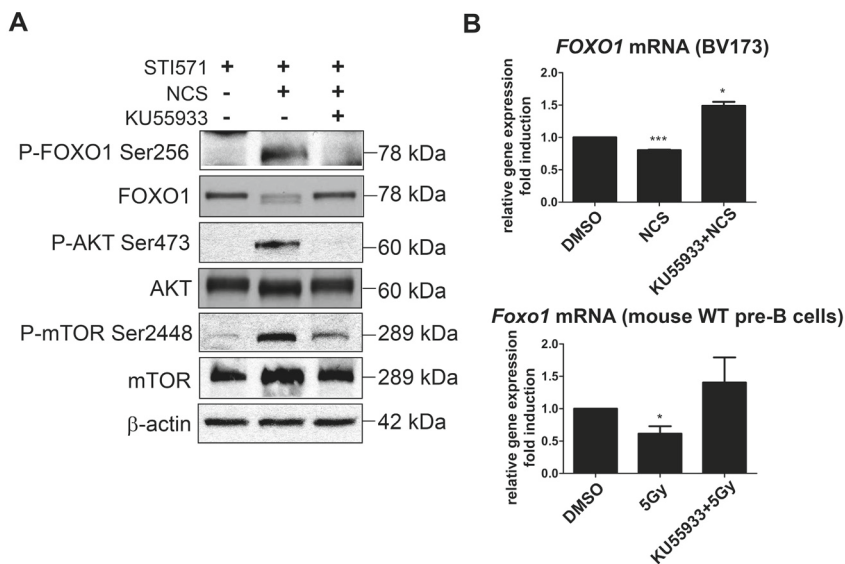


Figure 3. FOXO1 protein is cleaved/degraded upon DNA damage.

(A) Western blot analysis of FOXO1, AKT and mTOR phosphorylation in BV173 cells treated as indicated, the β -actin blot was used to control for loading. (B) Realtime quantitative RT-PCR analysis of *FOXO1* mRNA expression in BV173 cells treated as indicated, means \pm SEM are shown (upper graph, n=4, *** p=0.0003, one-sample t test), and *Foxo1* mRNA in WT mouse IL-7 dependent pre-B cell cultures, cells were treated as indicated 48h after IL7 withdrawal, cultures from 4 mice were analyzed independently, means \pm SEM are shown (lower graph, n=4, * p=0.02, one-sample t test).

We observed FOXO1 phosphorylation on Ser²⁵⁶ upon NCS treatment (**Figure 3A**). Because FOXO1 Ser²⁵⁶ phosphorylation has previously been linked to ubiquitin-mediated FOXO1 degradation by Skp2, a subunit of the Skp1/Cul1/F-box protein complex^{35,36}, we examined the level of FOXO1 protein following DNA damage. In response to NCS treatment, decreased levels of FOXO1 protein were detected in BV173 cells by immunoblot analysis (**Figure 3A**), coinciding with the appearance of a faster migrating band, suggestive of a FOXO1 cleavage product. Of note, this FOXO1 cleavage product was not prevented by pre-treatment with the pan-caspase inhibitor Z-VAD, or the acidic protease inhibitors chloroquine and NH₄Cl (data not shown). Furthermore, *FOXO1* mRNA levels were modestly but significantly reduced in BV173 cells (80% of DMSO-treated controls, $p=0.0003$) and in primary mouse WT pre-B cells (61% of DMSO-treated controls, $p=0.02$) upon induction of DNA damage (**Figure 3B**). Interestingly, DNA damage-induced FOXO1 phosphorylation and cleavage/degradation were prevented pre-treating BV173 cells with the ATM inhibitor KU55933 (**Figure 3A**). Similarly, KU55933 prevented the DNA damage-induced decrease of *FOXO1* mRNA levels (**Figure 3B**). DNA damage thus seems to control the availability and expression of FOXO1 in an ATM-dependent manner. The fact that DNA damage had a modest effect on FOXO1 protein stability/cleavage, whereas it greatly impacted on the *Erag*-binding capacity of FOXO1 suggests that DNA damage regulates RAG1/2 expression primarily by modulating DNA binding of FOXO1 and that FOXO1 degradation/cleavage may be a secondary event.

PI3K-AKT signaling is not involved in the regulation of RAG1 expression in response to DNA damage

Because DNA damage induced FOXO1 phosphorylation on Ser²⁵⁶, which is an established AKT phosphorylation site that affects FOXO1 protein stability, we also explored the contribution of PI3K-AKT signaling in the regulation of FOXO1 and RAG1 following DNA damage. We found that induction of DNA damage resulted in the ATM-dependent phosphorylation of AKT on Ser⁴⁷³ in BV173 cells (**Figure 3A**), similar to that reported earlier for other cell types³⁷. Besides FOXO1, mTOR has been suggested to be a direct target of AKT, phosphorylating mTOR on Ser²⁴⁴⁸³⁸. We assessed mTOR phosphorylation as a positive control for activation of AKT kinase, and consistently, in our experiments DNA damage-dependent AKT Ser⁴⁷³ phosphorylation coincided with increased mTOR Ser²⁴⁴⁸ phosphorylation (**Figures 3A and 4A**). Interestingly, inhibition of AKT kinase activity by increasing amounts of GSK690693 prevented NCS-induced phosphorylation of mTOR, but surprisingly, had no effect on the loss of RAG1 protein (**Figure 4A**). Pre-treatment with the AKT inhibitor had no appreciable effect on the DNA damage-induced p53 Ser¹⁵ phosphorylation. The use of a different structurally unrelated AKT kinase inhibitor, AKT inhibitor VIII, did not prevent the DNA damage-induced loss of RAG1 protein either (**Figure 4B**).

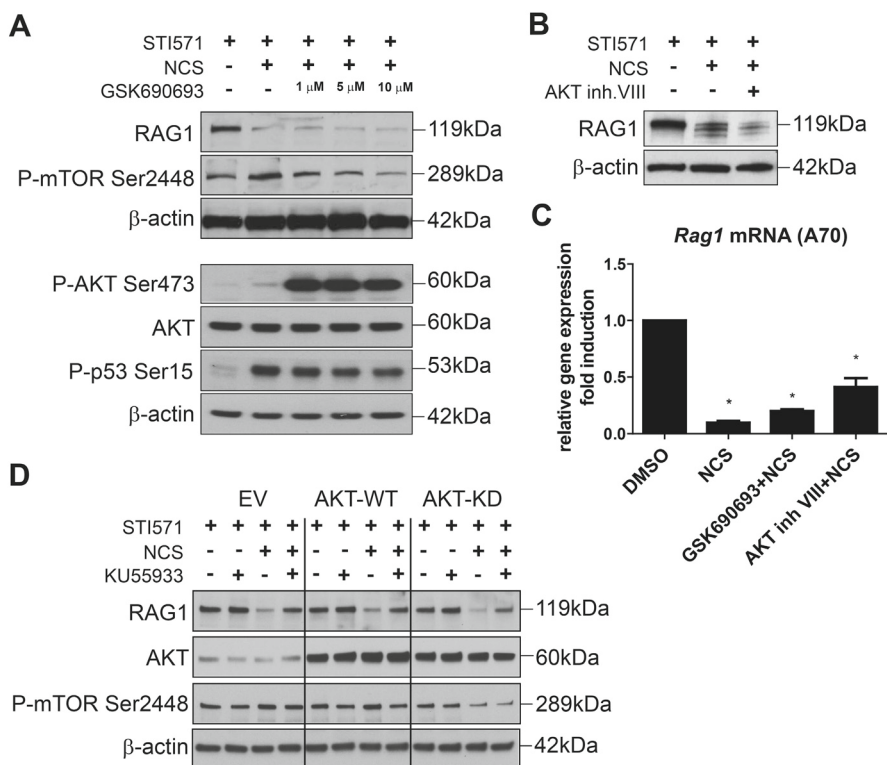


Figure 4. AKT is not involved in regulating RAG1 expression following DNA damage.

(A) Western blot analysis of STI571-treated BV173 BCR-ABL-positive B-ALL cells treated as indicated. DNA damage-induced RAG1 down-regulation could not be prevented by pretreatment with the AKT kinase inhibitor GSK690693. Effective inhibition of AKT kinase was shown by accumulation of AKT Ser⁴⁷³ phosphorylation and diminished mTOR Ser²⁴⁴⁸ phosphorylation. The β -actin blot was used to control for loading. (B) Western blot analysis of STI571-treated BV173 cells treated as indicated. Pretreatment with 10 μ M AKT inhibitor VIII did not prevent DNA damage-induced RAG1 downregulation. The β -actin blot was used to control for loading. (C) Realtime quantitative RT-PCR analysis of *Rag1* mRNA expression in A70 WT mouse *v-Abl* pre-cells treated as indicated, means \pm SEM are shown (n=4, * p<0.05, one-sample *t* test). (D) Western blot analysis of STI571-treated BV173 cells transduced with empty vector (EV), wild type AKT (AKT-WT), or kinase-dead AKT (AKT-KD), and treated as indicated. The AKT blot was used to show AKT overexpression; mTOR Ser²⁴⁴⁸ phosphorylation was diminished upon DNA damage in AKT-KD overexpressing cells. The β -actin blot was used to control for loading.

Treatment with GSK690693 resulted in the accumulation of AKT Ser⁴⁷³ phosphorylation, probably due to disturbed negative feedback regulation impinging on AKT, as was previously reported for this particular AKT kinase inhibitor³⁹⁻⁴¹. Moreover, treatment with either AKT inhibitor had no effect on the down-modulation of *Rag1* mRNA in A70 mouse *v-Abl* pre-B cells following DNA damage (Figure 4C). Furthermore, inhibition of the PI3K p110 δ isoform, which is an upstream regulator of AKT, by the specific inhibitor CAL101

(Idelalisib) did not prevent NCS-induced down-regulation of RAG1 protein either (data not shown). To firmly establish that AKT is not involved in the regulation of RAG1 expression following DNA damage we show that RAG1 protein is decreased equivalently in BV173 cells overexpressing WT-AKT or a dominant-negative kinase-dead mutant of AKT (K179M/T308A/S473A) upon NCS treatment (**Figure 4D**). These combined results clearly indicate that in pre-B cells the effect of DNA damage on RAG1 expression and FOXO1 stability does not involve the PI3K-AKT pathway.

ATM interacts with FOXO1 but does not phosphorylate FOXO1 on SQ/TQ residues

To gain more insight into how the stability and DNA binding activity of FOXO1 is regulated by ATM upon induction of DNA damage, we assessed whether ATM physically interacted with FOXO1 in RAG1-expressing pre-B cells using the proximity ligation assay (PLA), which detects two proteins in close spatial proximity (<30 nm distance)⁴². We observed specific interactions between activated ATM (phosphorylated on Ser¹⁹⁸¹) and FOXO1 in NCS-treated BV173 cells in which RAG1 expression was induced by STI571 (**Figure 5A**). Strikingly, using antibodies that detected both phosphorylated and unphosphorylated (inactive) ATM we found specific interactions between ATM and FOXO1 regardless of whether DNA damage was induced (**Figure 5B**), suggesting that FOXO1 and ATM constitutively interact in RAG1-expressing pre-B cells, and that autophosphorylated ATM is associated with FOXO1 upon induction of DNA damage. In conjunction with the ChIP results that showed enrichment of phosphorylated ATM at the *Erag* enhancer in NCS-treated cells and loss of FOXO1 binding (**Figure 2E**), these data suggest that phosphorylated ATM could be involved in the release of FOXO1 from *Erag*. To confirm the specificity of the PLA experiments we assessed the interaction between ATM and phosphorylated p53 (Ser¹⁵; an ATM kinase substrate), and as expected the interaction was induced by DNA damage and inhibited by KU55933 pre-treatment (**Figure 5C**). In addition, for each of the antibody combinations, PLA experiments in which one of the antibodies was omitted were performed as negative controls, showing no specific PLA signals (**SUPPL Figure 2**).

A functional consequence of the interaction between ATM and FOXO1 might be the ATM-dependent phosphorylation of FOXO1, which may regulate its DNA-binding capacity and stability. Interestingly, a previously performed proteomic screen for ATM and ATR (ATM and Rad3-related) substrates in HEK293T cells that were exposed to 10 Gy of γ -irradiation suggested that FOXO1 may be phosphorylated on residue Ser⁵⁰⁹ by ATM and/or ATR⁴³. To explore whether FOXO1 is phosphorylated by ATM/ATR in RAG1-expressing BV173 cells following induction of DNA damage we performed immunoprecipitations with the ATM/ATR substrate-specific antibody (phospho-SQ/TQ). However, using this approach we could not detect SQ/TQ-phosphorylated FOXO1 upon NCS treatment, whereas ATM-dependent phosphorylation of an established ATM/ATR target such as Nijmegen Breakage Syndrome

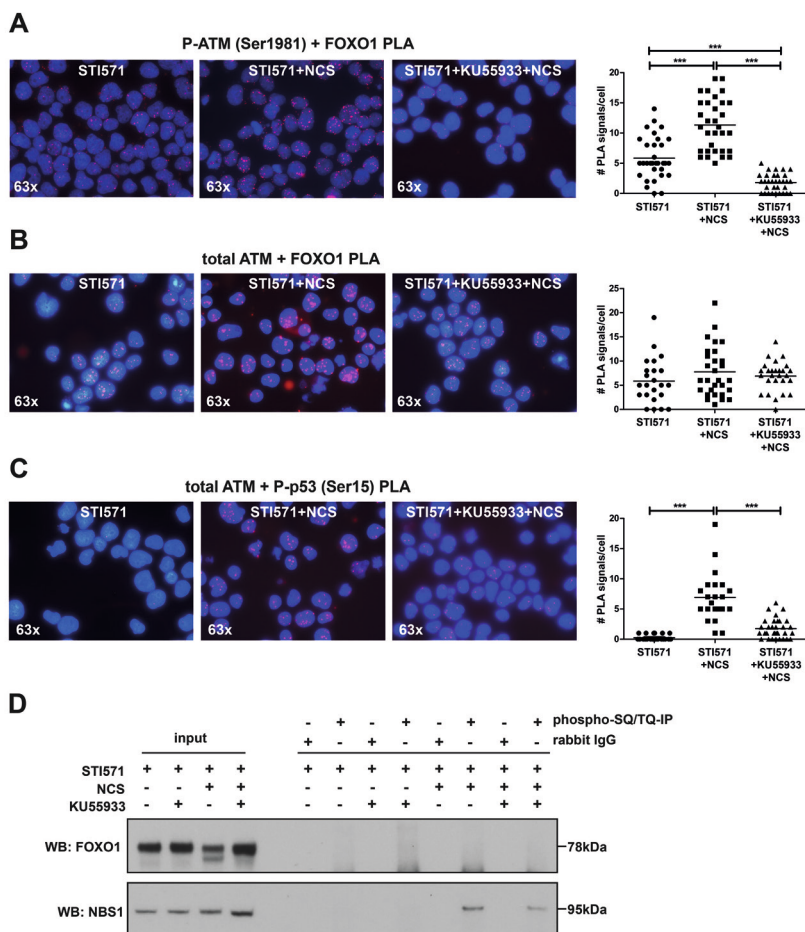


Figure 5. ATM interacts with FOXO1 but does not phosphorylate FOXO1 on SQ/TQ residues.

(A) Proximity ligation assay (PLA) shows the DNA damage-induced interaction between Ser¹⁹⁸¹-phosphorylated ATM and FOXO1 in STI571-treated BV173 BCR-ABL-positive B-ALL cells. Cells were treated as indicated. (B) Constitutive interactions between total ATM (phosphorylated and unphosphorylated) and FOXO1 in STI571-treated BV173 cells. (C) DNA damage-induced interactions between total ATM and Ser¹⁵-phosphorylated p53. Red fluorescent foci represent *in situ* protein proximity (<30 nm). The number of PLA signals per cell in at least 20 cells per condition was quantified. Horizontal lines represent means; statistical significances were determined by one-way ANOVA (***) ($p < 0.001$). (D) Western blot analysis of anti-phospho SQ/TQ (ATM/ATR substrate) immunoprecipitated proteins in STI571-treated BV173 cells that were treated as indicated. Input represents total lysates from treated cells. Immunoprecipitation using polyclonal rabbit IgG served as a negative control for each condition. FOXO1 was not detected in the immunoprecipitates whereas NBS1 was readily detected in NCS-treated cells. Phosphorylation of SQ/TQ residues on NBS1 was reduced by pretreatment of the cells with KU55933 prior to induction of DNA damage, indicating ATM-dependent phosphorylation. A representative example of two independent immunoprecipitation experiments is shown.

1 (NBS1)^{44,45} was readily detected (**Figure 5D**). The fact that we could ChIP phospho-ATM at the *Erag* enhancer region in NCS-treated cells whereas FOXO1 DNA-binding was abolished under these conditions (**Figure 2D**) suggests that ATM may locally regulate/impair the DNA occupancy of FOXO1, but most likely this does not involve direct phosphorylation of FOXO1 by ATM.

Of note, the interaction between phosphorylated ATM and FOXO1 was already observable in STI571-treated cells and was further increased after induction of DNA damage. This suggests that there is already some degree of DNA damage in cells treated with STI571. Since RAG expression is induced by STI571 we proposed that RAG-mediated DNA cleavage could be the source of this DNA damage, thereby activating negative feedback regulation of RAG expression.

RAG-dependent DNA breaks regulate RAG1 expression through a negative feedback mechanism

To assess whether the RAG-dependent endogenous DNA breaks are able to regulate RAG1 expression, WT (A70) and *Rag2*^{-/-} (R2K3) mouse *v-Abl* cells were treated with STI571 for 72 hours and *Rag1* mRNA expression was quantified. Because both RAG1 and RAG2 are needed to form the RAG1/2 complex that possesses the endonuclease activity, no *Ig* rearrangement-related DNA breaks are generated upon STI571-treatment in *Rag2*^{-/-} *v-Abl* cells²⁷. Interestingly, *Rag1* mRNA expression was 2.7-fold higher in STI571-treated *Rag2*^{-/-} as compared to WT *v-Abl* cells (**Figure 6A**). Inhibition of ATM kinase activity increased *Rag1* mRNA expression in WT *v-Abl* cells to a similar level as observed in *Rag2*^{-/-} *v-Abl* cells, but did not alter *Rag1* mRNA expression levels in *Rag2*^{-/-} *v-Abl* cells. In accordance, *Rag2*^{-/-} *v-Abl* cells showed enhanced *Erag-Rag1* luciferase reporter activity compared to WT *v-Abl* cells upon STI571 treatment (**Figure 6B**). To further substantiate the point that DNA breaks can regulate the *Rag1* expression levels in *Rag2*^{-/-} *v-Abl* cells, we show that exogenously induced DNA breaks by NCS also provoked the ATM-dependent inhibition of *Rag1* transcription in these cells (**Figure 6C**). In addition, we show that in the absence of Artemis nuclease, which is required for the repair of RAG1/2-dependent coding joint hairpins, *Rag2*-deficient cells have significantly increased *Rag1* mRNA expression compared to *Rag2*-proficient cells (**Figure 6D**). Also, the expression level of *Rag1* mRNA is about twofold lower in STI571-treated Artemis^{-/-} versus wildtype *v-Abl* cells (compare **Figures 6A** and **6D**), which may be caused by the accumulation of RAG1/2-dependent breaks in Artemis-deficient cells, due to the lack of repair of coding ends.

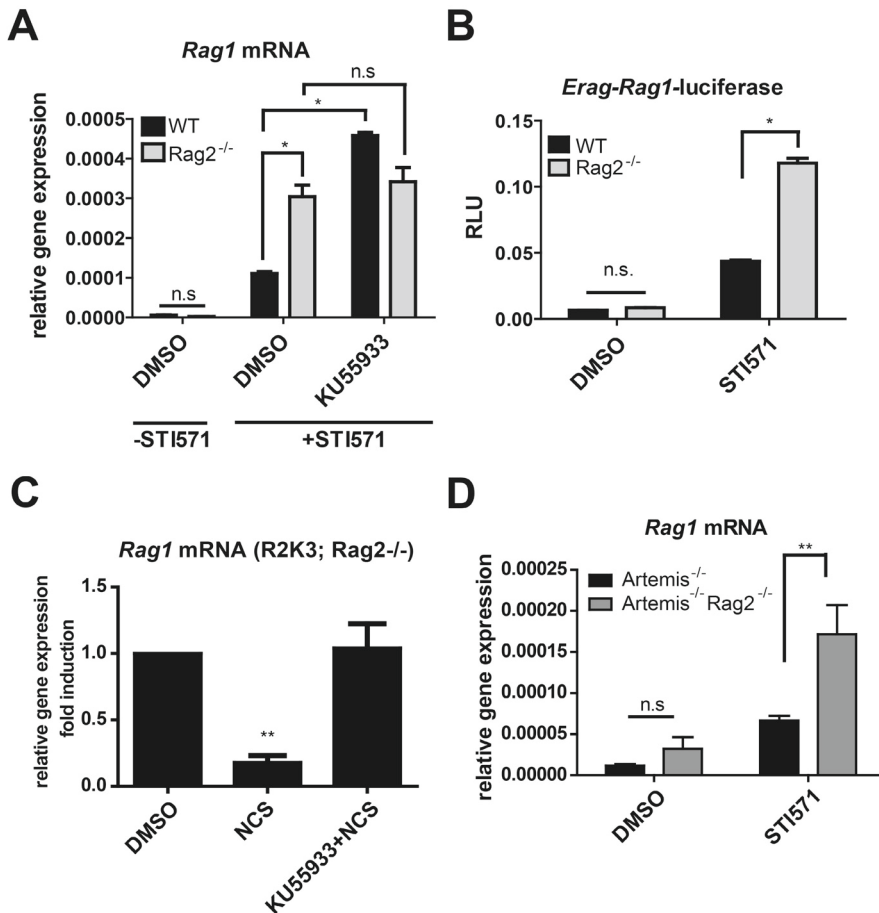


Figure 6. *Rag1* mRNA expression is regulated by RAG-dependent DNA breaks.

(A) Realtime quantitative RT-PCR analysis of *Rag1* mRNA expression in A70 (WT, black bars) and R2K3 (*Rag2*^{-/-}, grey bars) mouse *v-Abl* cells treated for 72h with 5 μ M STI571 and 5 μ M KU55933 or vehicle (DMSO), *Rag1* mRNA expression relative the housekeeping gene *18S rRNA* is shown. Means \pm SEM are shown ($n=3$, * $p<0.05$, one-way ANOVA). (B) *Erag-Rag1*-driven luciferase activity was measured by transient transfection of the *Erag-Rag1* luciferase construct in A70 (WT, black bars) and R2K3 (*Rag2*^{-/-}, grey bars) mouse *v-Abl* pre-B cells treated for 72h with 5 μ M STI571 or vehicle (DMSO). Relative light units (RLU) normalized to the TK *Renilla* luciferase reporter vector are shown. Following transfection, cells were treated for 24h with 5 μ M KU55933. Means \pm SEM are shown ($n=3$, * $p<0.05$, two-way ANOVA). (C) Realtime quantitative RT-PCR analysis *Rag1* mRNA expression in R2K3 (*Rag2*^{-/-}) treated overnight with 5 μ M STI571. DNA damage induction by 2h treatment with 50 ng/mL NCS resulted in a rapid down-regulation of *Rag1* mRNA expression in *Rag2*-deficient cells, which was prevented by 2h pretreatment with 5 μ M KU55933. Means \pm SEM are shown ($n=3$, ** $p=0.004$). (D) Realtime quantitative RT-PCR analysis of *Rag1* mRNA expression in *Artemis*^{-/-} (black bars) and *Artemis*^{-/-} *Rag2*^{-/-} (grey bars) mouse *v-Abl* cells treated for 72h with 5 μ M STI571 or vehicle (DMSO). Means \pm SEM are shown ($n=3$, ** $p<0.01$, two-way ANOVA).

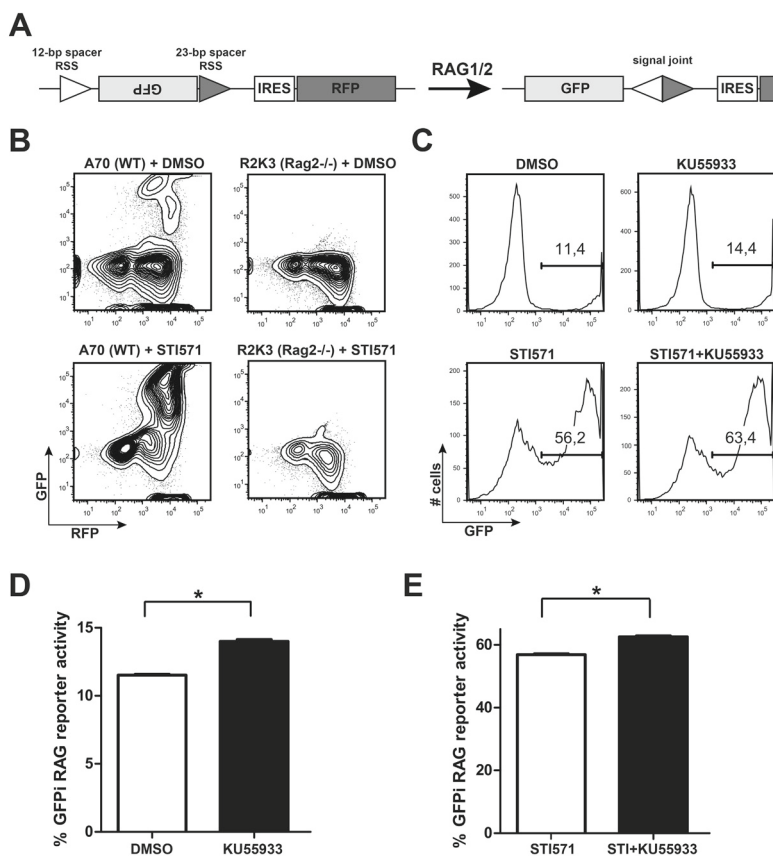


Figure 7. Inhibition of ATM kinase function augments RAG1/2 recombination activity.

(A) Schematic depiction of the fluorescent RAG1/2 activity reporter construct. White and grey triangles represent 12-bp spacer RSS and 23-bp spacer RSS, respectively. RAG1/2-mediated inversional recombination results in the formation of a signal joint and the sense orientation of the GFP cassette. (B) Representative FACS plots of A70 (WT) and R2K3 (*Rag2*^{-/-}) mouse *v-Ab1* cells treated with vehicle (DMSO; upper panels) or treated with 5 μ M STI571 for 96h (lower panels). (C) Representative FACS histograms showing GFP expression within RFP-gate (indicative of RAG1/2 activity) in A70 pre-B cells treated for 96h with vehicle (DMSO) (upper left panel) 5 μ M KU55933 (upper right panel), 5 μ M STI571 (lower left panel) or 5 μ M KU55933 + 5 μ M STI571 (lower right panel). Percentages of GFP-positive cells are indicated in FACS plots. (D) Bar graph depicting percentages of GFP-positive cells within RFP-gate in A70 pre-B cells treated for 96h with vehicle (DMSO, white bar) or 5 μ M KU55933 (black bar). Means \pm SEM are shown (n=4, * p<0.05, Mann-Whitney *U* test). (E) Bar graph depicting percentages of GFP-positive cells within RFP-gate in A70 pre-B cells treated for 96h with 5 μ M STI571 (white bar) or 5 μ M STI571 + 5 μ M KU55933 (black bar). Means \pm SEM are shown (n=4, * p<0.05, Mann-Whitney *U* test).

Taken together, these results suggest that DNA breaks that originate from RAG1/2 activity and *Ig* gene rearrangements are involved in the down-regulation of *Rag1* mRNA expression in ATM-dependent manner. Moreover, it suggests that the kinase function of ATM restricts the activity of the RAG1/2 endonuclease complex. To directly assess the impact of ATM kinase on RAG1/2 activity we made use of a novel fluorescent reporter system that has an antisense green fluorescent protein (GFP) cassette, which is flanked by a 12-basepair spacer RSS and a 23-basepair spacer RSS²⁶. Functional expression of the RAG1/2 complex mediates inversional recombination that results in the sense orientation of the GFP cassette, which can be monitored in cells that co-express control red fluorescent protein (RFP) (**Figures 7A, 7B**). Treatment of mouse *v-Abl* cells with KU55933 resulted in a modest but reproducible increase in spontaneous (**Figure 7C upper panels and Figure 7D**) and STI571-induced RAG-dependent reporter activity (**Figure 7C lower panels and Figure 7E**), consistent with a modest increase in *Igh* allelic inclusion in ATM-deficient mouse splenic and bone marrow B cells⁴⁶. Collectively, these results show that ATM kinase activity is involved in limiting the activity of the RAG1/2 complex.

Discussion

The strict and ordered regulation of the RAG1/2 complex in developing B cells ensures the expression of a functional B-cell receptor required for B-cell maturation, while minimizing the risk of collateral damage emanating from this endonuclease. As there is ample evidence for the involvement of illegitimate RAG1/2 activity in genomic alterations found in mouse and human B-cell malignancies^{15-17,47}, a thorough understanding of the mechanisms that control RAG1/2 expression will provide insight into the etiology of these malignancies and may even yield strategies to curb this potentially hazardous endonuclease.

Previously, it was shown that RAG1/2 activity is restricted in a cell-cycle dependent manner⁴⁸, which involves the cyclinA/CDK2-triggered proteasomal destruction of the RAG2 protein¹⁵, whereas RAG1 protein stability does not appear to be cell-cycle regulated¹³. At the transcriptional level, the expression of the RAG1 and RAG2 genes, residing in the same locus, is coordinately regulated by the binding of several transcription factors to *cis*-acting sequences¹², of which FOXO1 and FOXP1 binding to the *Erag* enhancer emerge as major players in the regulation of RAG expression in B lymphocytes^{32,49}. In this study, we investigated whether additional mechanisms, other than cell cycle-dependent RAG2 protein degradation, are involved limiting RAG-dependent DNA damage.

In agreement with previous studies, we find that the DNA damage response regulates RAG in normal and malignant pre-B cells^{46,50}. We show that DNA damage induces a rapid ATM-dependent down-regulation of RAG1 and RAG2 mRNA and protein expression. Our finding that recombinant expression of RAG1 in HEK293 cells was not affected by DNA damage suggests a predominantly transcriptional regulatory mechanism, although in

pre-B cells the stability/turnover of RAG1 was clearly affected by DNA damage, suggesting that a post-translational regulatory mechanism exists that may be cell-type specific. However, in further support of a transcriptional regulatory mechanism, we show that DNA damage abolished FOXO1 binding to the *Erag* enhancer, which was restored by pre-treatment with the ATM kinase inhibitor. Furthermore, DNA damage resulted in the partial cleavage/degradation of FOXO1. However, the dramatic reduction of RAG1 transcription upon DNA damage suggests that the incomplete loss of FOXO1 protein integrity is a secondary event following the loss of FOXO1 DNA-binding activity. The very short half-life of RAG1 protein and mRNA of approximately 15 minutes and 30 minutes, respectively^{29,30}, allows for the dynamic regulation of expression at the transcriptional level, falling well within the range of 2 hours, after which we analyzed RAG1 protein and mRNA expression upon induction of DNA damage. Also from our experiments, we conclude that caspase-mediated proteolysis is not involved in the regulation of RAG1 expression, as pre-treatment with the pan-caspase inhibitor Q-VD-OPH did not prevent RAG1 downregulation upon DNA damage.

In previous studies, it was shown that treatment with PI3K inhibitors or the specific lack of the p85 α subunit of PI3K in immature B cells increased the expression of RAG1⁵¹, whereas the overexpression of myristoylated (constitutively active) AKT suppressed RAG1 expression in developing B cells³². Since the FOXO transcription factors are bona fide phosphorylation targets of the PI3K-AKT kinase pathway, acting downstream from the pre-BCR and BCR⁵¹ and resulting in nuclear exclusion and degradation of FOXO, we assessed the role of AKT signaling in the downmodulation of RAG1 expression following DNA damage. We found that both AKT and FOXO1 were phosphorylated in an ATM-dependent manner upon NCS treatment, but surprisingly, inhibition of AKT kinase activity did not prevent the downregulation of RAG1. In addition to AKT, several other kinases have been reported to regulate the subcellular distribution and activity of FOXO1, such as p38 MAPK, I κ B kinase ERK, and JNK^{27,52}. Pretreatment of RAG-expressing pre-B cells with small molecule inhibitors for neither of these kinases prior to induction of DNA damage was able to prevent RAG1 down-regulation, suggesting that these kinases are not involved in the regulation of RAG1 expression upon DNA damage (data not shown).

Using PLA, we show that the ATM kinase and FOXO1 can be found in close proximity (<30 nm). This interaction was found irrespective of the induction of exogenous DNA damage suggesting a constitutive association. Despite the physical interaction, we found no evidence for the ATM-dependent phosphorylation of FOXO1 upon induction of DNA damage. Using CHIP, we detected phosphorylated ATM at the *Erag* enhancer region in NCS-treated cells, suggesting that DNA damage activates ATM to locally release FOXO1 binding to *Erag*. Previously, a similar local effect on the transactivation of RAG expression by FOXO1 was described by Chow *et al.* who showed that MAPK-activated protein kinase (MAPKAPK5) phosphorylates FOXO1 on Ser²¹⁵, which is required for binding to the

RAG locus and RAG expression, but not for the expression of several other FOXO1 target genes⁵³. Unfortunately, we could not assess the effects of DNA damage on FOXO1 Ser²¹⁵ phosphorylation, as antibodies recognizing this specific FOXO1 phospho-protein are not available. It was shown that MAPKAPK5 expression is required for RAG expression in pre-B cells, leaving open the possibility that MAPKAPK5 levels itself could be regulated by DNA damage. To address this possibility we assessed the levels of MAPKAPK5 in STI571-treated BV173 pre-B cells but found no difference in MAPKAPK5 levels upon DNA damage and/or ATM kinase inhibition (**SUPPL Figure 3**). Additionally, it was shown that the BCL11a transcription factor activates RAG1/2 expression in pre-B cells and is critical component of the gene regulatory network controlling early B-cell development⁵⁴. However, we neither found evidence for the DNA damage-mediated regulation of BCL11a in STI571-treated BV173 pre-B cells (**SUPPL Figure 3**).

Based on the above we hypothesize that the ATM kinase may possibly function by recruiting or activating additional factors that regulate the DNA-binding capacity and stability of FOXO1 in RAG-expressing pre-B cells, of which the identity remains to be elucidated. The ATM kinase may be involved in post-translational modifications that affect the DNA-binding properties of FOXO1, other than phosphorylation. For instance, it was shown that acetylation of FOXO1 decreased its affinity for the target DNA⁵⁵. The acetylation status of FOXO1 is regulated by the acetyltransferase C-AMP response element-binding protein (CBP) and the NAD-dependent histone deacetylase sirtuin 1 (SIRT1)^{56,57}. Of interest, ATM was shown to activate the deleted in breast cancer 1 (DBC1) protein upon induction of DNA damage, which is a negative regulator of SIRT1^{58,59}. A possible scenario might be that ATM inhibits the deacetylation of FOXO1 by activating DBC1, thereby regulating the DNA-binding capacity of FOXO1. In an earlier study in A549 lung carcinoma cells, the acetylation of overexpressed FLAG-tagged FOXO1 could be detected upon induction of DNA damage⁵⁸. However, we were unable to convincingly show acetylation of endogenous FOXO1 in BV173 cells exposed to NCS (data not shown).

Consistent with earlier reports, we show that DNA breaks resulting from RAG1/2 activity trigger an ATM-dependent negative feedback loop that limits the expression and activity of RAG1/2^{46,50}. Previously, it was shown that this negative feedback regulation contributes to *Igκ* allelic exclusion by suppressing secondary *Vκ* to *Jκ* rearrangements and therefore is an integral part of B-cell development⁴⁶. In agreement with this, we find that the activity of RAG1/2 is slightly enhanced upon inhibition of the ATM kinase function. It was suggested that ATM regulates RAG1/2 expression by repressing the growth arrest and DNA-damage-inducible protein (GADD45α)⁴⁶, which is important for RAG1/2 transcription in mouse *v-Abl* transformed pre-B cells³². However, we could not detect any alterations in the mRNA or protein levels of Gadd45α in mouse *v-Abl* transformed pre-B cells and BV173 BCR-ABL-positive B-ALL cells 2h after DNA damage induction by NCS, nor after (pre-) treatment of these cells with the ATM kinase inhibitor (**SUPPL Figure 4**).

In a recent study, it was shown that RAG2 is also affected by DNA damage, triggering its nuclear export. However, only a modest fraction of RAG2 was shown to undergo sub-cellular redistribution, making it unlikely that this mechanism is involved in regulating V(D)J recombination⁶⁰.

Previously, in severe combined immune deficient (SCID) mice it was shown that irradiation promotes the aberrant joining of RAG1/2-dependent DNA breaks to random DNA breaks, leading to chromosomal translocations that promote thymic lymphomagenesis⁶¹. We speculate that the rapid downregulation of RAG1 upon DNA damage may be important in preventing such aberrant recombinations in pro- and pre-B cells that have initiated V(D)J recombination, by limiting the co-existence of RAG-dependent and RAG-independent DNA breaks. Our data suggest that ATM imposes an important barrier for the generation of RAG-dependent DNA damage not only by regulating DNA repair of these lesions^{62,63} but also by transcriptional regulation of RAG1, thereby preventing excessive and inappropriate RAG activity.

Conflict of interest statement

The authors declare that there are no conflicts of interest.

Acknowledgements

We thank Dr. Craig Bassing (University of Pennsylvania School of Medicine, Philadelphia, PA), Drs. Inês Trancoso and Jocelyne Demengeot (Instituto Gulbenkian, Oeiras, Portugal); Prof. Mark Schlissel (University of Michigan, Ann Arbor, MI) and Dr. Mirjam van der Burg (Erasmus Medical Center, Rotterdam, The Netherlands) for providing reagents and cell lines, and Yanís Pelinski Carmona for excellent technical assistance.

References

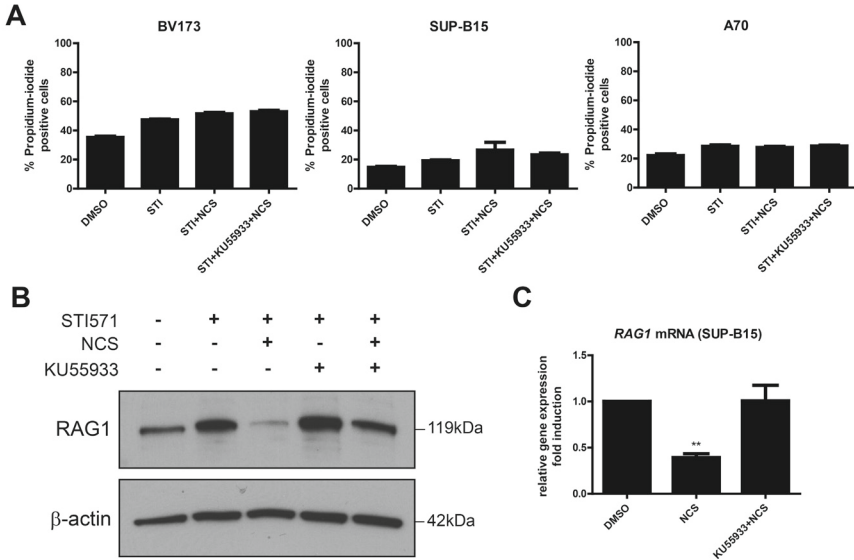
1. Tonegawa, S. 1983. Somatic generation of antibody diversity. *Nature* 302: 575–581.
2. Fugmann, S. D., A. I. Lee, P. E. Shockett, I. J. Villey, and D. G. Schatz. 2000. The RAG proteins and V(D)J recombination: complexes, ends, and transposition. *Annu. Rev. Immunol.* 18: 495–527.
3. Boboila, C., F. W. Alt, and B. Schwer. 2012. Classical and alternative end-joining pathways for repair of lymphocyte-specific and general DNA double-strand breaks. *Adv. Immunol.* 116: 1–49.
4. Clark, M. R., M. Mandal, K. Ochiai, and H. Singh. 2014. Orchestrating B cell lymphopoiesis through interplay of IL-7 receptor and pre-B cell receptor signalling. *Nat. Rev. Immunol.* 14: 69–80.
5. Herzog, S., M. Reth, and H. Jumaa. 2009. Regulation of B-cell proliferation and differentiation by pre-B-cell receptor signalling. *Nat. Rev. Immunol.* 9: 195–205.
6. Mandal, M., S. E. Powers, K. Ochiai, K. Georgopoulos, B. L. Kee, H. Singh, and M. R. Clark. 2009. Ras orchestrates exit from the cell cycle and light-chain recombination during early B cell development. *Nat. Immunol.* 10: 1110–1117.
7. Shaw, A. C., W. Swat, R. Ferrini, L. Davidson, and F. W. Alt. 1999. Activated Ras Signals Developmental Progression of Recombinase-activating Gene (RAG)-deficient Pro-B Lymphocytes. *J. Exp. Med.* 189: 123–129.
8. Stadhouders, R., M. J. W. de Bruijn, M. B. Rother, S. Yuvaraj, C. Ribeiro de Almeida, P. Kolovos, M. C. Van Zelm, W. van Ijcken, F. Grosveld, E. Soler, and R. W. Hendriks. 2014. Pre-B cell receptor signaling induces immunoglobulin κ locus accessibility by functional redistribution of enhancer-mediated chromatin interactions. *PLoS Biol.* 12: e1001791.
9. Jumaa, H., B. Wollscheid, M. Mitterer, J. Wienands, M. Reth, and P. J. Nielsen. 1999. Abnormal development and function of B lymphocytes in mice deficient for the signaling adaptor protein SLP-65. *Immunity* 11: 547–554.
10. Yu, W., Z. Misulovin, H. Suh, R. R. Hardy, M. Jankovic, N. Yannoutsos, and M. C. Nussenzweig. 1999. Coordinate regulation of RAG1 and RAG2 by cell type-specific DNA elements 5' of RAG2. *Science* 285: 1080–1084.
11. Hsu, L.-Y., J. Lauring, H.-E. Liang, S. Greenbaum, D. Cado, Y. Zhuang, and M. S. Schlissel. 2003. A conserved transcriptional enhancer regulates RAG gene expression in developing B cells. *Immunity* 19: 105–117.
12. Kuo, T. C., and M. S. Schlissel. 2009. Mechanisms controlling expression of the RAG locus during lymphocyte development. *Curr. Opin. Immunol.* 21: 173–178.
13. Lin, W. C., and S. Desiderio. 1994. Cell cycle regulation of V(D)J recombination-activating protein RAG-2. *Proc Natl Acad Sci U S A* 91: 2733–2737.
14. Li, Z., D. I. Dordai, J. Lee, and S. Desiderio. 1996. A conserved degradation signal regulates RAG-2 accumulation during cell division and links V(D)J recombination to the cell cycle. *Immunity* 5: 575–589.
15. Lee, J., and S. Desiderio. 1999. Cyclin A/CDK2 regulates V(D)J recombination by coordinating RAG-2 accumulation and DNA repair. *Immunity* 11: 771–781.
16. Zhang, L., T. L. Reynolds, X. Shan, and S. Desiderio. 2011. Coupling of V(D)J recombination to the cell cycle suppresses genomic instability and lymphoid tumorigenesis. *Immunity* 34: 163–174.

17. Papaemmanuil, E., I. Rapado, Y. Li, N. E. Potter, D. C. Wedge, J. Tubio, L. B. Alexandrov, P. Van Loo, S. L. Cooke, J. Marshall, I. Martincorena, J. Hinton, G. Gundem, F. W. van Delft, S. Nik-Zainal, D. R. Jones, M. Ramakrishna, I. Tittley, L. Stebbings, C. Leroy, A. Menzies, J. Gamble, B. Robinson, L. Mudie, K. Raine, S. O'Meara, J. W. Teague, A. P. Butler, G. Cazzaniga, A. Biondi, J. Zuna, H. Kempinski, M. Muschen, A. M. Ford, M. R. Stratton, M. Greaves, and P. J. Campbell. 2014. RAG-mediated recombination is the predominant driver of oncogenic rearrangement in ETV6-RUNX1 acute lymphoblastic leukemia. *Nat. Genet.* 46: 116–125.
18. Steenbergen, E. J., O. J. Verhagen, E. F. van Leeuwen, A. E. von dem Borne, and C. E. van der Schoot. 1993. Distinct ongoing Ig heavy chain rearrangement processes in childhood B-precursor acute lymphoblastic leukemia. *Blood* 82: 581–589.
19. Landau, D. A., S. L. Carter, G. Getz, and C. J. Wu. 2014. Clonal evolution in hematological malignancies and therapeutic implications. *Leukemia* 28: 34–43.
20. Pegoraro, L., L. Matera, J. Ritz, A. Levis, A. Palumbo, and G. Biagini. 1983. Establishment of a Ph1-positive human cell line (BV173). *J. Natl. Cancer Inst.* 70: 447–453.
21. Muljo, S. A., and M. S. Schlissel. 2003. A small molecule Abl kinase inhibitor induces differentiation of Abelson virus-transformed pre-B cell lines. *Nat. Immunol.* 4: 31–37.
22. Barlow, C., S. Hirotsune, R. Paylor, M. Livanage, M. Eckhaus, F. Collins, Y. Shiloh, J. N. Crawley, T. Ried, D. Tagle, and A. Wynshaw-Boris. 1996. Atm-deficient mice: a paradigm of ataxia telangiectasia. *Cell* 86: 159–171.
23. DiRenzo, J., S. Signoretti, N. Nakamura, R. Rivera-Gonzalez, W. Sellers, M. Loda, and M. Brown. 2002. Growth factor requirements and basal phenotype of an immortalized mammary epithelial cell line. *Cancer Res.* 62: 89–98.
24. Weber, K., U. Bartsch, C. Stocking, and B. Fehse. 2008. A multicolor panel of novel lentiviral “gene ontology” (LeGO) vectors for functional gene analysis. *Mol. Ther.* 16: 698–706.
25. Frecha, C., C. Costa, C. Lévy, D. Nègre, S. J. Russell, A. Maisner, G. Salles, K.-W. Peng, F.-L. Cosset, and E. Verhoeven. 2009. Efficient and stable transduction of resting B lymphocytes and primary chronic lymphocyte leukemia cells using measles virus gp displaying lentiviral vectors. *Blood* 114: 3173–3180.
26. Trancoso, I., M. Bonnet, R. Gardner, J. Carneiro, V. M. Barreto, J. Demengeot, and L. M. Sarmiento. 2013. A Novel Quantitative Fluorescent Reporter Assay for RAG Targets and RAG Activity. *Front. Immunol.* 4: 110.
27. Ochodnicka-Mackovicova, K., M. Bahjat, T. A. Bloedjes, C. Maas, A. M. de Bruin, R. J. Bende, C. J. M. van Noesel, and J. E. J. Guikema. 2015. NF- κ B and AKT signaling prevent DNA damage in transformed pre-B cells by suppressing RAG1/2 expression and activity. *Blood* 10: 1324–1335.
28. Hittelman, W. N., and M. Pollard. 1982. Induction and repair of DNA and chromosome damage by neocarzinostatin in quiescent normal human fibroblasts. *Cancer Res.* 42: 4584–4590.
29. Sadofsky, M. J., J. E. Hesse, J. F. McBlane, and M. Gellert. 1993. Expression and V(D) J recombination activity of mutated RAG-1 proteins. *Nucleic Acids Res.* 21: 5644–5650.
30. Verkoczy, L., D. Ait-Azzouzene, P. Skog, A. Mårtensson, J. Lang, B. Duong, and D. Nemazee. 2005. A role for nuclear factor kappa B/rel transcription factors in the regulation of the recombinase activator genes. *Immunity* 22: 519–531.
31. Cullen, S. P., and S. J. Martin. 2009. Caspase activation pathways: some recent progress. *Cell Death Differ.* 16: 935–938.
32. Amin, R. H., and M. S. Schlissel. 2008. Foxo1 directly regulates the transcription of recombination-activating genes during B cell development. *Nat. Immunol.* 9: 613–622.

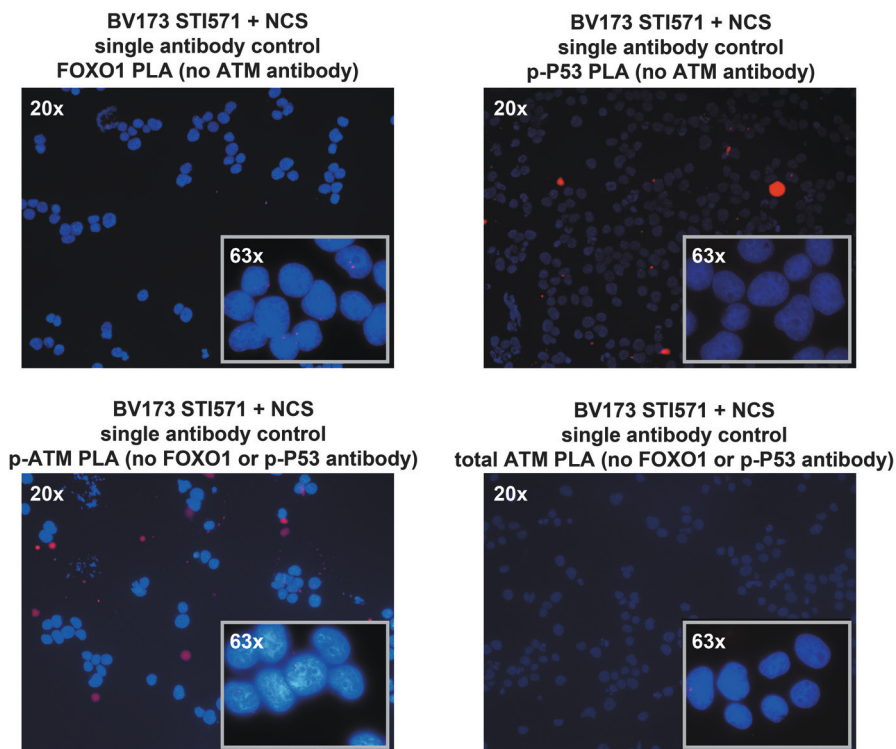
33. Dengler, H. S., G. V Baracho, S. A. Omori, S. Bruckner, K. C. Arden, D. H. Castrillon, R. A. DePinho, and R. C. Rickert. 2008. Distinct functions for the transcription factor Foxo1 at various stages of B cell differentiation. *Nat. Immunol.* 9: 1388–1398.
34. Ochiai, K., M. Maienschein-Cline, M. Mandal, J. R. Triggs, E. Bertolino, R. Sciammas, A. R. Dinner, M. R. Clark, and H. Singh. 2012. A self-reinforcing regulatory network triggered by limiting IL-7 activates pre-BCR signaling and differentiation. *Nat. Immunol.* 13: 300–307.
35. Calnan, D. R., and A. Brunet. 2008. The FoxO code. *Oncogene* 27: 2276–2288.
36. Huang, H., K. M. Regan, F. Wang, D. Wang, D. I. Smith, J. M. A. van Deursen, and D. J. Tindall. 2005. Skp2 inhibits FOXO1 in tumor suppression through ubiquitin-mediated degradation. *Proc. Natl. Acad. Sci. U. S. A.* 102: 1649–1654.
37. Fraser, M., S. M. Harding, H. Zhao, C. Coackley, D. Durocher, and R. G. Bristow. 2011. MRE11 promotes AKT phosphorylation in direct response to DNA double-strand breaks. *Cell Cycle* 10: 2218–2232.
38. Sekulić, A., C. C. Hudson, J. L. Homme, P. Yin, D. M. Otterness, L. M. Karnitz, and R. T. Abraham. 2000. A direct linkage between the phosphoinositide 3-kinase-AKT signaling pathway and the mammalian target of rapamycin in mitogen-stimulated and transformed cells. *Cancer Res.* 60: 3504–3513.
39. Rhodes, N., D. A. Heerding, D. R. Duckett, D. J. Eberwein, V. B. Knick, T. J. Lansing, R. T. McConnell, T. M. Gilmer, S.-Y. Zhang, K. Robell, J. A. Kahana, R. S. Geske, E. V Klyemenova, A. E. Choudhry, Z. Lai, J. D. Leber, E. A. Minthorn, S. L. Strum, E. R. Wood, P. S. Huang, R. A. Copeland, and R. Kumar. 2008. Characterization of an Akt kinase inhibitor with potent pharmacodynamic and antitumor activity. *Cancer Res.* 68: 2366–2374.
40. Levy, D. S., J. A. Kahana, and R. Kumar. 2009. AKT inhibitor, GSK690693, induces growth inhibition and apoptosis in acute lymphoblastic leukemia cell lines. *Blood* 113: 1723–1729.
41. Altomare, D. A., L. Zhang, J. Deng, A. Di Cristofano, A. J. Klein-Szanto, R. Kumar, and J. R. Testa. 2010. GSK690693 delays tumor onset and progression in genetically defined mouse models expressing activated Akt. *Clin. Cancer Res.* 16: 486–496.
42. Söderberg, O., M. Gullberg, M. Jarvius, K. Ridderstråle, K.-J. Leuchowius, J. Jarvius, K. Wester, P. Hydbring, F. Bahram, L.-G. Larsson, and U. Landegren. 2006. Direct observation of individual endogenous protein complexes in situ by proximity ligation. *Nat. Methods* 3: 995–1000.
43. Matsuoka, S., B. A. Ballif, A. Smogorzewska, E. R. McDonald III, K. E. Hurov, J. Luo, C. E. Bakalarski, Z. Zhao, N. Solimini, Y. Lerenthal, Y. Shiloh, S. P. Gygi, and S. J. Elledge. 2007. ATM and ATR substrate analysis reveals extensive protein networks responsive to DNA damage. *Science (80-.)*. 316: 1160–1166.
44. Gatei, M., D. Young, K. M. Cerosaletti, A. Desai-Mehta, K. Spring, S. Kozlov, M. F. Lavin, R. A. Gatti, P. Concannon, and K. Khanna. 2000. ATM-dependent phosphorylation of nibrin in response to radiation exposure. *Nat. Genet.* 25: 115–119.
45. Lim, D. S., S. T. Kim, B. Xu, R. S. Maser, J. Lin, J. H. Petrini, and M. B. Kastan. 2000. ATM phosphorylates p95/nbs1 in an S-phase checkpoint pathway. *Nature* 404: 613–617.
46. Steinel, N. C., B.-S. Lee, A. T. Tubbs, J. J. Bednarski, E. Schulte, K. S. Yang-Lott, D. G. Schatz, B. P. Sleckman, and C. H. Bassing. 2013. The ataxia telangiectasia mutated kinase controls Igk allelic exclusion by inhibiting secondary Vκ-to-Jκ rearrangements. *J. Exp. Med.* 210: 233–239.
47. Waanders, E., B. Scheijen, L. T. van der Meer, S. V van Reijmersdal, L. van Emst, Y. Kroeze, E. Sonneveld, P. M. Hoogerbrugge, A. G. van Kessel, F. N. van Leeuwen, and R. P. Kuiper. 2012. The origin and nature of tightly clustered BTG1 deletions in precursor B-cell acute lymphoblastic leukemia support a model of multiclonal evolution. *PLoS Genet.* 8: e1002533.

48. Schlissel, M., A. Constantinescu, T. Morrow, M. Baxter, and A. Peng. 1993. Double-strand signal sequence breaks in V(D)J recombination are blunt, 5'-phosphorylated, RAG-dependent, and cell cycle regulated. *Genes Dev.* 7: 2520–2532.
49. Hu, H., B. Wang, M. Borde, J. Nardone, S. Maika, L. Allred, P. W. Tucker, and A. Rao. 2006. Foxp1 is an essential transcriptional regulator of B cell development. *Nat Immunol* 7: 819–826.
50. Steinel, N. C., M. R. Fisher, K. S. Yang-lott, and C. H. Bassing. 2014. The ataxia telangiectasia mutated and cyclin D3 proteins cooperate to help enforce TCR β and IgH allelic exclusion. *J. Immunol.* 193: 2881–2890.
51. Verkoczy, L., B. Duong, P. Skog, D. Ait-Azouzene, K. Puri, J. L. Vela, and D. Nemazee. 2007. Basal B cell receptor-directed phosphatidylinositol 3-kinase signaling turns off RAGs and promotes B cell-positive selection. *J. Immunol.* 178: 6332–6341.
52. Eijkelenboom, A., and B. M. T. Burgering. 2013. FOXOs: signalling integrators for homeostasis maintenance. *Nat. Rev. Mol. Cell Biol.* 14: 83–97.
53. Chow, K. T., G. A. Timblin, S. M. McWhirter, and M. S. Schlissel. 2013. MK5 activates Rag transcription via Foxo1 in developing B cells. *J. Exp. Med.* 210: 1621–1634.
54. Lee, B., J. D. Dekker, B. Lee, V. R. Iyer, B. P. Sleckman, A. L. Shaffer, G. C. Ippolito, and P. W. Tucker. 2013. The BCL11A transcription factor directly activates RAG gene expression and V(D)J recombination. *Mol. Cell. Biol.* 33: 1768–1781.
55. Matsuzaki, H., H. Daitoku, M. Hatta, H. Aoyama, K. Yoshimochi, and A. Fukamizu. 2005. Acetylation of Foxo1 alters its DNA-binding ability and sensitivity to phosphorylation. *Proc. Natl. Acad. Sci. U. S. A.* 102: 11278–11283.
56. Daitoku, H., M. Hatta, H. Matsuzaki, S. Aratani, T. Ohshima, M. Miyagishi, T. Nakajima, and A. Fukamizu. 2004. Silent information regulator 2 potentiates Foxo1-mediated transcription through its deacetylase activity. *Proc. Natl. Acad. Sci. U. S. A.* 101: 10042–10047.
57. Motta, M. C., N. Divecha, M. Lemieux, C. Kamel, D. Chen, W. Gu, Y. Bultsma, M. McBurney, and L. Guarente. 2004. Mammalian SIRT1 represses forkhead transcription factors. *Cell* 116: 551–563.
58. Yuan, J., K. Luo, T. Liu, and Z. Lou. 2012. Regulation of SIRT1 activity by genotoxic stress. *Genes Dev.* 26: 791–796.
59. Zannini, L., G. Buscemi, J.-E. Kim, E. Fontanella, and D. Delia. 2012. DBC1 phosphorylation by ATM/ATR inhibits SIRT1 deacetylase in response to DNA damage. *J. Mol. Cell Biol.* 4: 294–303.
60. Rodgers, W., J. N. Byrum, H. Sapkota, N. S. Rahman, R. C. Cail, S. Zhao, D. G. Schatz, and K. K. Rodgers. 2015. Spatio-temporal regulation of RAG2 following genotoxic stress. *DNA Repair (Amst).* 27: 19–27.
61. Williams, C. J., I. Grandal, D. J. Vesprini, U. Wojtyra, J. S. Danska, and C. J. Gidos. 2001. Irradiation promotes V(D)J joining and RAG-dependent neoplastic transformation in SCID T-cell precursors. *Mol. Cell. Biol.* 21: 400–413.
62. Bredemeyer, A. L., G. G. Sharma, C. Y. Huang, B. A. Helmink, L. M. Walker, K. C. Khor, B. Nuskey, K. E. Sullivan, T. K. Pandita, C. H. Bassing, and B. P. Sleckman. 2006. ATM stabilizes DNA double-strand-break complexes during V(D)J recombination. *Nature* 442: 466–470.
63. Callen, E., M. Jankovic, S. Difilippantonio, J. A. Daniel, H. T. Chen, A. Celeste, M. Pellegrini, K. McBride, D. Wangsa, A. L. Bredemeyer, B. P. Sleckman, T. Ried, M. Nussenzweig, and A. Nussenzweig. 2007. ATM prevents the persistence and propagation of chromosome breaks in lymphocytes. *Cell* 130: 63–75.

Supplement

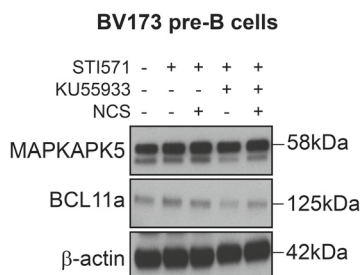


Supplemental Figure 1. Short term exposure to neocarzinostatin does not result in appreciable cell death, and DNA damage regulates RAG1 expression in SUP-B15 pre-B cells. (A) Overnight STI571-treated (STI) BV173, SUPB15 and A70 pre-B cells were treated for 2.5hrs with 200 ng/mL neocarzinostatin (NCS). STI, NCS and KU5933 treatment did not result in increased cell death as judged by propidium-iodide (PI) staining and flow-cytometry analysis. (n=3, independent replicate experiments). (B) Western blot analysis of SUP-B15 pre-B cells. DNA damage resulted in the ATM-kinase dependent down-regulation of RAG1 protein levels. The β -actin blot was used to control for loading. (C) Realtime quantitative RT-PCR analysis of *RAG1* mRNA expression in SUP-B15 pre-B cells treated overnight with 5 μ M STI571. DNA damage induction by 2h treatment with 50 ng/mL NCS resulted in the down-regulation of *RAG1* mRNA expression, which was prevented by 2h pretreatment with 5 μ M KU5933. Means +/- SEM are shown (n=3, ** p<0.01, one-sample t test).



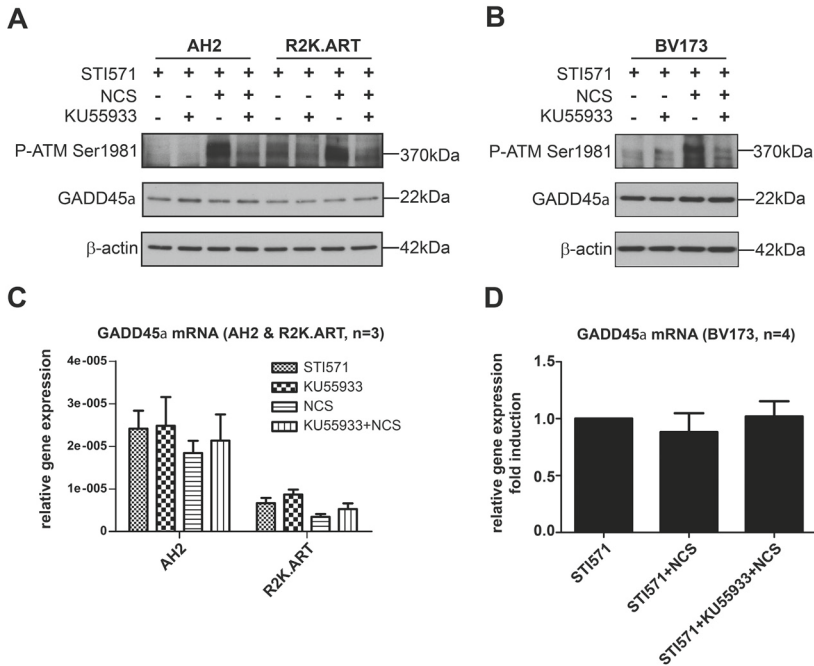
Supplemental Figure 2. Single antibody specificity controls for Proximity Ligation Assay.

BV173 cells treated overnight with 5 μ M STI571 and subsequently treated with 50 ng/mL neocarzinostatin for 2 hrs. Cells were cytocentrifuged and incubated overnight with the indicated single antibodies and developed as indicated in Figure 5. In none of the single antibody controls >5 specific PLA signals were observed in the DAPI-stained nuclei.



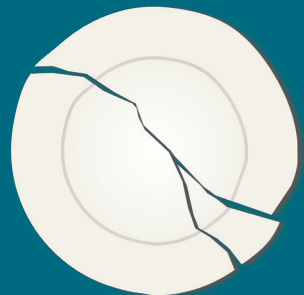
Supplemental Figure 3. Expression levels of MAPKAPK5 and BCL11a are not affected by DNA damage in STI571-treated BV173 pre-B cells.

BV173 cells treated overnight with 5 μ M STI571 and subsequently treated with 50 ng/mL neocarzinostatin for 2 h. Western blot analysis for MAPKAPK5 and BCL11a protein levels. The β -actin blot was used to control for loading.



Supplemental Figure 4. GADD45 α expression is not affected by DNA damage and inhibition of ATM kinase activity.

(A) Western blot analysis of STI571-treated (72h) AH2 (Artemis^{-/-}) and R2K.ART (Artemis^{-/-} / Rag2^{-/-}) mouse *v-Abl* cell lines. DNA damage (2h treatment with 50 ng/mL NCS) did not affect GADD45 α protein levels. Effective induction of DNA damage was shown by phosphorylation of ATM (Ser¹⁹⁸¹), which was inhibited by treatment of cells with the ATM kinase inhibitor KU55933 2h prior to induction of DNA damage by NCS. The β -actin blot was used to control for loading. (B) Western blot analysis of STI571-treated (72h) BV173 pre-B cells. DNA damage did not affect GADD45 α protein levels. The β -actin blot was used to control for loading. (C) Realtime quantitative RT-PCR analysis of *Gadd45a* mRNA expression in STI571-treated (72h) AH2 and R2K.ART mouse *v-Abl* cell lines. *Gadd45a* mRNA expression was not affected by DNA damage and inhibition of ATM kinase activity. (n=3, independent replicate experiments). (D) Realtime quantitative RT-PCR analysis of GADD45a mRNA expression in BV173 pre-B cells. DNA damage did not affect GADD45a mRNA expression levels. (n=4, independent replicate experiments).



CHAPTER

NF- κ B and AKT signaling prevent DNA damage in transformed pre-B cells by suppressing RAG1/2 expression and activity

Katarina Ochodnicka-Mackovicova, Mahnoush Bahjat,
Timon A. Bloedjes, Chiel Maas, Alexander M. de Bruin,
Richard J. Bende, Carel J. M. van Noesel
and Jeroen E. J. Guikema

5

Blood (2015) 126 (11): 1324–1335.



Abstract

In developing lymphocytes, expression and activity of the recombination activation gene protein 1 (RAG1) and RAG2 endonuclease complex is tightly regulated to ensure ordered recombination of the immunoglobulin genes and to avoid genomic instability. Aberrant RAG activity has been implicated in the generation of secondary genetic events in human B-cell acute lymphoblastic leukemias (B-ALLs), illustrating the oncogenic potential of the RAG complex. Several layers of regulation prevent collateral genomic DNA damage by restricting RAG activity to the G₁ phase of the cell cycle. In this study, we show a novel pathway that suppresses RAG expression in cycling-transformed mouse pre-B cells and human pre-B B-ALL cells that involves the negative regulation of FOXO1 by nuclear factor kappa B (NF- κ B). Inhibition of NF- κ B in cycling pre-B cells resulted in upregulation of RAG expression and recombination activity, which provoked RAG-dependent DNA damage. In agreement, we observe a negative correlation between NF- κ B activity and the expression of *RAG1*, *RAG2*, and *TdT* in B-ALL patients. Our data suggest that targeting NF- κ B in B-ALL increases the risk of RAG-dependent genomic instability.

Introduction

The adaptive immune system plays a crucial role in the defense against pathogens, functioning by virtue of highly specific antigen receptors expressed on B and T cells. Effective immunity requires a diverse repertoire of these antigen receptors, which is achieved by recombination of variable (V), diversity (D), and joining (J) gene segments of the immunoglobulin (*Ig*) and T-cell receptor (*Tcr*) loci.¹ VDJ recombination requires the recombination activation gene proteins 1 and 2 (RAG1 and RAG2) to instigate DNA breaks in recombination signal sequences (RSSs) that flank the recombining gene segments.^{2,3} At the pro-B-cell stage, RAG1/2 initiates *Ig* heavy chain (*Igh*) recombination after which RAG is downregulated, followed by several rounds of cell division at the large pre-B-cell stage. Subsequently, pre-B cells exit the cell cycle, and RAG expression is upregulated resulting in *Ig* light chain (*Igl*) recombination. The functional expression of a tolerant (non-self) B-cell receptor (BCR) switches off RAG, whereas expression of an autoreactive BCR leads to prolonged RAG expression, thereby allowing secondary *Igl* recombinations in a process known as receptor editing.^{4,5}

Signals emanating from the interleukin-7 receptor (IL7R) and the pre-B-cell receptor (pre-BCR) regulate the dynamic pattern of RAG expression, which involves phosphoinositide-3 kinase (PI3K) and protein kinase B (PKB, also known as AKT) impinging on forkhead box O (FOXO) transcription factors that are required for RAG expression.^{6,7} The interplay between these signals ensures a sharp demarcation between proliferation and *Ig* gene recombinations in order to conserve genomic stability in pre-B cells. Additionally, RAG2 protein is phosphorylated at threonine 490 (T490) by the cyclin A/cyclin-dependent kinase 2 (CDK2) complex, eliciting S phase kinase-associated protein 2 (SKP2) –mediated ubiquitination and protein degradation in S phase.^{8,9} A breach of this regulation results in genomic instability that activates a p53-dependent checkpoint, as was shown by the increased lymphomagenesis in p53-deficient RAG2-T490A mice.¹⁰

There is ample evidence for the involvement of RAG in chromosomal aberrations in lymphomas and leukemias, which underscores the importance of proper regulation of this potentially harmful recombination mechanism.¹¹ Moreover, B-cell acute lymphoblastic leukemias (B-ALLs) show a developmental block at the pro- to pre-B cell stage and frequently display constitutive RAG, terminal deoxy-transferase (TdT) expression, and ongoing *Ig* gene recombinations.^{12,13} Recent genome-wide analyses of BCR-ABL-positive and ETV6-RUNX1-positive B-ALL have shown that breakpoints of secondary genetic events frequently map near RSS motifs, suggesting the involvement of RAG.^{14,15} Given its oncogenic potential, a deeper understanding of the regulation of RAG expression and activity is warranted. About 25% of adult B-ALL and 5% of childhood B-ALL patients carry the BCR-ABL1 fusion gene,¹⁶ a tyrosine kinase that mimics IL7R and pre-BCR signaling.¹⁷ Here, we made use of human BCR-ABL-positive B-ALL cell lines, Abelson-transformed (Abl) mouse

pre-B cells, and IL7-dependent mouse pre-B cell cultures representing tractable models to study the regulation of RAG expression in (transformed) pre-B cells because inhibition and/or abrogation of BCR-ABL, Abl, or IL7 signaling induces differentiation that is accompanied by RAG expression and *IgI* recombination.^{18,19} In addition, we studied RAG expression in BCR-ABL-negative primary human B-ALL samples. We report the unexpected finding that nuclear factor kappa B (NF- κ B) and AKT signaling suppresses RAG expression and activity in cycling-transformed mouse pre-B cells and in human B-ALL cells and show that inhibition of NF- κ B and AKT signaling results in RAG-dependent DNA damage.

Materials and methods

Cell culture and small molecule inhibitors

Abl-transformed mouse pre-B cell lines generated from wild-type (WT) and RAG2^{-/-} mice carrying an E μ -Bcl2 transgene were kindly provided by Dr Craig Bassing (University of Pennsylvania School of Medicine, Philadelphia, PA). The human BCR-ABL-positive B-ALL cell lines BV173 and SUP-B15 were obtained from Deutsche Sammlung von Mikroorganismen und Zellkulturen (Braunschweig, Germany). Cells were treated with the following small molecule inhibitors at 10⁶ cells per milliliter as indicated: STI571 (imatinib methanesulfonate, LC Laboratories, Woburn, MA), BMS-345541 (Sigma Aldrich), GSK-690693 (Selleckchem, Houston, TX), MLN120B (MCE MedChem Express, Princeton, NJ), CAL-101 (Idelalisib; Selleckchem), and PD-0332991 (Palbociclib; Selleckchem).

Immunoblotting

Protocols for immunoblotting experiments are available in the supplemental Data available at the *Blood* Web site.

Flow cytometry

Intracellular, intranuclear, and 5-bromo-2'-deoxyuridine (BrdU) stainings were done as previously described.^{20,21} Detailed protocols are available in the supplemental Data.

PCR analysis and real-time reverse transcription PCR

V κ 6-23 to J κ 1 coding joins were determined in mouse Abl cells by semiquantitative polymerase chain reaction (PCR) by using previously published primers.²² PCR was performed on 100, 25, and 6.25 ng of DNA. For expression analysis by quantitative real-time reverse transcription PCR, RNA was isolated by using TRI Reagent (Sigma Aldrich), and equal amounts of RNA (0.5 μ g) were first-strand transcribed into complementary DNA by using random primers (Promega Corp., Fitchburg, WI) and Moloney murine leukemia virus reverse transcriptase (Invitrogen, Carlsbad, CA). Gene expression levels were normalized by using *RPLP0* (ribosomal protein, large, P0) and 18S ribosomal RNA (rRNA) housekeeping

genes for human and mouse samples, respectively. Primer sequences are listed in **SUPPL Table 1**.

Analysis of J κ 2-RSS signal-end DNA breaks in G1 and S phase cell cycle cells

Ligation-mediated PCR (LM-PCR) for J κ 2-RSS signal-end DNA breaks in cell cycle phase sorted WT and RAG2^{-/-} Abl-transformed pre-B cells was performed essentially as described earlier,^{23,24} with minor modifications. A detailed protocol is available in the supplemental Data.

NF- κ B transcription factor activity assay

NF- κ B transcription factor p65 and p50 DNA-binding activity was measured in 5 μ g of nuclear extracts from stimulated BV173 and SUP-B15 cells by using a commercially available enzyme-linked immunosorbent assay kit (p50/p65 Transcription Factor Assay Kit; ab133128, Abcam, Cambridge, MA) according to the manufacturer's instructions.

Expression constructs and retroviral transductions

The RAG-reporter construct was used as described previously.²⁵ The retroviral RAG-reporter and I κ B α SR (I κ B α S32A/S36A) constructs were co-transfected with the pCL-ECO plasmid in Phoenix-A cells. For retroviral transduction, cells and retroviral supernatants were spun for 90 minutes at 2000g onto retronectin-coated 24-well plates (5 \times 10⁵ cells per well) according to the manufacturer's instructions (Takara Bio Inc., Otsu, Shiga, Japan).

Primary mouse bone marrow pre-B-cell cultures

C57Bl/6 WT mice were housed in the animal research facility of the Academic Medical Center under specific pathogen-free conditions. Animal experiments were approved by the Animal Ethics Committee and were performed in agreement with national and institutional guidelines. Primary mouse pre-B-cell cultures were performed as described previously²⁰; details are available in the supplemental Data.

Patient samples

Bone marrow aspirates and peripheral blood mononuclear cells from B-ALL patients containing >90% blasts were obtained and prepared according to ethical standards of our institutional medical ethical committee, as well as in agreement with the Helsinki Declaration of 1975, as revised in 1983. Cells were cultured for 48 hours in supplemented Iscove's modified Dulbecco's medium with 20% fetal calf serum, in the presence of 2.5 μ M NF- κ B kinase β (IKK β) inhibitor (IKK β i) and 2.5 μ M AKT inhibitor (AKTi), or vehicle (dimethylsulfoxide; untreated). Patient cytogenetic characteristics are listed in **SUPPL Table 2**.

Gene expression analysis

Data from a previously published study in which the gene expression profiles of 207 untreated B-ALL patients were determined^{26,27} were reanalyzed using the R2 microarray analysis and visualization platform developed in our institute and publicly available (<http://r2.amc.nl>).

Statistics

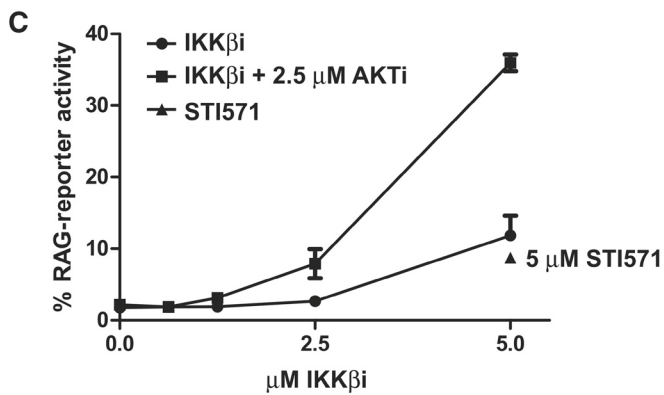
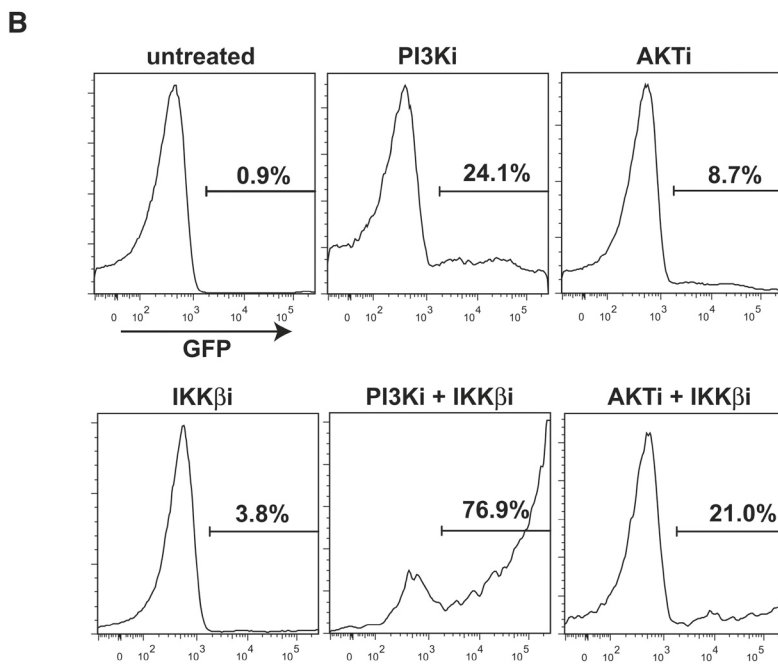
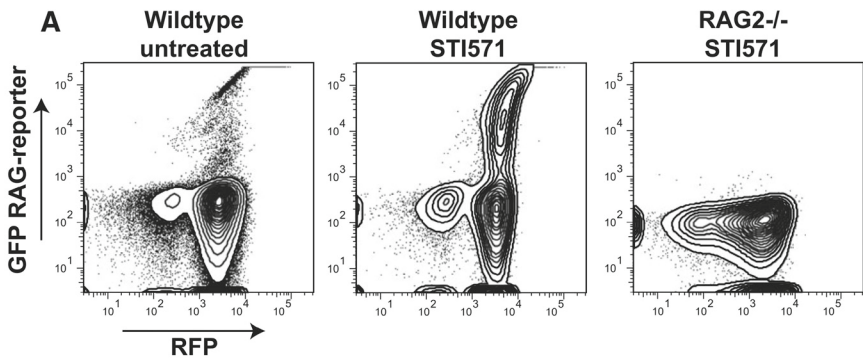
The GraphPad Prism software package (GraphPad Software, La Jolla, CA) was used for statistical testing.

Results**AKT and NF- κ B suppress RAG activity in Abl mouse pre-B cells**

RAG activity in mouse Abl pre-B cells was assessed by using a green fluorescence protein (GFP)-based RAG activity reporter.²⁵ Abl-transformed pre-B cells can be induced to undergo differentiation toward small pre-B cells with the Abl kinase inhibitor STI571.^{18,22} As expected, STI571 induced GFP expression in WT but not in RAG2^{-/-} Abl cells (**Figure 1A**). The PI3K p110 δ inhibitor CAL-101 (PI3Ki) and AKTi GSK-690693 increased RAG-reporter activity, showing that RAG activity is suppressed by PI3K and AKT (**Figure 1B**). Treatment with IKK β i BMS-345541 resulted in a modest but consistent increase in RAG activity. Strikingly, combined treatment with IKK β i and PI3Ki or AKTi synergistically increased RAG activity (**Figure 1B-C**). A structurally unrelated IKK β i (MLN120B) yielded similar results, demonstrating the specificity of this effect (**SUPPL Figure 1**).

► Figure 1. AKT and NF- κ B regulate RAG activity in mouse Abl pre-B cells.

(A) Representative fluorescence-activated cell sorter plots of the WT and RAG2^{-/-} mouse Abl pre-B cells transduced with the retroviral RAG-reporter construct consisting of an antisense GFP complementary DNA flanked by a 12-bp spacer RSS and a 23-bp spacer RSS, followed by an IRES-RFP cassette. RAG activity mediates inversional recombination of the antisense GFP gene, which can be quantified by flow cytometry. WT and RAG2^{-/-} mouse Abl pre-B cells were treated for 96 hours with 10 μ M STI571. **(B)** WT mouse Abl pre-B cells transduced with the RAG-reporter construct stimulated with 5 μ M PI3Ki, 2.5 μ M AKTi, 2.5 μ M IKK β i, or untreated (dimethylsulfoxide [DMSO] vehicle) for 96 hours. GFP histograms (RAG-reporter activity) of transduced cells are shown by gating on RFP⁺ cells. **(C)** Titration curve for IKK β i and for IKK β i plus 2.5 μ M AKTi. RAG-reporter activity (y-axis) of WT mouse Abl pre-B cells is plotted against the concentration of IKK β i (x-axis). RAG-reporter activity of mouse Abl pre-B cells treated with 5 μ M STI571 is shown. Cells were treated for 72 hours. A representative example of 3 independent experiments is shown, 4 replicate measurements were performed per experiment, and error bars show means \pm standard deviation (SD).



AKT and NF- κ B regulate RAG transcription by inhibiting FOXO1

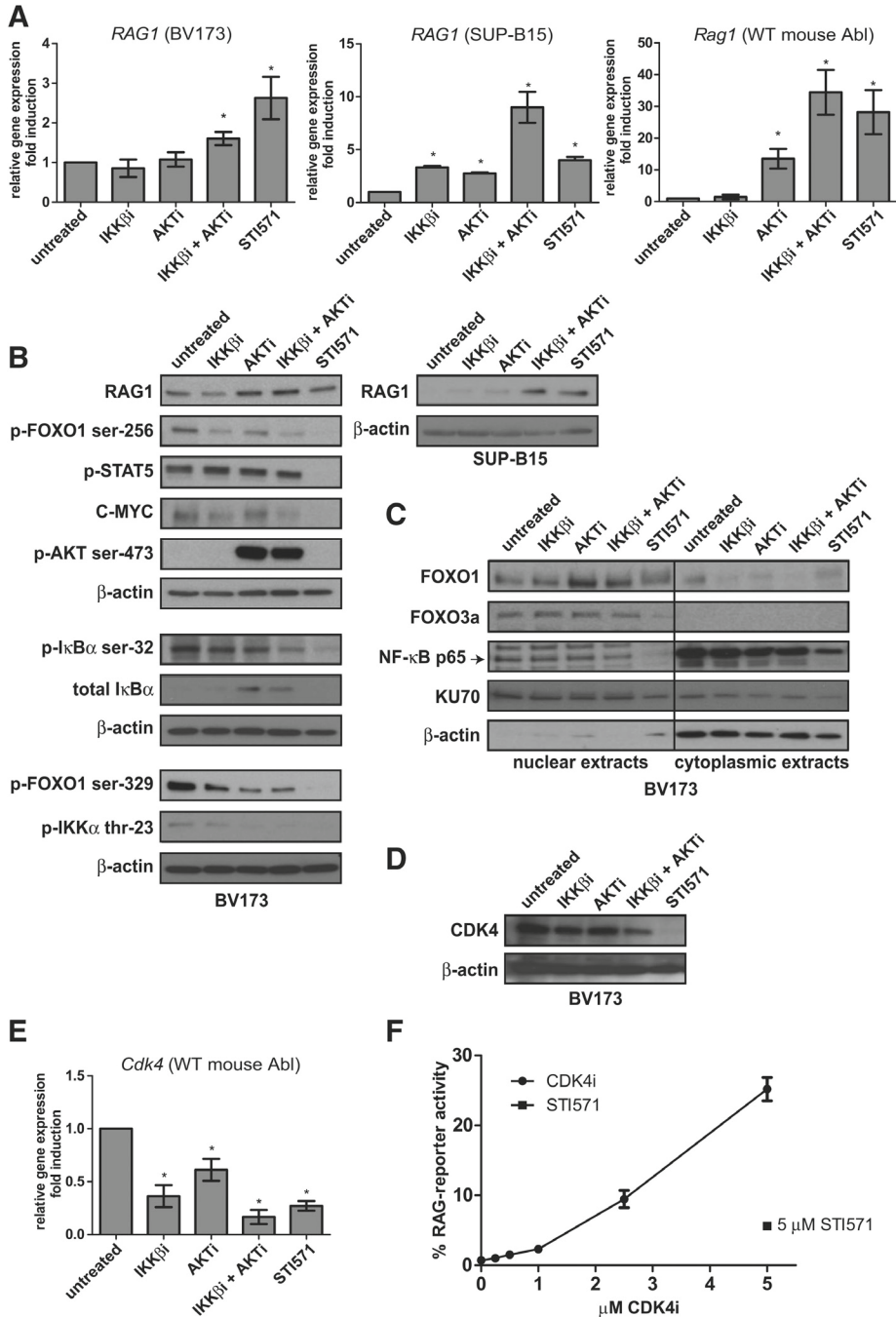
Combined treatment with IKK β i and AKTi induced RAG1 and RAG2 messenger RNA (mRNA) expression in Abl mouse pre-B cells and in two human BCR-ABL-positive B-ALL cell lines (BV173 and SUP-B15) at levels comparable to those observed after STI571 treatment (**Figure 2A** and **SUPPL Figure 2**); RAG1 protein expression was correspondingly induced (**Figure 2B**). We next studied the expression of FOXO1 and FOXO3a, which are known regulators of RAG transcription.^{6,7} Nuclear FOXO1 levels were increased upon AKTi treatment and upon combined AKTi and IKK β i treatment, whereas FOXO3a levels remained unchanged (**Figure 2C**). Concomitantly, phosphorylation of FOXO1 on serine 256 and serine 329, which negatively regulate its stability, was decreased in cells treated with IKK β i and AKTi (**Figure 2B**). Recently, it was demonstrated that cyclin-dependent kinase 4 (CDK4) suppresses RAG expression in *Myc*-driven lymphomas by phosphorylating FOXO1 at serine 329.²⁸ In line with this, we found that CDK4 protein and mRNA expression was decreased in IKK β i- and AKTi-treated cells (**Figure 2D-E**). Moreover, treatment with the CDK4-specific inhibitor PD-0332991 (CDK4i) increased RAG activity to a degree comparable to that with IKK β i and AKTi treatment (**Figure 2F**).

AKT and NF- κ B inhibition does not interfere with Abl signaling

In Abl-transformed pre-B cells, the Abl kinase activity results in constitutive STAT5 phosphorylation, which is inhibited by STI571 (**Figure 2B**). However, phospho-STAT5 remained unchanged in cells treated with IKK β i and AKTi, showing that Abl kinase signaling was not abrogated. In addition, C-MYC was detectable in IKK β i- and AKTi-treated cells, whereas

► **Figure 2. Transcriptional regulation of RAG1 by the AKT and NF- κ B pathways.**

(A) Real-time reverse transcription PCR (RT-PCR) analysis of *RAG1* mRNA in the human BCR-ABL-positive B-ALL cell lines BV173 (left) and SUP-B15 (middle) and *Rag1* mRNA in the WT mouse Abl pre-B cell line (right). Cells were treated with 2.5 μ M IKK β i, 2.5 μ M AKTi, or 10 μ M STI571 for 48 hours. **(B)** Immunoblot analysis of whole-cell extracts from BV173 and SUP-B15 cells treated as in (A). **(C)** Immunoblot analysis of nuclear and cytoplasmic extracts from BV173 cells treated as in (A). **(D)** Immunoblot analysis of CDK4 cells treated as in (A). β -actin was used as loading control in (B) and (D). KU70 is expressed in the nucleus and the cytoplasm and was used as loading control in (C). **(E)** *Cdk4* real-time RT-PCR analysis of the WT mouse Abl pre-B cell line; cells were treated as in (A), and results were normalized to those in untreated cells (DMSO vehicle). Real-time RT-PCR results are presented relative to the expression of the housekeeping genes *RPLPO* (for human cells) and *18S* ribosomal RNA (rRNA) (mouse cells); PCRs were performed at least in duplicate, and error bars show means \pm SD of 3 independent experiments. **(F)** Titration curve of CDK4i. RAG-reporter activity of WT mouse Abl pre-B cells treated with 5 μ M STI571 is plotted against the concentration of CDK4i. Cells were stimulated for 96 hours. A representative example of 3 independent experiments is shown, 4 replicate measurements were performed per experiment, and error bars represent means \pm SD. * P < .05, as determined by the 1-sample Student *t* test.



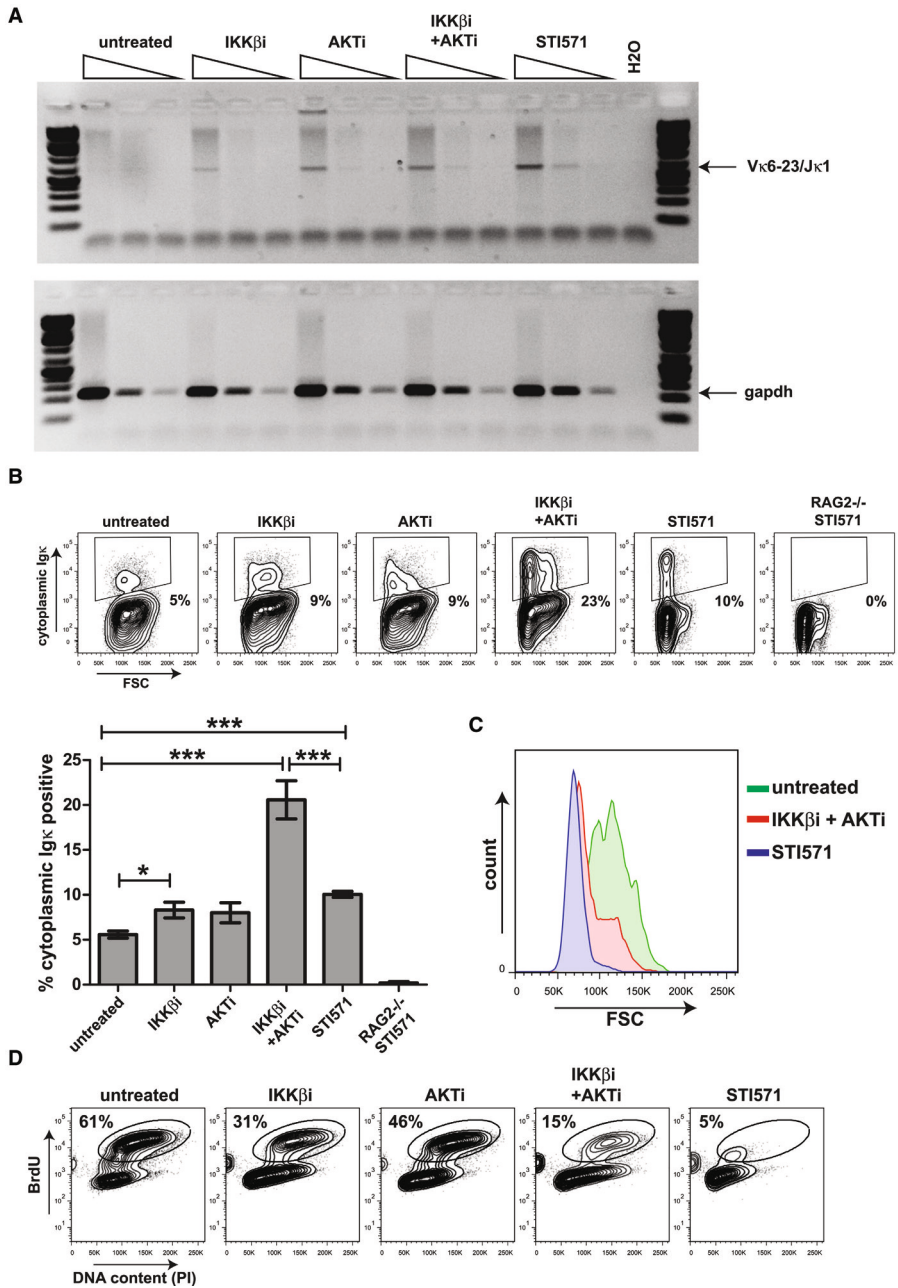
STI571 treatment led to the loss of C-MYC (**Figure 2B**) and the induction of a G₁ cell cycle arrest (data not shown). The DNA binding activities of p65 and p50 NF- κ B transcription factors were modestly but significantly decreased after IKK β i and AKTi treatment (~50% reduction) (**SUPPL Figure 3**), consistent with a decreased level of phosphorylated inhibitor of κ B α (I κ B α) and a modest decrease in nuclear p65 (**Figure 2C**). We also show that AKT is involved in NF- κ B signaling because I κ B α was increased whereas phosphorylation of IKK α on threonine 23 was decreased by AKTi treatment. Treatment with AKTi resulted in increased phosphorylation of AKT on serine 473 (**Figure 2B**) as a result of disturbed negative feedback regulation, which was previously described.²⁹⁻³¹

AKT and NF- κ B inhibit endogenous Ig κ recombination

To determine whether endogenous *Ig κ* recombination was regulated by NF- κ B, we assessed V κ 6-23 to J κ 1 coding joins by semiquantitative PCR. Coding joins were observed in Abl cells treated with STI571 and also in cells treated with IKK β i, AKTi, or IKK β i and AKTi combined (**Figure 3A**). In addition, cytoplasmic Ig κ light chain expression was significantly induced in Abl cells treated with IKK β i and AKTi, exceeding induction by STI571 (**Figure 3B**). Cytoplasmic κ light chain expression upon treatment with STI571 was accompanied by the transition from large to small pre-B cells, as shown by forward scatter (FSC) analysis. However, a sizeable fraction of IKK β i- and AKTi-treated cells expressing cytoplasmic κ light chain remained large, suggesting that these cells did not exit the cell cycle (**Figure 3C**), which is in agreement with our finding that C-MYC is still detectable under these conditions (**Figure 2B**). In addition, a considerable portion of the cells (15%) incorporated BrdU. Although BrdU incorporation in the IKK β i- and AKTi-treated cultures was diminished compared with that in untreated cells (15% vs 61%), it was clearly higher than that in STI571-treated cells (15% vs 5%) (**Figure 3D**).

► **Figure 3. Inhibition of AKT and NF- κ B signaling results in recombination of the endogenous *Ig κ* locus in mouse Abl pre-B cells.**

(A) Semiquantitative PCR analysis of V κ 6-23 to J κ 1 coding joins in mouse Abl pre-B cells treated with 2.5 μ M IKK β i, 2.5 μ M AKTi, or 10 μ M STI571 for 72 hours. Semiquantitative PCR analysis for *Gapdh* was performed as a loading control. **(B)** Representative fluorescence-activated cell sorter (FACS) plots showing cytoplasmic Ig κ expression vs forward scatter (FSC) in mouse Abl pre-B cells stimulated as in (A). Numbers below outlined gates indicate percentage of cells. Graph depicts percentages of cytoplasmic Ig κ -positive cells in mouse Abl pre-B cell cultures stimulated for 72 hours. A representative example of 2 independent experiments is shown, 4 replicate measurements were performed per experiment, and error bars represent means \pm SD. Statistical significances between groups were determined by 1-way analysis of variance (ANOVA) using a Bonferroni's posttest. **(C)** Representative FACS plot showing overlay FSC histograms of cytoplasmic Ig κ -positive mouse Abl pre-B cells treated as indicated. **(D)** Representative FACS plots showing BrdU incorporation vs DNA content as measured by propidium iodide (PI) staining in mouse Abl pre-B cells treated for 48 hours as indicated above FACS plots. Numbers above outlined gates indicate percentage of cells. **P* < .05; ****P* < .001.



AKT and NF- κ B signaling prevents RAG-dependent DNA damage in cycling-transformed pre-B cells

Flow cytometric analysis of phosphorylated H2AX (γ H2AX) in WT and RAG2^{-/-} Abl cells revealed that treatment with IKK β i and AKTi resulted in significantly higher levels of intracellular γ H2AX in RAG-proficient cells, indicating that these cells experienced RAG-dependent DNA damage. RAG-dependent DNA damage was also increased in cells treated with IKK β i alone, but not with AKTi (**Figure 4A**). Strikingly, RAG-dependent γ H2AX staining was exclusively observed in the large cells (FSC high), suggesting that the cycling cells sustained DNA damage (**Figure 4B**). In cycling cells, RAG2 protein expression is restricted by cyclin A/CDK2-mediated phosphorylation, whereas RAG1 is not regulated in a cell cycle-dependent manner.^{32,33} Interestingly, the levels of *cyclin* and *CDK2* mRNA expression were significantly decreased in IKK β i- and AKTi-treated Abl cells at a level comparable to that in STI571-treated cells, whereas the level of *cyclin D1* was unaffected in contrast to STI571-treated cells (**Figure 4C**). The low levels of cyclin A/CDK2 could provide a window for RAG2 protein expression and RAG activity in cycling cells. To provide additional evidence that RAG is active in cycling cells under these conditions, we performed J κ 2-RSS signal-end LM-PCR on IKK β i- and AKTi-treated WT and RAG2^{-/-} mouse Abl pre-B cells sorted according to the G₁ and S phase of the cell cycle. This approach detects transient RAG-dependent DNA breaks at the J κ 2-RSS upstream of the J κ 2 coding region. Upon visual inspection, J κ 2-RSS breaks appeared most prevalent in the G₁ phase but were also detectable in S phase cells (**Figure 4D**). Cloning and sequencing of the PCR products obtained from G₁ phase cells showed that 3 of 7 clones harbored the correct insert, whereas 2 of 7 clones obtained from S phase cells contained J κ 2-RSS linker fragments, indicating RAG activity in S phase. Negative clones harbored PCR products caused by promiscuity of the J κ 2-ko5 LM-PCR forward primer (data not shown). J κ 2-RSS LM-PCR products were not detected in RAG2^{-/-} cells, confirming their RAG-dependence. Moreover, J κ 2-RSS breaks were not detected in untreated WT mouse Abl pre-B cells, consistent with the absence of endogenous *Igk* recombinations in untreated cells as shown in **Figure 3A**.

Expression of NF- κ B superrepressor stimulates RAG activity

To provide further evidence that NF- κ B signaling suppresses RAG activity, we introduced the NF- κ B superrepressor I κ B α SR-IRES-YFP cassette together with the RAG-reporter construct into the WT mouse Abl pre-B cell line. NF- κ B signaling was effectively repressed as shown by diminished lipopolysaccharide-induced CD69 expression in I κ B α SR-transduced cells (**SUPPL Figure 4**). We found that I κ B α SR-expressing cells (YFP⁺RFP⁺) had ~10-fold higher RAG activity compared with the control cell population (YFP⁺RFP⁺) (mean of 24% vs 2% GFP⁺ cells) (**Figure 5A**). In agreement, *Rag1* mRNA expression was ~10-fold higher in

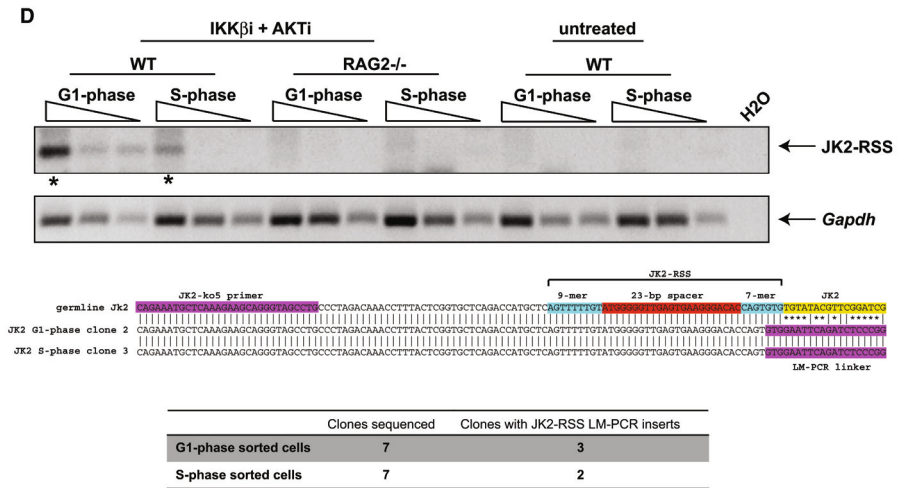


Figure 4. Inhibition of AKT and NF- κ B signaling induces RAG-dependent DNA damage in mouse Abl pre-B cells.

(A) Mean fluorescence intensity (MFI) of intracellular γ H2AX staining in mouse Abl pre-B cells treated as indicated on x-axis. Red symbols represent γ H2AX MFI in WT cells, and blue symbols represent γ H2AX MFI in RAG2^{-/-} cells. MFIs of untreated controls were subtracted to correct for background staining. Three independent experiments were performed, and horizontal lines represent means. Statistical significances between groups were determined by ANOVA using a Bonferroni's posttest. (B) Overlay FACS histograms of intracellular γ H2AX staining in IKK β i- and AKTi-treated cells. Small B cells (FSC low; left gate) vs large B cells (FSC high; right gate) are shown. (C) Real-time RT-PCR of *Cyclin-A*, *Cdk2*, and *Cyclin-D1* mRNA expression in WT mouse Abl pre-B cells. Cells were treated with 2.5 μ M IKK β i, 2.5 μ M AKTi, or 10 μ M STI571 for 48 hours. Real-time RT-PCR results are presented relative to the expression of the 18S rRNA housekeeping gene. Three independent experiments were performed, PCRs were performed at least in duplicate, and error bars represent means \pm SD of 3 independent experiments. (D) Jk2-RSS DNA breaks are detected by LM-PCR in cell-cycle sorted (G₁ and S phase) WT mouse Abl pre-B cells that were treated with 2.5 μ M IKK β i and 2.5 μ M AKTi. Threefold dilutions of linker-ligated DNA were amplified with a Jk2-specific forward primer and an LM-PCR linker-specific reverse primer. PCR products indicated with an asterisk were excised from the gel, cloned, and sequenced. The middle section of panel D shows the alignments of sequences obtained from G₁ and S phase cells to the germline Jk2 sequence. Jk2-ko5 primer site, Jk2-RSS, and the Jk2 coding region are indicated by colored boxes. Sequencing results are listed at the bottom of panel D. **P* < .05; ***P* < .01; ****P* < .001. ns, not significant.

fluorescence-activated cell sorter-purified I κ B α SR-YFP⁺ cells compared with I κ B α SR-YFP⁻ cells (SUPPL Figure 5). Treatment with IKK β i and AKTi increased RAG activity in the control cell population (increasing from a mean of 2% to 32% GFP⁺ cells), reaching a level similar to that in I κ B α SR-transduced cells (Figure 5B), showing limited increase of RAG activity upon treatment (~1.5-fold). We assessed whether NF- κ B is also involved in suppressing RAG expression in untransformed primary mouse pro-B cells. In vitro expanded primary

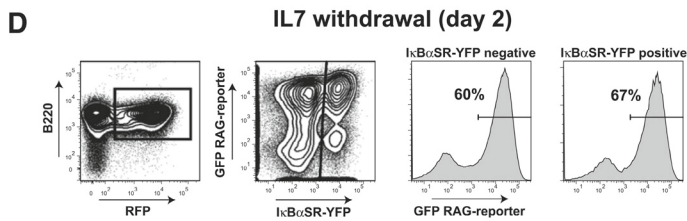
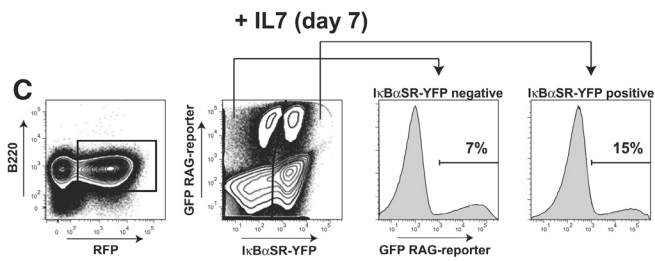
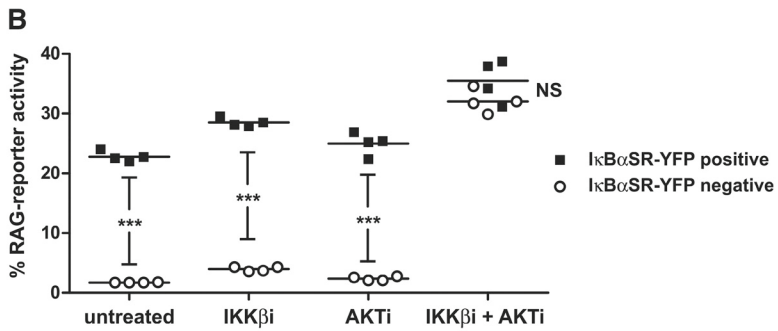
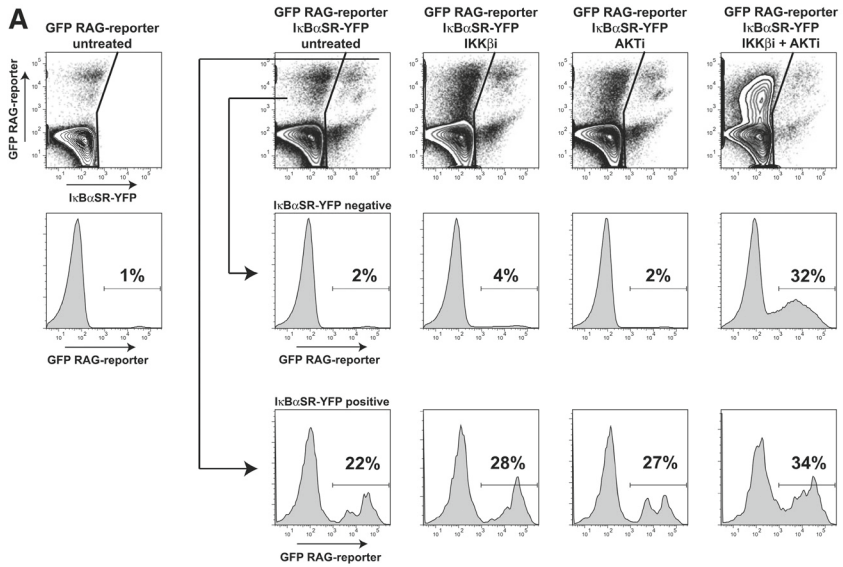
mouse pre-B cells were transduced with the $\text{I}\kappa\text{B}\alpha\text{SR}$ and the RAG-reporter constructs and analyzed by flow cytometry 7 days after transduction. In the presence of IL7 and Flt3L, RAG activity was approximately twofold higher in the $\text{I}\kappa\text{B}\alpha\text{SR}$ -transduced cells compared with the control cell population (15% vs 7% GFP⁺ cells) (**Figure 5C**). Withdrawal of IL7 increased RAG activity, upon which inhibition of NF- κ B signaling had no substantial effect (60% vs 67% GFP⁺ cells) (**Figure 5D**).

NF- κ B and AKT suppress RAG expression in primary human pre-B ALL cells

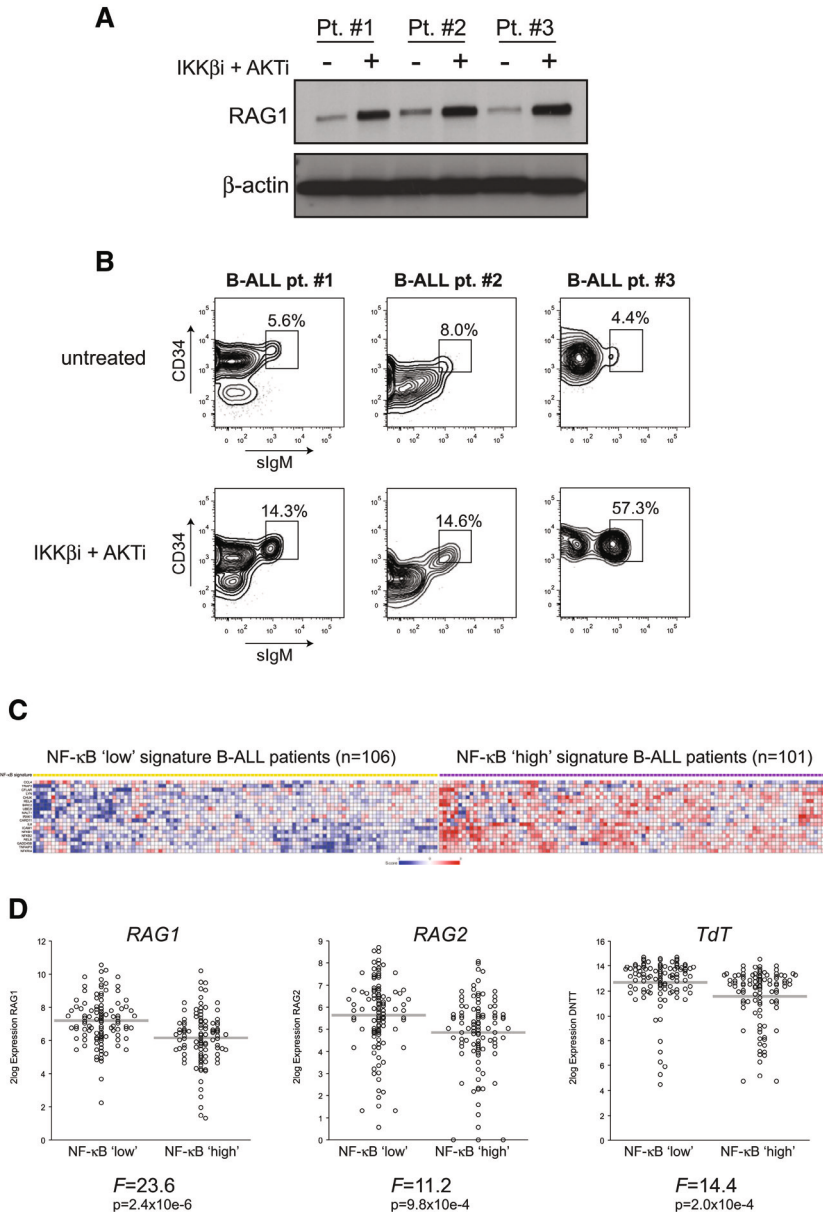
To confirm that the NF- κ B and AKT pathways regulate RAG in primary human B-ALL cells, we stimulated B-ALL blasts in vitro from 3 (BCR-ABL⁻) patients with the combination of IKK β i and AKTi. RAG1 protein expression was increased in all 3 patients (**Figure 6A**). In addition, surface IgM expression on B-ALL blasts (CD19⁺CD10⁺CD34^{+/-}) from these patients was increased (ranging from 1.8-fold to 13-fold) after treatment (**Figure 6B**), which may suggest increased RAG activity resulting in productive IgM expression in these cells. To further explore whether the activity of the NF- κ B pathway is related to RAG expression in primary B-ALL patients, we reanalyzed the gene expression profiles of a previously published cohort of BCR-ABL-negative childhood B-ALL patients.^{26,27} This heterogeneous patient group consists of 207 untreated high-risk B-ALL patients. We performed unsupervised clustering based on the expression of 19 NF- κ B pathway/target genes by using a *k*-means clustering algorithm that identified an NF- κ B low signature B-ALL patient group (*n* = 106) and an NF- κ B high signature patient group (*n* = 101) (**Figure 6C**). Although there is considerable overlap between the patient groups that reflects their heterogeneous nature, the NF- κ B low signature group displayed significantly increased *RAG1*, *RAG2*, and *TdT* mRNA expression compared with the NF- κ B high signature group (**Figure 6D**), highlighting the

► **Figure 5. NF- κ B superrepressor augments RAG activity in mouse Abl pre-B cells and in IL7-dependent untransformed mouse pre-B cell cultures.**

(A) FACS plots of WT mouse Abl pre-B cells transduced with $\text{I}\kappa\text{B}\alpha\text{SR}$ -YFP and RAG-reporter (GFP) IRES-RFP. Scatter plots show YFP (*x*-axis) vs GFP (*y*-axis) within RFP-positive gate. Histograms show RAG-reporter (GFP) in $\text{I}\kappa\text{B}\alpha\text{SR}$ -YFP-negative cells (middle row) and in $\text{I}\kappa\text{B}\alpha\text{SR}$ -YFP-positive cells (bottom row). Cells were treated for 96 hours as indicated above FACS plots. Numbers above outlined gates indicate percentage of cells. **(B)** Graph depicting percentage of RAG-reporter activity (GFP) in $\text{I}\kappa\text{B}\alpha\text{SR}$ -YFP-positive cells and $\text{I}\kappa\text{B}\alpha\text{SR}$ -YFP-negative cells. Horizontal lines represent means, and 4 independent experiments were performed. Statistical significances were determined by two-way ANOVA. **(C)** FACS scatter plots of untransformed mouse pre-B cells cultured for 7 days with IL7. Pre-B cells (B220⁺, IgM⁻CD43⁺) were retrovirally transduced with $\text{I}\kappa\text{B}\alpha\text{SR}$ -YFP and RAG-reporter (GFP) IRES-RFP constructs. Gating strategy is shown (B220⁺RFP⁺). FACS histograms show RAG-reporter activity (GFP) in $\text{I}\kappa\text{B}\alpha\text{SR}$ -YFP-negative and $\text{I}\kappa\text{B}\alpha\text{SR}$ -YFP-positive cells. A representative example of 3 independent experiments is shown. **(D)** RAG-reporter activity (GFP) 2 days after IL7 withdrawal. Numbers above outlined gates indicate percentage of cells. A representative example of 2 independent experiments is shown. ****P* < .001.



negative correlation between NF- κ B activity and RAG expression in primary B-ALL patients. Of interest, pathway analysis showed that the DNA replication pathway was significantly associated with the NF- κ B signature groups ($P < .0001$), whereas the NF- κ B low signature group showed higher expression of DNA replication genes and had significantly higher white blood cell counts (**SUPPL Figure 6A-B**).



Discussion

In B-ALL, many secondary genetic events bear the hallmarks of being derived from aberrant RAG activity, suggesting that RAG is an important instigator of genomic instability.^{14,15} Aberrant RAG activity also contributes to subclonal diversification of B-ALL, which results in the development of therapy-resistant subclones.³⁴ Despite these recent insights, the (mis) regulation of RAG expression in B-ALL remains poorly understood. During B-cell development, pre-B cell proliferation and RAG expression and/or activity are strictly separated, preventing genomic instability. Multiple layers of regulation safeguard this separation, which may be disrupted in proliferating leukemic cells that constitutively express RAG. In BCR-ABL-positive B-ALL, large cycling pre-B cells are transformed by the Abl kinase activity, preventing their differentiation toward the immature B-cell stage. Typically, proliferating BCR-ABL-positive B-ALL cells do not show RAG activity, indicating that the separation between proliferation and recombination is (still) enforced.^{19,35} Inhibition of the Abl kinase with STI571 leads to induction of RAG expression and activity accompanied by cell cycle exit, similar to that in normal pre-B or immature B cells.^{18,19} In proliferating pre-B cells, RAG expression is repressed by AKT signaling that negatively regulates FOXO1. Our results show that the NF- κ B pathway contributes to the repression of RAG activity in cycling-transformed pre-B cells by regulating FOXO1. NF- κ B was implicated in regulating *Igk* locus accessibility³⁶; however, it is unlikely that increased RAG activity upon NF- κ B inhibition can be ascribed to effects on locus accessibility because the RAG reporter used in this study measured RAG activity independently of *Igk* accessibility.

The role of AKT in the regulation of RAG expression in Abl cells is not entirely clear; previous results with an Abl cell line generated from a *RAG1^{GFP}* knock-in mouse showed that AKT inhibition by the AKTVIII inhibitor did not result in increased *RAG1^{GFP}* expression,³⁷ whereas the expression of constitutively active AKT suppressed *RAG1^{GFP}* expression in un-

◀ **Figure 6. Inhibition of AKT and NF- κ B signaling induces RAG1 protein expression in primary human B-ALL cells, and NF- κ B gene expression signature negatively correlates with *RAG1*, *RAG2*, and *TdT* mRNA expression in untreated B-ALL patients.**

(A) Immunoblot analysis of whole-cell extracts from primary (BCR-ABL-negative) B-ALL blasts ($n = 3$) cultured for 48 hours with 2.5 μ M IKK β i and 2.5 μ M AKTi or vehicle (DMSO; untreated). (B) FACS plots of primary human B-ALL cells from 3 patients cultured for 48 hours with 2.5 μ M IKK β i and 2.5 μ M AKTi or vehicle (DMSO; untreated). FACS plots show CD34 vs surface IgM (sIgM) expression within the CD19⁺ gate; gated events were CD10⁺ (data not shown). Numbers above outlined gates indicate percentage of cells. (C) Heatmap showing NF- κ B low (yellow squares) and NF- κ B high (purple squares) B-ALL patient subgroups based on a 19 NF- κ B pathway/target classifier gene expression profile. Each column represents a B-ALL patient, and each row represents a unique gene classifying the 2 subgroups. (D) Relative *RAG1*, *RAG2*, and *TdT* mRNA expression in NF- κ B low and NF- κ B high signature B-ALL patients. Each circle represents an individual patient, 2log expression is depicted, and gray bars indicate means. The ANOVA *F*-statistic and *P* value are given below each graph.

transformed B220⁺IgM⁻ cells.⁷ We show that the specific AKTi GSK-690693²⁹ increased RAG activity in Abl cells. Interestingly, the AKT-mediated RAG repression may operate by direct inhibition of FOXO1 and by feeding into NF- κ B-mediated FOXO1 regulation, because simultaneous inhibition of the AKT and the NF- κ B pathways resulted in increased levels of nuclear FOXO1, a concomitant decrease in FOXO1 phosphorylation, and a synergistic effect on RAG activity. In support, we show that AKT is involved in NF- κ B activation by phosphorylating IKK α on serine 23, as was shown previously.³⁸ In addition, we demonstrate that expression of I κ B α SR had a stimulatory effect on RAG activity in Abl cells and in primary mouse pre-B cells, albeit to a lesser extent.

Several studies addressed the role of NF- κ B in early B-cell development with discordant results. NF- κ B was shown to be involved in *Ig κ* germline transcription but not RAG activity.³⁶ Other studies suggest that NF- κ B is dispensable for B-cell development.^{39,40} More recently, it was shown that NF- κ B is active in pre-B cells and in immature B cells engaged in receptor editing during *Ig λ* recombination.^{41,42} Strikingly, in an earlier study, it was shown that NF- κ B1/p50-deficient B cells had elevated RAG expression and activity.⁴³ To add to the complexity, kinase-dead IKK α knockin mice showed defective B-cell development because of decreased *PAX5* and *IRF4* gene expression.⁴⁴ It is likely that different modalities of NF- κ B signaling exist in normal and transformed developing B cells that determine the outcome of this pleiotropic signaling pathway.

Recently, it was shown that CDK4 suppresses RAG expression in B-cell lymphomas in E μ -Myc-transgenic mice. In that model, CDK4 deficiency accelerated lymphomagenesis in a RAG-dependent fashion by regulating FOXO1 levels. The authors showed that CDK4 phosphorylates FOXO1 on residue serine 329, which provokes nuclear exclusion.²⁸ Of interest, CDK4 activity is regulated by NF- κ B,⁴⁵ and it was shown that I κ B α binds to CDK4 thereby inhibiting its kinase function.⁴⁶ We demonstrated that simultaneous inhibition of the NF- κ B and the AKT pathways resulted in diminished *Cdk4* mRNA and CDK4 protein levels and decreased FOXO1-serine 329 phosphorylation. In addition, specific inhibition of CDK4 increased RAG activity. On the basis of these observations, we speculate that I κ B α stabilization could promote RAG expression by inhibition of CDK4, which acts as a negative regulator of FOXO1 (**Figure 7**). The NF- κ B pathway is one of the major regulators of antiapoptotic gene expression during B-cell development, which makes it intrinsically difficult to assess other functions of this pathway because perturbation of NF- κ B has detrimental effects on cell survival. It is possible that the antiapoptotic function of NF- κ B is (partly) uncoupled from its other functions in Abl cells because Abl kinase activity can prevent apoptosis independently of NF- κ B.⁴⁷ Moreover, the mouse Abl cells used in this study harbor the E μ -Bcl2 transgene and express the antiapoptotic BCL2 protein, which may have helped to uncover the role of NF- κ B in the regulation of RAG expression. In support of this, treatment of the mouse and human BCR-ABL-positive cell lines with the IKK β i and AKTi resulted in only a minor increase in cell death (<10% specific cell death) over

the course of the experiments described, whereas the primary human (BCR-ABL-negative) B-ALL samples displayed a much greater induction of cell death (ranging from 50% to 80% specific cell death) upon treatment (data not shown).

Our findings indicate that RAG expression induced after AKT and NF- κ B inhibition does not coincide with cell cycle exit in Abl cells, which could have oncogenic potential because RAG activity during S phase is linked to lymphomagenesis.¹⁰ Consistent with this, our study shows that AKT and NF- κ B inhibition leads to increased RAG-dependent DNA damage, most prominently in large cycling cells, which may provoke genomic instability. In agreement, our LM-PCR analysis confirms that RAG is active in S phase under these conditions.

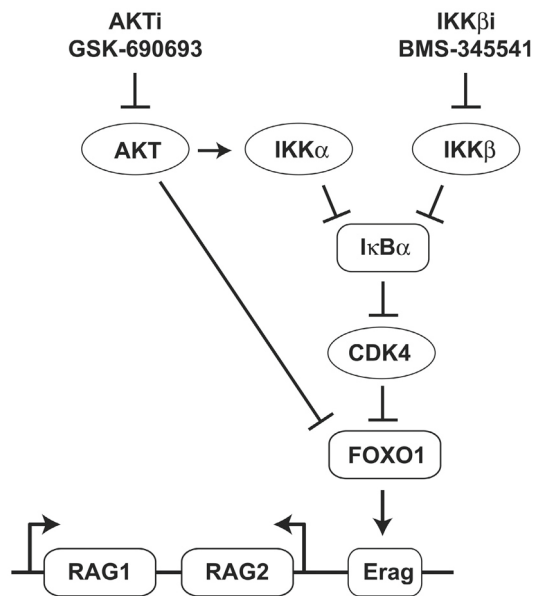


Figure 7. Model indicating the potential mechanism by which IKK β i and AKTi stimulate RAG expression in pre-B cells.

Arrows represent positive and/or stimulatory effects. Horizontal bars represent inhibitory and/or repressive effects. *Erag*, conserved transcriptional enhancer in the RAG locus.

Inhibition of NF- κ B and AKT also increased RAG protein expression in primary BCR-ABL-negative human B-ALL cells, similar to that in mouse Abl cells and human BCR-ABL-positive B-ALL cell lines, suggesting that these pathways are important for suppressing RAG expression in primary human leukemic cells. Moreover, NF- κ B and AKT inhibition resulted in increased surface IgM expression on leukemic blasts, which suggests that these cells may have experienced RAG activity. In support, by reanalysis of gene expression data, we found that NF- κ B negatively correlated with RAG expression in primary BCR-ABL-negative B-ALL patients, although it must be noted that the differences between

the NF- κ B signature patient groups were small, reflecting the heterogeneity within these groups. In addition, NF- κ B activity negatively correlated with the expression of DNA replication genes, and patients with an NF- κ B low signature had higher white blood cell counts, suggesting that these patients may suffer from a more aggressive disease. These results indicate that NF- κ B could have tumor-suppressive qualities in B-ALL, as was suggested previously for other cell types.⁴⁸ Importantly, several novel therapies for leukemias and lymphomas are aimed at the NF- κ B and PI3K-AKT pathways and at CDK4.⁴⁹⁻⁵² In light of our data, it is conceivable that such treatments might have adverse effects in leukemia patients by unleashing the oncogenic potential of RAG, thus driving (sub)clonal diversification and genomic instability of leukemic pre-B cells.

Acknowledgements

The authors thank Dr Craig Bassing (University of Pennsylvania School of Medicine, Philadelphia, PA) for providing wild-type and RAG2^{-/-} mouse Abl pre-B cell lines; Drs Inês Trancoso and Jocelyne Demengeot (Instituto Gulbenkian, Oeiras, Portugal) for the RAG-reporter (green fluorescence protein) IRES-RFP construct; Dr Hergen Spits (Academic Medical Center, Amsterdam, The Netherlands) for the κ B α SR-IRES-YFP construct; Prof Dr Ellen van der Schoot and Dr Christa Homburg (Sanquin Research Institute, Amsterdam, The Netherlands) and Dr Edwin Sonneveld (Children's Oncology Foundation [within the Stichting Kinderoncologie Nederland], The Hague, The Netherlands) for sharing patient material and data; and Dr Carol Schrader (University of Massachusetts Medical School, Worcester, MA) for helpful discussions.

This work was supported by a fellowship from the Academic Medical Center and Innovational Research Incentives Scheme VIDI grant 016126355 from The Netherlands Organization for Scientific Research (both to J.E.J.G).

References

1. Tonegawa S. Somatic generation of antibody diversity. *Nature*. 1983;302(5909):575-581.
2. Schatz DG, Oettinger MA, Baltimore D. The V(D)J recombination activating gene, RAG-1. *Cell*. 1989; 59(6):1035-1048.
3. Oettinger MA, Schatz DG, Gorka C, Baltimore D. RAG-1 and RAG-2, adjacent genes that synergistically activate V(D)J recombination. *Science*. 1990;248(4962):1517-1523.
4. Gay D, Saunders T, Camper S, Weigert M. Receptor editing: an approach by autoreactive B cells to escape tolerance. *J Exp Med*. 1993; 177(4):999-1008.
5. Tiegs SL, Russell DM, Nemazee D. Receptor editing in self-reactive bone marrow B cells. *J Exp. Med*. 1993;177(4):1009-1020.
6. Herzog S, Hug E, Meixlsperger S, et al. SLP-65 regulates immunoglobulin light chain gene recombination through the PI(3)K-PKB-Foxo pathway. *Nat Immunol*. 2008;9(6):623-631.
7. Amin RH, Schlissel MS. Foxo1 directly regulates the transcription of recombination-activating genes during B cell development. *Nat Immunol*. 2008;9(6):613-622.
8. Li Z, Dordai DI, Lee J, Desiderio S. A conserved degradation signal regulates RAG-2 accumulation during cell division and links V(D)J recombination to the cell cycle. *Immunity*. 1996;5(6):575-589.
9. Lee J, Desiderio S. Cyclin A/CDK2 regulates V(D)J recombination by coordinating RAG-2 accumulation and DNA repair. *Immunity*. 1999; 11(6):771-781.
10. Zhang L, Reynolds TL, Shan X, Desiderio S. Coupling of V(D)J recombination to the cell cycle suppresses genomic instability and lymphoid tumorigenesis. *Immunity*. 2011;34(2):163-174.
11. Küppers R, Dalla-Favera R. Mechanisms of chromosomal translocations in B cell lymphomas. *Oncogene*. 2001;20(40):5580-5594.
12. Gawad C, Pepin F, Carlton VEH, et al. Massive evolution of the immunoglobulin heavy chain locus in children with B precursor acute lymphoblastic leukemia. *Blood*. 2012;120(22): 4407-4417.
13. Steenbergen EJ, Verhagen OJ, van Leeuwen EF, von dem Borne AE, van der Schoot CE. Distinct ongoing Ig heavy chain rearrangement processes in childhood B-precursor acute lymphoblastic leukemia. *Blood*. 1993;82(2):581-589.
14. Papaemmanuil E, Rapado I, Li Y, et al. RAG-mediated recombination is the predominant driver of oncogenic rearrangement in ETV6-RUNX1 acute lymphoblastic leukemia. *Nat Genet*. 2014; 46(2):116-125.
15. Mullighan CG, Miller CB, Radtke I, et al. BCRABL1 lymphoblastic leukaemia is characterized by the deletion of Ikaros. *Nature*. 2008;453(7191): 110-114.
16. Kurzrock R, Gutterman JU, Talpaz M. The molecular genetics of Philadelphia chromosome positive leukemias. *N Engl J Med*. 1988;319(15): 990-998.
17. Rickert RC. New insights into pre-BCR and BCR signalling with relevance to B cell malignancies. *Nat Rev Immunol*. 2013;13(8):578-591.
18. Muljo SA, Schlissel MS. A small molecule Abl kinase inhibitor induces differentiation of Abelson virus-transformed pre-B cell lines. *Nat Immunol*. 2003;4(1):31-37.
19. Klein F, Feldhahn N, Mooster JL, et al. Tracing the pre-B to immature B cell transition in human leukemia cells reveals a coordinated sequence of primary and secondary IGK gene rearrangement, IGK deletion, and IGL gene rearrangement. *J Immunol*. 2005;174(1):367-375.
20. Guikema JE, Gerstein RM, Linehan EK, et al. Apurinic/aprimidinic endonuclease 2 is necessary for normal B cell development and recovery of lymphoid progenitors after chemotherapeutic challenge. *J Immunol*. 2011; 186(4):1943-1950.

21. Guikema JE, Linehan EK, Esa N, et al. Apurinic/aprimidinic endonuclease 2 regulates the expansion of germinal centers by protecting against activation-induced cytidine deaminase-independent DNA damage in B cells. *J Immunol*. 2014;193(2):931-939.
22. Bredemeyer AL, Sharma GG, Huang CY, et al. ATM stabilizes DNA double-strand-break complexes during V(D)J recombination. *Nature*. 2006;442(7101):466-470.
23. Vettermann C, Timblin GA, Lim V, Lai EC, Schlissel MS. The proximal J kappa germline transcript promoter facilitates receptor editing through control of ordered recombination. *PLoS One*. 2015;10(1):e0113824.
24. Schrader CE, Guikema JE, Linehan EK, Selsing E, Stavnezer J. Activation-induced cytidine deaminase-dependent DNA breaks in class switch recombination occur during G1 phase of the cell cycle and depend upon mismatch repair. *J Immunol*. 2007;179(9):6064-6071.
25. Trancoso I, Bonnet M, Gardner R, et al. A Novel Quantitative Fluorescent Reporter Assay for RAG Targets and RAG Activity. *Front Immunol*. 2013; 4:110.
26. Harvey RC, Mullighan CG, Wang X, et al. Identification of novel cluster groups in pediatric high-risk B-precursor acute lymphoblastic leukemia with gene expression profiling: correlation with genome-wide DNA copy number alterations, clinical characteristics, and outcome. *Blood*. 2010;116(23):4874-4884.
27. Kang H, Chen IM, Wilson CS, et al. Gene expression classifiers for relapse-free survival and minimal residual disease improve risk classification and outcome prediction in pediatric B-precursor acute lymphoblastic leukemia. *Blood*. 2010;115(7):1394-1405.
28. Lu Y, Wu Y, Feng X, et al. CDK4 deficiency promotes genomic instability and enhances Myc-driven lymphomagenesis. *J Clin Invest*. 2014; 124(4):1672-1684.
29. Rhodes N, Heerding DA, Duckett DR, et al. Characterization of an Akt kinase inhibitor with potent pharmacodynamic and antitumor activity. *Cancer Res*. 2008;68(7):2366-2374.
30. Levy DS, Kahana JA, Kumar R. AKT inhibitor, GSK690693, induces growth inhibition and apoptosis in acute lymphoblastic leukemia cell lines. *Blood*. 2009;113(8):1723-1729.
31. Altomare DA, Zhang L, Deng J, et al. GSK690693 delays tumor onset and progression in genetically defined mouse models expressing activated Akt. *Clin Cancer Res*. 2010;16(2):486-496.
32. Lin WC, Desiderio S. Cell cycle regulation of V(D)J recombination-activating protein RAG-2. *Proc Natl Acad Sci USA*. 1994;91(7):2733-2737.
33. Jiang H, Chang FC, Ross AE, et al. Ubiquitylation of RAG-2 by Skp2-SCF links destruction of the V(D)J recombinase to the cell cycle. *Mol Cell*. 2005; 18(6):699-709.
34. Anderson K, Lutz C, van Delft FW, et al. Genetic variegation of clonal architecture and propagating cells in leukaemia. *Nature*. 2011;469(7330): 356-361.
35. Ross ME, Zhou X, Song G, et al. Classification of pediatric acute lymphoblastic leukemia by gene expression profiling. *Blood*. 2003;102(8): 2951-2959.
36. Scherer DC, Brockman JA, Bendall HH, Zhang GM, Ballard DW, Oltz EM. Corepression of RelA and c-rel inhibits immunoglobulin kappa gene transcription and rearrangement in precursor B lymphocytes. *Immunity*. 1996;5(6):563-574.
37. Chow KT, Timblin GA, McWhirter SM, Schlissel MS. MK5 activates Rag transcription via Foxo1 in developing B cells. *J Exp Med*. 2013;210(8): 1621-1634.
38. Ozes ON, Mayo LD, Gustin JA, Pfeffer SR, Pfeffer LM, Donner DB. NF-kappaB activation by tumour necrosis factor requires the Akt serine-threonine kinase. *Nature*. 1999;401(6748):82-85.
39. Sasaki Y, Derudder E, Hobeika E, et al. Canonical NF-kappaB activity, dispensable for B cell development, replaces BAFF-receptor signals and promotes B cell proliferation upon activation. *Immunity*. 2006;24(6):729-739.

40. Igarashi H, Baba Y, Nagai Y, Jimi E, Ghosh S, Kincade PW. NF- κ B is dispensable for normal lymphocyte development in bone marrow but required for protection of progenitors from TNF α . *Int Immunol*. 2006;18(5):653-659.
41. Cadera EJ, Wan F, Amin RH, Nolla H, Lenardo MJ, Schlessel MS. NF- κ B activity marks cells engaged in receptor editing. *J Exp Med*. 2009;206(8):1803-1816.
42. Derudder E, Cadera EJ, Vahl JC, et al. Development of immunoglobulin lambda-chain positive B cells, but not editing of immunoglobulin kappa-chain, depends on NF- κ B signals. *Nat Immunol*. 2009;10(6):647-654.
43. Verkoczy L, Ait-Azzouzene D, Skog P, et al. A role for nuclear factor kappa B/rel transcription factors in the regulation of the recombinase activator genes. *Immunity*. 2005;22(4): 519-531.
44. Balkhi MY, Willette-Brown J, Zhu F, et al. IKK α -mediated signaling circuitry regulates early B lymphopoiesis during hematopoiesis. *Blood*. 2012;119(23):5467-5477.
45. Hinz M, Krappmann D, Eichten A, Heder A, Scheidereit C, Strauss M. NF- κ B function in growth control: regulation of cyclin D1 expression and G0/G1-to-S-phase transition. *Mol Cell Biol*. 1999;19(4):2690-2698.
46. Li J, Joo SH, Tsai M-D. An NF- κ B-specific inhibitor, I κ B α , binds to and inhibits cyclin-dependent kinase 4. *Biochemistry*. 2003;42(46):13476-13483.
47. Reuther JY, Reuther GW, Cortez D, Pendergast AM, Baldwin AS Jr. A requirement for NF- κ B activation in Bcr-Abl-mediated transformation. *Genes Dev*. 1998;12(7):968-981.
48. Chen F, Castranova V. Nuclear factor- κ B, an unappreciated tumor suppressor. *Cancer Res*. 2007;67(23):11093-11098.
49. Malumbres M, Barbacid M. Cell cycle, CDKs and cancer: a changing paradigm. *Nat Rev Cancer*. 2009;9(3):153-166.
50. Fruman DA, Rommel C. PI3K and cancer: lessons, challenges and opportunities. *Nat Rev Drug Discov*. 2014;13(2):140-156.
51. Braun T, Carvalho G, Fabre C, Grosjean J, Fenaux P, Kroemer G. Targeting NF- κ B in hematologic malignancies. *Cell Death Differ*. 2006;13(5):748-758.
52. Lim K-H, Yang Y, Staudt LM. Pathogenetic importance and therapeutic implications of NF- κ B in lymphoid malignancies. *Immunol Rev*. 2012; 246(1):359-378.

Supplement

Supplemental Table 1: Primer sequences

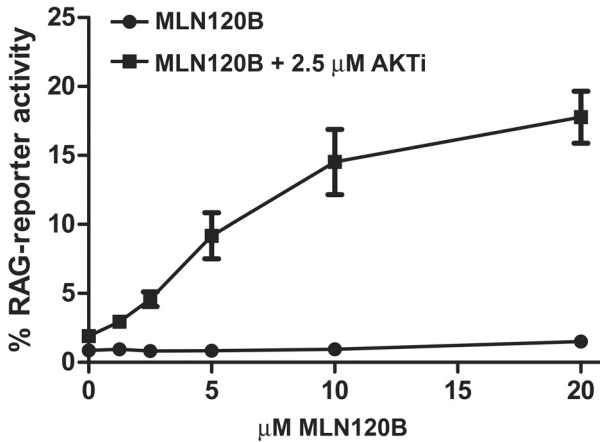
Target gene	5'-3' sequence	
<i>RAG1</i> (human)	Forward	GGCAAGGAGAGAGCAGAGAA
	Reverse	CTCACCCGGAACAGCTTAAA
<i>RAG1</i> (human)	Forward	CTTCCCAAGTGTGACAATT
	Reverse	AGTGAGAAGCCTGGCTGAAAT
<i>RPLPO</i> (human)	Forward	GCTTCTGGAGGGTGTCCGC
	Reverse	TCCGTCTCCACAGACAAGGCCA
<i>Rag1</i> (mouse)	Forward	AGCTATCACTGGGAGGCAGA
	Reverse	GAGGAGGCAAGTCCAGACAG
<i>Rag2</i> (mouse)	Forward	CTTCCCAAGTGTGACAATT
	Reverse	AGTGAGAAGCCTGGCTGAAT
<i>Cdk4</i> (mouse)	Forward	GATCTCATTGGATTGCCTCCAG
	Reverse	TTAAAGGTCAGCATTTCAGTAGC
<i>Cdk2</i> (mouse)	Forward	CCCTATTCCCTGGAGATTCTG
	Reverse	CAGCATTGCGATAACAAGCTC
<i>Cyclin-A</i> (mouse)	Forward	TGCTAGGGGTGTGACTGAA
	Reverse	CCCATGGTCAGAGAGCACTT
<i>Cyclin-D1</i> (mouse)	Forward	CGTGGCCTCTAAGATGAAGGA
	Reverse	AGTTCATTTGCAGCAGCTC
<i>Vk6-23/Jk1 rearr.</i> (mouse)	Forward	ACATGTTGCTGTGGTTGTCTGGTG
	Reverse	GGAGAGTGCCAGAATCTGGTTTCAG
<i>Gapdh</i> (mouse)	Forward	CAAATTC AACGGCACAGTC
	Reverse	TCACAAACATGGGGGCATC
<i>18S rRNA</i> (mouse)	Forward	TGGTGGAGGGATTTGTCTGG
	Reverse	TCAATCTCGGGTGGCTGAAC
<i>JK2-ko5</i> (mouse; LM-PCR)	Forward	CAGAAATGCTCAAAGAAGCAGGGTAGCCTG
BW-H (LM-PCR)	Reverse	CCGGGAGATCTGAATTCCAC
BW-1 (LM-PCR linker)	Sense	GCGGTGACCCGGGAGATCTGAATTC
BW-2 (LM-PCR linker)	Antisense	GAATTCAGATC

Supplemental Table 2: B-ALL patient cytogenetic characteristics

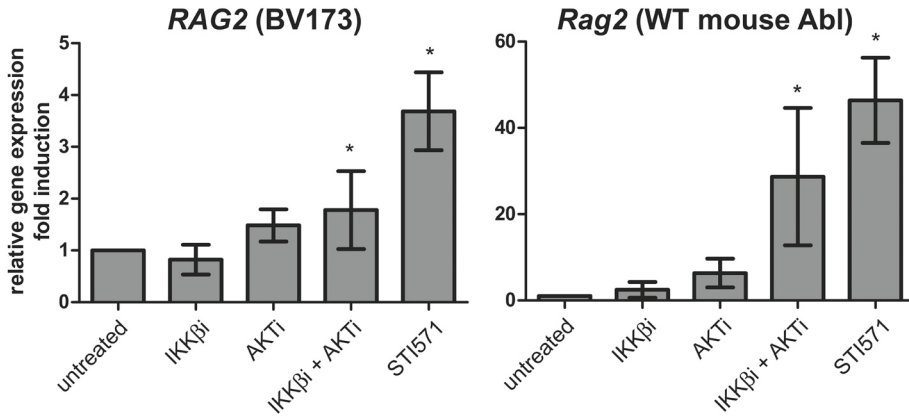
Patient	Cytogenetic profile	Other
1	53,XY,+X,+4,+6,+14,+17,+18,+21[2], add(16)(?q24)[4]/46,XY[14]	BCR-ABL negative TEL-AML1 negative MLL-AF4 negative E2A-PBX1 negative Δ IKZF1 ex4-7
2	5 2 ~ 5 3 , X Y , + 4 , + 9 , + 1 4 , + 1 7 , + 1 8 , + 2 1 , + 2 ~ 4 mar, inc[cp8]/46,XY[12]	BCR-ABL negative TEL-AML1 negative MLL-AF4 negative E2A-PBX1 negative Δ IKZF1 negative
3	Not available	BCR-ABL negative TEL-AML1 negative T(11;v) MLL partner unknown

Supplemental figures

5

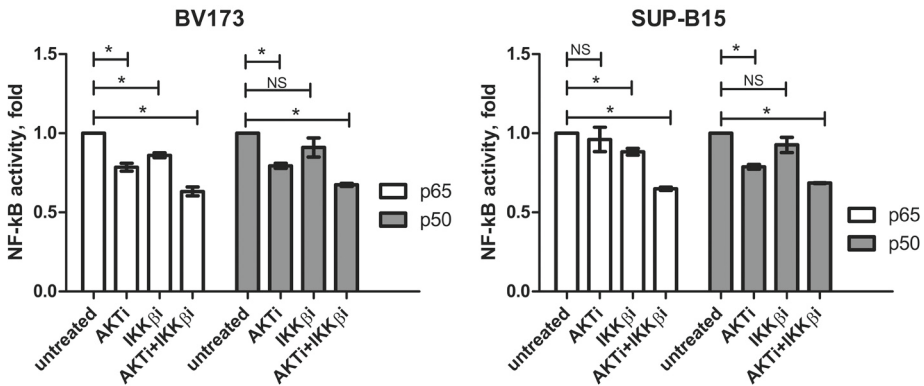
**Supplemental Figure 1.**

Combined treatment with MLN120B and AKTi stimulates RAG activity in mouse Abl pre-B cells. Titration curve of MLN120B (circles + line) and titration of MLN120B + 2.5 μ M AKTi (boxes + line). RAG-reporter activity (y-axis) of wildtype mouse Abl pre-B cells is plotted against the concentration of MLN120B (x-axis), cells were treated for 96h (n=4 independent cultures), means \pm SD are shown.



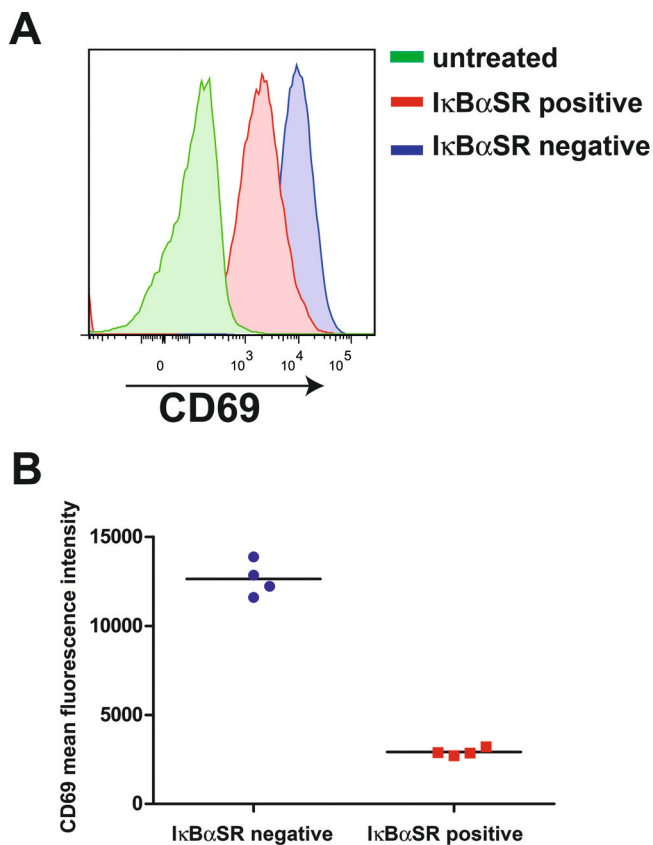
Supplemental Figure 2.

RAG2 mRNA expression in BV173 human pre-B ALL cell line and WT mouse Abl pre-B cells. Rag2 real-time RT-PCR analysis of the human BCR-ABL+ B-ALL cell line BV173 and WT mouse Abl pre-B cells. Cells were treated with 2.5 μM IKKβi, 2.5 μM AKTi or 10 μM STI571 for 48h. Means ± SD are shown (n=4 independent stimulations, PCR reactions were performed in duplicate), *p<0.05, as determined by the one sample t test.



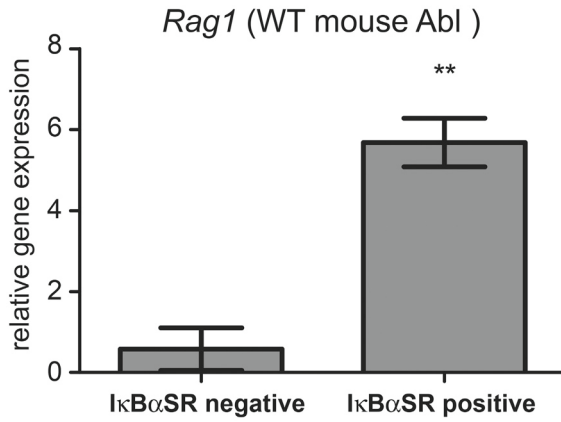
Supplemental Figure 3.

Combined treatment with IKKβi and AKTi inhibits NF-κB transcription factor activity in human pre-B ALL cell lines. BV173 and SUP-B15 cells were treated for 24h with 2.5 μM IKKβi, 2.5 μM AKTi, or with both. Equal amounts of nuclear lysates (5 μg) were analyzed for specific NF-κB p65 (white bars) and p50 (grey bars) transcription factor DNA binding activity using an enzyme-linked immunosorbent assay (ELISA) (Abcam ab133128). Each stimulation was performed in triplicate and each individual lysate was assayed in duplicate. Means ± SD of independent cultures are shown (n=3). *p<0.05, as determined by the one sample t test.



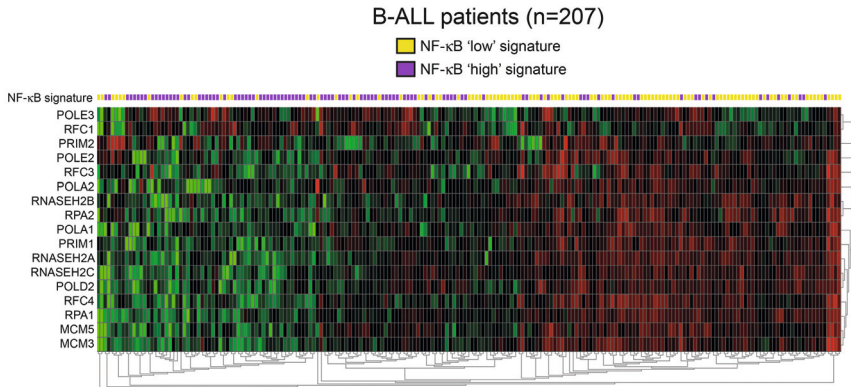
Supplemental Figure 4.

Expression of I κ B α super-repressor in mouse Abl pre-B cells inhibits LPS-induced upregulation of CD69 expression. CD69 expression was determined in LPS-treated (25 μ g/mL; 24h) mouse Abl pre-B cells retrovirally transduced with I κ B α SR-IRES-YFP. **(A)** Overlay FACS histograms are shown of untreated cells and LPS-stimulated cells gated on YFP-positive cells and YFP-negative cells. **(B)** Graph depicts CD69 mean fluorescence intensity within I κ B α SR negative (YFP-negative) and I κ B α SR-positive (YFP-positive) gates. Each symbol represents an individual stimulation (n=4)

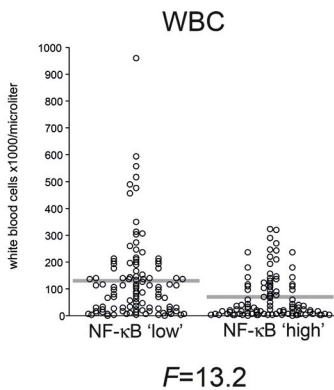
**Supplemental Figure 5.**

RAG1 mRNA expression in mouse Abl pre-B cells retrovirally transduced with IκBα super-repressor. IκBαSR-IRES-YFP positive and IκBαSR-IRES-YFP negative cells were FACS sorted and analyzed by quantitative real-time PCR. Means ± SD are shown (n=4; technical replicates). **p<0.01, as determined by Mann-Whitney *U*-test.

A



B



Supplemental Figure 6.

NF-κB gene expression signatures are associated with the expression of DNA replication pathway genes and white blood cell counts. **(A)** Heatmap showing expression of DNA replication pathway genes (Kyoto Encyclopedia of Genes and Genomes, KEGG). Each column represents a B-ALL patient. Yellow squares indicate NF-κB 'low' signature patients, purple squares indicate NF-κB 'high' signature patients. **(B)** White blood cell counts (x1000/microliter) in NF-κB 'low' and NF-κB 'high' signature B-ALL patients. Each circle represents an individual patient, grey bars indicate means. Below the graph the ANOVA F-statistic and p-value are given.

Supplemental materials and methods

Immunoblotting

For whole-cell lysates, cells were lysed in radioimmunoprecipitation assay (RIPA) buffer (50 mM Tris-HCl at pH 7.0, 150 mM NaCl, 0.1% SDS, 0.5% sodium deoxycholate, and 1% NP-40), supplemented with EDTA-free complete protease inhibitor cocktail and phosphatase inhibitor cocktail (PhosSTOP™) (both from Roche, Basel, Switzerland). For cytoplasmic and nuclear fractionation, the Nuclear/Cytosol Extraction kit was used according to the manufacturer's instructions (Biovision, Mountain View, CA). Equal amounts of lysates (10 μg) were separated on 4% to 20% gradient SDS page gels (Bio-Rad, Hercules, CA) and transferred to PVDF membranes (Fisher Thermo Scientific, Waltham, MA). Antibodies used for immunoblotting include RAG1 (D36B3), FOXO1 (C29H4), p-FOXO1-ser-256 (9461), FOXO3a (75D8), p-AKT-ser-473 (D9E) (Cell Signaling Technology, Danvers, MA), p-FOXO1-ser-329 (EP927Y), C-MYC (Y69), KU70 (N3H10) (Abcam, Cambridge, MA), IκBα (SC-371), p-IκBα-ser-32 (SC-8404), p-IKKα-thr-23 (SC-101706), NF-κB p65 (SC-372), CDK4 (SC-260), p-STAT5-tyr-694/tyr-699 (SC-11761) (Santa Cruz Biotechnology Inc. Dallas, TX), and β-Actin (AC-15, Sigma Aldrich).

Flow cytometry

Intracellular, intranuclear and BrdU stainings were done as previously described^{1,2}. Antibodies for mouse cells include B220-APC (RA3-6B2), CD43-PE (S7), kappa light chain-PE/Cy7 and kappa light chain-FITC (187.1) (BD Pharmingen, San Diego, CA), IgM-PE/Cy7 (II/41), p-H2AX-ser-139-Alexa-Fluor-647 (2F3) (eBioscience, San Diego, CA). Antibodies for human cells include CD19-APC/Cy7 (BD, Pharmingen) CD43-FITC (clone 581, Biolegend, San Diego, CA), CD10-PE/Cy5 (BD Pharmingen) and IgM-APC (BD Pharmingen). Intracellular Ig kappa light chains stainings and intranuclear γH2AX stainings were performed as described earlier^{1,2}. BrdU incorporation was measured by incubating cells for 2 hours with 20 μM BrdU (Sigma Aldrich), BrdU stainings were done as described previously^{1,2}. All populations were gated on viable cells by 7-aminoactinomycin-D exclusion or based on forward and side scatter. Doublets were excluded based on forward and side scatter height versus width profiles. Flow-cytometry was performed on a four-laser, thirteen-detector LSR Fortessa (BD Biosciences). Flowcytometry data was analyzed using FlowJo (Tree Star Inc., Ashland, OR).

Analysis of Jκ2-RSS signal end DNA breaks in G1- and S- cell-cycle phase cells

WT and RAG2^{-/-} Abl transformed pre-B cells were treated with 2.5 μM IKKβi + AKTi or left untreated for 48h and subsequently stained with 10 μM Vybrant® Dyecycle™ (Life Technologies, Carlsbad, CA) for 90 minutes at 37°C. G1- phase and S-phase cells were sorted according to their DNA content using a BD Influx™ cell-sorter (Becton & Dickinson. Exactly 1x10⁶ cells were sorted for each fraction, cells were washed and embedded in 0.5% low-melting

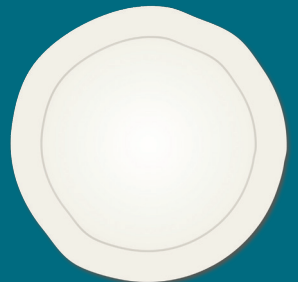
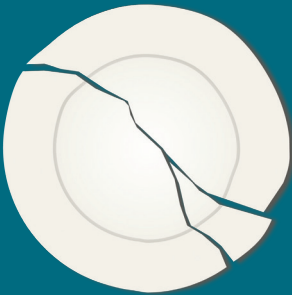
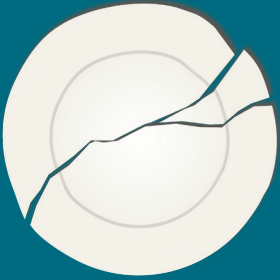
agarose in 20 mM EDTA. Genomic DNA was carefully isolated from agarose-embedded cells by sequential overnight proteinase K treatments (1 mg/mL proteinase K, 1% SDS, 50 mM Tris pH=8, 20 mM EDTA) to prevent mechanical shearing of the DNA. After proteinase K inactivation and washing, 1/5th of each sample (200,000 cell equivalents) was used for DNA doublestranded break linker ligation. Double-stranded linkers were prepared by allowing the oligonucleotides BW-1 and BW-2 to anneal. Linkers were annealed to genomic DNA by T4 ligase in 1x ligase buffer to which 3.5% polyethyleneglycol-4000 was added. Ligation-mediated PCR (LM-PCR) was performed using a J κ 2-specific forward primer (J κ 2-ko5) and a linker-specific primer (BW-H) in a touchdown-PCR: 95°C, 10'; 11x (94°C, 30" / 70-60°C, 2.5', with $\Delta T = 1^\circ\text{C}/\text{cycle}$); 29x (94°C, 30"; 60°C, 2.5'); 72°C, 10'. LM-PCR was performed on three-fold dilutions of linker-ligated genomic DNA, which was normalized for input by GAPDH PCR. PCR products were resolved in 3% agarose gels. Bands of the expected size were excised from the gel and cloned into the pCR2.1-TOPO vector for sequencing. After cloning, bacterial clones were sequenced using plasmid-specific M13 primers. Primer sequences are listed in Supplemental Table 1.

Primary mouse bone marrow pre-B cell cultures

Bone marrow (BM) cells were harvested from 8-20 wks old mice by flushing femurs and tibia. Total BM cells were cultured in 6-wells plates at a density of 2×10^6 cells/mL in RPMI1640 with 2 mM L-glutamine, 100 U/mL penicillin, 100 $\mu\text{g}/\text{mL}$ streptomycin, 10% fetal calf serum, 50 μM β -mercaptoethanol, 10 ng/mL recombinant mouse IL7, and 10 ng/mL Flt3L (both from ProSpec Inc., Ness-Ziona, Israel). Culture medium and cytokines were replaced every three days. Cells were harvested after 7-10 days and analyzed by flow-cytometry, typically yielding >95% B220⁺, IgM⁻, CD43⁺ progenitor B cells (data not shown). To induce large to small pre-B cell transition, cells were washed 3 times in culture medium without cytokines and placed back in 6-wells plates at 2×10^6 cells/mL in medium without cytokines (IL7 withdrawal).

Supplementary references

1. Guikema JE, Gerstein RM, Linehan EK, et al. Apurinic/Apyrimidinic endonuclease 2 is necessary for normal B cell development and recovery of lymphoid progenitors after chemotherapeutic challenge. *J Immunol.* 2010;186(4):1943–1950.
2. Guikema JE, Linehan EK, Esa N, et al. Apurinic/Apyrimidinic Endonuclease 2 Regulates the Expansion of Germinal Centers by Protecting against Activation-Induced Cytidine Deaminase-Independent DNA Damage in B Cells. *J. Immunol.* 2014;193(2):931–9.



CHAPTER

DNA damage-induced p53 downregulates expression of RAG1 through a negative feedback loop involving miR-34a and FOXP1

Katarina Ochodnicka-Mackovicova,
Martine van Keimpema, Marcel Spaargaren,
Carel J.M. van Noesel, Jeroen E.J. Guikema

A large, stylized pink number '6' is positioned on the right side of the page, partially overlapping a vertical teal line.

Abstract

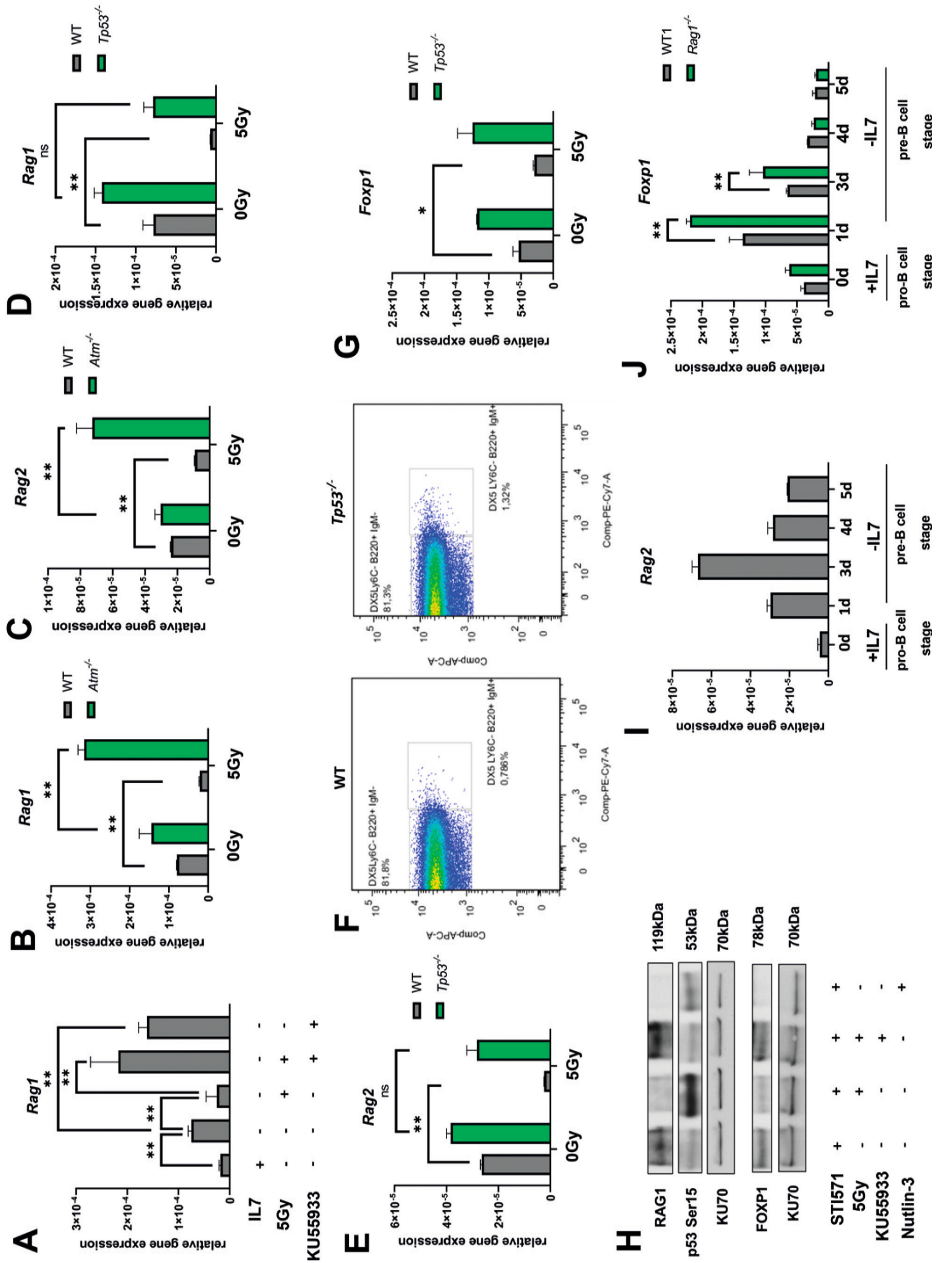
During the maturation of pre-B cells, the recombination activating gene 1 and 2 (RAG1/2) endonuclease complex plays a crucial role in coordinating V(D)J recombination by introducing DNA breaks in immunoglobulin (*Ig*) loci. Dysregulation of RAG1/2 has been linked to the onset of B-cell malignancies, yet the mechanisms controlling RAG1/2 in pre-B cells exposed to excessive DNA damage are not fully understood. In this study, we show that DNA damage-induced activation of p53 initiates a negative-feedback loop which rapidly downregulates RAG1 levels. This feedback loop involves ataxia telangiectasia mutated (ATM) activation, subsequent stabilization of p53, and modulation of microRNA-34a (miR-34a) levels, which is one of the p53 targets. Notably, this loop incorporates transcription factor forkhead box P1 (FOXP1) as a downstream effector. The absence of p53 resulted in an increased proportion of IgM⁺ cells prompted to upregulate RAG1/2 and to undergo *Ig* light chain (*IgI*) recombination. Similar results were obtained in primary pre-B cells with depleted levels of miR-34a. We propose that in pre-B cells undergoing *Ig* gene recombination, the DNA breaks activate a p53/miR-34a/FOXP1-mediated negative-feedback loop that contributes to the rapid downregulation of RAG. This regulation limits the RAG-dependent DNA damage, thereby protecting the stability of the genome during V(D)J rearrangement in developing B cells.

Results and discussion

In developing pre-B cells, V(D)J rearrangement is orchestrated by the RAG1/2 endonuclease complex. Aberrant regulation of this rearrangement process has been implicated in the development of B-cell malignancies, such as B-cell acute lymphoblastic leukemia (B-ALL) and follicular lymphoma (FL)¹⁻³. Persistent expression of RAG1 was shown to be an oncogenic driver in B-ALL⁴ and RAG1/2 regulators have been suggested as plausible therapeutic targets⁵⁻⁷. The double-stranded DNA breaks (DSBs) created by RAG activate the ATM kinase, which then recruits and activates other proteins to the site of the breaks in the efforts of its repair. Following the *Ig* kappa light chain (*Ig*κ) recombination on one allele, the RAG-dependent DNA breaks activate ATM, which was shown to limit RAG expression and accessibility of the *Ig*κ locus, thus enforcing allelic exclusion^{8,9}. Previously, we have demonstrated that in response to external DNA damage, RAG protein and mRNA levels are rapidly downregulated, and that the regulation involves the ATM-FOXO1 pathway, where pharmacological inhibition of ATM prevented the DNA damage-induced downregulation of *Rag1* and *Rag2*⁷.

To further validate the involvement of ATM in the DNA damage-dependent regulation of RAG we expanded progenitor B cells from *Atm*^{-/-} mouse bone marrows by IL7 and Flt3L stimulation *in vitro*. The large-to-small pre-B cell transition was induced by IL7 and Flt3L withdrawal. In agreement with our previous findings⁷, we show that IL7/Flt3L withdrawal induced *Rag1* and *Rag2* expression, which was downregulated upon 5 Grays (Gy) of γ-irradiation in wildtype (WT) pre-B cells, but not in *Atm*^{-/-} pre-B cells (**Figure 1A-C**).

ATM activation is known to stabilize TP53 via a complex downstream array of events, including phosphorylation of mouse double minute 2, also known as E3 protein ubiquitin ligase, (MDM2), which in its phosphorylated form cannot poly-ubiquitinate p53, thus leading to its stabilization^{10,11}. Here, we show that the ATM-mediated regulation of *Rag* also involves p53. *Rag1* and *Rag2* mRNA was rapidly downregulated in response to external DNA damage in mouse primary pre-B cells, with on average 89.9% reduction in *Rag1* and 90.7% in *Rag2* mRNA levels in 5 Gy-irradiated primary WT pre-B cells, whereas in *TP53*^{-/-} mouse primary pre-B cells γ-irradiation resulted in an on average 44.3% reduction in *Rag1* and 25.6% in *Rag2* mRNA levels (**Figure 1D-E**). In addition, in primary bone marrow pre-B-cell cultures prompted to undergo *Ig*λ recombination by IL7 and Flt3L withdrawal from the culture, the amount of surface IgM-expressing immature B cells (B220⁺DX6⁻Ly6C⁻IgM⁺) was higher in *TP53*^{-/-} cultures cells as compared to their WT counterparts (1.32% vs. 0.79%, respectively), suggesting that p53 activation interferes with the successful production and expression of surface IgM in developing B cells (**Figure 1F**).



◀ **Figure 1.**

(A) *Rag1* mRNA expression in primary murine WT bone marrow pre-B cells measured by quantitative RT-PCR; the cells were first cultured 7 days on the OP9 feeder layer cell line with IL7 and Flt3L: conditions that promote expansion of small pre-B cells that have not yet undergone the *Igk* recombination because of the low RAG1/2 expression. To induce the RAG1/2 expression, IL7 and Flt3L were withdrawn from the media for 24h. After that, the cells were treated either with DMSO, subjected to 5 Gy γ -irradiation with subsequent 2h recovery time, pre-treated with ATM inhibitor KU55933 for 2h prior to γ -irradiation, or treated for 4h with KU55933 with no irradiation (n=2, mean \pm SD, **p<0.05). (B) *Rag1* and (C) *Rag2* mRNA expression in primary WT and *Atm*^{-/-} bone marrow pre-B cells first cultured 7 days on OP9 cells with addition of IL7 and Flt3L, 24h after the withdrawal of Flt3L and IL7 the cells were treated either with either DMSO or subjected to 5 Gy γ -irradiation with subsequent 2h recovery time (n=2, mean \pm SD, **p<0.05). (D) and (E) *Rag1* and *Rag2* mRNA expression in primary WT and *Tp53*^{-/-} bone marrow pre-B cells treated, 24h after the withdrawal of Flt3L and IL7, with either DMSO or 5 Gy γ -irradiation with subsequent 2h recovery time (n=2, mean \pm SD, fold difference as compared to DMSO, *p<0.1). (F) Representative FACS staining of WT primary bone marrow cells and cells derived from *Tp53*^{-/-} mice. The bone marrow cells were first cultured 7 days on OP9, Flt3L, and IL7, then, the amounts of B220⁺IgM⁺ pre-B cells were measured 48h following the withdrawal of Flt3L and IL7 from the medium. (G) *Foxp1* mRNA expression in primary WT and *Tp53*^{-/-} bone marrow pre-B cells treated, 24h after the withdrawal of Flt3L and IL7, with either DMSO or 5 Gy γ -irradiation with subsequent 2h recovery time (n=2, mean \pm SD, fold difference as compared to DMSO, *p<0.1). (H) Western blotting analysis of RAG1, TP53 phosphorylated at Ser¹⁵ and FOXP1 protein levels in BV173 cells. The cells were treated with v-Abl kinase inhibitor STI571 for 72h to induce RAG1/2 expression and *Igk* recombination, after which the cells were exposed to 5Gy γ -irradiation with subsequent 2h recovery time or pre-treated with ATM inhibitor KU55933 for 2hours prior to the irradiation with subsequent 2h recovery time or treated with p53 stabilizer Nutlin-3 for 4 hours. KU70 was used as a control. (I) *Rag2* and (J) *Foxp1* mRNA expression in primary WT and *Rag1*^{-/-} bone marrow pre-B cells. After 7 days of culture, the Flt3L and IL7 were withdrawn from the media and the *Rag2* and *Foxp1* mRNA expression were measured on the day of the withdrawal and 1, 3, 4, and 5 days following the withdrawal (n=2, mean \pm SD, **p<0.05).

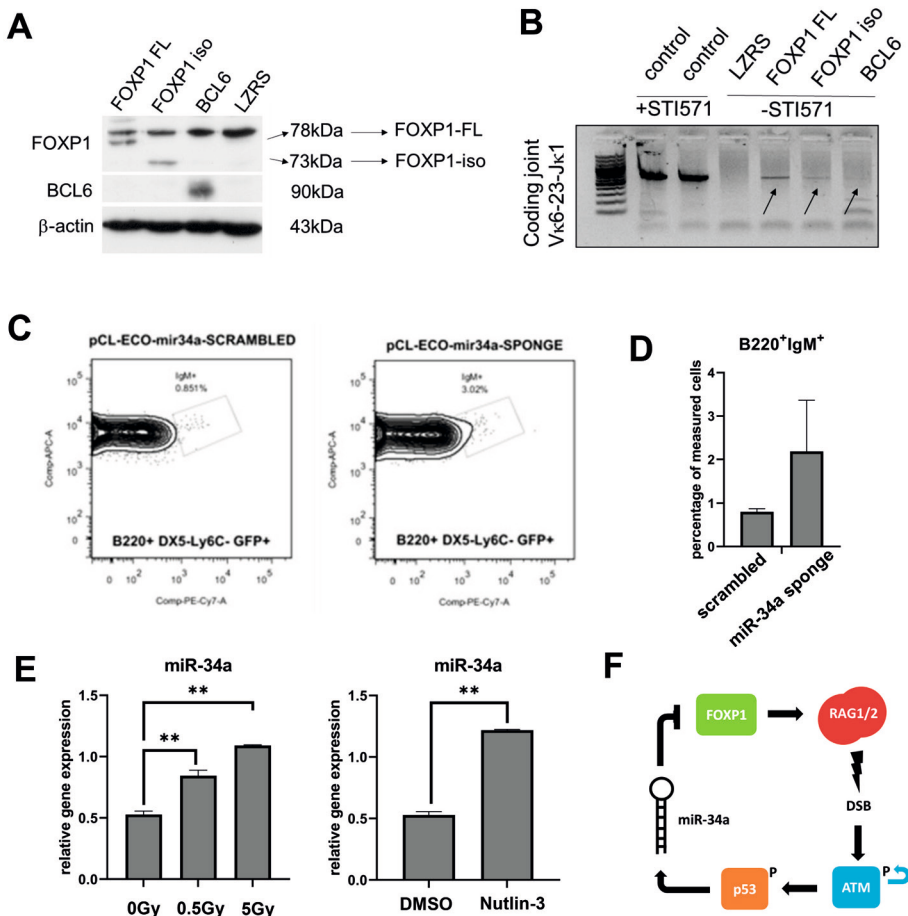
The transcription factor FOXP1 was shown to regulate RAG1 and RAG2 expression by binding to the *Erag* enhancer. The bone marrow from *Foxp1*^{-/-} mice showed impaired B-cell development, as the percentages of pro-B cells (IgM⁻B220⁺CD43⁺) and pre-B cells (IgM⁻B220⁺CD43⁻) were significantly lower than in *Foxp1*^{+/-} bone marrows¹². In our study, the mRNA expression of *Foxp1* was decreased by 45.5% in γ -irradiated WT primary pre-B-cell cultures undergoing light chain recombination following IL7 withdrawal, while the *Foxp1* expression in *Tp53*^{-/-} primary pre-B cells remained unaffected by irradiation (**Figure 1G**).

In the mouse A70 pre-B cell line, v-Abl creates a developmental block, arresting the B cells in a stage at which the RAG1/2 expression is low and the *Igk* is not yet recombined. Treatment with STI571, an Abelson-kinase inhibitor, alleviates this block, induces RAG1/2 expression and *Igk* recombination¹³. In agreement, in STI571-treated mouse v-Abl-transformed pre-B cells, 5Gy γ -irradiation or treatment with the p53-stabilizing agent Nutlin-3 resulted in the downregulation of RAG1 and FOXP1 protein expression, which was prevented by pretreatment with the ATM kinase inhibitor KU55933 (**Figure 1H**). The downregulation of RAG1 and FOXP1 following γ -irradiation was not caused by activation of caspases, as shown by pretreatment with the pan-caspase inhibitor Z-VAD-FMK, nor by cell death, as shown by the amount of sub-G1 phase cells analyzed by FACS for DNA-content (propidium-iodide). (**Suppl Figure 2A-B**).

► **Figure 2.**

(A) Western blotting analysis of FOXP1, BCL6, and β -actin (loading control) in mouse v-Abl WT (A70) cells transduced with either empty vector (LZRS), human full-length FOXP1 (FOXP1 FL), the isoform of human of FOXP1 (FOXP1 iso), or human BCL6. **(B)** The mouse v-Abl WT cells (A70) were transduced with either empty vector (LZRS), human full-length FOXP1 (FOXP1 FL), the isoform of human of FOXP1 (FOXP1 iso), or human BCL6. Control, untransduced A70 cells treated with STI571 for 72h to induce RAG1/2 expression and *Igk* recombination. The formation of coding joints following the treatment with STI571 was assessed by qualitative PCR analysis of one particular joint: V κ 6-23 to J κ 7²⁴ (bands representing coding joints in transduced cells are indicated by arrows). The PCR products were run in 2% agarose gel containing ethidium bromide. **(C)** Representative FACS staining of WT primary bone marrow cells, transduced either with pCL-ECO-miR-34a-sponge or with pCL-ECO-scrambled as a control. The cells were cultured for 7 days on OP9, Flt3L, and IL7, the amount of B220⁺IgM⁺ pre-B cells was measured 48h following the withdrawal of Flt3L and IL7 from the medium. **(D)** Quantification of the amount of B220⁺IgM⁺ pre-B cells by FACS staining as described in 2B (n=2, mean \pm SD, **p<0.05). **(E)** RT-PCR analysis of the relative miR-34a expression in primary WT bone marrow pre-B cells, initially cultured 7 days on OP9, Flt3L and IL7, then the Flt3L and IL7 were withdrawn from the medium for 72h and the cells were exposed to either 5 Gy or 0.5 Gy of γ -irradiation followed by 2h of recovery, or treated with p53 stabilizer Nutlin-3 (2.5 μ M) for 4 hours. Control cells were treated with DMSO (n=2, mean \pm SD, **p<0.05). **(F)** Schematic representation of the proposed self-regulating negative feedback loop. In response to excessive DNA damage ATM is phosphorylated which in turn activates the p53 pathway. Subsequently, one of the consequences of p53 activation of miR-34a, which is a negative regulator of FOXP1, the RAG1/2 transcription factor. This might represent a mechanism by which the B cells protect themselves against excessive DNA damage, and dysregulation of this pathway might contribute to the genetic instability in developing B cells.

Previously, we have shown that endogenous DNA damage emanating from RAG1/2 activity could trigger a similar regulatory response as provoked by γ -irradiation⁷. To study the effect of RAG1/2-dependent DNA damage on *Foxp1* expression we made use of pre-B cell cultures from *Rag1*^{-/-} mice, where the developmental block imposed by *Rag1* deficiency is rescued by the transgenic expression of a functionally rearranged VH81x IgH μ chain¹⁴. We observed that in *in vitro* cultured primary bone marrow B-cell progenitor cells prompted to undergo *IgI* recombination by IL7 and Flt3L withdrawal, *Foxp1* mRNA levels were approximately 2-fold higher in *Rag1*^{-/-} VH81x primary bone marrow as compared to their RAG-proficient counterparts (1.61-fold higher *Foxp1* levels, $p < 0.05$, on day 1 following IL7/Flt3L withdrawal in *Rag1*^{-/-} VH81x vs *Rag1*^{+/+} VH81x; and 1.59-fold higher *Foxp1* levels, $p < 0.05$, on day 3 after IL7/Flt3L withdrawal in *Rag1*^{-/-} VH81x versus *Rag1*^{+/+} VH81x) (**Figure 1I-J**).



To further substantiate the role of FOXP1 in driving RAG expression in pre-B cells, we overexpressed the full-length (FL) FOXP1 and its shorter isoform (iso), which were previously shown to have similar functions¹⁵, in the A70 v-Abl transformed mouse pre-B cell line (**Figure 2A**). Interestingly, FOXP1 overexpression was sufficient to induce productive recombination *Igκ* recombination, and partly overcame the development block imposed by v-Abl expression, as determined by the detection of productive by Vκ6-23-Jκ1 coding joints by PCR (**Figure 2B**). The FOXP1 isoform, truncated at the N-terminus, is overexpressed in subsets of B-cells lymphomas and has been suggested to have an oncogenic capacity¹⁵⁻¹⁷. Our results imply that the FOXP1 N-terminus is not required to partially override the v-Abl-induced developmental block in the A70 pre-B cell line. In addition, overexpression of BCL6¹⁸ a negative regulator of p53, also resulted in Vκ6-23-Jκ1 recombination events without STI571 treatment in A70 cells (**Figure 2A-B and Suppl Figure 3A-B**).

Previously, the regulation of FOXP1 in developing B cells was linked to the p53 pathway through miR-34a. The activation of p53 has been shown to drive the expression of miR-34a in cell lines of various origin¹⁹⁻²¹, and constitutive miR-34a expression resulted in a B-cell development blockade, where FOXP1 was identified as the key mediator of this effect²². Moreover, in chronic lymphocytic leukemia (CLL) cells, the p53/miR-34a pathway has been shown to be a negative regulator of FOXP1 expression, responding rapidly to DNA damage and limiting B-cell receptor (BCR) signaling in mature B cells²³. We therefore investigated the possible ties of ATM/p53 signaling induced by DSBs to the miR-34a/FOXP1/RAG axis. Our data show that γ -irradiation drives the miR-34a expression in *in vitro* expanded progenitor B cells from primary mouse bone marrow in a dose-dependent manner. In agreement, the level of miR-34a was significantly higher upon treatment with the MDM2 inhibitor Nutlin-3 (**Figure 2E**). Furthermore, in *in vitro* expanded progenitor B cells from primary bone marrow, depletion of miR-34a using a miR-34a-sponge construct resulted in an increase in B220⁺DX6⁺Ly6C⁺IgM⁺ B cells (2.19% in cells transduced with pCL-ECO-miR-34a-sponge vs. 0.80% in cells transduced with pCL-ECO-scrambled) following the IL-7 and Flt3L withdrawal from the cell culture, suggesting that depletion of miR-34a promotes successful *Igκ* recombination (**Figure 2C- D**).

In summary, we propose a negative-feedback regulatory mechanism involving p53, miR-34a, and FOXP1, where DNA breaks limit the expression of RAG1 and RAG2 (**Figure 2F**). In this regulatory mechanism, (RAG-dependent) DNA damage activates ATM, which in turn stabilizes p53 and activates the p53 effectors, including miR-34a, which affects Foxp1 levels and *Igκ* recombination in pre-B cells. In agreement, the levels of miR-34a as well as FOXP1 respond to exogenous and RAG-instigated DNA damage and limit the RAG1/2 expression and the V(D)J recombination. This regulatory process in developing B cells may serve as a self-protective mechanism against excessive RAG-dependent DNA damage and thus guards the stability of the genome.

Acknowledgements

This study was supported by the Academic Medical Center Fellowship program and a VIDI-grant from the Dutch Organization for Scientific Research (NWO VIDI 016126355), both awarded to JEJG.

References

- Papaemmanuil, E. *et al.* RAG-mediated recombination is the predominant driver of oncogenic rearrangement in ETV6-RUNX1 acute lymphoblastic leukemia. *Nat. Genet.* **46**, 116–125 (2014).
- Kuiper, R. P. & Waanders, E. A RAG driver on the road to pediatric ALL. *Nat. Genet.* **46**, 96–98 (2014).
- Bakhshi, A. *et al.* Mechanism of the t(14;18) chromosomal translocation: structural analysis of both derivative 14 and 18 reciprocal partners. *Proc. Natl. Acad. Sci. U. S. A.* **84**, 2396–2400 (1987).
- Han, Q. *et al.* RAG1 high expression associated with IKZF1 dysfunction in adult B-cell acute lymphoblastic leukemia. *J. Cancer* **10**, 3842–3850 (2019).
- Wang, F. *et al.* Tight regulation of FOXO1 is essential for maintenance of B-cell precursor acute lymphoblastic leukemia. *Blood* **131**, 2929–2942 (2018).
- Ochodnicka-Mackovicova, K. *et al.* NF- κ B and AKT signaling prevent DNA damage in transformed pre-B cells by suppressing RAG1/2 expression and activity. *Blood* **126**, 1324–1335 (2015).
- Ochodnicka-Mackovicova, K. *et al.* The DNA Damage Response Regulates RAG1/2 Expression in Pre-B Cells through ATM-FOXO1 Signaling. *J. Immunol.* **197**, 2918–2929 (2016).
- Glynn, R. A. & Bassing, C. H. Nemo-Dependent, ATM-Mediated Signals from RAG DNA Breaks at Ig κ Feedback Inhibit V(κ) Recombination to Enforce Ig κ Allelic Exclusion. *J. Immunol.* **208**, 371–383 (2022).
- Steinel, N. C. *et al.* The ataxia telangiectasia mutated kinase controls Ig κ allelic exclusion by inhibiting secondary V κ -to-J κ rearrangements. *J. Exp. Med.* **210**, 233–9 (2013).
- Shiloh, Y. & Ziv, Y. The ATM protein kinase: regulating the cellular response to genotoxic stress, and more. *Nat. Rev. Mol. Cell Biol.* **14**, 197–210 (2013).
- Cheng, Q. & Chen, J. Mechanism of p53 stabilization by ATM after DNA damage. *Cell Cycle* **9**, 472–478 (2010).
- Hu, H. *et al.* Foxp1 is an essential transcriptional regulator of B cell development. *Nat. Immunol.* **7**, 819–826 (2006).
- Muljo, S. A. & Schlissel, M. S. A small molecule Abl kinase inhibitor induces differentiation of Abelson virus-transformed pre-B cell lines. *Nat. Immunol.* **4**, 31–7 (2003).
- Stadhouders, R. *et al.* Pre-B cell receptor signaling induces immunoglobulin κ locus accessibility by functional redistribution of enhancer-mediated chromatin interactions. *PLoS Biol.* **12**, e1001791 (2014).
- van Keimpema, M. *et al.* The small FOXP1 isoform predominantly expressed in activated B cell-like diffuse large B-cell lymphoma and full-length FOXP1 exert similar oncogenic and transcriptional activity in human B cells. *Haematologica* **102**, 573–583 (2017).
- Brown, P. J. *et al.* Potentially oncogenic B-cell activation-induced smaller isoforms of FOXP1 are highly expressed in the activated B cell-like subtype of DLBCL. *Blood* **111**, 2816–2824 (2008).
- Green, M. R., Gandhi, M. K., Courtney, M. J., Marlton, P. & Griffiths, L. Relative abundance of full-length and truncated FOXP1 isoforms is associated with differential NF κ B activity in Follicular Lymphoma. *Leuk. Res.* **33**, 1699–1702 (2009).
- van Keimpema, M. *et al.* The forkhead transcription factor FOXP1 represses human plasma cell differentiation. *Blood* **126**, 2098–2109 (2015).
- Chang, T.-C. *et al.* Transactivation of miR-34a by p53 broadly influences gene expression and promotes apoptosis. *Mol. Cell* **26**, 745–752 (2007).
- Navarro, F. & Lieberman, J. miR-34 and p53: New Insights into a Complex Functional Relationship. *PLoS One* **10**, e0132767 (2015).

21. Okada, N. *et al.* A positive feedback between p53 and miR-34 miRNAs mediates tumor suppression. *Genes Dev.* **28**, 438–450 (2014).
22. Rao, D. S. *et al.* MicroRNA-34a perturbs B lymphocyte development by repressing the forkhead box transcription factor Foxp1. *Immunity* **33**, 48–59 (2010).
23. Cerna, K. *et al.* MicroRNA miR-34a downregulates FOXP1 during DNA damage response to limit BCR signalling in chronic lymphocytic leukaemia B cells. *Leukemia* **33**, 403–414 (2019).
24. Bredemeyer, A. L. *et al.* ATM stabilizes DNA double-strand-break complexes during V(D)J recombination. *Nature* **442**, 466–470 (2006).

Supplement

Materials and methods

Mouse and human v-Abl cells

The v-Abl transformed mouse pre-B cell lines were generated from wild type (WT) (A70) and *Rag2*^{-/-} (R2K3) mice that harbor the E μ -Bcl2 transgene and were kindly provided by Dr. Craig Bassing (University of Pennsylvania School of Medicine, Philadelphia, PA). The cells were cultured in RPMI1640 (Life Technologies, Bleiswijk, The Netherlands) supplemented with 2 mM of L-glutamine, 100 U/ml penicillin, 100 μ g/ml streptomycin, and 10% FCS (Thermo Scientific, Waltham, MA) and 50 μ M 2-mercaptoethanol (2-ME, Sigma Aldrich, Burlington, MA). The human BCR-ABL+ B-ALL cell line BV173 was obtained from DSMZ (Braunschweig, Germany) and cultured in RPMI1640 (Life Technologies, Bleiswijk, the Netherlands) supplemented with 2 mM of l-glutamine, 100 U/ml penicillin, 100 μ g/ml streptomycin, 20% FCS. The following small-molecule inhibitors/activators were used: STI571 (imatinib methanesulfonate; LC Laboratories, Woburn, MA) to induce RAG1/2 expression in v-Abl cells and *IgI* recombination, the cells were treated with 5 μ M STI571 as previously established^{1,2}, KU55933 (ATM kinase inhibitor; Selleckchem, Houston, TX), Nutlin-3 (non-genotoxic p53 activator³, Sigma Aldrich), Z-VAD-FMK (carbobenzoxy-valyl-alanyl-aspartyl-[O-methyl]-fluoromethyl ketone; a pan-caspase inhibitor) (Promega, Madison, WI), Staurosporine (inductor of apoptosis through caspase-activation⁴) (Selleckchem).

Mouse primary B cells

ATM-deficient mice⁵ (Jackson Laboratory stock 002753) and TP53-deficient mice⁶ were provided by Dr. Stephen Jones (University of Massachusetts Medical School, Worcester, MA). RAG1-deficient VH81x IgH μ chain transgenic mice were provided by Prof. Dr. Rudi Hendriks (Erasmus Medical Center, Rotterdam, the Netherlands), C57BL/6 WT mice were housed in the animal research facility of the Academic Medical Center under specific pathogen-free conditions. Animal experiments were approved by the Animal Ethics Committee and performed in agreement with national and institutional guidelines. Bone marrow cells were harvested from 8- to 20-wk-old mice by flushing femurs and tibia. Total bone marrow cells were cultured in six-well plates in RPMI1640 with 2 mM of L-glutamine, 100 U/ml penicillin, 100 μ g/ml streptomycin, 10% FCS, 50 μ M 2-ME, 10 ng/ml recombinant mouse IL-7, and 10 ng/ml Flt3L (both from ProSpec, Ness-Ziona, Israel). The culture medium and cytokines were replaced every 3 days. Cells were harvested after 7–10 d and analyzed by flow cytometry, typically yielding > 95% B220⁺IgM⁺ progenitor cells (**Suppl Figure 1A**). To induce large to small pre-B cell transition, RAG1/2 expression, and *Igk* recombination, the cells were washed three times in culture medium without cytokines and placed back in six-well plates at 2×10^6 cells/ml in medium without cytokines (IL-7 withdrawal) (**Suppl Figure 1B**).

The formation of coding joints was assessed by qualitative PCR analysis of $V\kappa 6-23$ to $J\kappa 1$ rearrangement using previously published primers⁷. The PCR products were separated in 2% agarose gel containing ethidium bromide.

Exogenous DNA damage and p53 induction

DNA damage was induced by irradiating the cells (^{137}Cs), 5 Gy, 0.50 Gy/min) at a dose of 5 Gy. In some experiments, dose dependency was studied, in these cases, where indicated so, also a 0.5 Gy dose was applied. After γ -irradiation, the cells were allowed to recover for 2 h at 37°C in an atmosphere of 5% CO₂ and subsequently harvested. To study the effect on p53 activation without the genotoxic element, the cells were treated with Nutlin-3 by adding 2.5 μM of the compound into the cell culture and after 2h the cells were thoroughly washed and collected.

Western Blot

The protein pellets were homogenized passing through a 27G needle, and protein concentrations were measured using the bicinchoninic acid assay (Sigma-Aldrich). For each sample, 15 μg of protein lysate was used for protein separation in Precise 4–20% gradient Tris-SDS gels (Thermo Fisher Scientific). Subsequently, separated protein lysates were transferred onto polyvinylidene difluoride membranes (Immobilon-P; EMD Millipore, Burlington, MA); membranes were blocked in 5% BSA (BSA Fraction V, Roche Life Sciences, Almere, The Netherlands) in TBS-T or 5% milk in TBS-T for 2 h. Primary antibodies (Ab) were incubated overnight at 4°C. After a series of thorough washes with TBS-T, membranes were incubated with secondary Abs (goat anti-rabbit HRP or rabbit anti-mouse HRP; DAKO, Agilent Technologies, Heverlee, Belgium) for 2h at room temperature. Ab binding (protein expression) was visualized using Amersham ECL Prime Western blotting detection reagent (GE Healthcare Bio-Sciences AB, Uppsala, Sweden). The following Abs were used in this study: rabbit anti-RAG1 (D36B3), rabbit anti-FOXP1, rabbit anti-phospho-p53 (Ser¹⁵) (9284), rabbit anti-cleaved caspase-3 (Asp¹⁷⁵) (9661), rabbit anti-BCL6, rabbit anti- KU70 (D10A7), all from Cell Signaling Technology, Danvers, MA, rabbit anti-FOXP1 ab16645 (Abcam), and mouse anti- β -actin (C4) (EMD Millipore).

Real-Time quantitative PCR

The RNA isolation from the cells was performed using TRIreagent (Sigma-Aldrich) according to the manufacturer's protocol. MicroRNA isolation was performed using mirVana miRNA isolation kit (ThermoFisher) according to the manufacturer's protocol.

Levels of mRNA expression were determined using the CFX384 (Bio-Rad, Hercules, CA) real-time PCR platform. For each sample, cDNA was synthesized from 500 ng of RNA, using random primers (Promega) and Moloney murine leukemia virus reverse transcriptase (Invitrogen-Life Technologies, Bleiswijk, the Netherlands). For each sample, cDNA was

diluted 1:5 with PCR-grade water. The PCR master mix contained 5 μ l of Sso Fast EvaGreen supermix (Bio-Rad, Hercules, CA) and 0.5 μ l of 10 μ M reverse and forward primers (Biolegio, Nijmegen, the Netherlands). The final volume was adjusted to 9 μ l using PCR-grade water, to which 1 μ l of diluted cDNA was added. The following PCR conditions were used: initial denaturation at 95°C for 5 min, followed by 40 cycles of denaturation at 95°C for 15 s, annealing at 65°C for 5 s, and extension at 72°C for 10 s. The fluorescent product was measured by a single acquisition mode at 72°C after each cycle. For distinguishing specific from nonspecific products and primer dimers, a melting curve was obtained after amplification by holding the temperature at 65°C for 15 s followed by a gradual increase in temperature to 95°C at a rate of 2.5°C s⁻¹, with the signal acquisition mode set to continuous. For each cDNA preparation, PCRs were performed at least in duplicate, and for each condition, at least three independent experiments were performed. Expression of target gene mRNAs was normalized to the housekeeping genes large ribosomal protein PO (*RPLPO*) for human samples and 18S rRNA (*18S rRNA*) for mouse samples. Expression of miR-34a was assessed by Taqman MicroRNA assay and normalized to snoRNA429 (Applied; now ThermoFisher) as per manufacturer's protocol.

The following primers were used: mouse Rag1-forward (5'-AGCTATCACTGGGAGGCA-GA-3'), mouse Rag1-reverse (5'-GAGGAGGCAAGTCCAGACAG-3'), mouse Rag2-forward (5'-CTTCCCAAGTGCTGACAAT-3'), mouse Rag2-reverse (5'-AGTGAGAAGCCTGGCT-GAAT-3'), mouse Foxp1-forward (5'-AGTCATGATGCAAGAATCTGGGT-3'), mouse Foxp1-reverse (5'-TCTCCGTTGGACCGAGTGTCAG-3') mouse 18S rRNA-forward (5'-TGGTGGAGG-GATTTGTCTGG-3'), and mouse 18S rRNA-reverse (5'-TCAATCTCGGGTGGCTGAAC-3'). The data were analyzed in GraphPad, on figures expressed as mean \pm SD, ANOVA statistical analysis was used for multiple comparisons with the alpha threshold of 0.05. Where data are compared as fold induction/reduction against a control group, a non-parametric Kruskal-Wallis test was used with the alpha threshold set to 0.1 due to a low number of repeats.

FACS

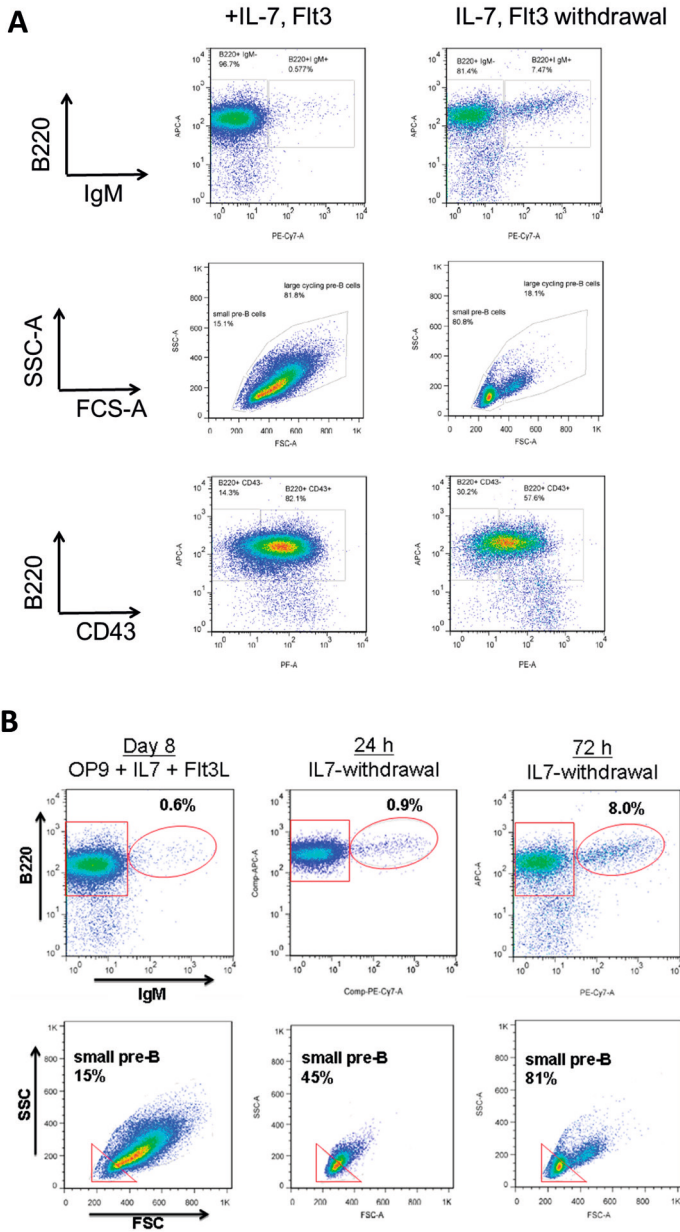
Flow-cytometry stainings and analyses were performed according to the protocol as described earlier⁸. Briefly, 1x10⁶ cells were washed 2x with 2mL of cold FACS buffer (1x PBS + 0.2% NaN₃ + 1% FCS) and spun at 1100 rpm for 5 minutes. After the addition of the antibodies, the cells were incubated on ice in the dark for 30min and then washed again with the cold FACS buffer. Next, the cells were resuspended in 1 mL 1x PBS + 1% paraformaldehyde and incubated for 5 minutes at room temperature. Finally, the cells were spun at 1100rpm and re-suspended again in 400 μ L of FACS buffer. The doublets were excluded based on forward and side scatter height versus width profiles. Flow cytometry was performed on a four-laser, thirteen-detector LSR Fortessa (BD Biosciences). Flow cytometry data were analyzed using FlowJo (Tree Star Inc., Ashland). The following antibodies were used to

perform the stainings: rat-anti-mouse CD45R/B220 (BD Pharmingen, San Diego, CA, clone RA3-682) rat-anti-mouse CD43(BD Pharmingen, clone S7), rat-anti-mouse Ig kappa light chain (BD Pharmingen, clone 187.1), rat-anti-mouse IgM (eBioscience, San Diego, CA, clone II/41), rat-anti-mouse IgD (Southern Biotech, Birmingham, AL, clone 11-26), rat-anti-mouse CD49b (BD Pharmingen, clone DX5), rat-anti-mouse Ly-6C (BD Pharmingen, clone AL-21).

Retroviral transductions

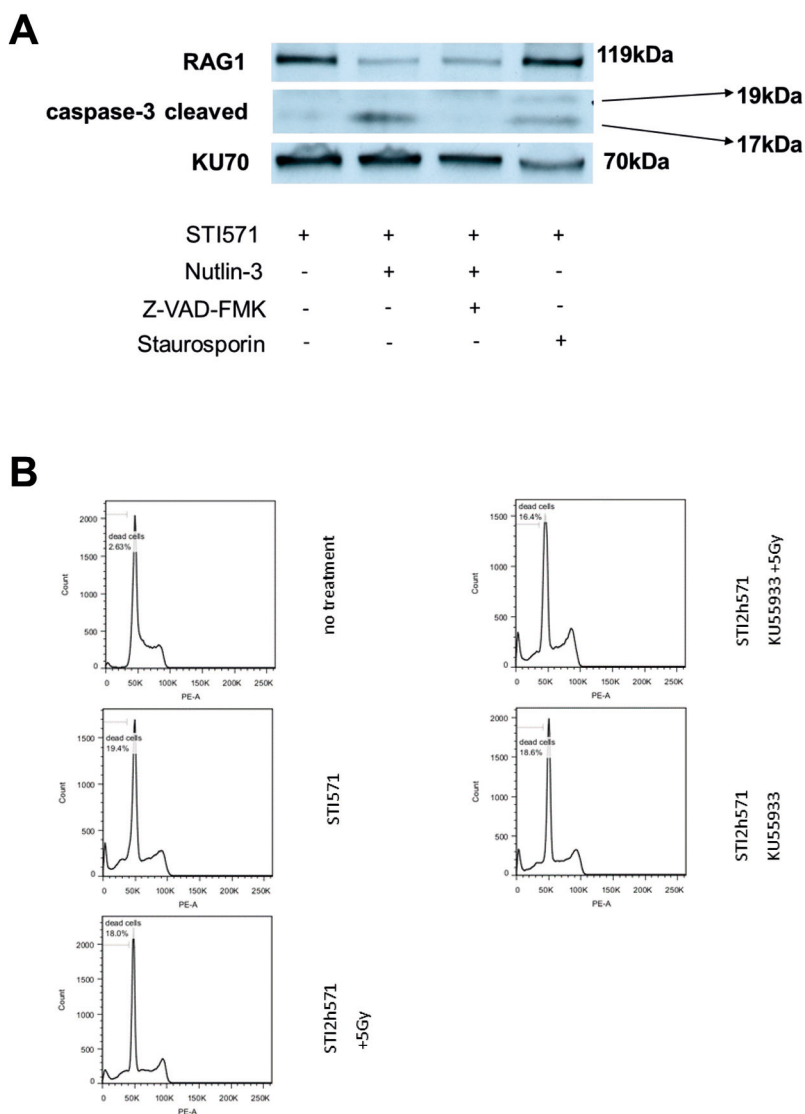
LZRS-FOXP1-IRES-YFP (FOXP1 FL) and LZRS-BCL6-IRES-GFP (BCL6) were generated as previously described^{9,10}. A FOXP1-iso construct that starts translation from the second coding ATG (in exon 6; M101), encoding a 100 AA N-terminally deleted FOXP1, was PCR-cloned and subcloned into LZRS-IRES-YFP (FOXP1 iso). Cells transduced with an empty LZRS-IRES-YFP were used as a control.

The pCL-ECO-miR-34a-sponge and pCL-ECO-scrambled were kindly provided by Dr. J. Kluiver, University Medical Center Groningen, The Netherlands. The viral transductions were performed as previously described⁹⁻¹¹. Transduced cells were FACS-sorted based on GFP expression 5 d after transduction.



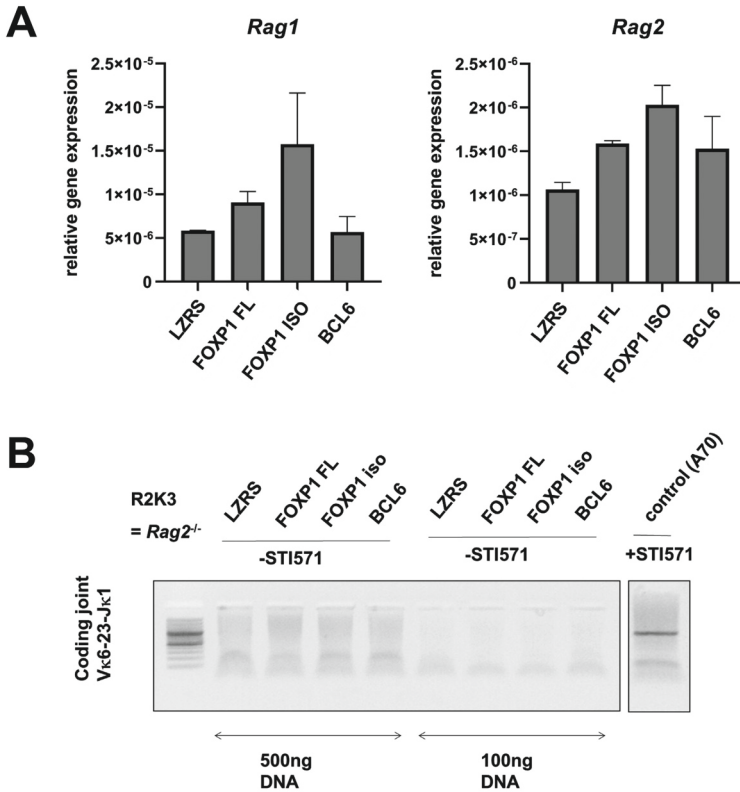
Supplemental Figure 1.

(A) Depiction of the gating strategy used to determine the amount of IgM⁺ cells after they have undergone successful V(D)J rearrangement. Primary WT bone marrow cells were cultured for 7 days on OP9 feeder cells, Flt3L, and IL7. Under these conditions on day 7, the cells acquire pro-to-pre B-cell phenotype assessed by FACS staining with B220-APC, CD34-PE, and IgM-PE/Cy7. On average 0.5% of the pre-B cells at this stage are IgM⁺ (B), 72 hours following the IL7 and Flt3L withdrawal, the portion of IgM⁺ cells increases to an average of 8%.



Supplemental Figure 2.

(A) Western Blot staining of RAG1, cleaved caspase-3 and KU70, used as a housekeeper, in BV173 cells, treated first with STI571 for 24 hours to induce RAG1/2 expression and *Igκ* recombination. Then, the cells split into 4 groups, a control group, a group treated with p53 stabilizer Nutlin-3 (2.5 μ M) for 4 hours, a group treated simultaneously with Nutlin-3 (2.5 μ M) and the pan-caspase inhibitor Z-VAD-FMK (50 μ M) for 4 hours and a group treated with caspase-activator Staurosporine (200nM) for 4 hours. **(B)** FACS staining for propidium iodide showing the % of sub-G1 cells, defined as dead cells, in mouse v-Abl WT cells (A70) treated initially for 72 hours with STI571 to induce RAG1/2 expression and *Igκ* recombination. After 72 hours, the cells were either subjected to 5Gy γ -irradiation and left to recover for 2 hours or pre-treated with ATM inhibitor KU55933 for 2 hours prior to the γ -irradiation or treated for 4 hours with KU55933 with no irradiation. The DMSO-treated group was taken as a control.

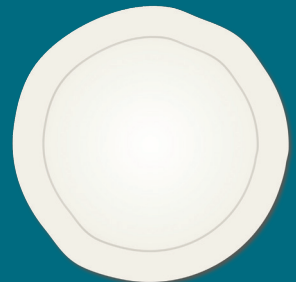
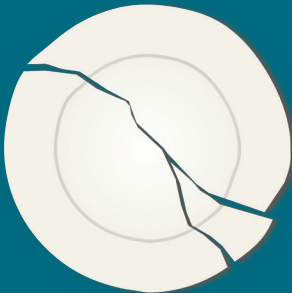
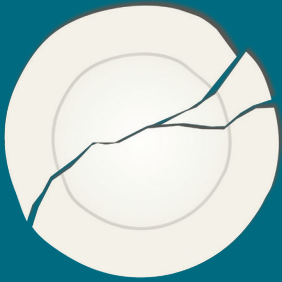


Supplemental Figure 3.

(A) *Rag1* and *Rag2* mRNA expression measured by RT-PCR in mouse v-Abl WT cells (A70) transduced with either empty vector (LZRS), human full-length FOXP1 (FOXP1 FL), the isoform of human of FOXP1 (FOXP1 iso) or human BCL6. The transduced cells were not treated with STI571, therefore this expression reflects the *Rag1* and *Rag2* mRNA expression before the alleviation of the developmental block at the pre-to-pre-B cell stage. ($n=2$, mean \pm SD, * $p<0.05$). (B) *Rag2*^{-/-} mouse v-Abl cells were transduced with either empty vector (LZRS), human full-length FOXP1 (FOXP1 FL), the isoform of human of FOXP1 (FOXP1 iso) or human BCL6, the formation of coding joints was assessed by qualitative PCR of V κ 6-23 to J κ 1 joint, using 100ng and 500ng DNA, showing that the absence of a PCR product is not a result of too little DNA input in the PCR reaction. Control mouse WT v-Abl cells (A70) were treated with STI571 to induce RAG1/2 expression and recombination at *Ig* κ . The PCR products were run in 2% agarose gel containing ethidium bromide.

Supplemental references

1. Pegoraro, L. *et al.* Establishment of a Ph1-positive human cell line (BV173). *J. Natl. Cancer Inst.* **70**, 447–53 (1983).
2. Muljo, S. A. & Schlissel, M. S. A small molecule Abl kinase inhibitor induces differentiation of Abelson virus-transformed pre-B cell lines. *Nat. Immunol.* **4**, 31–7 (2003).
3. Shen, H. & Maki, C. G. Pharmacologic activation of p53 by small-molecule MDM2 antagonists. *Curr. Pharm. Des.* **17**, 560–568 (2011).
4. Chae, H. J. *et al.* Molecular mechanism of staurosporine-induced apoptosis in osteoblasts. *Pharmacol. Res.* **42**, 373–381 (2000).
5. Barlow, C. *et al.* Atm-deficient mice: a paradigm of ataxia telangiectasia. *Cell* **86**, 159–171 (1996).
6. Donehower, L. A. *et al.* Mice deficient for p53 are developmentally normal but susceptible to spontaneous tumours. *Nature* **356**, 215–221 (1992).
7. Bredemeyer, A. L. *et al.* ATM stabilizes DNA double-strand-break complexes during V(D)J recombination. *Nature* **442**, 466–470 (2006).
8. Ochodnicka-Mackovicova, K. *et al.* NF- κ B and AKT signaling prevent DNA damage in transformed pre-B cells by suppressing RAG1/2 expression and activity. *Blood* **126**, 1324–1335 (2015).
9. van Keimpema, M. *et al.* The forkhead transcription factor FOXP1 represses human plasma cell differentiation. *Blood* **126**, 2098–2109 (2015).
10. van Keimpema, M. *et al.* The small FOXP1 isoform predominantly expressed in activated B cell-like diffuse large B-cell lymphoma and full-length FOXP1 exert similar oncogenic and transcriptional activity in human B cells. *Haematologica* **102**, 573–583 (2017).
11. van Keimpema, M. *et al.* FOXP1 directly represses transcription of proapoptotic genes and cooperates with NF- κ B to promote survival of human B cells. *Blood* **124**, 3431–3440 (2014).



CHAPTER
General discussion

7

General discussion

The adaptive immune system is characterized by its ability to mount specific responses against pathogens, mediated by lymphocytes and antigen-presenting cells. B cells produce antibodies and use B-cell receptors (BCR, also termed antigen receptor or immunoglobulin) to recognize and eliminate pathogens, damaged or non-self cells; these responses are called humoral immunity. T cells also use specific receptors— T-cell receptors (TCR) to eliminate foreign antigens in responses that constitute the cellular adaptive immunity. To generate a diverse array of antigen receptors, a sophisticated system of somatic gene recombination called V(D)J recombination is employed, in which the V (variable), D (diversity), and J (joining) segments of the immunoglobulin chains are reorganized to form a new sequence. The process of gene recombination, specific for B and T cells, is initiated by the recombination activating gene 1 and 2 (RAG1/2) endonuclease complex, introducing DNA breaks at recombination signal sequences (RSS), specific sequences that flank the recombining gene segments within the immunoglobulin (*Ig*) and *Tcr* loci. During V(D)J recombination additional variability at junctions of coding segments is introduced by terminal deoxynucleotidyl transferase (TdT), further increasing receptor diversity¹. However, due to the introduction of DNA breaks during the V(D)J recombination, this intricate system poses a risk to genome integrity. The stringent and well-orchestrated control of the RAG1/2 complex during B-cell development ensures minimization of the unintended damage caused by the RAG1/2 complex while allowing the formation of functional BCR necessary for B-cell maturation. Acute lymphoblastic leukemia (ALL) is a type of blood cancer characterized by the rapid expansion of malignant B- or T-cell precursors. Genomic instability is the hallmark of ALL, including the *ETV6-RUNX1*, *BCR-ABL1*, and *E2A-PBX1* translocations². Footprints of RAG1/2 activity, such as insertion of N-nucleotides, or presence of sequences resembling RSS, were found in the proximity of genomic lesions in both mouse and human B-cell malignancies, including ALL. This implicates aberrant RAG1/2 targeting and/or activity in the development of lymphoid malignancies. A thorough understanding of the mechanisms governing the (mis)-regulation and the (mis)-targeting of RAG1/2 within the genome may offer insights into the molecular pathogenesis of pre-B-cell malignancies.

Key findings of this thesis:

1. The RAG1/2 endonuclease complex is able to introduce DNA breaks outside of the *Ig* loci in mouse developing B cells. Using a genome-wide approach, RAG-dependent DNA breaks were mapped in the mouse genome. The motif analysis revealed that simple repeat sequences and GC-rich regions were identified in the proximity of the RAG1/2-dependent DNA breaks. The simple repeat sequences and GC-rich regions are known to form alternative DNA structures. We propose that in the genome-wide context, such structures are targeted by the RAG1/2 endonuclease complex. **(Chapter 3)**
2. DNA breaks trigger a negative feedback loop that limits RAG1/2 expression in developing B cells. In response to external and RAG1/2-derived DNA damage in pre-B cells, the DNA damage sensor ataxia telangiectasia mutated (ATM) negatively regulates the RAG1/2 transcription factor forkhead box protein O1 (FOXO1), resulting in downregulation of RAG1/2. This describes how DNA breaks, which result from the activity of RAG1/2, control the expression of RAG1/2. **(Chapter 4)**
3. Several layers of regulation ensure genome stability by restricting RAG1/2 activity to the G1 cell cycle phase in developing lymphocytes. In proliferating pre-B cells, RAG1/2 expression and activity are suppressed, preventing collateral DNA damage. We identified a novel regulatory mechanism suppressing RAG1/2 in proliferating pre-B cells. The nuclear factor kappaB protein (NF- κ B) and phosphoinositide-3 kinase (PI3K/AKT) signaling pathways suppressed RAG expression in cycling mouse and human pre-B cells. Inhibition of NF- κ B resulted in increased RAG expression, and recombination activity, and led to RAG-dependent DNA damage in proliferating pre-B cells. **(Chapter 5)**
4. DNA breaks trigger the DNA damage response (DDR) with the tumor suppressor p53 being a central downstream molecular mediator. We have identified a novel regulatory pathway in which activation and stabilization of p53 suppressed RAG expression in mouse pre-B cells. This regulatory mechanism involved the p53 target miR-34a and the RAG1/2 transcription factor forkhead box protein P1 (FOXP1). We propose that in this way the DNA breaks limit RAG1/2 expression, thus protecting the pre-B cell genome stability. **(Chapter 6)**

RAG1/2 off-target DNA cleavage in developing B cells

During B-cell development, gene recombination follows a specific order of events to ensure the creation of a diverse repertoire of immunoglobulins. Initially, the immunoglobulin heavy chain (*Igh*) locus undergoes recombination, where V(D)J gene segments

rearrange to form the hypervariable parts of the BCR/antibody heavy chain. This is followed by the expression of the pre-B cell receptor complex consisting of the rearranged *Igh* and a surrogate light chain. Once the *Igh* locus has successfully rearranged, it becomes inaccessible, thereby preventing multiple productive locus recombinations. Subsequently, the immunoglobulin light chain (*Igl*) loci recombine and give rise to the hypervariable parts of the BCR/antibody light chain. In this process, immunoglobulin kappa light chain (*Igκ*) locus recombinations precede immunoglobulin lambda light chain (*Igλ*) locus recombinations³. RAG1/2 complex is targeted to RSS sequences in the genome, consisting of conserved heptamer and nonamer sequences separated by a less conserved spacer sequence⁴. The location of the RSSs is primarily adjacent to the variable (V), diversity (D), and joining (J) gene segments of (*Ig*) and *Tcr* loci, restricting RAG1/2 activity to these segments. However, sequences that resemble RSS, so-called cryptic RSS (cRSS), were identified throughout the mouse and human genomes. The presence of cRSS has been observed near the recurring genomic lesions in leukemia patients, thereby implicating the participation of RAG1/2 in the formation of the genomic lesions⁵⁻⁷.

In **Chapter 3** we investigated on a genome-wide scale, whether the RAG1/2 recombinase complex is able to introduce double-stranded DNA breaks (DSBs) in regions outside of the *Ig* loci. We used the Nijmegen breakage syndrome 1 (NBS1) protein as a surrogate marker for DSBs. NBS1 binds to DSBs as a part of the Mre11-Rad50-NBS1 (MRN) complex, which is integral to the recognition and repair of DSBs. NBS1 recognizes and binds to the broken DNA ends, acting as a sensor of DNA damage⁸. In our study, the RAG off-target activity was assessed by differential binding of NBS1 to DNA in RAG-proficient and RAG2-deficient v-Abl-transformed cell lines, lacking Artemis which is indispensable for hairpin opening formed after the DNA is nicked. In the absence of Artemis, the DSBs cannot be resolved and accumulate. This is an important feature of the experimental cell system, which we leveraged in our study to increase the resolution of the off-target RAG-induced DNA breaks that would have otherwise been resolved and repaired. The v-Abl in the used cell lines introduces a developmental block, arresting the cells in the pro-to-pre-B cell stage. At this stage, the *Igl* is still in the germline configuration. Treatment with Abelson-kinase inhibitors, such as STI571 (imatinib) alleviates this block, whereupon the cells begin to express RAG1, RAG2 and the gene recombination of the *Igl* is initiated⁹. This model system enables the examination of DSBs in the chromosomal context of living pre-B cells undergoing *Ig* recombination. The use of NBS1 chromatin immunoprecipitation (ChIP) followed by massive parallel sequencing (ChIP-Seq) to detect DSBs has been validated and employed previously to study activation-induced cytidine deaminase (AID)-dependent DNA breaks on a genome-wide scale in splenic B cells activated to undergo *Ig* class switch recombination¹⁰.

In our study, we have identified 1489 putative RAG1/2 DSBs throughout the genome in mouse v-Abl cells, with a clear accumulation of the RAG1/2-dependent NBS1 signals at

chromosome 6 at the *Ig* loci, which we used as a positive control. In our study we did not identify RAG1/2-dependent NBS1 binding sites at the genes or breakpoints frequently seen translocated or deleted in B-ALL patients, such as *ETV6/RUNX1*, *BCR/ABL1* or *E2A*, early B-cell factor 1 (*EBF1*), lymphoid enhancer-binding factor-1 (*LEF1*), IKAROS family zinc finger 1 (*IKZF1*) and IKAROS family zinc finger 3 (*IKZF3*)^{11–13}. We hypothesize that differences between murine and human chromatin configuration might account for this observation. In addition, the employed cell lines already harbor a transforming element (i.e. *v-Abl*), which could change the accessibility of genes. Though the most “obvious suspects” were not implicated in our study, we have detected RAG1/2-dependent DNA breaks in the proximity of several other genes previously associated with B-cell malignancies in mouse and/or human. For instance, in the proximity of *Klf4*, previously shown to be a putative tumor suppressor in pre-B cells and B-cell malignancies¹⁴, in the proximity of *Abl2* which, next to the frequently rearranged *ABL1*, has also been reported to be rearranged in some cases of high-risk B-ALL¹⁵; or in the proximity of MADS box transcription enhancer factor 2 (*Mef2c*). The enforced overexpression of MEF2C resulted in lymphoid tumors co-expressing CD3 and CD19, resembling the human phenotype of mixed ALL¹⁶.

The group of David Schatz (Yale University, New Haven, CT) has previously demonstrated that RAG1 and RAG2 can bind DNA throughout the genome and suggested that their DNA cleaving activity may not be restricted to canonical RSS sequences. In one of their studies, RAG1 was found to bind to approximately 3400 RAG1 binding sites in mouse pre-B cells, and around 18300 RAG2 binding sites throughout the genome of mouse pre-B cells. The binding of RAG1 and RAG2 however, did not correlate with the presence of spontaneous RAG-dependent translocations, concluding that *in vivo* such events must be rare¹⁷. When we compared our data with the publicly available data from the aforementioned study, we found only around 3% overlap between the RAG1 binding sites, as identified by the Schatz lab, and our RAG1/2-dependent NBS1 binding sites. This rather low overlap can be attributed to the use of different cell systems— primary mouse pre-B cells as compared to the *v-Abl*-transformed pre-B cells used in our study. Also, it is important to emphasize that the study of the Schatz lab mapped RAG1 and RAG2 binding to DNA, while our study mapped the DSBs resulting from RAG1/2 activity on the genome-wide scale. It is unknown to what extent the binding of RAG1 and RAG2 to chromatin results in the formation of DSBs. The overlap between the RAG1 or RAG2 binding profile and the RAG-dependent NBS1 binding profile within one cell system has not been studied yet, opening up possibilities for follow-up investigations of actual the extent, to which the binding of RAG to DNA effectively results in DSBs.

Next, we examined the NBS1 binding pattern in more detail and aimed to identify common denominators of the RAG-mediated NBS1 binding sites. What makes these sequences RAG (off) targets? In the mouse *v-Abl* pre-B cell line used in our study, *v-Abl* transformation was shown to arrest the developing B cells at the pro-to-pre B-cell stage,

where the *Igh* recombination already took place while the *Igl* are still in their germline configuration. An accumulation of RAG-specific NBS1 peaks was observed at the *Igk* locus, as expected. However, we also observed an accumulation of RAG1/2-dependent DNA breaks at the *Igh* heavy chain (*Igh*) locus on chromosome 12. The abundant binding of RAG1/2-dependent NBS1 to *Igh* suggests concomitant induction of RAG1/2-mediated DNA breaks at *Igh* and *Igl*, potentially breaching the concept of strictly serial fashion of gene recombination¹⁸. Some earlier studies propose that while v-Abl transformed cells are able to initiate gene recombination, they fail to terminate the process. Perhaps due to the v-Abl presence, which antagonizes the pre-B cell receptor (pre-BCR) signaling and causes the pre-B cells with one functional *Igh* allele to persistently transcribe and rearrange the non-recombined allele^{19,20}. Another explanation for the continuous presence of RAG-dependent NBS1 binding to *Igh* could come from the previous work on “receptor editing” showing that functional B-cell receptors can re-engage in further recombination. This may result in the editing of the receptor’s specificity, allowing the cells with auto-reactive B-cell receptors to escape elimination²¹.

The discovery that human and mouse genomes are densely populated with sequences that resemble RSS, so-called cryptic RSS^{22,23}, begs the question of whether the RAG1/2 recombinase complex is able to target and cleave such sequences in regions outside of the *Ig* loci. Several studies have demonstrated that in extrachromosomal assays RAG1/2 was able to cleave cRSS, and similar observations were made in a v-Abl pre-B cell lines transformed with constructs containing cRSS-substrates^{24,25}. However, the evidence for RAG1/2 off-target activity on the chromatin in living cells is challenging to capture. We investigated the presence of RSS motifs in the proximity of the RAG-dependent NBS1 binding sites and found enrichment for canonical RSS around the NBS1 peaks at the *Igk* locus, which served as a positive control. Outside of the *Ig* loci, in the 500-1000bp proximity to RAG-dependent NBS1 binding sites, we observed an enrichment for nonamers, but not for heptamers. Similar observations were made in another study that showed an enrichment for nonamers, but not heptamers in the proximity of RAG1 binding sites in mouse v-Abl cell lines and in mouse thymocytes¹⁷. We have also examined the presence of several selected cRSS^{26,27} in the proximity of RAG-dependent NBS1 binding sites but found no enrichment (unpublished data, data not shown). However, there are hundreds of possible cRSS sequences, therefore a more systematic approach to investigating the cRSS enrichment around RAG-dependent DNA breaks would be more appropriate in a follow-up study.

In addition to the RSS motif analysis, we performed an unsupervised motif analysis to determine if there are any other motifs enriched in the vicinity of the RAG-dependent NBS1 binding sites. The motifs we have identified were predominantly zinc-finger-binding sequences, abundant in eukaryotic cells. Intriguingly, several of these motifs corresponded to known binding sites of proteins such as PR domain zinc finger protein 9 (PRDM9), early

growth response 1 (EGR1), or Ras responsive element binding protein 1 (RREB1)²⁸⁻³⁰, as well as modulators of p53 signaling and apoptosis, such as POZ/BTB And AT Hook Containing Zinc Finger 1 (PATZ1) or specificity protein 1 (SP1)^{31,32}. PRDM9 is a zinc finger protein with histone methyltransferase activity, catalyzing the methylation of lysine (K) 4 of the H3 histone (H3K4me3), primarily during meiosis³³. Interestingly, the H3K4me3 histone epigenetic mark was associated with open chromatin configuration and with transcriptionally active promoters of genes regulating cell growth, cell migration, or angiogenesis, all of which makes H3K4me3 an important regulator in cancer immunity^{34,35}. EGR1 is a zinc-finger transcription factor regulating cell growth, differentiation and participating in the regulation of B-cell development³⁶. Another identified motif was linked to the MYC-associated zinc-finger protein (MAZ), a transcription factor known to regulate the expression of MYC oncogene and affect the large-scale genome organization through its interaction with cohesins^{37,38}. The off-target RAG activity in the aforementioned regions poses a potential threat of introducing a genomic lesion in these genes, making pre-B cells susceptible to malignant transformation.

Another recurrent motif type observed in our study was simple dinucleotide sequence repeats, such as CA and GA or TA repeats. Our supervised motif analysis of the CA and GA repeats revealed strong enrichment in the regions 500-1000bp around (5' and 3') RAG-dependent NBS1 peaks. Naturally occurring repetitive sequences have been demonstrated to assume non-canonical DNA structures, so-called non-B DNA. These structures include G-quadruplexes, which are guanine-rich sequences, H-DNA which are mirrored repeats of oligopurine sequences forming triplex DNA, Z-DNA which are AT/GC-rich sequences, or cruciform and other hairpin-forming DNA structures. Such structures are known for adopting an open chromatin configuration and for affecting DNA replication and transcription, which makes them more susceptible to genomic instability^{39,40}. In the context of hematological malignancies, non-B DNA structures were observed in the proximity of the breakpoints of the hallmark genomic lesions. For instance, in Burkitt's lymphoma and in mouse t(12;15) BALB/c plasmacytomas, H-DNA forming regions have been identified near the breakpoints of the translocated *c-myc* locus. The presence of non-B DNA structures has also been demonstrated in the proximity of the major breakpoint region (Mbr) of Bcl-2 in follicular lymphoma⁴¹. Notably, RAG1/2 has exhibited the ability to cleave non-B DNA structures in the absence of RSS, acting as a structure-specific endonuclease. In fact, CA repeats were shown to mimic cRSS with their nonamer and heptamer elements, and have been identified as specific targets of RAG1/2 activity. Consequently, RAG1/2 inadvertently introduced DNA breaks at CA-rich sites^{42,43}. In addition, a more recent study highlighted the essential role of the zinc-binding domain (ZnC2) of RAG1 in its binding to non-B DNA structures. Mutations in the ZnC2 domain have been found to impede the RAG's nicking capacity on DNA G-quadruplexes and on the single-stranded DNA regions⁴⁴.

In summary, we demonstrated that RAG1/2 can introduce DNA breaks in non-*Ig* regions. While the previous studies implicated RAG1/2 activity in the formation of genomic lesions based on the composition of the breakpoint sequences and *in-vitro* cleavage assays, our study provides more specific evidence for RAG1/2 activity outside of the *Ig* loci and maps the genome-wide location of RAG-dependent DNA breaks in mouse *v-Abl* pre-B cell line. The presence of simple sequence repeat motifs, especially CA and GA repeats, and GC-rich regions around RAG-dependent NBS1 peaks may reflect the affinity of the RAG's off-target activity to non-B DNA structures.

DNA breaks are important regulators of RAG1/2 expression and activity

In B-ALL, numerous secondary genetic events bear characteristics arising from aberrant RAG activity, implicating RAG as a key contributor to genomic instability. Aberrant RAG activity also plays a role in the sub-clonal diversification of B-ALL, leading to the emergence of therapy-resistant subclones^{45,46}. Despite available insights into the regulation of *Ig* gene recombination, regulation of RAG1/2 in pre-B cells exposed to excessive DNA damage remains poorly understood. In normal B-cell development, pre-B cell proliferation and RAG expression/activity are strictly separated, maintaining genomic stability. This separation is upheld by multiple layers of regulation, which may be disrupted in proliferating leukemic cells expressing RAG continuously.

In **Chapter 4** we showed that in pre-B cells undergoing V(D)J recombination, *Rag1* and *Rag2* mRNA and protein expression rapidly respond to genotoxic stress induced by DSBs. DNA breaks activate ATM, a protein kinase that plays a crucial role in cellular responses to DNA damage⁴⁷. ATM acts as a sensor of DSBs and orchestrates activation of signaling pathways, such as checkpoint kinase 2 (CHK2), p53, and breast cancer 1 (BRCA1), which in turn regulate processes like DNA repair, cell cycle checkpoint activation, and apoptosis. In the context of pre-B cells, ATM ensures the fidelity of this process by coordinating the repair of DSBs introduced during V(D)J recombination, thereby preventing genomic instability and the potential development of leukemia or lymphoma. In our study, treatment of mouse pre-B cells, undergoing light chain recombination, with ionizing radiation mimetic neocarzinostatin (NCS), resulted in ATM autophosphorylation at Ser¹⁹⁸¹ and RAG downregulation. The ATM autophosphorylation at Ser¹⁹⁸¹ has previously been shown to stabilize ATM at the site of the DSBs and it is required for proper DNA damage response (DDR)⁴⁸. In our study, we demonstrated an efficient activation of ATM/DDR following the NCS treatment. The pre-treatment with an ATM kinase inhibitor prevented the NCS-induced RAG downregulation. In addition, RAG levels in pre-B cells derived from *Atm*^{-/-} mouse bone marrow did not respond to NCS treatment.

RAG2 was shown to accumulate in the G1 phase of the cell cycle, but it degraded quickly when the cell entered the G1-S transition and the levels remained low until the

next G1 phase. RAG2 regulation at the G1-S transition has been attributed to cyclin-A/cyclin-dependent kinase 2 (CDK2) which phosphorylates RAG2 at Thr490. This facilitates the formation of an S-phase kinase-associated protein 2 (SKP2) binding site, which ultimately results in ubiquitylation and degradation of RAG2^{49,50}. While CDK2 was shown to trigger proteasomal degradation of RAG2, RAG1 stability appears independent of the cell cycle⁵¹⁻⁵³. Interestingly, we observed that DNA damage negatively affects the protein stability of RAG1, as in human v-Abl transformed pre-B cells co-treatment with NCS and the protein synthesis inhibitor cycloheximide (CHX) shortened the RAG1 half-life as compared to CHX-only treatment. The N-terminus of RAG1 contains a functional E3 ubiquitin ligase domain called Really Interesting New Gene (RING)⁵⁴, which is known to catalyze the ubiquitination of H3, but also of RAG1 itself^{55,56}. Recently, it was discovered that mouse mutants carrying P326G mutation in the RAG1 RING domain accumulate RAG1 protein, probably due to the inability to degrade RAG by autoubiquitylation⁵⁷. We further demonstrated that the DNA damage-induced RAG1 protein downregulation cannot be attributed to damage-induced caspase cleavage, leaving the mechanism of the DNA damage-induced shortened RAG1 protein half-life incompletely understood with an open possibility for ubiquitin-mediated regulation. Recently, the Swanson group reported that VprBP/DCAF1, functioning as a substrate adaptor within the cullin-RING E3 ubiquitin ligase 4 (CRL4) ubiquitin ligase complex, plays a crucial role in regulating the levels of RAG1 protein in murine B cells, facilitating the turnover of RAG1. *In vivo* depletion of VprBP/DCAF1 leads to increased expression of RAG1, resulting in excessive V(D)J recombination and a skewed repertoire of Ig light chains^{58,59}. It is therefore conceivable that a part of the DNA damage-induced rapid loss of RAG1 protein is conveyed by a reduction of RAG1 protein stability. However, whether VprBP/DCAF1 responds to DNA damage and whether it could be the missing link for a mechanistic explanation of DNA damage-induced reduction in RAG1 protein stability is yet to be investigated.

The regulation of *Rag1* and *Rag2* gene transcription involves various transcription factors binding to cis-acting sequences, mainly FOXO1 and FOXO1 binding the *Erag* enhancer, inducing RAG1 and RAG2 expression during B-cell development^{60,61}. We therefore investigated whether the DNA damage-induced RAG1/2 downregulation is linked to transcriptional regulation by FOXO1. Our study shows that DNA damage abolished FOXO1 binding to *Erag* enhancer, and that the ATM kinase inhibition is able to restore the FOXO1 binding to *Erag*, linking both ATM and FOXO1 to the DNA damage-induced downregulation of RAG1. Moreover, we found that DNA damage-activated ATM phosphorylated at Ser¹⁹⁸¹ was bound to *Erag*, possibly locally releasing FOXO1 from binding to *Erag*. Specifically, the phosphorylation of FOXO1 on Ser²¹⁵ has previously been shown to be required for FOXO1 binding to *Erag*, and the FOXO1 Ser²¹⁵ phosphorylation was demonstrated to be dependent on MAPK-activated protein kinase (MAPKAPK5)⁶². We could not investigate the effect of DNA damage on FOXO1 Ser²¹⁵, nor its binding to *Erag*, due to the unavailability of reagents

specifically recognizing the phosphorylation of the Ser²¹⁵ residue of FOXO1. However, in our study, we found that DNA damage did not have any effect on MAPKAPK5 protein levels. We further hypothesized that the activated ATM may possibly recruit other proteins that are able to modulate the stability of FOXO1. For instance, it has been demonstrated that silent information regulator 2 (Sir2) binds and deacetylates FOXO1 at Lys²⁴², Lys²⁴⁵, and Lys²⁶² residues acetylated by cAMP-response element-binding protein (CREB)-binding protein (CBP)⁶³. The acetylation of FOXO1 results in decreased DNA binding and expression of FOXO1 target genes⁶⁴. In addition, in response to DNA damage, ATM was shown to inhibit SIRT1, the mammalian Sir2 orthologue⁶⁵. We therefore speculate that upon induction of DNA damage, ATM might inhibit SIRT1, leading to increased FOXO1 acetylation, and consequently decreased FOXO1 DNA-binding capacity, thereby reducing the expression of *Rag1* and *Rag2* mRNA. However, our data did not convincingly show that DNA damage affected FOXO1 acetylation in a human BCR-ABL1⁺ pre-B-cell line after NCS exposure.

To further provide a mechanistic explanation of how FOXO1 regulates RAG1/2 expression in pre-B cells, we investigated signaling pathways involved in the regulation of FOXO1. The PI3K/AKT pathway plays a pivotal role in regulating the activity of the transcription factor FOXO1. In response to pre-B cell receptor (pre-BCR) signals, AKT phosphorylates FOXO1 at Ser²⁵⁶. Phosphorylation at this residue by AKT leads to the nuclear exclusion and subsequent degradation of FOXO1, inhibiting its transcriptional activity and preventing the expression of its target genes. Additionally, AKT can phosphorylate other serine and threonine residues on FOXO1, contributing to the regulation of FOXO1 activity in response to signaling through the PI3K/AKT pathway⁶⁶. In our study, we observed that DNA damage resulted in ATM-dependent phosphorylation of AKT at Ser⁴⁷³. In response to DSBs, ATM-dependent AKT activation was shown to be critical for downstream transmission of signals to extracellular signal-regulated kinase (ERK), thereby triggering either cell proliferation and survival, or apoptosis, depending on the extent of the DNA damage⁶⁷. Moreover, we found other downstream AKT targets⁶⁸ to be phosphorylated in response to NCS-induced DNA damage, such as mTOR on Ser²⁴⁴⁸. We therefore hypothesized that PI3K/AKT might play a role in DNA damage-induced downregulation of RAG. However, contrary to our hypothesis, AKT inhibition failed to prevent the DNA damage-induced downregulation of RAG. We used 2 different small-molecule AKT inhibitors (GSK690693 and AKT inhibitor VIII), none of which was able to prevent the damage-induced RAG downregulation. In addition, overexpression of the dominant-negative kinase-dead mutant of AKT did not prevent the NCS-induced RAG downregulation either. Though under circumstances that do not involve exposure to DNA damage, the PI3K/AKT pathway has been shown to modulate RAG expression in developing B cells⁶⁹, we conclude that the DNA damage-induced downregulation of RAG in pre-B cells is not mediated through AKT signaling. In addition to AKT, we investigated the effect of pharmacological inhibition of other kinases that have been reported to regulate FOXO1 activity and subcellular localization, such as p38 mito-

gen-activated protein kinase (MAPK), ERK or c-Jun N-terminal kinase (JNK)^{70,71}. However, the inhibition of these kinases by small molecule inhibitors did not prevent the rapid DNA damage-induced downregulation of RAG.

Allelic exclusion refers to a phenomenon in the immune system in which each lymphocyte expresses only one functional allele of its antigen receptor gene, ensuring specificity in immune responses. This process is crucial for generating a diverse repertoire of antigen receptors while preventing self-reactivity and autoimmune reactions. There are several proposed models explaining the mechanisms of allelic exclusion. The asynchronous recombination model, for instance, assumes that the probability of simultaneous bi-allelic recombinations is limited by the chromatin configurations, allowing recombination on one allele, while preventing recombination on the other allele. The feedback inhibition models suggest that the products or intermediates of *Ig* gene rearrangements act to inhibit the recombination process. According to the classical feedback inhibition model, successful *Ig* gene rearrangements induce signals via pre-BCRs or B-cell receptors (BCRs) to suppress additional allelic recombination⁷²⁻⁷⁴. In line with the current models, DSBs are thought to help enforce the allelic exclusion; the DNA breaks activate ATM, which in turn phosphorylates a plethora of downstream targets, including histone H2AX, modulating the accessibility of *Ig* loci for the RAG recombination machinery. Phosphorylated histone H2AX leads to the recruitment of chromatin remodeling complexes, such as the switch/Sucrose non-fermenting (SWI/SNF) complex⁷⁵. Based on the results of our study, we hypothesize that activation of ATM induces multiple negative feedback loops leading to transcriptional downregulation of RAG1/2 protein and mRNA, and thus enforcing allelic exclusion by limiting RAG's availability for further recombinations. Previous studies have also demonstrated that ATM prevents secondary *Igκ* recombinations by triggering a negative feedback loop, where the DSBs, generated during V to J recombination, eventually lead to inhibition of RAG1/2 recombinase⁷⁶. Mechanistically, ATM-mediated repression of growth arrest and DNA-damage-inducible protein alpha (GADD45α) was suggested to contribute to this negative feedback loop^{69,76}. However, in contrast to these previous studies, we did not detect any changes in protein or mRNA expression of GADD45α following NCS-induced DNA damage neither in human BCR-ABL1⁺ cell line nor in mouse v-Abl transformed cells. Consistent with our findings, the Bassing lab also demonstrated that in mouse pre-B cells the changes in GADD45α did not modulate the transcriptional expression of *Rag1/2* in response to DNA damage⁷⁷. Moreover, the Bassing lab also showed that in mouse pre-B cells, the inactivation of NF-κB essential modulator (Nemo), a known ATM signaling effector, resulted in increased *Rag1* and *Rag2* transcription, increased *Igκ* accessibility, and triggered RAG-dependent DSBs. The inactivation of Nemo disrupted the repression of *Rag1/2* mRNA and increased the simultaneous bi-allelic cleavage. Moreover, the induction of Spi-C transcription factor (SpiC) by RAG-mediated DSBs, led to a decrease

in Jk accessibility. However, inactivation of SpiC, alone was not sufficient to provoke a breach of allelic exclusion⁷⁷.

Next, we explored the possible involvement of other transcription factors in the DNA damage-driven regulation of RAG1/2. The transcription factor B-cell leukemia 11a (BCL11a) is known to be a component of the transcriptional network regulating RAG expression. The major isoform of BCL11a, the BCL11a-XL, was shown to bind directly to the *RAG1* promoter as well as to regulatory regions of other transcription factors involved in regulating RAG1 and RAG2, such as IKZF1, FOXO1, PAX5, Transcription Factor 3 (TCF3), SPIB, and interferon regulatory factor 4 (IRF4). Moreover, BCL11A was found to bind directly to the surrogate light chain VPRED1 promoter region.⁷⁸ In our study, the NCS-induced DNA damage in human BCR-ABL1⁺ pre-B cells did not have any effect on the protein levels of BCL11a. However, whether the DNA breaks modulate the ability of BCL11a to bind to *RAG1* promoter, has not been investigated.

Recently, growth factor-independent 1b (Gfi1b) has been demonstrated to be a transcriptional repressor of RAG. Using mouse v-Abl cell lines, the repression of RAG transcription was achieved by direct binding of Gfi1b to the 5' of the *Erag*, causing epigenetic changes in the *Rag* locus, as well as through repression of FOXO1 by Gfi1b⁷⁹. Whether DNA damage triggers the binding of Gfi1b to the *Erag* enhancer has not been investigated, leaving a possibility of Gfi1b's contribution to the RAG downregulation in response to genotoxic stress.

Chapter 5 reveals that the NF- κ B pathway plays an important role in the repression of RAG activity in pre-B cells. Several layers of regulations limit the expression of RAG1/2 in pre-B cells to the G1 phase of the cell cycle. The inappropriate activity of RAG1/2 during the S phase can contribute to chromosomal translocations, deletions, and other genomic alterations, ultimately leading to cellular dysfunction and disease development. Also, the RAG1/2 expression and activity in the S phase have previously been linked to an increase in genomic instability and lymphomagenesis⁸⁰.

In the course of B-cell development, there is a strict separation between pre-B cell proliferation and RAG expression/activity, serving as a safeguard against genomic instability⁸¹. Following the successful *Igh* recombination, the developing B cells at this stage are rather large, they divide fast and are in cycle. Before moving on to the next developmental stage, the cells go out of cycle, become smaller, re-activate expression of RAG1/2, and initiate recombination on the *IgI*⁸². In our study⁸³, we used a mouse v-Abl-transformed pre-B cell line, where the Abelson virus introduces a developmental block and keeps the cells at large cycling pre-B cells stage. Notably, in the large cycling v-Abl transformed pre-B cells do not express RAG and their *Igk* or *Igl* is still in the germline configuration. Treatment with Abelson kinase inhibitor STI571 alleviates the differentiation block and induces a G1 arrest, at which the cells upregulate RAG1/2 and initiate *IgI* gene recombination^{9,81}. In the cycling pre-B cells, AKT has been shown to repress the FOXO1 expression⁸⁴. Our study showed

that in cycling v-Abl transformed pre-B cells, inhibition of AKT kinase activity led to an increase in RAG-reporter activity and similar results were obtained when inhibiting PI3K with small molecule inhibitors in these cells, suggesting that in proliferating pre-B cells, RAG expression is actively suppressed by the PI3K/AKT pathway. The PI3K/AKT-mediated suppression of RAG was mediated by the RAG1/2 transcription factor FOXO1. Our data showed that AKT inhibition resulted in upregulation of nuclear FOXO1 and concomitant decrease of the phosphorylated forms of FOXO1 on Ser²⁵⁶ and Ser³²⁹, which are associated with FOXO1 destabilization^{50,85}.

The NF- κ B signaling pathway has been demonstrated to play a role in B-cell development. It is intricately regulated by various upstream signaling pathways, including the B-cell receptor (BCR), toll-like receptors (TLRs), cytokine receptors, and co-stimulatory molecules⁸⁶. The NF- κ B family of transcription factors consists of 5 members, NF- κ B1 (p50 and its precursor p105), NF- κ B2 (p52 and its precursor p100), which are synthesized as precursor molecules and catalytically processed into the active form, and RelA (p65), RelB, and c-Rel which are synthesized in their mature form and interact in the cytoplasm with inhibitors until they receive activating signals⁸⁷. Generally, there are 2 ways of NF- κ B pathway activation: the classical and alternative. In the classical pathway, IKK- β phosphorylates the inhibitory subunits of I κ B- α , I κ B- β , or I κ B- ϵ , leading to their degradation and causing the accumulation of RelA, c-Rel, and p50 in the nucleus where it delivers mainly survival and proliferation signals. In the alternative pathway, NF- κ B-inducing kinase (NIK) activates IKK- α , which phosphorylates NF- κ B2. This results accumulation of p52/RelB heterodimers in the nucleus. The alternative NF- κ B pathway is regulated mainly through the control of NIK turnover, with TNF receptor-associated factor 3 (TRAF3), TNF receptor-associated factor 2 (TRAF2), and Baculoviral IAP repeat-containing protein 1 and 2 (cIAP1/2) critically involved in this process^{88,89}. Numerous mouse and cell line knock-in and knock-out studies have highlighted the complexity of the role of NF- κ B in B-cell development, and the results provided sometimes contradicting conclusions, probably due to the many redundancies in NF- κ B subunits. For instance, mice expressing a dominant negative form of I κ B α exhibited reduced pre-B cell numbers, potentially as a result of altered PAX5 and IRF4 expression⁹⁰. Additionally, constitutive NF- κ B activation via p100 deletion resulted in arrested B-cell development at the pro-B cell stage⁹¹. However, the constitutive activation of alternative NF- κ B pathway, achieved by B-cell specific knock out of Traf3 (CD19^{Traf3-/-} mice), or constitutive activation of the classical pathway in mice expressing *IKK2ca* in B cells, did not affect B-cell development^{92,93}. Also, a study of mice simultaneously carrying inactivating mutations in RelA and c-Rel showed inhibition in germline *Igk* transcription but not RAG⁹⁴, whereas another study demonstrated that NF- κ B1/p50-deficient B cells do show an increase in RAG1/2 expression and activity⁹⁵.

In our study, using an inducible RAG recombination-reporter cell line, we show that two structurally different I κ B small molecule inhibitors (BMS-345541 and MLN120B, to-

gether referred to as Ikk β i) resulted in an increase in RAG-reporter activity, and strikingly, we observed a clear synergistic effect of concomitant Ikk β and PI3K/AKT inhibition on the increase in RAG activity and expression, and on the upregulation of RAG transcription factor FOXO1. Importantly, unlike upon the treatment of the v-Abl transformed pre-B cells with Abelson kinase inhibitor STI571, the cells treated with AKT and NF- κ B inhibitor did not exit the cell cycle and showed RAG activity in the S-phase, which has previously been linked to increase in genomic instability and lymphomagenesis⁸⁰. This can be partially attributed to the fact that during S phase of the cell cycle, when DNA replication takes place, the chromatin structure becomes more accessible, potentially allowing RAG1/2 to access DNA sequences they wouldn't normally have access to. Also, RAG-induced DSBs occurring during this phase can coincide with DNA replication forks, leading to the formation of complex DNA structures that are prone to errors in repair. Also, the non-homologous end-joining (NHEJ) pathway, used to resolve RAG-induced DSBs is known to be error-prone, which in the G1 phase is beneficial as it further increases the diversity of the recombined V(D)J regions, however in the S phase, the use of the error-prone DNA repair pathway might result in translocations, deletions and an overall increase in genomic instability⁹⁶⁻⁹⁸. In line with this observation, our data show that Ikk β inhibition resulted in a RAG-dependent increase in genomic instability, measured by the levels of intranuclear γ H2AX in cycling v-Abl wildtype as compared to *Rag2*^{-/-} pre-B cells. AKT inhibition alone did not increase the intranuclear γ H2AX. Notably, the γ H2AX staining was only observed in large cells, in further support of the notion that induction of RAG expression and activity was provoked in cycling cells.

Previously, the cell cycle was shown to be an important regulator of RAG expression: in the *E μ -Myc* transgenic mouse model of B-cell lymphoma, the cyclin-dependent kinase 4 (CDK4) phosphorylated FOXO1, which resulted in FOXO1 degradation and abolished the FOXO-dependent induction of *Rag1* and *Rag2* expression⁹⁹. In our study we observed that the levels of cyclin-A and CDK2 were significantly decreased following the IKK β i and AKTi treatment of v-Abl transformed cells; in fact, the degree of cyclin-A and CDK2 downregulation was similar to the one observed following the treatment with Abelson kinase inhibitor. Also, CDK4 protein and mRNA expression were decreased following the treatment with IKK β i and AKTi. Inversely, treatment with the small molecule inhibitor of CDK4/6 kinase activity PD-0332991 resulted in increased RAG activity. Previous studies have shown that CDK4 is regulated by NF- κ B and also, I κ B α binding to CDK4 was demonstrated to inhibit its kinase function^{90,100}. We therefore hypothesize that I κ B α might be involved in RAG regulation through CDK4 inhibition, which in turn acts as a negative regulator of FOXO1. We further hypothesize that the synergistic effect of combined inhibition of AKT and IKK β might be explained by the fact that both pathways impinge on the expression of RAG transcription factor FOXO1.

Also, following the NF- κ B and AKT inhibition in *in vitro* cultures of BCR-ABL negative primary human B-ALL cells, we observed an increase in RAG protein levels, and an increase in surface IgM expression as assessed by FACS, suggesting that in addition to murine cells, this regulatory pathway is also active in human cells. Our re-analysis of the publicly available mRNA expression profiles from previously published childhood B-ALL cohort showed that NF- κ B was negatively correlated with *Rag1*, *Rag2*, and *TdT* expression. These findings suggest that NF- κ B may possess tumor-suppressive properties in B-ALL, aligning with previous observations in different cell types. It is noteworthy that several emerging therapies targeting NF- κ B, PI3K-AKT, and CDK4 are being tested in leukemias and lymphomas¹⁰¹⁻¹⁰³. Given our results, it is conceivable that such treatments could inadvertently stimulate the oncogenic activity of RAG in leukemia patients, potentially exacerbating clonal diversification and genomic instability in pre-B cells.

In **Chapter 6** we uncovered an additional novel mechanism that regulates RAG1/2 expression upon induction of DNA damage. We found that the RAG protein and mRNA downregulation in response to DNA damage is also dependent on p53. This regulatory mechanism acts as a negative feedback loop, likely involving microRNA-34a (miR-34a), which is a p53 downstream target, and the RAG transcription factor FOXP1, which is one of the established targets of miR-34a^{104,105}.

TP53, a well-known tumor suppressor gene, plays a pivotal role in preventing cancer development by regulating cell growth and apoptosis. Alterations in p53, such as mutations, deletion, or dysregulation in signaling upstream from p53 have been associated with tumorigenesis, which underscores the tumor-suppressor role of p53¹⁰⁶. In the context of lymphoid malignancies, aberrant functioning of p53 was clearly shown to contribute to tumor formation, as previously extensively reviewed¹⁰⁷. Because p53 is a very well-established substrate of activated ATM¹⁰⁸, we explored the role of p53 in the regulation of RAG1/2 expression upon induction of DNA damage. Downregulation of *Rag1* and *Rag2* mRNA expression was partially prevented in *p53*^{-/-} primary pre-B cells exposed to γ -irradiation in contrast to their wild-type counterparts. Moreover, in the absence of p53, primary mouse pre-B cells undergoing light chain rearrangement, showed increased surface IgM expression, emphasizing the functional consequences of p53 modulation. In the severe combined immunodeficiency (*scid*) mouse model, the mutation in the catalytic subunit of DNA-dependent protein kinase (DNA-Pkcs) results in a developmental block of B and T cells at a very early stage¹⁰⁹. Notably, p53 deficiency in the *scid* model, achieved by crossing the *scid* mice with *Tp53*^{-/-} mice, was able to partially overcome the *scid*-conferred developmental block and allowed TCR β protein production¹¹⁰. In germinal center B cells and pre-B cells¹¹¹, the proto-oncogene BCL6 was shown to repress p53 expression by binding to two specific sites within p53 promoter¹¹². In our study, the overexpression of BCL6 in mouse v-Abl pre-B cells was sufficient to produce productive *Igk* recombination and partially overcome the developmental block imposed by v-Abl, similar to the results observed

when overexpressing FOXP1 in mouse v-Abl pre-B cells. We speculate that the BCL6-driven inhibition of p53 might have consequently limited the expression of miR-34a and alleviated the miR-34a-driven repression of the RAG1/2 transcription factor FOXP1. Collectively, our data, and the data of others, suggest that activation or stabilization of p53 suppresses gene recombination in developing B cells, thereby maintaining genomic stability.

FOXP1 is known RAG1/2 transcription factor and has been shown to bind to *Erag* enhancer to regulate the expression of *Rag1* and *Rag2*¹¹³. In our study, expression of *Foxp1* mRNA and protein was rapidly downregulated after induction of the DNA damage in the form of γ -irradiation, in v-Abl mouse pre-B cells treated with STI571; the absence of p53 partially prevented the downregulation of *Foxp1* following the induction of DNA damage. Interestingly, a recent study by Cerna *et al* showed that also in chronic lymphocytic leukemia (CLL) cells, activation of the DDR resulted in rapid downmodulation of FOXP1. Furthermore, the study of Cerna *et al* provided compelling evidence that the p53/miR-34a pathway is involved in the regulation of FOXP1 levels in response to DNA damage. Silencing FOXP1, or overexpressing miR-34a mimics was shown to result in lower protein levels of phospho-AKT and phospho-ERK after BCR-crosslinking, thereby contributing to BCR signaling modulation in CLL cells¹⁰⁵. Downregulation of miR-34a has been observed in various types of cancers and its expression level profiling holds promise as a prognostic indicator, as low miR-34a levels were associated with poor patients' outcome¹¹⁴. Though some studies showed a clear decrease in miR-34a transcripts in cell lines lacking p53 or containing a mutant p53^{115,116}, in other studies the correlation between p53 status and miR-34a expression was not established¹¹⁷. In the HCT116 colon cancer cell line miR-34a has been identified as a direct transcriptional target of p53 in response to genotoxic stress. Expression profiling further revealed that transcripts of genes involved in cell proliferation were significantly downregulated, whereas transcripts of genes involved in DNA repair and DNA checkpoints were significantly upregulated following the retroviral overexpression of miR-34a¹¹⁷. In the context of B cells, in human (NALM-6) and murine (70Z/3) pre-B cell lines and mouse bone marrow cells, the viral overexpression of miR-34a resulted in repression of *Foxp1* and displayed an increase in CD19⁺c-kit⁺IgM⁻ pre-B cells, while the levels of B220⁺CD43⁻IgM⁻ pre-B cells were significantly reduced, suggesting that the miR-34a overexpression caused a partial block of B-cell development at the pre-to-pre-B cell stage. In fact, this study identified FOXP1 to be a *bona fide* target of miR-34a, and overexpression of the *Foxp1* gene lacking the 3'-UTR rescued the miR-34a-induced B-cell developmental block¹¹⁸. This conflicting evidence might be related to the intrinsic variability between the used cell line models and cell types.

Our data suggest that a regulatory circuit, involving p53/miR-34a/FOXP1 might exist in pre-B cells, where the DNA breaks drive expression levels of miR-34a in mouse primary pre-B cells that are undergoing light-chain recombination. Moreover, a decrease of miR-34a levels using the miR-34a sponge resulted in an increase of surface IgM⁺ in B-cells after the

light chain recombination, similar to the increase observed in *Tp53*^{-/-} primary pre-B cells, suggesting that more pre-B cells have undergone *Igκ* recombination. In addition, the absence of RAG1, and thus absence of RAG-dependent DSBs in primary pre-B cells coincided with higher *Foxp1* mRNA levels. We propose that the increase in *Foxp1* levels might be related to the lack of gene recombination-mediated activation of p53 DNA damage responses, including the miR-34a.

In search of a more detailed mechanistic explanation of the DNA damage-driven RAG1/2 regulation, we speculate about several possible scenarios: The pro-survival factor B-cell leukemia/lymphoma 2 (BCL2) has also been identified as one of the transcripts downregulated upon overexpression of miR-34a. Interestingly, BCL2 has been shown to partially compensate for the loss of Vpr-binding protein (VprBP, also known as DCAF1), which is a substrate adaptor protein, associating with the N-terminus of RAG1 and is required for B-cell development and V(D)J recombination^{119,120}. Whether in our model the effect of the loss of p53 or miR-34a on the amount of B220⁺DX6⁺Ly6C⁺IgM⁺ B cells following the IL7 withdrawal could be (partially) attributed to BCL2 remains an open question. Another possible mechanistic explanation could be provided by the study showing that in the induction of miR-34a expression by cisplatin treatment downregulates Sirtuin 1 (*Sirt1*), which in turn increased the NF-κB activity¹¹⁶. Previously, we have established that in cycling pre-B cells, the NF-κB pathway inhibits RAG1/2 expression through AKT and CDK4⁸³. Whether the DNA damage-driven expression of miR-34a in pre-B cells could contribute to RAG1/2 downregulation through NF-κB activation is yet to be established.

In summary, we propose a negative feedback regulatory mechanism involving p53, miR-34a, and FOXP1, whereby DNA damage limits the expression of RAG1 and RAG2. In this regulatory pathway, DNA damage (exogenous as well as RAG-induced) triggers the activation of ATM, which subsequently stabilizes p53 and initiates the downstream effects of p53, including the upregulation of miR-34a. MiR-34a then modulates the levels of FOXP1 and the recombination of *Igκ* in pre-B cells. Consistent with this model, both miR-34a and FOXP1 levels respond to both exogenous and RAG-induced DNA damage, thereby constraining the expression of RAG1/2 and V(D)J recombination. This regulatory mechanism in developing B cells likely functions as a self-protective mechanism against excessive RAG-induced DNA damage, thereby safeguarding genome stability.

Final thoughts

The RAG-mediated DSBs are vital for the assembly of BCR (and TCR), without which our immune system would not be able to adapt and to protect us from the armada of different pathogens, they are also seen as a potentially hazardous product of RAG1/2 activity. Research data in this thesis indicate that the RAG-induced DSBs also display regulatory capacities and are capable of triggering a self-regulatory mechanism, where the RAG-produced

DNA breaks signal to shut down RAG expression to prevent unnecessary DNA damage. That RAG-derived DSBs have an important regulatory function is also illustrated in the recent study of Johnston et al, demonstrating that non-RAG induced DSBs at *Ig* loci of pre-B cells result in different gene expression profiles than the DSBs instigated by RAG: while other endonucleases, such as Cas9 endonuclease, was also capable of introducing DNA breaks at *Ig* loci, and triggering the “canonical DDR”, leading to the DNA break repair, measured by the degree of tumor protein p53-binding protein 1 (TP53BP1) foci generation, only RAG1/2-mediated DSBs triggered the “non-canonical DDR”, such as processes regulating B-cell development, as measured by the degree of NF- κ B2 activation and the CD40 and proviral integration site for Moloney murine leukemia virus 2 (Pim2) expression¹²¹.

The studies of the RAG regulatory pathways in this thesis underscore how temporal and qualitative circumstances determine the outcome of a signaling pathway modulation: **Chapter 5** shows that in cycling pre-B cells AKT signaling regulates RAG expression, while **Chapter 4** demonstrates that once the pre-B cells exit the cell cycle, AKT signaling is not involved in the regulation of RAG expression under the DNA damage conditions.

Moreover, the mechanisms uncovered in **Chapters 5 and 6**, where we demonstrated that the regulation of RAG expression involves a negative feedback loop that hinges on the kinase activity of the DNA damage sensor ATM. The degree of crosstalk between these are 2 pathways, (ATM/FOXO1 and ATM/p53/miR-34a/FOXP1), if any, is yet to be determined. We hypothesize that on the one hand, ATM is able to regulate the RAG transcription directly, by binding to *Erag* and thereby evicting the RAG transcription factor FOXO1 from its binding to *Erag*, and on the other hand, that ATM activation triggers several regulatory pathways (ATM/FOXO1 or ATM/p53/miR-34a/FOXP1) affecting the availability of the RAG transcription factors. These two effects of ATM activation may co-exist, potentiate each other or fine-tune the expression and activity of RAG1/2 in response to DNA damage.

References

1. Marshall JS, Warrington R, Watson W, Kim HL. An introduction to immunology and immunopathology. *Allergy, asthma, Clin Immunol Off J Can Soc Allergy Clin Immunol*. 2018;14(Suppl 2):49. doi:10.1186/s13223-018-0278-1
2. Woo JS, Alberti MO, Tirado CA. Childhood B-acute lymphoblastic leukemia: a genetic update. *Exp Hematol Oncol*. 2014;3:16. doi:10.1186/2162-3619-3-16
3. Jung D, Alt FW. Unraveling V(D)J recombination; insights into gene regulation. *Cell*. 2004;116(2):299-311. doi:10.1016/s0092-8674(04)00039-x
4. Akamatsu Y, Oettinger MA. Distinct roles of RAG1 and RAG2 in binding the V(D)J recombination signal sequences. *Mol Cell Biol*. 1998;18(8):4670-4678. doi:10.1128/MCB.18.8.4670
5. Score J, Calasanz MJ, Ottman O, et al. Analysis of genomic breakpoints in p190 and p210 BCR-ABL indicate distinct mechanisms of formation. *Leukemia*. 2010;24(10):1742-1750. doi:10.1038/leu.2010.174
6. Wiemels J. Chromosomal translocations in childhood leukemia: natural history, mechanisms, and epidemiology. *J Natl Cancer Inst Monogr*. 2008;(39):87-90. doi:10.1093/jncimonographs/lgn006
7. Wiemels JL, Leonard BC, Wang Y, et al. Site-specific translocation and evidence of postnatal origin of the t(1;19) E2A-PBX1 fusion in childhood acute lymphoblastic leukemia. *Proc Natl Acad Sci U S A*. 2002;99(23):15101-15106. doi:10.1073/pnas.222481199
8. Stracker TH, Theunissen JWF, Morales M, Petrini JHJ. The Mre11 complex and the metabolism of chromosome breaks: the importance of communicating and holding things together. *DNA Repair (Amst)*. 2004;3(8-9):845-854. doi:10.1016/j.dnarep.2004.03.014
9. Muljo SA, Schlissel MS. A small molecule Abl kinase inhibitor induces differentiation of Abelson virus-transformed pre-B cell lines. *Nat Immunol*. 2003;4(1):31-37. doi:10.1038/ni870
10. Khair L, Baker RE, Linehan EK, Schrader CE, Stavnezer J. Nbs1 ChIP-Seq Identifies Off-Target DNA Double-Strand Breaks Induced by AID in Activated Splenic B Cells. *PLoS Genet*. 2015;11(8):e1005438. doi:10.1371/journal.pgen.1005438
11. Kaczmarek A, Derebas J, Pinkosz M, Niedźwiecki M, Lejman M. The Landscape of Secondary Genetic Rearrangements in Pediatric Patients with B-Cell Acute Lymphoblastic Leukemia with t(12;21). *Cells*. 2023;12(3). doi:10.3390/cells12030357
12. Ryan SL, Peden JF, Kingsbury Z, et al. Whole genome sequencing provides comprehensive genetic testing in childhood B-cell acute lymphoblastic leukaemia. *Leukemia*. 2023;37(3):518-528. doi:10.1038/s41375-022-01806-8
13. Papaemmanuil E, Rapado I, Li Y, et al. RAG-mediated recombination is the predominant driver of oncogenic rearrangement in ETV6-RUNX1 acute lymphoblastic leukemia. *Nat Genet*. 2014;46(2):116-125. doi:10.1038/ng.2874
14. Kharas MG, Yusuf I, Scarfone VM, et al. KLF4 suppresses transformation of pre-B cells by ABL oncogenes. *Blood*. 2007;109(2):747-755. doi:10.1182/blood-2006-03-011106
15. Rohil Y, Shetty D, Narula G, Banavali SD. A Novel Case of ABL2 Chromosomal Rearrangement in High-Risk B-Cell Acute Lymphoblastic Leukemia. *J Assoc Genet Technol*. 2019;45(2):73-76.
16. Canté-Barrett K, Meijer MT, Cordo' V, et al. MEF2C opposes Notch in lymphoid lineage decision and drives leukemia in the thymus. *JCI insight*. 2022;7(13). doi:10.1172/jci.insight.150363

17. Teng G, Maman Y, Resch W, et al. RAG Represents a Widespread Threat to the Lymphocyte Genome. *Cell*. 2015;162(4):751-765. doi:10.1016/j.cell.2015.07.009
18. Collins AM, Watson CT. Immunoglobulin Light Chain Gene Rearrangements, Receptor Editing and the Development of a Self-Tolerant Antibody Repertoire. *Front Immunol*. 2018;9:2249. doi:10.3389/fimmu.2018.02249
19. Muljo SA, Schlissel MS. Pre-B and pre-T-cell receptors: conservation of strategies in regulating early lymphocyte development. *Immunol Rev*. 2000;175:80-93.
20. Schlissel MS, Corcoran LM, Baltimore D. Virus-transformed pre-B cells show ordered activation but not inactivation of immunoglobulin gene rearrangement and transcription. *J Exp Med*. 1991;173(3):711-720. doi:10.1084/jem.173.3.711
21. Luning Prak ET, Monestier M, Eisenberg RA. B cell receptor editing in tolerance and autoimmunity. *Ann N Y Acad Sci*. 2011;1217:96-121. doi:10.1111/j.1749-6632.2010.05877.x
22. Merelli I, Guffanti A, Fabbri M, et al. RSSsite: a reference database and prediction tool for the identification of cryptic Recombination Signal Sequences in human and murine genomes. *Nucleic Acids Res*. 2010;38(Web Server issue):W262-7. doi:10.1093/nar/gkq391
23. Lieber MR, Yu K, Raghavan SC. Roles of non-homologous DNA end joining, V(D)J recombination, and class switch recombination in chromosomal translocations. *DNA Repair (Amst)*. 2006;5(9-10):1234-1245. doi:10.1016/j.dnarep.2006.05.013
24. Marculescu R, Le T, Simon P, Jaeger U, Nadel B. V(D)J-mediated translocations in lymphoid neoplasms: a functional assessment of genomic instability by cryptic sites. *J Exp Med*. 2002;195(1):85-98. doi:10.1084/jem.20011578
25. Raghavan SC, Kirsch IR, Lieber MR. Analysis of the V(D)J recombination efficiency at lymphoid chromosomal translocation breakpoints. *J Biol Chem*. 2001;276(31):29126-29133. doi:10.1074/jbc.M103797200
26. Davila M, Liu F, Cowell LG, et al. Multiple, conserved cryptic recombination signals in VH gene segments: detection of cleavage products only in pro B cells. *J Exp Med*. 2007;204(13):3195-3208. doi:10.1084/jem.20071224
27. Rahman NS, Godderz LJ, Stray SJ, Capra JD, Rodgers KK. DNA cleavage of a cryptic recombination signal sequence by RAG1 and RAG2. Implications for partial V(H) gene replacement. *J Biol Chem*. 2006;281(18):12370-12380. doi:10.1074/jbc.M507906200
28. Deng YN, Xia Z, Zhang P, Ejaz S, Liang S. Transcription Factor RREB1: from Target Genes towards Biological Functions. *Int J Biol Sci*. 2020;16(8):1463-1473. doi:10.7150/ijbs.40834
29. Paigen K, Petkov PM. PRDM9 and Its Role in Genetic Recombination. *Trends Genet*. 2018;34(4):291-300. doi:10.1016/j.tig.2017.12.017
30. Wang B, Guo H, Yu H, Chen Y, Xu H, Zhao G. The Role of the Transcription Factor EGR1 in Cancer. *Front Oncol*. 2021;11:642547. doi:10.3389/fonc.2021.642547
31. Keskin N, Deniz E, Eryilmaz J, et al. PATZ1 Is a DNA Damage-Responsive Transcription Factor That Inhibits p53 Function. *Mol Cell Biol*. 2015;35(10):1741-1753. doi:10.1128/MCB.01475-14
32. Chuang JY, Wu CH, Lai MD, Chang WC, Hung JJ. Overexpression of Sp1 leads to p53-dependent apoptosis in cancer cells. *Int J Cancer*. 2009;125(9):2066-2076. doi:10.1002/ijc.24563
33. Powers NR, Parvanov ED, Baker CL, Walker M, Petkov PM, Paigen K. The Meiotic Recombination Activator PRDM9 Trimethylates Both H3K36 and H3K4 at Recombination Hotspots In Vivo. *PLoS Genet*. 2016;12(6):e1006146. doi:10.1371/journal.pgen.1006146
34. Li S, Shen L, Chen KN. Association between H3K4 methylation and cancer prognosis: A meta-analysis. *Thorac cancer*. 2018;9(7):794-799. doi:10.1111/1759-7714.12647

35. Xiao C, Fan T, Zheng Y, et al. H3K4 trimethylation regulates cancer immunity: a promising therapeutic target in combination with immunotherapy. *J Immunother cancer*. 2023;11(8). doi:10.1136/jitc-2022-005693
36. Gururajan M, Simmons A, Dasu T, et al. Early growth response genes regulate B cell development, proliferation, and immune response. *J Immunol*. 2008;181(7):4590-4602. doi:10.4049/jimmunol.181.7.4590
37. Xiao T, Li X, Felsenfeld G. The Myc-associated zinc finger protein (MAZ) works together with CTCF to control cohesin positioning and genome organization. *Proc Natl Acad Sci U S A*. 2021;118(7). doi:10.1073/pnas.2023127118
38. Zheng C, Wu H, Jin S, Li D, Tan S, Zhu X. Roles of Myc-associated zinc finger protein in malignant tumors. *Asia Pac J Clin Oncol*. 2022;18(6):506-514. doi:10.1111/ajco.13748
39. McGinty RJ, Sunyaev SR. Revisiting mutagenesis at non-B DNA motifs in the human genome. *Nat Struct Mol Biol*. 2023;30(4):417-424. doi:10.1038/s41594-023-00936-6
40. Guiblet WM, Cremona MA, Harris RS, et al. Non-B DNA: a major contributor to small- and large-scale variation in nucleotide substitution frequencies across the genome. *Nucleic Acids Res*. 2021;49(3):1497-1516. doi:10.1093/nar/gkaa1269
41. Wang G, Vasquez KM. Naturally occurring H-DNA-forming sequences are mutagenic in mammalian cells. *Proc Natl Acad Sci U S A*. 2004;101(37):13448-13453. doi:10.1073/pnas.0405116101
42. Agard EA, Lewis SM. Postcleavage sequence specificity in V(D)J recombination. *Mol Cell Biol*. 2000;20(14):5032-5040. doi:10.1128/MCB.20.14.5032-5040.2000
43. Lewis SM, Agard E, Suh S, Czyzyk L. Cryptic signals and the fidelity of V(D)J joining. *Mol Cell Biol*. 1997;17(6):3125-3136. doi:10.1128/MCB.17.6.3125
44. Nilavar NM, Nishana M, Paranjape AM, et al. Znc2 module of RAG1 contributes towards structure-specific nuclease activity of RAGs. *Biochem J*. 2020;477(18):3567-3582. doi:10.1042/BCJ20200361
45. Iacobucci I, Mullighan CG. Genetic Basis of Acute Lymphoblastic Leukemia. *J Clin Oncol Off J Am Soc Clin Oncol*. 2017;35(9):975-983. doi:10.1200/JCO.2016.70.7836
46. Thomson DW, Shahrin NH, Wang PPS, et al. Aberrant RAG-mediated recombination contributes to multiple structural rearrangements in lymphoid blast crisis of chronic myeloid leukemia. *Leukemia*. 2020;34(8):2051-2063. doi:10.1038/s41375-020-0751-y
47. Ochodnicka-Mackovicova K, Bahjat M, Maas C, et al. The DNA Damage Response Regulates RAG1/2 Expression in Pre-B Cells through ATM-FOXO1 Signaling. *J Immunol*. 2016;197(7):2918-2929. doi:10.4049/jimmunol.1501989
48. So S, Davis AJ, Chen DJ. Autophosphorylation at serine 1981 stabilizes ATM at DNA damage sites. *J Cell Biol*. 2009;187(7):977-990. doi:10.1083/jcb.200906064
49. Minton K. How RAG2 cycles. *Nat Rev Immunol*. 2005;5(8):591. doi:10.1038/nri1673
50. Huang H, Regan KM, Wang F, et al. Skp2 inhibits FOXO1 in tumor suppression through ubiquitin-mediated degradation. *Proc Natl Acad Sci U S A*. 2005;102(5):1649-1654. doi:10.1073/pnas.0406789102
51. Schlissel M, Constantinescu A, Morrow T, Baxter M, Peng A. Double-strand signal sequence breaks in V(D)J recombination are blunt, 5'-phosphorylated, RAG-dependent, and cell cycle regulated. *Genes Dev*. 1993;7(12B):2520-2532. doi:10.1101/gad.7.12b.2520
52. Lin WC, Desiderio S. Cell cycle regulation of V(D)J recombination-activating protein RAG-2. *Proc Natl Acad Sci U S A*. 1994;91(7):2733-2737. doi:10.1073/pnas.91.7.2733
53. Lee J, Desiderio S. Cyclin A/CDK2 regulates V(D)J recombination by coordinating RAG-2 accumulation and DNA repair. *Immunity*. 1999;11(6):771-781. Accessed September 10, 2014. <http://www.ncbi.nlm.nih.gov/pubmed/10626899>

54. Yurchenko V, Xue Z, Sadofsky M. The RAG1 N-terminal domain is an E3 ubiquitin ligase. *Genes Dev.* 2003;17(5):581-585. doi:10.1101/gad.1058103
55. Jones JM, Gellert M. Autoubiquitylation of the V(D)J recombinase protein RAG1. *Proc Natl Acad Sci U S A.* 2003;100(26):15446-15451. doi:10.1073/pnas.2637012100
56. Grazini U, Zanardi F, Citterio E, Casola S, Goding CR, McBlane F. The RING domain of RAG1 ubiquitylates histone H3: a novel activity in chromatin-mediated regulation of V(D)J joining. *Mol Cell.* 2010;37(2):282-293. doi:10.1016/j.molcel.2009.12.035
57. Beilinson HA, Glynn RA, Yadavalli AD, et al. The RAG1 N-terminal region regulates the efficiency and pathways of synapsis for V(D)J recombination. *J Exp Med.* 2021;218(10). doi:10.1084/jem.20210250
58. Schabla NM, Swanson PC. The CRL4VPRB-P(DCAF1) E3 ubiquitin ligase directs constitutive RAG1 degradation in a non-lymphoid cell line. *PLoS One.* 2021;16(10):e0258683. doi:10.1371/journal.pone.0258683
59. Schabla NM, Perry GA, Palmer VL, Swanson PC. VprBP (DCAF1) Regulates RAG1 Expression Independently of Dicer by Mediating RAG1 Degradation. *J Immunol.* 2018;201(3):930-939. doi:10.4049/jimmunol.1800054
60. Dengler HS, Baracho G V, Omori SA, et al. Distinct functions for the transcription factor Foxo1 at various stages of B cell differentiation. *Nat Immunol.* 2008;9(12):1388-1398. doi:10.1038/ni.1667
61. Chen J, Limon JJ, Blanc C, Peng SL, Fruman DA. Foxo1 regulates marginal zone B-cell development. *Eur J Immunol.* 2010;40(7):1890-1896. doi:10.1002/eji.200939817
62. Chow KT, Timblin GA, McWhirter SM, Schlissel MS. MK5 activates Rag transcription via Foxo1 in developing B cells. *J Exp Med.* 2013;210(8):1621-1634. doi:10.1084/jem.20130498
63. Motta MC, Divecha N, Lemieux M, et al. Mammalian SIRT1 represses forkhead transcription factors. *Cell.* 2004;116(4):551-563. doi:10.1016/s0092-8674(04)00126-6
64. Matsuzaki H, Daitoku H, Hatta M, Aoyama H, Yoshimochi K, Fukamizu A. Acetylation of Foxo1 alters its DNA-binding ability and sensitivity to phosphorylation. *Proc Natl Acad Sci U S A.* 2005;102(32):11278-11283. doi:10.1073/pnas.0502738102
65. Oberdoerffer P, Michan S, McVay M, et al. SIRT1 redistribution on chromatin promotes genomic stability but alters gene expression during aging. *Cell.* 2008;135(5):907-918. doi:10.1016/j.cell.2008.10.025
66. Verkoczy L, Duong B, Skog P, et al. Basal B cell receptor-directed phosphatidylinositol 3-kinase signaling turns off RAGs and promotes B cell-positive selection. *J Immunol.* 2007;178(10):6332-6341. doi:10.4049/jimmunol.178.10.6332
67. Khalil A, Morgan RN, Adams BR, et al. ATM-dependent ERK signaling via AKT in response to DNA double-strand breaks. *Cell Cycle.* 2011;10(3):481-491. doi:10.4161/cc.10.3.14713
68. Sekulić A, Hudson CC, Homme JL, et al. A direct linkage between the phosphoinositide 3-kinase-AKT signaling pathway and the mammalian target of rapamycin in mitogen-stimulated and transformed cells. *Cancer Res.* 2000;60(13):3504-3513. Accessed November 21, 2014. <http://www.ncbi.nlm.nih.gov/pubmed/10910062>
69. Amin RH, Schlissel MS. Foxo1 directly regulates the transcription of recombination-activating genes during B cell development. *Nat Immunol.* 2008;9(6):613-622. doi:10.1038/ni.1612
70. Asada S, Daitoku H, Matsuzaki H, et al. Mitogen-activated protein kinases, Erk and p38, phosphorylate and regulate Foxo1. *Cell Signal.* 2007;19(3):519-527. doi:10.1016/j.cellsig.2006.08.015
71. Calnan DR, Brunet A. The FoxO code. *Oncogene.* 2008;27(16):2276-2288. doi:10.1038/onc.2008.21
72. Mårtensson IL, Keenan RA, Licence S. The pre-B-cell receptor. *Curr Opin Immunol.* 2007;19(2):137-142. doi:10.1016/j.coi.2007.02.006

73. Vettermann C, Schlissel MS. Allelic exclusion of immunoglobulin genes: models and mechanisms. *Immunol Rev.* 2010;237(1):22-42. doi:10.1111/j.1600-065X.2010.00935.x
74. Brady BL, Steinel NC, Bassing CH. Antigen receptor allelic exclusion: an update and re-appraisal. *J Immunol.* 2010;185(7):3801-3808. doi:10.4049/jimmunol.1001158
75. Sadek M, Sheth A, Zimmerman G, Hays E, Vélez-Cruz R. The role of SWI/SNF chromatin remodelers in the repair of DNA double strand breaks and cancer therapy. *Front cell Dev Biol.* 2022;10:1071786. doi:10.3389/fcell.2022.1071786
76. Steinel NC, Lee BS, Tubbs AT, et al. The ataxia telangiectasia mutated kinase controls Ig κ allelic exclusion by inhibiting secondary V κ -to-J κ rearrangements. *J Exp Med.* 2013;210(2):233-239. doi:10.1084/jem.20121605
77. Glynn RA, Bassing CH. Nemo-Dependent, ATM-Mediated Signals from RAG DNA Breaks at Igk Feedback Inhibit V (κ) Recombination to Enforce Igk Allelic Exclusion. *J Immunol.* 2022;208(2):371-383. doi:10.4049/jimmunol.2100696
78. Lee BS, Lee BK, Iyer VR, et al. Corrected and Republished from: BCL11A Is a Critical Component of a Transcriptional Network That Activates RAG Expression and V(D) J Recombination. *Mol Cell Biol.* 2018;38(1). doi:10.1128/MCB.00362-17
79. Schulz D, Vassen L, Chow KT, et al. Gfi1b negatively regulates Rag expression directly and via the repression of FoxO1. *J Exp Med.* 2012;209(1):187-199. doi:10.1084/jem.20110645
80. Zhang L, Reynolds TL, Shan X, Desiderio S. Coupling of V(D)J recombination to the cell cycle suppresses genomic instability and lymphoid tumorigenesis. *Immunity.* 2011;34(2):163-174. doi:10.1016/j.immuni.2011.02.003
81. Klein F, Feldhahn N, Mooster JL, et al. Tracing the pre-B to immature B cell transition in human leukemia cells reveals a coordinated sequence of primary and secondary IGK gene rearrangement, IGK deletion, and IGL gene rearrangement. *J Immunol.* 2005;174(1):367-375. doi:10.4049/jimmunol.174.1.367
82. Melchers F. Checkpoints that control B cell development. *J Clin Invest.* 2015;125(6):2203-2210. doi:10.1172/JCI78083
83. Ochodnicka-Mackovicova K, Bahjat M, Bloedjes TA, et al. NF- κ B and AKT signaling prevent DNA damage in transformed pre-B cells by suppressing RAG1/2 expression and activity. *Blood.* 2015;126(11):1324-1335. doi:10.1182/blood-2015-01-621623
84. Lees J, Hay J, Moles MW, Michie AM. The discrete roles of individual FOXO transcription factor family members in B-cell malignancies. *Front Immunol.* 2023;14:1179101. doi:10.3389/fimmu.2023.1179101
85. Zhang X, Jiang L, Liu H. Forkhead Box Protein O1: Functional Diversity and Post-Translational Modification, a New Therapeutic Target? *Drug Des Devel Ther.* 2021;15:1851-1860. doi:10.2147/DDDT.S305016
86. Guldenpfennig C, Teixeira E, Daniels M. NF- κ B's contribution to B cell fate decisions. *Front Immunol.* 2023;14:1214095. doi:10.3389/fimmu.2023.1214095
87. Yu H, Lin L, Zhang Z, Zhang H, Hu H. Targeting NF- κ B pathway for the therapy of diseases: mechanism and clinical study. *Signal Transduct Target Ther.* 2020;5(1):209. doi:10.1038/s41392-020-00312-6
88. Siebenlist U, Brown K, Claudio E. Control of lymphocyte development by nuclear factor-kappaB. *Nat Rev Immunol.* 2005;5(6):435-445. doi:10.1038/nri1629
89. Demchenko YN, Glebov OK, Zingone A, Keats JJ, Bergsagel PL, Kuehl WM. Classical and/or alternative NF-kappaB pathway activation in multiple myeloma. *Blood.* 2010;115(17):3541-3552. doi:10.1182/blood-2009-09-243535

90. Balkhi MY, Willette-Brown J, Zhu F, et al. IKK α -mediated signaling circuitry regulates early B lymphopoiesis during hematopoiesis. *Blood*. 2012;119(23):5467-5477. doi:10.1182/blood-2012-01-401547
91. Guo F, Tänzer S, Busslinger M, Weih F. Lack of nuclear factor-kappa B2/p100 causes a RelB-dependent block in early B lymphopoiesis. *Blood*. 2008;112(3):551-559. doi:10.1182/blood-2007-11-125930
92. Sasaki Y, Derudder E, Hobeika E, et al. Canonical NF-kappaB activity, dispensable for B cell development, replaces BAFF-receptor signals and promotes B cell proliferation upon activation. *Immunity*. 2006;24(6):729-739. doi:10.1016/j.immuni.2006.04.005
93. Xie P, Stunz LL, Larison KD, Yang B, Bishop GA. Tumor necrosis factor receptor-associated factor 3 is a critical regulator of B cell homeostasis in secondary lymphoid organs. *Immunity*. 2007;27(2):253-267. doi:10.1016/j.immuni.2007.07.012
94. Scherer DC, Brockman JA, Bendall HH, Zhang GM, Ballard DW, Oltz EM. Corepression of RelA and c-rel inhibits immunoglobulin kappa gene transcription and rearrangement in precursor B lymphocytes. *Immunity*. 1996;5(6):563-574. doi:10.1016/s1074-7613(00)80271-x
95. Verkoczy L, Ait-Azzouzene D, Skog P, et al. A role for nuclear factor kappa B/rel transcription factors in the regulation of the recombinase activator genes. *Immunity*. 2005;22(4):519-531. doi:10.1016/j.immuni.2005.03.006
96. Ramsden DA, Nussenzweig A. Mechanisms driving chromosomal translocations: lost in time and space. *Oncogene*. 2021;40(25):4263-4270. doi:10.1038/s41388-021-01856-9
97. Yu W, Lescale C, Babin L, et al. Repair of G1 induced DNA double-strand breaks in S-G2/M by alternative NHEJ. *Nat Commun*. 2020;11(1):5239. doi:10.1038/s41467-020-19060-w
98. Libri A, Marton T, Deriano L. The (Lack of) DNA Double-Strand Break Repair Pathway Choice During V(D)J Recombination. *Front Genet*. 2021;12:823943. doi:10.3389/fgene.2021.823943
99. Lu Y, Wu Y, Feng X, et al. CDK4 deficiency promotes genomic instability and enhances Myc-driven lymphomagenesis. *J Clin Invest*. 2014;124(4):1672-1684. doi:10.1172/JCI63139
100. Li J, Joo SH, Tsai MD. An NF-kappaB-specific inhibitor, I κ B α , binds to and inhibits cyclin-dependent kinase 4. *Biochemistry*. 2003;42(46):13476-13483. doi:10.1021/bi035390r
101. Bride KL, Hu H, Tikhonova A, et al. Rational drug combinations with CDK4/6 inhibitors in acute lymphoblastic leukemia. *Haematologica*. 2022;107(8):1746-1757. doi:10.3324/haematol.2021.279410
102. Oki Y, Fanale M, Romaguera J, et al. Phase II study of an AKT inhibitor MK2206 in patients with relapsed or refractory lymphoma. *Br J Haematol*. 2015;171(4):463-470. doi:10.1111/bjh.13603
103. Verzella D, Cornice J, Arboretto P, et al. The NF- κ B Pharmacopeia: Novel Strategies to Subdue an Intractable Target. *Biomedicines*. 2022;10(9). doi:10.3390/biomedicines10092233
104. Rao DS, O'Connell RM, Chaudhuri AA, Garcia-Flores Y, Geiger TL, Baltimore D. MicroRNA-34a perturbs B lymphocyte development by repressing the forkhead box transcription factor Foxp1. *Immunity*. 2010;33(1):48-59. doi:10.1016/j.immuni.2010.06.013
105. Cerna K, Oppelt J, Chochola V, et al. MicroRNA miR-34a downregulates FOXP1 during DNA damage response to limit BCR signalling in chronic lymphocytic leukemia B cells. *Leukemia*. 2019;33(2):403-414. doi:10.1038/s41375-018-0230-x
106. Mantovani F, Collavin L, Del Sal G. Mutant p53 as a guardian of the cancer cell. *Cell Death Differ*. 2019;26(2):199-212. doi:10.1038/s41418-018-0246-9

107. Aubrey BJ, Strasser A, Kelly GL. Tumor-Suppressor Functions of the TP53 Pathway. *Cold Spring Harb Perspect Med.* 2016;6(5). doi:10.1101/cshperspect.a026062
108. Shiloh Y. ATM and related protein kinases: safeguarding genome integrity. *Nat Rev Cancer.* 2003;3(3):155-168. doi:10.1038/nrc1011
109. Sealey AL, Hobbs NK, Schmidt EE. Molecular genotyping of the mouse scid allele. *J Immunol Methods.* 2002;260(1-2):303-304. doi:10.1016/s0022-1759(01)00524-5
110. Guidos CJ, Williams CJ, Grandal I, Knowles G, Huang MT, Danska JS. V(D)J recombination activates a p53-dependent DNA damage checkpoint in scid lymphocyte precursors. *Genes Dev.* 1996;10(16):2038-2054. doi:10.1101/gad.10.16.2038
111. Nahar R, Ramezani-Rad P, Mossner M, et al. Pre-B cell receptor-mediated activation of BCL6 induces pre-B cell quiescence through transcriptional repression of MYC. *Blood.* 2011;118(15):4174-4178. doi:10.1182/blood-2011-01-331181
112. Phan RT, Dalla-Favera R. The BCL6 proto-oncogene suppresses p53 expression in germinal-centre B cells. *Nature.* 2004;432(7017):635-639. doi:10.1038/nature03147
113. Hu H, Wang B, Borde M, et al. Foxp1 is an essential transcriptional regulator of B cell development. *Nat Immunol.* 2006;7(8):819-826. doi:10.1038/ni1358
114. Li S, Wei X, He J, et al. The comprehensive landscape of miR-34a in cancer research. *Cancer Metastasis Rev.* 2021;40(3):925-948. doi:10.1007/s10555-021-09973-3
115. Luan S, Sun L, Huang F. MicroRNA-34a: a novel tumor suppressor in p53-mutant glioma cell line U251. *Arch Med Res.* 2010;41(2):67-74. doi:10.1016/j.arcmed.2010.02.007
116. Tan J, Fan L, Mao JJ, et al. Restoration of miR-34a in p53 deficient cells unexpectedly promotes the cell survival by increasing NFκB activity. *J Cell Biochem.* 2012;113(9):2903-2908. doi:10.1002/jcb.24167
117. Chang TC, Wentzel EA, Kent OA, et al. Transactivation of miR-34a by p53 broadly influences gene expression and promotes apoptosis. *Mol Cell.* 2007;26(5):745-752. doi:10.1016/j.molcel.2007.05.010
118. Rao DS, O'Connell RM, Chaudhuri A a., Garcia-Flores Y, Geiger TL, Baltimore D. MicroRNA-34a perturbs B lymphocyte development by repressing the forkhead box transcription factor Foxp1. *Immunity.* 2010;33(1):48-59. doi:10.1016/j.immuni.2010.06.013
119. Palmer VL, Aziz-Seible R, Kassmeier MD, Rothermund M, Perry GA, Swanson PC. VprBP Is Required for Efficient Editing and Selection of Igκ+ B Cells, but Is Dispensable for Igλ+ and Marginal Zone B Cell Maturation and Selection. *J Immunol.* 2015;195(4):1524-1537. doi:10.4049/jimmunol.1500952
120. Kassmeier MD, Mondal K, Palmer VL, et al. VprBP binds full-length RAG1 and is required for B-cell development and V(D)J recombination fidelity. *EMBO J.* 2012;31(4):945-958. doi:10.1038/emboj.2011.455
121. Johnston R, Mathias B, Crowley SJ, et al. Nuclease-independent functions of RAG1 direct distinct DNA damage responses in B cells. *EMBO Rep.* 2023;24(1):e55429. doi:10.15252/embr.202255429



APPENDIX

English summary

Nederlandse samenvatting

Zhrnutie v slovenčine

**Authors' contributions &
Research funding**

PhD portfolio & Publications

About the author

Acknowledgements

A large, stylized, light pink letter 'A' is positioned on the right side of the page, partially overlapping a vertical teal line.

English summary

The adaptive immune system is renowned for its ability to elicit specific responses against pathogens, mediated by lymphocytes and antigen-presenting cells. B cells produce antibodies and utilize B cell receptors (BCR), also known as antigen receptors or immunoglobulins, to detect and eliminate pathogens, damaged, or non-self cells, leading to humoral immunity. T cells, on the other hand, employ T cell receptors (TCR) to eliminate foreign antigens, resulting in cellular immunity. The generation of a wide array of antigen receptors occurs through a sophisticated system called V(D)J recombination. Specifically found in precursor B and T cells, this process is initiated by the recombination activating gene 1 and 2 (RAG1/2) complex, which induces DNA breaks at recombination signal sequences (RSS), specific sequences abundant in immunoglobulin (*Ig*) and *Tcr* gene segments. These gene segments are brought together through a DNA recombination process in various combinations. RAG1/2 recognizes specific recombination signal sequences (RSS), flanking the coding V(D)J segments, and introduces a break in one of the DNA strands, called a single-stranded break. Subsequently, the 3' hydroxyl end of the broken DNA strand induces a break in the opposite DNA strand, ultimately forming the double-strand DNA break (DSB). These types of DNA breaks are recognized by the MRE11/RAD50/NBS1 (MRN) protein complex, which binds near DNA breaks and recruits other DNA repair-associated proteins such as DNA-dependent protein kinase, catalytic subunit (DNA-PKcs), ataxia telangiectasia mutated (ATM), and Artemis. Cells use a process called non-homologous end joining (NHEJ) to repair double-strand DNA breaks. This means that no homology is required (no sister chromatid or homologous chromosome) to repair the break. Compared to other DNA repair processes, such as homologous recombination (HR), NHEJ is a much less accurate process: nucleotides, that were not originally in the germ line configuration, are incorporated into the junction, resulting in a shift in the genetic reading frame. This form of genetic "sloppiness" is advantageous for precursor B cells. On one hand, by introducing new nucleotides/mutations into the recombinant V(D)J gene segments, new, unique *Ig* receptors with unique specificities are constantly generated. However, on the other hand, this process can also introduce genetic errors elsewhere in the genome that may contribute to the malignant transformation of precursor B cells.

Considering that DNA breaks are introduced during V(D)J gene recombination, this process must be tightly regulated to prevent DNA breaks from being introduced into non-*Ig* gene segments in the genome. How is RAG1/2-mediated DNA cutting kept within the boundaries of *Ig* genes? Is the regulation indeed so strict, or can RAG1/2 occasionally introduce DNA breaks in genes unrelated to *Ig* rearrangement, so-called "off-targets"? If this is the case, what if these breaks are also repaired with errors? Is there a link between the off-target RAG1/2 activity and the occurrence of genetic lesions that underlie the for-

mation of cancer? For example, an oncogene that cannot be “turned off” due to incorrectly repaired DNA breaks, causing the cells to continuously divide.

Acute lymphoblastic leukemia (ALL) is a type of blood cancer characterized by rapid expansion of malignant B and T cell precursors. Genomic instability, including translocations such as ETV6-RUNX1, BCR-ABL1, and E2A-PBX1, is a feature of ALL. Traces of RAG1/2 activity, or the presence of sequences resembling RSS, have been found in the vicinity of genomic lesions in both mouse and human B-cell malignancies, including ALL. This suggests that aberrant targeting and/or activity of RAG1/2 may play a role in the development of lymphoid malignancies. However, the precise mechanism of the malignant derailment of precursor B cells in the onset of ALL, and the exact role of the RAG1/2 complex in this process, are currently unknown. The research in this thesis focuses on detecting and characterizing the “off-target” activity of RAG1/2 and the potential consequences thereof on the genomic integrity of precursor B cells. We also meticulously studied the regulation of the RAG1/2 complex in the context of DNA damage and discovered several novel regulatory mechanisms.

In **Chapter 2**, we extensively described the process of B-cell development and V(D)J gene rearrangement. Here, we paid particular attention to the role of DNA damage and DNA damage signaling. We discuss the molecular mechanisms involved and how the balance between DNA damage and DNA repair is maintained, as well as the possible consequences of disrupting this balance. We summarized evidence from other studies showing that a significant portion of the genetic errors in patients with B-cell acute lymphoblastic leukemia (B-ALL) exhibit characteristics of dysregulated RAG1/2 activity, which may arise due to failed RAG1/2 regulation.

First, we investigated whether the activity of the RAG1/2 complex in precursor B cells is limited to *Ig* genes, or if it can also introduce DNA breaks elsewhere in the genome. Previous studies conducted by other research groups demonstrated that the RAG1/2 complex can bind to DNA at locations other than *Ig* genes. However, those studies could not conclude whether the RAG1/2 binding to the DNA also results in the formation of RAG1/2-dependent DNA breaks. In **Chapter 3**, we demonstrated that RAG1/2 does not only introduce DSBs at *Ig* genes but also at thousands of other locations in the genome. In a mouse precursor B-cell line, we identified approximately 1500 sites where RAG1/2 introduces a DNA break. In addition to the known “hot spots” on the *Ig* gene segments on chromosome 6 (immunoglobulin light chain genes in mice) and chromosome 12 (immunoglobulin heavy chain genes in mice), RAG1/2-dependent DNA breaks were found throughout the entire genome. RAG1/2-dependent DNA breaks were identified near genes previously associated with the development of B-cell malignancies such as *Ikzf4*, *Abl2*, *Klf4*, *Tcf4*, *Tcf7*, *Rassf8*, *Mef2c*, or near genes involved in DNA break repair such as *Rad51ap1*. We further investigated the DNA sequences in the vicinity of RAG1/2-dependent DNA breaks, showing that these breaks are predominantly found near simple repetitive sequences such

as CA or GA dinucleotide combinations. It is known that such sequences can adopt an alternative DNA structure, also called non-B DNA structure. These non-B DNA structures can form a triple helix or so-called G-quadruplexes, or DNA hairpin structures. Several biochemical studies have shown that the RAG1/2 complex is indeed capable of recognizing and cleaving these structures, with non-B structures identified around some genetic abnormalities commonly found in malignant B cells.

In Chapters 4, 5, and 6, we describe new mechanisms of deregulation of the RAG1/2 complex. In **Chapter 4**, we describe a novel mechanism that causes B cells to shut down the RAG1/2 complex in response to DNA damage. This mechanism can be activated by DNA damage caused by external factors (γ -radiation, or chemical substances that introduce DNA breaks), as well as when the RAG1/2 complex itself is the source of the DNA damage. We have demonstrated that the activation of the ATM protein by DNA damage is crucial for this regulation. Pharmacological inhibition of ATM activation prevents the deactivation of the RAG1/2 complex following DNA damage induction. The DNA damage-dependent activation of ATM reduces the binding of the transcription factor FOXO1 to the RAG1 and RAG2 genes, thereby silencing the expression of these genes. We propose that this mechanism may play a significant role in protecting cells against multiple DNA damages during the gene rearrangement process.

In **Chapter 5**, we have discovered another novel regulatory mechanism that controls the activity and availability of RAG. We show that the nuclear factor kappa-B (NF- κ B) and the phosphoinositide 3-kinase (PI3K)/AKT signaling pathways are significant suppressors of RAG1/2 activity, ensuring that the RAG1/2 complex is expressed and active at the appropriate time during cell division. We demonstrate that inhibition of NF- κ B results in an increase in RAG1/2 activity and RAG-mediated DNA breaks. The use of potential new therapeutic agents that inhibit NF- κ B components may therefore have implications for the genomic stability of precursor B cells developing in the bone marrow.

Finally, in **Chapter 6**, we showed that the tumor suppressor p53 also plays a crucial role in the regulation of the RAG1/2 complex in response to DNA damage. In precursor B cells lacking the p53 gene (p53 knockouts), the expression of RAG1/2 following DNA damage is not deactivated as in normal precursor B cells. Additionally, we have shown that the absence of p53 resulted in an increase in precursor B cells that have successfully undergone *Ig* gene rearrangement. We have demonstrated that the activation of p53 by DNA damage leads to an increase in the expression of microRNA-34a (miR-34a). miR-34a subsequently partially deactivates the transcription factor forkhead box P1 (FOXP1) protein, which plays a crucial role in the expression of the RAG1/2 complex. We have shown that DNA damage results in a reduction in FOXP1 expression, and that increased expression of FOXP1 in precursor B cells accelerates gene rearrangement.

Nederlandse samenvatting

Het adaptieve immuunsysteem staat bekend om zijn vermogen om specifieke reacties tegen pathogenen te veroorzaken, dankzij lymfocyten en antigeen-presenterende cellen. B-cellen maken antilichamen aan en maken gebruik van B-celreceptoren (BCR), ook bekend als antigeenreceptoren of immunoglobulinen, om pathogenen, beschadigde of niet-zelfcellen te detecteren en te verwijderen, wat leidt tot humorale immuniteit. T-cellen, aan de andere kant, gebruiken T-celreceptoren (TCR) om vreemde antigenen te elimineren, wat leidt tot cellulaire immuniteit. Het genereren van een breed scala aan antigeenreceptoren gebeurt door middel van een geavanceerd systeem genaamd V(D)J-genherschikking. Dit proces, specifiek voor voorloper B- en T-cellen, wordt gestart door het recombinerende activerende gen 1 en 2 (RAG1/2) complex, dat DNA-breuken induceert op recombinatiesignaalsequenties (RSS), specifieke sequenties die overvloedig aanwezig zijn op immunoglobuline (*Ig*) en *Tcr* gensegmenten. Deze gensegmenten worden door een DNA-herschikkingsproces in verschillende combinaties samengebracht. Hierbij introduceert RAG1/2 allereerst een onderbreking van een van de DNA strengen, een zogenaamde enkelstrengsbreuk. RAG1/2 herkent specifieke recombinatie signaal sequenties (RSS) die de coderende V(D)J segmenten flankeren. Het 3' hydroxyl-einde van de gebroken DNA-streng veroorzaakt vervolgens een onderbreking van de tegenoverliggende DNA-streng, wat uiteindelijk tot de vorming van een dubbelstrengs DNA-breuk leidt. Dit type DNA-breuken worden herkend door het MRE11/RAD50/NBS1 (MRN) eiwitcomplex dat in de buurt van DNA-breuken bindt en andere DNA reparatie-geassocieerde eiwitten rekruteert, zoals het DNA-dependent protein kinase, catalytic subunit (DNA-PKcs), ataxia telangiectasia mutated (ATM) en Artemis. Voor het repareren van de dubbelstrengs DNA-breuken gebruiken de cellen het zogenaamde niet-homologe eindverbindingsproces (NHEJ). Dit betekent dat er geen gebruik wordt gemaakt van de informatie van dezelfde regio aanwezig op de tweede DNA streng om de breuk te herstellen. In vergelijking met andere DNA-herstel processen, zoals homologe recombinatie (HR), is NHEJ een veel minder accuraat proces: er worden bijvoorbeeld nucleotiden in de breuk geïncorporeerd die er oorspronkelijk (in de kiembaanconfiguratie) niet waren, wat kan resulteren in de verschuiving van het genetische lees kader. Deze vorm van genetische "slordigheid" is aan de ene kant heel voordelig voor de voorloper B-cellen: door het introduceren van nieuwe nucleotiden/mutaties in de recombinerende V(D)J gensegmenten ontstaan telkens nieuwe, unieke, *Ig* receptoren met ieder een unieke specificiteit. Maar tegelijkertijd heeft dit het risico dat er genetische fouten die mogelijk bijdragen aan de kwaadaardige ontsporing van de voorloper B-cellen.

Omdat het RAG1/2 complex tijdens de genherschikking in staat is het DNA te knippen, moet dit proces bijzonder strikt gereguleerd worden om te voorkomen dat er DNA-breuken op andere plekken dan het *Ig* locus in het genoom geïntroduceerd worden. Hoe wordt het knippen van het DNA binnen de kaders van *Ig* genen gehouden? Is de regulatie

inderdaad zo strikt, of kan het incidenteel voorkomen dat RAG1/2 DNA-breuken in genen introduceert die met *Ig* herschikking niets te maken hebben, zogeheten “off-targets”? Indien dit het geval is, wat als deze breuken ook nog met fouten hersteld worden? Wat zijn de consequenties van deze gebeurtenissen voor het ontstaan van genetische fouten die ten grondslag kunnen liggen aan de vorming van kanker? Bijvoorbeeld een oncogen dat door incorrect herstelde DNA-breek niet meer “uitgezet” kan worden en de cellen aanzet om voortdurend te delen.

Acute lymfoblastische leukemie (ALL) is een type bloedkanker dat gekenmerkt wordt door een snelle uitbreiding van kwaadaardige B-cel en T-celvoorlopers. Genomische instabiliteit, inclusief chromosomale translocaties zoals *ETV6-RUNX1*, *BCR-ABL1* en *E2A-PBX1*, is een kenmerk van ALL. Sporen van RAG1/2-activiteit, of aanwezigheid van sequenties die lijken op RSS en dus herkent en gekleefd zouden kunnen worden door RAG1/2, zijn gevonden in de nabijheid van genomische laesies in B-cel tumoren in patiënten (zoals ALL) en in muismodellen voor deze ziekten. Dit suggereert een afwijkende doelgerichtheid en/of activiteit van RAG1/2 tijdens de ontwikkeling van lymfoïde maligniteiten. Echter, het precieze mechanisme van de kwaadaardige ontsporing van voorloper B-cellen in het ontstaan van ALL, en de rol van het RAG1/2 complex hierbij zijn vooralsnog niet bekend. Het onderzoek in dit proefschrift richt zich op het detecteren en karakteriseren van de “off-target” activiteit van RAG1/2 en de potentiële consequenties hiervan op de genomische integriteit van voorloper B-cellen. Ook hebben we de regulatie van het RAG1/2 complex nauwkeurig bestudeert en meerdere nieuwe regulatiemechanismen ontdekt.

In **Hoofdstuk 2** hebben we het proces van B-cel ontwikkeling en V(D)J genherschikking, uitgebreid beschreven. Hierbij hebben we vooral veel aandacht besteedt aan de rol van DNA-schade en DNA-schade signalering. We bespreken de moleculaire mechanismen die hierbij een rol spelen, en hoe de balans tussen DNA-schade en DNA-reparatie in evenwicht worden gehouden, en wat de mogelijke gevolgen zijn van het verstoren van deze balans. We hebben aanwijzingen uit andere studies samengevat die laten zien dat een belangrijk deel van de genetische fouten in patiënten met B-cel acute lymfoblastische leukemie (B-ALL) kenmerken dragen van een ontregelde RAG1/2 activiteit, en dat deze mogelijk ontstaan zijn als gevolg van verstoorde RAG1/2 regulatie.

Als eerste hebben we onderzocht of de activiteit van het RAG1/2 complex in voorloper B-cellen zich beperkt tot de *Ig* genen, of dat het daarnaast ook DNA-breuken kan veroorzaken in de rest van het genoom. Eerdere studies die uitgevoerd zijn door andere onderzoekers lieten zien dat het RAG1/2 complex zich aan het DNA kan binden op andere plekken dan de *Ig* genen. Echter, uit die studies kon niet worden geconcludeerd of deze binding ook resulteert in de vorming van RAG1/2-afhankelijke DNA-breuken. In **Hoofdstuk 3** laten we zien dat RAG1/2 niet alleen dubbelstrengs DNA-breuken kan veroorzaken op de *Ig* genen, maar ook op duizenden andere plekken in het genoom. In een voorloper B-cellijn uit de muis hebben we ongeveer 1500 plekken geïdentificeerd waar RAG1/2 een

DNA-brek heeft veroorzaakt. Naast de bekende “hot-spots” op de *Ig* gensegmenten op chromosoom 6 (immunoglobuline lichte keten genen in de muis) en chromosoom 12 (immunoglobuline zware keten genen in de muis), waren er RAG1/2-specifieke DNA-breken gevonden door het hele genoom heen. Er zijn RAG1/2-specifieke DNA-breken geïdentificeerd in de buurt van de genen die eerder geassocieerd zijn met de ontwikkeling van B-cel maligniteiten zoals *Ikzf4*, *Abl2*, *Klf4*, *Tcf4*, *Tcf7*, *Rassf8*, *Mef2c*, of in de buurt van de genen die rol spelen het herstel van DNA-breken zoals *Rad51ap1*. We hebben verder onderzocht wat de DNA-volgordes (sequenties) in de buurt van RAG1/2-specifieke DNA-breken gemeen hebben, waarbij we hebben laten zien dat deze breken met name gevonden worden in de buurt van simpele herhaalsequenties zoals van CA of GA dinucleotide combinaties. Het is bekend dat zulke sequenties een alternatieve DNA-structuur kunnen aannemen, ook wel non-B DNA-structuur genoemd. Deze non-B DNA-structuren kunnen een driedubbele helix zijn, of zogenaamde G-kwartetten, en DNA-haarspeld structuren. Verschillende biochemische studies hebben aangetoond dat RAG1/2 complex inderdaad in staat is om deze structuren te herkennen en te knippen, waarbij bijvoorbeeld non-B-structuren geïdentificeerd zijn rondom sommige genetische afwijkingen die veel voorkomen in kwaadaardige B-cellen.

In de hoofdstukken 4, 5 en 6 beschrijven we nieuwe mechanismen van deregulatie van het RAG1/2 complex. In **Hoofdstuk 4** beschrijven we een nieuw mechanisme dat ervoor zorgt de B-cellen het RAG1/2 complex afschakelen na het ontstaan van DNA-schade. Dit mechanisme treedt in werking bij zowel DNA-schade veroorzaakt door externe factoren (γ -straling, of chemische stoffen die DNA-breken introduceren) maar ook door het RAG1/2 complex zelf. We hebben laten zien dat de activatie van het ATM-eiwit door DNA-schade cruciaal is voor deze regulatie. Bij farmacologische remming van de activatie van het ATM vindt afschakeling van het RAG1/2 complex niet plaats na inductie van DNA-schade. De DNA-schade-afhankelijke activatie van ATM vermindert de binding van de transcriptie factor forkhead box O1 (FOXO1) aan de RAG1 en RAG2 genen waardoor de expressie van deze genen wordt uitgeschakeld. We stellen voor dat dit een mechanisme is dat een belangrijke rol kan spelen in het beschermen van cellen tegen veelvoudige DNA-schade tijdens het genherschikkingproces.

In **Hoofdstuk 5** beschrijven we een ander nieuw regulatiemechanisme ontdekt dat de activiteit en beschikbaarheid van RAG controleert. We laten zien dat het nucleaire factor kappa-B (NF- κ B) en de fosfoinositol-3-kinase (PI3K)/AKT-sigtaalpaden belangrijke onderdrukkers zijn van RAG1/2-activiteit, en ervoor zorgen dat het RAG1/2 complex op het juiste moment tijdens de celdeling tot expressie komt en actief is. We laten zien dat de remming van NF- κ B resulteert in een toename van RAG1/2-activiteit en RAG-gemedieerde DNA-breken. Het gebruik van de nieuwe potentiële therapeutische stoffen die de NF- κ B-componenten remmen kunnen daarom implicaties hebben voor de genomische stabiliteit van voorloper B-cellen die zich ontwikkelen in het beenmerg.

En tot slot in **Hoofdstuk 6** laten we zien dat de tumorsuppressor p53 ook een belangrijke rol speelt in de regulatie van het RAG1/2 complex. In voorloper B-cellen die het p53 gen missen (p53-knockouts) wordt de RAG1/2 expressie als gevolg van DNA-schade niet uitgeschakeld zoals in normale voorloper B-cellen. Daarbij hebben we ook laten zien dat de afwezigheid van p53 resulteert in een toename van voorloper B-cellen die de *Ig* generschikking succesvol hebben ondergaan. We hebben aangetoond dat activatie van p53 door DNA-schade leidt tot de toename van het microRNA-34a (miR-34a) expressie. Het miR-34a resulteert vervolgens in de gedeeltelijke afschakeling van het forkhead box P1 (FOXP1) eiwit, welke een belangrijke rol speelt in de expressie van het RAG1/2 complex. We hebben aangetoond dat DNA-schade leidt tot vermindering van FOXP1 expressie, en dat een verhoogde expressie van FOXP1 in voorloper B-cellen resulteert in een versnelde generschikking.

Zhrnutie v slovenčine

Adaptívny imunitný systém má schopnosť vyvolávať špecifickú odpoveď na prítomnosť patogénov, prostredníctvom lymfocytov a antigén prezentujúcich buniek. B bunky (tiež nazývané B lymfocyty) produkujú protilátky a využívajú B bunkové receptory (BCR), známe tiež ako antigénové receptory alebo imunoglobulíny, na detekciu a elimináciu patogénov, poškodených alebo telu nevlastných buniek. Tento typ imunitnej odpovede sa taktiež nazýva humorálna imunita. T bunky (tiež nazývané T lymfocyty) využívajú T bunkové receptory (TCR) na elimináciu cudzích antigénov, čo vedie k imunitnej odpovedi nazývanej bunková imunita. Produkcia širokej škály antigénových receptorov (BCR aj TCR) sa uskutočňuje prostredníctvom sofistikovaného systému preskupovania génových segmentov, nazývaného V(D)J rekombinácia. Tento molekulárny proces, prebiehajúci v prekursoroch B a T buniek, je iniciovaný komplexom rekombináciu aktivujúcich génov 1 a 2 (RAG1/2). RAG1/2 vyvoláva zlomy v DNA na signálnych sekvenciách pre rekombináciu (RSS), špecifických sekvenciách výrazne zastúpených v génových segmentoch kódujúcich hypervariabilnú časť imunoglobulínov (Ig) a TCR receptorov. Tieto génové segmenty sú rozštiepené a znova preskupené prostredníctvom procesu DNA rekombinácie, čím vznikajú segmenty s novou kombináciou V, (D) a J génov. RAG1/2 rozpoznáva RSS sekvencie, ktoré ohraničujú každý z V(D)J segmentov, a spôsobuje rozštiepenie jedného z vlákien DNA, takzvaný jednovláknový zlom. Následne 3' hydroxyl koniec rozštiepeného vlákna DNA vyvolá zlom v druhom vlákne DNA, čo nakoniec vedie k dvojláknovému zlomu DNA (DSB). Tieto typy zlomov DNA sú rozpoznávané proteínovým komplexom MRE11/RAD50/NBS1 (MRN), ktorý sa viaže na chromatin v blízkosti DNA zlomov a pritiahne ďalšie proteíny podieľajúce sa na oprave DNA, ako napríklad proteínovú kinázu závislú od DNA (DNA-PKcs), kinázu zmutovanú pri ataxii telangiektázii (ATM) a Artemis. Bunky využívajú na opravu dvojláknových zlomov DNA proces nazývaný nehomologické spájanie voľných koncov (NHEJ). To znamená, že na opravu zlomu nie je potrebná žiadna predloha (sesterská chromatída alebo homologický chromozóm). V porovnaní s inými procesmi opravy DNA, ako je napríklad homologická rekombinácia (HR), je NHEJ oveľa menej presný proces: nukleotidy, ktoré neboli v zárodnej DNA konfigurácii, sú začlenené do nových V(D)J spojov, čo vedie k posunu v genetickom čítacom rámci. Tento druh genetickej „nepresnosti“ je pre prekursorov B buniek výhodný. Na jednej strane, začleňovaním nových nukleotidov/mutácií do preskupených V(D)J génových segmentov, sú neustále generované novo vytvorené, unikátne Ig receptory s osobitou špecifitou. Na druhej strane, tento proces môže viesť ku genetickým chybám na iných miestach genómu, ktoré môžu prispievať ku rakovinovej transformácii B buniek.

Proces rekombinácie génov V(D)J do DNA musí byť dôsledne regulovaný, aby sa zabránilo zavedeniu zlomov DNA na iných miestach genómu mimo *Ig* segmentov. Akými mechanizmami je fyziologická aktivita RAG1/2 udržiavaná v rámci *Ig* génových segmentov? Je regulácia RAG1/2 skutočne taká dôsledná, alebo je možné, že RAG1/2 v niektorých prípadoch

spôsobuje zlomy DNA aj v génoch, ktoré nehrajú úlohu pri preskupovaní *Ig* segmentov, tzv. nežiadúca alebo „off-target“ aktivita? Čo ak by boli tieto nežiadúce zlomy navyše tiež opravené s chybami? Existuje súvislosť medzi „off-target“ aktivitou RAG1/2 a výskytom genetických chýb (mutácií, translokácií, delécií), ktoré tvoria základ pre vznik rakoviny B lymfocytov? Napríklad je možné predpokladať, že onkogén, ktorý sa nemôže „vypnúť“ v dôsledku nesprávne opravených zlomov DNA, by mohol viesť ku nekontrolovateľnému deleniu buniek. Akútna lymfoblastická leukémia (ALL) je typom krvnej rakoviny, ktorý sa vyznačuje rýchlym množením zhubných prekursorov B a T buniek. ALL je charakterizovaná genomickou nestabilitou, vrátane translokácií ako ETV6-RUNX1, BCR-ABL1 a E2A-PBX1. Náznaky aktivity RAG1/2, alebo prítomnosť sekvencií pripomínajúcich RSS, boli zaznamenané v blízkosti genetických mutácií nielen v myšiacích, ale aj v ľudských B-bunkových, vrátane ALL. Toto Tieto poznatky môžu naznačovať, že nepresná alebo chybná aktivita RAG1/2 by mohla zohrávať úlohu pri rozvoji lymfoidných malignít. Avšak presný mechanizmus malígnej transformácie prekursorov B buniek, a úloha komplexu RAG1/2 v tomto procese, zostávajú v súčasnosti nepreskúmané. Výskum v tejto dizertačnej práci sa zameriava na detekciu a charakterizáciu nežiadúcej, „off-target“, aktivity RAG1/2 a jej možné dôsledky pre genomickú integritu. Dôkladne sme skúmali aj reguláciu komplexu RAG1/2 v kontexte poškodenia DNA a objavili sme niekoľko nových regulačných mechanizmov tohto komplexného procesu.

V **Kapitole 2** sme v aktuálnom prehľade literatúry podrobne opísali proces vývoja B buniek a rekombináciu génov V(D)J. Osobitnú pozornosť sme venovali úlohe poškodenia DNA a signálnej transdukcii, ktorú DNA poškodenie spúšťa. Popisujeme molekulárne mechanizmy zapojené do procesu rekombinácie génov V(D)J, mechanizmy udržiavania rovnováhy medzi poškodením a opravou DNA, ako aj možné dôsledky narušenia tejto rovnováhy. Sumarizujeme výsledky zo štúdií, ktoré ukazujú, že významná časť genetických chýb u pacientov s akútnou lymfoblastickou leukémiou B-buniek (B-ALL) vykazuje charakteristiky nežiadúcej aktivity RAG1/2, ktorá sa môže objaviť v dôsledku chybných regulačných mechanizmov.

V úvode experimentálnej práce sme skúmali, či je aktivita komplexu RAG1/2 v prekursoroch B buniek obmedzená len na *Ig* gény, alebo môže RAG1/2 tiež zavádzať zlomy DNA na iných miestach genómu. Predchádzajúci výskum iných autorov naznačuje, že komplex RAG1/2 by sa mohol viazať na DNA aj na iných miestach ako *Ig* gény. Avšak z týchto štúdií nie je jednoznačné, či väzba RAG1/2 na DNA taktiež vedie na týchto miestach k aktívnej tvorbe DNA zlomov. V **Kapitole 3** sme preukázali, že RAG1/2 nespôsobuje DSB zlomy len v *Ig* génoch, ale aj na tisícoch ďalších miest v genóme. V bunkovej línii prekursorov B buniek sme identifikovali približne 1500 miest, kde RAG1/2 aktívne vytvoril zlom DNA. Okrem predpokladanej aktivity na segmentoch *Ig* génov na chromozóme 6 (gény ľahkého reťazca imunoglobulínu u myši) a na chromozóme 12 (gény ťažkého reťazca imunoglobulínu u myši) sme identifikovali zlomy spôsobné aktivitou RAG1/2 naprieč celým genómom. DNA zlomy vyvolané aktivitou RAG1/2 boli identifikované v blízkosti génov, ktoré zohrávajú úlohu vo vývoji malignít, ako sú *Ikzf4*, *Abl2*, *Klf4*, *Tcf4*, *Tcf7*, *Rassf8*, *Mef2c*, alebo blízko génov zapojených do opravy zlomov DNA,

ako je Rad51ap. Bližšia analýza DNA sekvencií v blízkosti DNA zlomov spôsobných aktivitou RAG1/2 ukázala, že tieto zlomy sa nachádzajú predovšetkým v blízkosti jednoduchých repetitívnych sekvencií, ako sú napríklad CA alebo GA repetitívne dinukleotidové kombinácie. Je známe, že takéto sekvencie sa môžu usporiadať do alternatívnej konformácie DNA, nazývanej aj non-B DNA štruktúra. Tieto non-B DNA konformácie môžu vytvárať trojvláknovú DNA, takzvané G-kvadruplexy, alebo vlásenkové štruktúry. Niekoľko biochemických štúdií preukázalo, že RAG1/2 komplex je schopný rozpoznávať takéto DNA štruktúry a zavádzať do nich DNA zlomy. Je zaujímavé, že non-B štruktúry boli identifikované aj v blízkosti niektorých genetických abnormalít často sa vyskytujúcich v malígnych B bunkách.

V kapitolách 4, 5 a 6 popisujeme nové mechanizmy patologickej regulácie komplexu RAG1/2. V **Kapitole 4** študujeme nový molekulárny mechanizmus, ktorý je zodpovedný za vypnutie expície komplexu RAG1/2 v B bunkách v reakcii na poškodenie DNA. Tento mechanizmus môže byť aktivovaný poškodením DNA vonkajšími faktormi (γ -žiarenie alebo chemické látky, ktoré indukujú zlomy DNA), ale aj v prípade, keď je zdrojom poškodenia DNA samotný komplex RAG1/2. Preukázali sme, že kľúčovým faktorom tejto regulácie je aktivácia proteínu ATM poškodením DNA. Farmakologická inhibícia ATM kinázy v našej štúdii zabránila inaktivácii komplexu RAG1/2 po indukcii DNA poškodenia. Naše výsledky ukázali, že aktivácia ATM znižuje viazanie transkripčného faktora FOXO1 na gény RAG1 a RAG2, čím sa utlmuje ich expresia. Navrhujeme, že tento mechanizmus môže zohrávať významnú úlohu pri ochrane B buniek pred nadmerným nežiaducim poškodením DNA počas procesu rekombinácie *Ig* génov. V **Kapitole 5** sme objavili ďalší nový regulačný mechanizmus, ktorý kontroluje aktivitu a dostupnosť RAG1/2 komplexu. Preukázali sme, že jadrový faktor kappa-B (NF- κ B) a signálna dráha fosfoinozitol-3-kinázy (PI3K)/AKT sú významnými inhibítormi aktivity RAG1/2. Navrhujeme, že tento regulačný mechanizmus zabezpečuje, expresiu a aktiváciu RAG1/2 iba v správnej fáze bunkového cyklu počas delenia buniek. Inhibícia NF- κ B vedie k zvýšeniu aktivity RAG1/2 a ku vzniku zlomov DNA. Použitie nových liečivých látok, ktoré inhibujú komponenty NF- κ B, môže mať preto nežiaduce dôsledky pre genomickú stabilitu prekurzorov B buniek vyvíjajúcich sa v kostnej dreni.

Na záver sme ukázali v **Kapitole 6**, že tumorový supresor p53 taktiež zohráva kľúčovú úlohu v regulácii komplexu RAG1/2 v reakcii na poškodenie DNA. Prekurzorom B buniek s vyradeným génom p53 (p53 knockout) sa expresia RAG1/2 po poškodení DNA nevypne, na rozdiel od "normálnych" prekurzorov B buniek. Okrem toho sme zistili, že absencia p53 vedie k zvýšeniu počtu prekurzorov B buniek, ktoré úspešne prešli rekombináciou *Ig* génov. Aktivácia p53 po poškodení DNA vedie k zvýšeniu expície mikroRNA-34a (miR-34a). miR-34a následne čiastočne deaktivuje transkripčný faktor forkhead box P1 (FOXP1) proteín, ktorý zohráva kľúčovú úlohu pri regulácii expície RAG1/2 komplexu. Naša štúdia ďalej ukázala, že poškodenie DNA vedie k zníženiu expície FOXP1, a že zvýšená expresia FOXP1 v prekurzoroch B buniek urýchljuje rekombináciu *Ig* génov.

Authors' contributions and Research funding

Affiliations of the authors:

(at the moment of study conduct)

Katarina Ochodnicka-Mackovicova (K.O-M):

Department of Pathology, Amsterdam University Medical Centers, Location AMC, University of Amsterdam, the Netherlands

Lymphoma and Myeloma Center Amsterdam (LYMMCARE), the Netherlands

Jeroen E.J. Guikema (J.E.J.G):

Department of Pathology, Amsterdam University Medical Centers, Location AMC, University of Amsterdam, the Netherlands

Lymphoma and Myeloma Center Amsterdam (LYMMCARE), the Netherlands

Carel J.M. van Noesel (C.J.M.v N):

Department of Pathology, Amsterdam University Medical Centers, Location AMC, University of Amsterdam, the Netherlands

Lymphoma and Myeloma Center Amsterdam (LYMMCARE), the Netherlands

Ted E. Bradley (T.E.B):

Core Facility Genomics, dept. Clinical Genetics, Amsterdam UMC, the Netherlands

Martin Haagmans (M.H.):

Core Facility Genomics, dept. Clinical Genetics, Amsterdam UMC, the Netherlands

Michal Mokry (M.M):

Laboratory of Experimental Cardiology, University Medical Center Utrecht, Utrecht University, Utrecht, the Netherlands

Central Diagnostics Laboratory, University Medical Center Utrecht, University Utrecht, Utrecht, the Netherlands

Mahnoush Bahjat (M.B):

Department of Pathology, Amsterdam University Medical Centers, Location AMC, University of Amsterdam, the Netherlands

Lymphoma and Myeloma Center Amsterdam (LYMMCARE), the Netherlands

Timon A. Bloedjes (T.A.B):

Department of Pathology, Amsterdam University Medical Centers, Location AMC, University of Amsterdam, the Netherlands

Lymphoma and Myeloma Center Amsterdam (LYMMCARE), the Netherlands

Chiel Maas (C.M):

Department of Pathology, Amsterdam University Medical Centers, Location AMC, University of Amsterdam, the Netherlands

Lymphoma and Myeloma Center Amsterdam (LYMMCARE), the Netherlands

Alexander M. de Bruin (A.M.d.B):

Department of Pathology, Amsterdam University Medical Centers, Location AMC, University of Amsterdam, the Netherlands

Lymphoma and Myeloma Center Amsterdam (LYMMCARE), the Netherlands

Richard J. Bende (R.J.B):

Department of Pathology, Amsterdam University Medical Centers, Location AMC, University of Amsterdam, the Netherlands

Lymphoma and Myeloma Center Amsterdam (LYMMCARE), the Netherlands

Amelie van der Veen (A.vdV.):

Department of Pathology, Amsterdam University Medical Centers, Location AMC, University of Amsterdam, the Netherlands

Lymphoma and Myeloma Center Amsterdam (LYMMCARE), the Netherlands

Harmen van Andel (H.vA.):

Department of Pathology, Amsterdam University Medical Centers, Location AMC, University of Amsterdam, the Netherlands

Lymphoma and Myeloma Center Amsterdam (LYMMCARE), the Netherlands

Carol E. Schrader (C.E.S.):

Department of Microbiology and Physiological Systems, University of Massachusetts Medical School, Worcester, MA 01655

Rudi W. Hendriks (R.W.H.):

Department of Pulmonary Medicine, Erasmus MC, 3000 CA Rotterdam, the Netherlands

Els Verhoeyen (E.V.):

Centre International de Recherche en Infectiologie, Virus Enveloppés, Vecteurs et Réponses Innées Équipe, INSERM U1111, CNRS, UMR5308, Université de Lyon-1, École Normale Supérieure de Lyon, 69007 Lyon, France

INSERM, U1065, Centre de Médecine Moléculaire, Équipe 3, 06204 Nice, France.

Martine van Keimpema (M.vK.):

Department of Pathology, Amsterdam University Medical Centers, Location AMC, University of Amsterdam, the Netherlands

Lymphoma and Myeloma Center Amsterdam (LYMMCARE), the Netherlands

Marcel Spaargaren (M.S.):

Department of Pathology, Amsterdam University Medical Centers, Location AMC, University of Amsterdam, the Netherlands

Lymphoma and Myeloma Center Amsterdam (LYMMCARE), the Netherlands

Author's contribution:

Chapter 1: K.O-M wrote the manuscript, J.E.J.G. and C.J.M.v N. edited the manuscript

Chapter 2: K.O-M wrote the manuscript, J.E.J.G. edited the manuscript

Chapter 3: K.O-M and J.E.J.G. designed the research, K.O.-M., J.E.J.G. and T.E.B. performed the research, K.O.-M., J.E.J.G., M.H., M.M., C.J.M.v N. and T.E.B. analyzed the data, K.O-M wrote the manuscript, all authors edited the manuscript

Chapter 4: K.O-M and J.E.J.G. designed the research, K.O.-M., M.B., T.A.B., C.M., A.vdV., H.vA., and J.E.J.G. performed the research, C.E.S, R.W.H, E.V, and A.M.d.B provided mouse material, expertise or reagents, K.O.-M., M.B., T.A.B., R.J.B, C.J.M.v N. and J.E.J.G. analyzed the data, K.O.-M, M.B. and J.E.J.G. wrote the manuscript, all authors edited the manuscript

Chapter 5: K.O-M and J.E.J.G designed the research, K.O-M, M.B. T.A.B., C.M., and J.E.J.G performed the research, A.M.de B. and R.J.B provided analytical tool and reagents, K.O-M, M.B., C.M. and J.E.J.G analyzed the data, K.O.-M, M.B. and J.E.J.G. wrote the manuscript, all authors edited the manuscript

Chapter 6: K.O-M and J.E.J.G. designed the research, K.O-M, J.E.J.G., M.v K. performed the research, M.S. provided tool and reagents, K.O-M, J.E.J.G. and C.J.M.v N. analyzed the data, K.O-M wrote the manuscript, all authors edited the manuscript

Chapter 7: K.O-M wrote the manuscript, J.E.J.G edited the manuscript

Research funding

This research, originating from Dr. Guikema's laboratory, was funded by the AMC Fellowship program and by Nederlandse Organisatie voor Wetenschappelijk Onderzoek (NWO) VIDI grant 016126355 both obtained by Dr. Guikema.

PhD portfolio

Name PhD student: Katarina Ochodnicka (née Mackovicova)

PhD period: August 2010 – August 2014

Promotor: prof. dr. Carel J.M. van Noesel

Co-promotor: dr. Jeroen E.J. Guikema

1. PhD training		
	Year	Workload
Specific courses		
• AMC world of science	2010	0.7
• Advanced immunology (AMC)	2011	2.9
• Dutch course NT2 pre-intermediate (UvA)	2012	1.8
• Radiation protection / Stralingsbescherming deskundigheidsniveau 5B (AMC)	2012	0.6
• Project management (AMC)	2012	0.6
• Next generation sequencing data analysis (NBIC)	2012	0.7
• Computing in R, basics (AMC)	2013	0.7
• Entrepreneurship in health and life sciences (AMC)	2014	1.5
Seminars, workshops and masterclasses		
• Weekly LYMMCARE meeting series	2010-2014 and 2022-2023	7.5
• OASIS seminar series	2010-2014	2.2
• Amsterdam Immunology (AIM) seminar series	2010-2014	2.2
• Pathology seminar series	2010-2014	3.5
Presentations		
• Oral presentation OOA retreat	2011	0.5
• Oral presentation NVVI annual meeting	2012	0.5
• Oral presentation Pathology seminars	2013	0.5
• Oral presentation Triple I retreat	2013	0.5
• Oral presentation AIMM seminar	2012, 2013, 2014	1.5
• Oral presentation Dutch hematology congress	2012, 2013, 2014	1.5
• Oral presentation LYMMCARE	2010-2014	2
• Poster presentation Mutation, Malignancy and Memory symposium	2013	1.5
(Inter)national conferences		
• NVVI annual meeting, Noordwijkerhout, the Netherlands	2011, 2012, 2014	1.8
• Dutch hematology congress, Papendal, the Netherlands	2012, 2013, 2014	1.8
• Mutation, Malignancy and Memory symposium, Boston, Massachusetts	2012	1.5
• B-cell development and Function symposium, Keystone, Colorado (presented by J.E.J.G)	2013	0.2
Other		
• Annual graduate student retreat of the Oncology Graduate School Amsterdam (OOA)	2011, 2012, 2013	1.8
• Tripple I PhD retreat	2013	0.6
• Journal clubs	2010-2014	3.3

2. Teaching		
	Year	Workload
Supervising		
• Michaela de Barberis (master student)	2013	3.5
• Dat Le Quang (master student)	2014	3.5
3. Parameters of Esteem		
	Year	Workload
Grants		
NVVI Travel grant	2012	0.1
4. Publications		
	Year	
Deli Zhang, Lei Ke, Katarina Mackovicova , Johannes J L Van Der Want, Ody C M Sibon, Robert M Tanguay, Genevieve Morrow, Robert H Henning, Harm H Kampinga, Bianca J J M Brundel. Effects of different small HSPB members on contractile dysfunction and structural changes in a <i>Drosophila melanogaster</i> model for Atrial Fibrillation. <i>J Mol Cell Cardiol</i> , 2011 Sep;51(3):381-9.	2011	
Katarina Mackovicova , Andrea Gazova, Dana Kucerova, Beata Gajdacova, Jan Klimas, Peter Ochodnický, Eva Goncalvesova, Jan Kyselovic, Peter Krenek. Enalapril decreases cardiac mass and fetal gene expression without affecting the expression of endothelin-1, transforming growth factor β -1, or cardiotrophin-1 in the healthy normotensive rat. <i>Can J Physiol Pharmacol</i> , 2011 Mar;89(3):197-205.	2011	
Kati Juuti-Uusitalo, Leon J Klunder, Klaas A Sjollema, Katarina Mackovicova , Ryuichi Ohgaki, Dick Hoekstra, Jan Dekker, Sven C D van Ijzendoorn. Differential effects of TNF (TNFSF2) and IFN- γ on intestinal epithelial cell morphogenesis and barrier function in three-dimensional culture. <i>PLoS One</i> , 2011;6(8):e22967.	2011	
Lei Ke, Roelien A M Meijering, Femke Hoogstra-Berends, Katarina Mackovicova , Michel J Vos, Isabelle C Van Gelder, Robert H Henning, Harm H Kampinga, Bianca J J M Brundel. HSPB1, HSPB6, HSPB7 and HSPB8 protect against RhoA GTPase-induced remodeling in tachypaced atrial myocytes. <i>PLoS One</i> , 2011;6(6):e20395.	2011	
Hana Cernecka, Katarina Ochodnicka-Mackovicova , Dana Kucerova, Jana Kmecova, Viera Nemcekova, Gabriel Doka, Jan Kyselovic, Peter Krenek, Peter Ochodnický, Jan Klimas. Enalaprilat increases PPAR β/δ expression, without influence on PPAR α and PPAR γ , and modulate cardiac function in sub-acute model of daunorubicin-induced cardiomyopathy. <i>Eur J Pharmacol</i> , 2013 Aug 15;714(1-3):472-7.	2013	
Jan Klimas, Michael Olvedy, Katarina Ochodnicka-Mackovicova , Peter Kruzliak, Sona Cacanyiova, Frantisek Kristek, Peter Krenek, Peter Ochodnický. Perinataly administered losartan augments renal ACE2 expression but not cardiac or renal Mas receptor in spontaneously hypertensive rats. <i>J Cell Mol Med</i> , 2015 Aug;19(8):1965-74.	2015	

4. Publications <i>continued.</i>	
	Year
Katarina Ochodnicka-Mackovicova , Mahnoush Bahjat, Timon A Bloedjes, Chiel Maas, Alexander M de Bruin, Richard J Bende, Carel J M van Noesel, Jeroen E J Guikema. NF- κ B and AKT signaling prevent DNA damage in transformed pre-B cells by suppressing RAG1/2 expression and activity. <i>Blood</i> , 2015 Sep 10;126(11):1324-35.	2015
Katarina Ochodnicka-Mackovicova , Mahnoush Bahjat, Chiel Maas, Amélie van der Veen, Timon A Bloedjes, Alexander M de Bruin, Harmen van Andel, Carol E Schrader, Rudi W Hendriks, Els Verhoeven, Richard J Bende, Carel J M van Noesel, Jeroen E J Guikema. The DNA Damage Response Regulates RAG1/2 Expression in Pre-B Cells through ATM-FOXO1 Signaling. <i>J Immunol</i> , 2016 Oct 1;197(7):2918-29	2016
Katarina Hadova , Jana Kmecova, Katarina Ochodnicka-Mackovicova , Eva Kralova, Gabriel Doka, Lenka Bies Pivackova, Peter Vavrinec, Tatiana Stankovicova, Peter Krenek, Jan Klimas. Rapid changes of mRNA expressions of cardiac ion channels affected by Torsadogenic drugs influence susceptibility of rat hearts to arrhythmias induced by Beta-Adrenergic stimulation. <i>Pharmacol Res Perspect</i> , 2023 Oct;11(5):e01134	2023
Katarina Ochodnicka-Mackovicova , Michal Mokry, Martin Haagmans, Ted E. Bradley, Carel J.M. van Noesel, Jeroen E.J. Guikema. RAG1/2 induces double-stranded DNA breaks at non-Ig loci in the proximity of single sequence repeats in developing B cells. <i>Manuscript under revision at European Journal of Immunology</i>	2024
Katarina Ochodnicka-Mackovicova , Martine van Keimpema, Marcel Spaargaren, Rudi W. Hendriks, Carel van Noesel, Jeroen J.E. Guikema. DNA damage-induced p53 downregulates expression of RAG1 through a negative feedback loop involving miR-34a and FOXP1. <i>Manuscript under consideration at Journal of Biological Chemistry</i>	2024
Role of RAG1 and RAG2 in pre-B cell development, signaling and (off)target DNA damage. Katarina Ochodnicka-Mackovicova , Jeroen J.E. Guikema. <i>Manuscript in preparation.</i>	2024

About the author

Katarína Ochodnická (née Mackovičová) was born on the 3rd of June 1986 in Bratislava, Slovakia (then Czechoslovakia). She pursued her undergraduate studies in Pharmacy at Comenius University in Bratislava. Alongside her studies, she actively engaged in various scientific student projects at the Faculty of Pharmacology and Toxicology, fostering a profound interest in research and innovation within pharmaceutical sciences.

Driven by her passion, Katarína ventured to the Netherlands, where she obtained her Master of Science degree in Medical and Pharmaceutical Drug Innovation from the University of Groningen. During her master's studies, she undertook two enriching internships. First, she worked in the lab of Professor van IJzendoorn at the Department of Cell Biology of University Medical Center Groningen (UMCG), focusing on 3D-organoid and *C.elegans* models to investigate the origin of Microvillus Inclusion Disease. Second, she conducted research in the lab of Professor Brundel at the Department of Clinical Pharmacology, UMCG, exploring the role of Heat Shock Proteins in Atrial Fibrillation using *D. melanogaster* as a model organism. Her contributions to various Bachelor's and Master's research projects at both universities were recognized in numerous scientific publications.

Continuing her academic pursuits, Katarína conducted her doctoral research studies at the University of Amsterdam/ University Medical Center Amsterdam. Under the guidance of Professor Carel van Noesel and Dr. Jeroen Guikema at the Department of Pathology, she conducted fundamental research on the origin of genomic instability in B-cell acute lymphoblastic leukemia (B-ALL), the culmination of which is presented in this thesis.

Following the four productive years as a PhD candidate, Katarína transitioned into roles within the pharmaceutical industry, while continuing working on publishing her research and completing her thesis. She dedicated six years to various quality assurance positions, including Qualified Person, Responsible Person, and QA Manager at Nordic Pharma. Subsequently, she served as an EU-Qualified Person/Senior QA Manager at Bristol Myers Squibb (BMS) for nearly two years.

However, balancing the career demands, and those of raising a young family, was structurally leaving insufficient time for thesis completion. Therefore, in the summer of 2023, she made the decision to temporarily step away from her paid job and concentrate full-time on finalizing her doctoral studies.

As of May 2024, Katarína holds the position of Qualified Person for Advanced Therapy Medicinal Products (ATMP) at the Cell Therapy facility of the University Medical Center patient care.



Acknowledgements

Life often happens while we are busy planning it. This certainly applied to my PhD trajectory; spending almost 15 years from the beginning to the end was definitely not part of the initial plan. But luckily, as it turns out, there indeed are more ways leading to Rome. And after all, I have always been more of a long-distance runner anyway. However, none of this would be possible if I was running alone. This thesis was really a team effort and I am truly grateful to the many who directly or indirectly contributed to its realization.

First of all, I am grateful for being granted the opportunity to conduct independent research at the **University of Amsterdam / University Medical Center Amsterdam**, namely at the **Pathology department**. To my promotors: **Prof. Dr. Carel van Noesel** and **Dr. Jeroen Guikema**, you shaped me academically, you challenged me. **Carel**, I am grateful for your guidance, I admire your profound insights and enjoyed our many scientific discussions very much. **Jeroen**, it is so much fun to work alongside someone whose unbridled enthusiasm for science is so genuine. The level of your attention to details has always been an example to me. In the last phase, I especially want to thank you for shaping and lifting my scientific writing. Carel and Jeroen, I am grateful to both of you for your dedication to our research projects, from the beginning to the end, and wish both of you lots of success in your further scientific and personal endeavors!

To the members of my **doctoral committee**: I sincerely appreciate that you agreed to take on the task of serving on my doctoral committee and wish to thank you for taking the time to read and evaluate my doctorate thesis.

To all **co-authors** (see Appendix): thank you very much for the fruitful collaboration! I am grateful for your feedback, your fine efforts and inputs; you were instrumental for the success of the various projects and publications. Also, many thanks to the colleagues from AMC FACS facility (**Berend**) and the AMC Core facility genomics (**Ted, Linda K.**) for the help with setting up protocols, troubleshooting, or operating the devices. **Michal, Martin H.**, thank you for your help with the initial analysis of the sequencing data.

To **Nike**: you are a great lab manager, relentlessly taking care of the lab supplies and making sure the labs run smoothly! Thank you very much for all your help with ordering primers, kits, and antibodies, as well as for the troubleshooting, administrative support (especially in the last few years), for the CDs that I once borrowed from you, and which took me like forever to return (CDs!! Haha, can you imagine!), and for all the nice talks.

To my paranympths: Martin and Martine, *tegenwoordig praten we met elkaar gewoon in het Nederlands. Sommigen van ons blijven dan wel Broabants pratuh, maar dat gaat de anderen van ons petje te boven*. I am thrilled that you accepted the role of paranympths, it was so much fun planning the final phase with you! **Martin**, I am amazed by the ease with which you sail through your academic career. Where others are in despair due to the pile of failed experiments, frustrated by the endless writing, or discouraged by the too-critical

feedback of the reviewers, you always seem so jolly, never complaining about any of that, you go around and cheer others up! Also, your neatly organized system of documenting the experiments and archiving the data puts any corporate good documentation practice policy to shame. (*Martine, wat ben jij een vrolijk en optimistisch ingesteld mens! En wat was jouw labjournaal altijd keurig bijgewerkt! Knap, hoor! Heel erg bedankt voor je praktische tips voor het afronden van het proefschrift. Ik wens je nog heel veel succes met jouw onderzoek, vele Nature papers, natuurlijk, maar vooral ook veel plezier thuis met jullie prachtige tweeling!*) **Martine**, we pipetted several experiments together and eventually turned that into a paper, ran a half-marathon in Vienna together and several other runs, were expecting at the same time (a coincidence), and now our kids are running and sporting together, followed by an occasional cake eating on Sundays (not a coincidence). I am grateful for your friendship, the many fun memories we share and happy that we keep creating new ones. Also together with Linda, you, and Martin, we stayed quite close after the AMC years (also geographically close; somehow, we ended up living quite close to each other). **Linda**, you and I are late bloomers, the timelines of our theses followed similar paths and we were both finishing the writing around the same time. A suffering shared is a suffering halved, I appreciate our regular check-ins and your supportive words. I wish you the best of luck with your last pieces, almost there! It takes much effort and discipline to write a thesis while taking care of a young family and working on a career at the same time, and you did it!! Well done!

To my former AMC colleagues: The two offices, the so-called *AIO kamers* (though in fact there were very few real “AIO’s”...) hosted many of us in the course of the years. It has been a long time since then, so I apologize in advance if I have forgotten someone: **Martine, Martin, Linda, Timon, Harmen, Mahnoush, Zemin, Richard, Sander, Robert, Patricia, Kinga, Diewertje, Nerissa, Arwen**, but also colleagues from adjacent *kamers* and labs: **Hans, Loes B., Elena, Alessandra, Nike, Leonie, Anand, Lucia, Avanita, Frederike, Thera, Roy, Lotte, Anneke, Annemieke, Wilco, Emanuele, Patrick, Chiel, Gwen, Willem, Marcel J., Marcel S., Jeroen B., Michaela, Dat, Alex dB., Alex M., Robert, Jasper, Remco, Sandrine, Mark, Jaklien, Monique, Jitske, Esther, Lionel** and the PhD students from other groups or institutes: **Anouk, Rebecca, Jan-Jaap, Malou, Nazanin, Dita, Loes J, Christina, Arnold, Katka**, I am grateful to have shared the PhD experience with you, many thanks for all the lab/office/conference/retreat *gezelligheid!*

Here, I would also like to highlight our periodic outings to the gym. Martine, Martin, Linda, Wilco, Marcel J., Hans, and Lotte as the core-group, and the very occasional visits of Jeroen B., Harmen, and Elena. This initiative, named *Sporten en Saunen bij Science Park*, kept us healthy and in shape during our academic endeavors. Which was also very much needed considering the damage inflicted by the *borrels* on the bridge, *kerst borrels, borrels* in Het Oude Gasthuis, Pinkpop weekend, *stappen* in Groningen, the 80’s and 90’s in Panama, Epsteinbar visits, etc. Last year we organized a revival of this initiative with few of

us, ended up doing Prison Island, which we decided to count as “sport”. Hopefully more sportive revivals are to come!

Marcel J, thank you very much for designing the cover of the thesis! You did a great job visualizing my scattered ideas, and you were very patient with the questions, comments and adjustments! Best of luck with your adventures in Switzerland!

Patrick, thank you for your help, especially in the last few years, with IT matters like re-suscitating my old AMC guest account, helping me to set up remote access, and with other IT questions and problems I was coming up with. Best of luck with your football-coaching dream.

In the last years, I have also had the pleasure of meeting some of the more current PhD students in the Pathology labs: **Hildo, Guus, Tijmen, Linda G.** and **Maria**: best of luck with your research and (sooner or later) with completing your doctorates!

Analyzing data, writing and publishing articles, writing the thesis: all of this was the giant mountain that still needed to be climbed after the 4 years in the lab, and it was following me like a shadow during my career outside of academia (until the day of the PhD defense). At this place, I would like to express my gratitude to my current and previous managers who showed a great deal of understanding for the shadows that were following me, and who made it possible to balance work, writing and family. **André**, on several occasions I heard you saying that an employee cannot flourish if their private life is out of balance. In relation to this thesis, about a year after starting my new job, you made it possible for me to temporarily work fewer hours and dedicate that time to writing, for which I am very grateful to you! In this period Chapter 4 was written. **Jan**, you expressed a lot of understanding and support when I presented to you my rather radical plans for the finalization of this thesis. Thank you for exploring the options and for thinking along. In this period, and especially in the period hereafter, Chapters 1, 2, 3 and 6 were written. **Gera** and **Wilma**, you hired me while knowing that you will need to wait quite some time for me to finalize all the remaining chapters before actually coming on board. In this period Chapter 7 and the Appendix chapters were written. Thank you for your patience, for understanding just how much *de laatste loodjes wegen*, and for making it possible in my first months to work fewer hours, leaving enough “thesis time” to round everything up.

Importantly, I appreciate the supportive words of many of my (ex)colleagues from the post-academic era, and I am grateful for us staying in touch, following each other’s lives, becoming friends! Likewise, to all the friends outside of research/work area: my heartfelt thank you for all your support at some point along this journey!

And then, none of this would really be possible if it was not for the unlimited support provided by my beloved family. To my in-laws **Milan** and **Eva**: thank you for your continued interest in my research, and especially many thanks to Milan for the long list of scientific articles you sent me over the course of this journey! (*Svokrovcom: Ďakujem vám za vašu podporu, prejavovaný záujem o môj výskum a za množstvo zaslaných separátok! Veľmi si to*

vážim!) To my parents **Ivan** and **Maria**: you created a stable basis in my life, you recognized the value of good education, stimulated me to aspire to higher goals and supported my academic efforts from the earliest of years, even if that meant moving to a different country later on. Without this support, without you, I would be nowhere. (*Rodičom: Ďakujem vám za stabilné rodinné zázemie, ktoré ste pre nás deti vytvorili. Vždy ste si vážili hodnotu kvalitného vzdelania, podporovali ste moje akademické ambície a povzbudzovali ma vzhliadať ku vysokým cieľom, aj keď to neskôr znamenalo študovať v inom štáte. Bez tejto podpory, bez vás, by som nebola nič z toho, čo som.*) I enjoy good teamwork and bringing people together. So fun fact, I team-worked my **father** and my brother **Jakub** into Chapter 3, and at this place, I want to thank you both for your active participation and all your help. My father created a server storage space for the big data generated in Chapter 3 and helped me to figure out how to transfer such data from the server into the various programs for data analysis or visualization. My brother wrote a Python script that enabled us to find overlaps between our data and the publicly available data generated by another research group. Thank you also for your help with testing and adjusting the script, and for patiently teaching your IT-alphabet sister how to use it ;-D

To **Peter**: we met each other when my research career was at its beginnings. We shared passion for science, worked on several research projects together, and even did many experiments together. However, the most beautiful experiment we have ever done is our life together and raising our two daughters. This thesis would not have seen the daylight if it was not for your unwavering support, your funny pep-talks, silly jokes at times when I was losing my mind, and especially all the adjustments we needed to make during the last years in order to make this happen. Thank you for being my rock! And finally, to my daughters **Barbora** and **Julia**, my sweet girls. I am so grateful that I get to be your mom! You supported me more than you realize. You always took very active interest in the progress of my thesis (*Mama, hoeveel had je vandaag geschreven? Waarover heb je geschreven? Wat voor berekeningen heb je gedaan? Mag ik de plaatjes zien die je had gemaakt? Ik kan ook plaatjes voor je maken als je wil...*) Day after day, you inspire me and you teach me, you make me want to be the best version of myself -for you! It is all for you. *Ik ben heel trots op jullie en ik hou van jullie onwijs veel!*

ERRATUM

Chapter 5, page 127, Figure 4 should be displayed as follows:

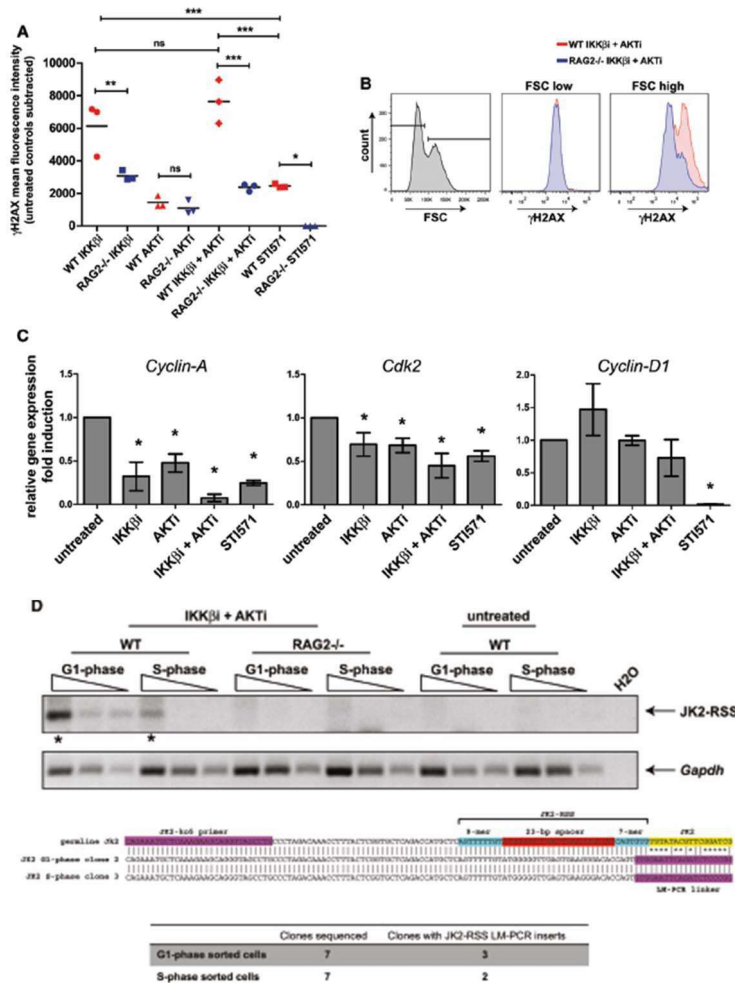


Figure 4. Inhibition of AKT and NF- κ B signaling induces RAG-dependent DNA damage in mouse Abl pre-B cells.

(A) Mean fluorescence intensity (MFI) of intracellular γ H2AX staining in mouse Abl pre-B cells treated as indicated on x-axis. Red symbols represent γ H2AX MFI in WT cells, and blue symbols represent γ H2AX MFI in RAG2^{-/-} cells. MFIs of untreated controls were subtracted to correct for background staining. Three independent experiments were performed, and horizontal lines represent means. Statistical significances between groups were determined by ANOVA using a Bonferroni's posttest. (B) Overlay FACS histograms of intracellular γ H2AX staining in IKK β i- and AKTI-treated cells. Small B cells (FSC low; left gate) vs large B cells (FSC high; right gate) are shown. (C) Real-time RT-PCR of *Cyclin-A*, *Cdk2*, and *Cyclin-D1* mRNA expression in WT mouse Abl pre-B cells. Cells were treated with 2.5 μ M IKK β i, 2.5 μ M AKTI, or 10 μ M STI571 for 48 hours. Real-time RT-PCR results are presented relative to the expression of the 18S rRNA housekeeping gene. Three independent experiments were performed, PCRs were performed at least in duplicate, and error bars represent means \pm SD of 3 independent experiments. (D) Jk2-RSS DNA breaks are detected by LM-PCR in cell-cycle sorted (G₁ and S phase) WT mouse Abl pre-B cells that were treated with 2.5 μ M IKK β i and 2.5 μ M AKTI. Threefold dilutions of linker-ligated DNA were amplified with a Jk2-specific forward primer and an LM-PCR linker-specific reverse primer. PCR products indicated with an asterisk were excised from the gel, cloned, and sequenced. The middle section of panel D shows the alignments of sequences obtained from G₁ and S phase cells to the germline Jk2 sequence. Jk2-ko5 primer site, Jk2-RSS, and the Jk2 coding region are indicated by colored boxes. Sequencing results are listed at the bottom of panel D. **P* < .05; ***P* < .01; ****P* < .001. ns, not significant.

